

Individual Source Measurements of Anthropogenic Methane Emissions from Canada and the United States

James P. Williams

Department of Civil Engineering

McGill University, Montreal

May 2023

A thesis submitted to McGill University in partial fulfillment of the requirements
of the degree of Doctor of Philosophy

©James P. Williams, 2023

*This thesis is dedicated to my aunt Susan,
my grandmother Ola,
and my godfather Don,
whose memories I will forever cherish,
and to my family for their continued support.*

Table of Contents

List of Figures	viii
List of Tables	x
Abstract	xiv
Résumé	xvii
Acknowledgements	xx
Preface	xxiii
1 Introduction	1
1.1 Introduction	1
1.2 Problem statement and hypotheses	6
1.3 Research objectives	7
1.4 Thesis organization	8
1.5 Contribution to original knowledge	10
2 Literature Review	19
2.1 Methane measurement methods	19
2.1.1 Indirect methods	20
2.1.2 Direct methods	23
2.1.3 Methane source attribution and geochemistry	24
2.2 Methane sources: emission inventories	26
2.2.1 Energy	26
2.2.2 Waste	29

2.2.3	Agriculture, forestry, and other land-use	31
3	Controlled release testing of the static chamber methodology for direct measurements of methane emissions	44
3.1	Introduction	46
3.2	Methodology	49
3.3	Results	54
3.3.1	Prior controlled methane releases and component level methane emissions .	54
3.3.2	Controlled releases of methane	56
3.3.3	Effects of leak properties	60
3.3.4	Optimizing the static chamber method for accuracy	61
3.4	Discussion	63
3.5	Acknowledgements	68
3.6	Supplementary information	69
3.6.1	Effects of chamber seal	69
4	Methane emissions from abandoned oil and gas wells in Canada and the United States	83
4.1	Introduction	84
4.2	Methods	87
4.2.1	Methane flow rate measurements and emission factors	87
4.2.2	Number of AOG wells	87
4.2.3	Emission factor attribution scenarios	89
4.2.4	Uncertainty analysis	91
4.3	Results	91
4.3.1	Methane flow rates and emission factors	91
4.3.2	Number of AOG wells	92
4.3.3	National methane emission estimates	95
4.4	Discussion	97
4.5	Acknowledgements	100

4.6	Supplementary information	101
4.6.1	Treatment of zeroes	101
4.6.2	Uncertainties in the number of AOG wells	101
5	Differentiating and mitigating methane emissions from fugitive leaks from natural gas distribution, historic landfills, and WUH in Montréal, Canada	111
5.1	Introduction	113
5.2	Methods	115
5.3	Results	118
5.3.1	Methane emissions by source	118
5.3.2	Geochemical analysis	122
5.3.3	Mitigation options: costs, technology readiness, and potential CH ₄ reductions	123
5.4	Discussion	126
5.4.1	Wastewater utility holes and historic landfills: larger CH ₄ sources than previously thought	126
5.4.2	CH ₄ source subcategories are generally not identifiable using geochemistry alone	128
5.4.3	Mitigation options vary in readiness, impact, and cost effectiveness	129
5.5	Acknowledgements	131
5.6	Supplementary information	132
5.6.1	Mobile surveying and site selection	132
5.6.2	Static chamber measurements	133
5.6.3	Description of source subcategories	133
5.6.4	Annual methane emissions calculations	135
5.6.5	Geochemical analysis and Keeling plot regressions	136
5.6.6	Methane mitigation costs	137

6	Characterizing and quantifying methane emissions from wastewater collection systems and urban water bodies	151
6.1	Introduction	152
6.2	Methods	154
6.2.1	Defining urban extents and site description	154
6.2.2	Emission factors	156
6.2.3	Activity data	157
6.2.4	Temporal analysis and mobile surveys	158
6.2.5	Annual methane emissions estimates	159
6.3	Results	160
6.3.1	Wastewater collection systems	160
6.4	Discussion	166
6.4.1	Comparisons to prior measurements	167
6.4.2	Temporal patterns in methane emissions	169
6.4.3	Mitigation avenues	170
6.4.4	Future work	171
6.5	Acknowledgements	172
6.6	Supplementary information	173
6.6.1	Methane emission rates and activity data	173
6.6.2	Representativity of emission factors	174
7	General discussion and conclusions	182
7.1	General discussions	182
7.2	Limitations and Uncertainties	185
7.3	Recommendations	188
7.3.1	Future research directions	188
7.3.2	For policy-makers	191
7.4	Conclusions	193

List of Figures

2.1	Summary of methane controlled release tests showing the range of methane flowrates tested and the type of measurement platform	22
2.2	Pie charts of annual methane emissions from Canada and the U.S. in 2021 categorized according to the major sectors and sub-sectors in each countries inventory	26
3.1	Diagram of the controlled release experiments for the static chamber method, with photos of chamber deployments in both field settings and during controlled release testing.	51
3.2	Component level methane emission factors from the IPCC emission factor database.	55
3.3	Summary of published literature of controlled releases of methane.	56
3.4	Parity plot showing the true versus measured measured methane flowrates for different chamber volumes.	57
3.5	Parity plot showing the true versus measured measured methane flowrates for different chamber shapes.	58
3.6	Parity plot showing the true versus measured measured methane flowrates for experiments with and without fans present.	59
3.7	Violin plots of the percentage errors of true versus measured methane flowrates under varying mass flowrates, volumetric flowrates, and gas concentrations of methane.	61
3.8	Four examples of raw controlled release data showing methane concentrations versus time.	64
3.9	Scatter-plots of methane concentration over time for all 64 controlled release tests (1/2).	77

3.10	Scatter-plots of methane concentration over time for all 64 controlled release tests (2/2).	78
4.1	Empirical cumulative distributions of measured methane flow rate from unplugged and plugged abandoned oil and gas wells in the U.S. and Canada.	93
4.2	Map of all active and abandoned onshore well locations gathered from publicly available databases for the U.S. and Canada.	95
4.3	Annual growth rates of abandoned oil and gas well counts in Canada from 1956 to 2017 and the U.S. from 2000 to 2013.	96
4.4	Bar plot of annual methane emissions from abandoned oil and gas wells from the U.S., Canada, and the most recent national inventory estimates.	97
4.5	Maps of five emission factor attribution scenarios and a map of oil and gas basins used to obtain emission factors.	103
4.6	Barplots of methane emissions from abandoned oil and gas wells from each state in the U.S. based on well type and plugging status for all five emission factor attribution scenarios.	106
4.7	Barplots of methane emissions from each province/territory in Canada based on well type and plugging status for all three emission factor attribution scenarios.	107
5.1	Map of sampled sites and gridded inventories (500m by 500m) of CH ₄ emissions from historic landfills, WUHs, and NG distribution emissions in the Island of Montréal.	118
5.2	Distributions of direct measurements of CH ₄ emissions released from NG stations, soil gas fluxes from historic landfills, above-ground infrastructure (LFG vents and observation wells) at historic landfill sites, and WUHs.	120
5.3	Annual CH ₄ emission estimates from fugitive NG distribution systems, historic landfills, and WUHs.	122
5.4	Average CO ₂ :CH ₄ ratios, C ₂ :C ₁ ratios, and δ ¹³ C-CH ₄ signatures of historic landfill, WUH, and NG distribution source groups.	124

5.5	Mitigation costs (USD) per tonne of CH ₄ versus the potential CH ₄ emissions reductions for Montréal for fugitive NG distribution, historic landfills, and WUHs.	125
5.6	Stepwise methodology of uncertainty range calculations for CH ₄ source subcategories in this work.	143
5.7	Photos of two CH ₄ source types encountered at some historic landfill locations.	143
5.8	Static chambers installed over three different source types.	144
5.9	Sensitivity analysis of Keeling plot regressions of geochemical source signatures.	145
6.1	Maps of Toronto, Canada, with the Keating Channel and northeastern corner of High Park highlighted.	155
6.2	Map of all cities in Canada and the U.S. with open-access data related to WUH counts.	160
6.3	Barplot of methane emission rates measured from WUHs in Toronto and Montreal, Canada, and Indianapolis, United States. Bars are coloured according the type of WUH.	162
6.4	Barplots of methane flux rates from urban water bodies in Canada.	164
6.5	Methane plumes measured during mobile surveys from the cluster of wastewater utility holes in High Park, and the Keating Channel.	165
6.6	Relative contributions annual methane emissions from source subcategories of wastewater utility holes and urban water bodies.	167
6.7	Linear regression of methane screening value (ppm) versus the measured methane flow rate for 43 wastewater utility holes measured in Indianapolis, Ohio.	176
6.8	Linear regressions of total population counts versus total and sewer WUH counts by population.	177

List of Tables

3.1	Physical descriptions of chambers used for the controlled release experiments. . . .	51
3.2	Leak properties of ten different leaks used in controlled release experiments including percentage errors associated with mass flow controllers (MFC).	53
3.3	IPCC Emission factor database – summary of assumptions used for component level methane emission factor calculations.	70
3.4	Physical chamber factors and leak properties of all 64 controlled release tests. . . .	71
3.5	Summary of controlled release experiments examined for literature review.	74
4.1	Emission factor spatial attribution scenarios for abandoned oil and gas wells in the U.S. and Canada.	90
4.2	Annual anthropogenic methane emissions and associated uncertainties for Canada and the U.S.	104
4.3	Counts of unplugged and plugged abandoned oil and gas wells assigned to each state/province/territory in the U.S. and Canada with the corresponding data sources.	105
5.1	Ranking of CH ₄ emission sources from Montréal’s 2018 greenhouse gas inventory.	140
5.2	Activity data used for all source types and sub-types considered in this study. Units for each source are unique to the type of emissions present.	141
5.3	Classification of methane plumes measured during mobile surveys.	141
5.4	Source category and mitigation activity, potential reduction in methane emissions and reasoning, and source of costs.	142

6.1 Total area covered by urban water bodies (i.e., lakes, canals, creeks, bays, rivers, and ponds) in urban areas in the Greater Toronto Area, Canada. 162

6.2 Summary of activity data, methane emission factors, and annual methane emissions estimates for each source category of urban water bodies and WUHs. 166

6.3 Classification of urban water bodies according to sub-types included in the Government of Canada geospatial data-set. 176

List of Abbreviations and Symbols

δ Delta

μg Microgram

τ Residence time

AD Activity data

AFOLU Agriculture, forestry, and other land-use

AOG Abandoned oil and gas

AVIRIS-NG Airborne Visible InfraRed Imaging Spectrometer - Next Generation

$\text{C}_2:\text{C}_1$ ratio Ethane to methane ratio

CAD Canadian dollar

CAPP Canadian Association of Petroleum Producers

CO_{2-eq} Carbon dioxide equivalent

dc Change in methane concentration

dt Change in time

ECCC Environment and Climate Change Canada

EF Emission factor

EPA Environmental Protection Agency

FLIR Forward looking infrared

g Gram

GHG Greenhouse gas

GTA Greater Toronto Area

hr Hour

IPCC Intergovernmental Panel on Climate Change

kg Kilogram

km Kilometer

kt Metric kiloton

kWh Kilowatt hour

L Litre

LDAR Leak detection and repair

LEL Lower explosive limit of methane

LFG Landfill gas

LiDAR Light detection and ranging

M Mass flowrate of methane

MFC Mass flow controller

MMBtu Metric million British thermal units

MMt Million metric tons

NG Natural gas

NHN National Hydro Network

NIST National Institute of Standards and Technology

OGI Optical gas imaging

ppb Parts per billion

ppm Parts per million

QGIS Quantum Geographic Information System

SLPM Standard litres per minute

SWIR Shortwave infrared

t Metric ton

TROPOMI TROPOspheric Monitoring Instrument

U.S. United States of America

UAV Unmanned aerial vehicle

USD United States dollar

V Volume

WCM Wastewater collection manhole

yr Year

Abstract

Anthropogenic methane emissions have been identified as a strategic greenhouse gas emission reduction target. In the field of methane emissions research, the scientific consensus is that for a given methane source category, the majority of cumulative methane emissions are emitted by a small percentage of high-emitting sites (i.e., super-emitters). However, distinct methane sources will have different emission rate thresholds that define a super-emitting site, and could emit methane at lower rates than what is easily captured by some methane measurement methods. Cumulative methane emissions from lower-emitting sources can be significant if the site counts (i.e. activity data) are high. Accurately quantifying methane emissions from all sources, including low-emitting sources, is a critical component of tracking progress towards methane mitigation goals and reducing emissions. In this thesis, data analysis and field measurements are used to study methane emissions from abandoned oil and gas wells, historic landfills, manholes, and natural gas distribution systems, all sources that have relatively low site level emission rates and require direct on-site measurement methods with to accurately capture the full range of emissions distributions and develop actionable mitigation strategies.

The static chamber methodology, a direct measurement method, was the primary method used in the field measurements of methane emissions presented in this thesis. We conducted controlled release experiments and explored the role of chamber design parameters. We found that static chambers can quantify methane flowrates ranging from 1 to 500 g/hr, which represents the lower range of emission rates when compared to other methane sources such as active oil and gas wells, with an accuracy of $\pm 14\%$.

Within the oil and gas sector, abandoned oil and gas (AOG) wells have the largest activity data, with ≥ 4 million wells in the U.S. and $\geq 370,000$ in Canada. Methane emissions from AOG wells were first included in the Canadian and U.S. national inventory reports in 2019, but estimates were based on a small dataset of 226 direct measurements spread across five U.S. states and no measurement data from Canada. As such, we analyzed methane emissions from 598 published measurements, including previously unpublished measurements of methane emissions we made from 54 AOG wells in Oklahoma and 17 in British Columbia using a static chamber methodology. We developed attribute- and region-specific emission factors of wells which ranged from 1.8×10^{-3} to 48 g/hour of methane for AOG wells in the U.S. and Canada. We estimated that, as of 2020, the annual methane emissions from AOG wells are 20% higher than inventory estimates for the U.S. and 150% higher for Canada.

Municipal greenhouse gas inventories have been shown to underestimate their annual methane emissions when compared to independent research studies. The discrepancy can be, in part, attributed to the missing contributions from smaller diffuse methane sources. To address this question, we quantified methane emissions from wastewater utility holes (WUHs) and historic landfills in Montreal (Canada), two sources with high population counts and few, if any, direct measurement data. In addition, we quantified emissions from natural gas (NG) distribution systems within the city, which is recognized as a significant methane source for cities. We extrapolated the methane emissions to city-wide estimates and performed a cost-benefit analysis of mitigation strategies. We estimated that historic landfills and WUHs, which are methane sources not considered in current greenhouse gas inventories, emitted 901 (452 – 1,541) and 786 (32 – 2,602) t/yr of methane respectively, making them the second and third highest methane sources in Montreal. We found that historic landfills have high potential for methane reductions at high mitigation costs, methane mitigation from WUHs is low-cost but the methods require further research, and increasing repair rates of NG distribution leaks are a cost-effective mitigation strategy.

Recent studies, including our study on methane emissions for Montreal, showed that biogenic sources of methane (e.g., WUHs and urban water bodies) were significant sources in cities, despite not being included in GHG inventories. To address this discrepancy, we directly measured methane

emissions from WUHs and urban water bodies in the Greater Toronto Area (GTA), the largest urban agglomeration in Canada. We found that annual methane emissions from urban water bodies totaled 2,737 t/yr of methane, or 26.4% of emissions from agriculture and wetlands, and that emissions from WUHs totaled 9,122 t/yr of methane, which is more than 10% of the total GTA methane budget.

Our findings address several knowledge gaps in methane emissions quantification of sources requiring direct on-site measurements, which are needed to improve greenhouse gas inventories and guide mitigation strategy development. Overall, multi-scale measurements including direct measurements are needed to fill gaps in current inventories and improved data sharing can reduce current limitations and uncertainties.

Résumé

Les émissions anthropiques de méthane ont été identifiées comme un objectif stratégique de réduction des émissions de gaz à effet de serre. Dans le domaine de la recherche sur les émissions de méthane, le consensus scientifique est que pour une catégorie donnée de sources de méthane, la majorité des émissions cumulées de méthane est émise par un petit pourcentage de sites fortement émetteurs (c'est-à-dire les super-émetteurs). Cependant, des sources de méthane distinctes auront des seuils de taux d'émission différents pour définir un site super-émetteur, et pourraient émettre du méthane à des taux inférieurs à ce qui est facilement capturé par certaines méthodes de mesure du méthane. Les émissions cumulées de méthane provenant de sources faiblement émettrices peuvent être importantes si le nombre de sites (c'est-à-dire les données d'activité) est élevé. La quantification précise des émissions de méthane provenant de toutes les sources, y compris les sources à faible émission, est un élément essentiel du suivi des progrès réalisés pour atteindre les objectifs d'atténuation des émissions de méthane et pour réduire les émissions. Dans cette thèse, l'analyse des données et les mesures sur le terrain sont utilisées pour étudier les émissions de méthane provenant de puits de pétrole et de gaz abandonnés, de décharges historiques, de trous d'homme et de systèmes de distribution de gaz naturel, toutes sources dont les taux d'émission au niveau du site sont relativement faibles et qui nécessitent des méthodes de mesure directe sur le site afin de capturer avec précision toute la gamme des distributions d'émissions et de développer des stratégies d'atténuation exploitables.

La méthodologie de la chambre statique, une méthode de mesure directe, a été la principale méthode utilisée pour les mesures sur le terrain des émissions de méthane présentées dans cette thèse. Nous avons mené des expériences de libération contrôlée et exploré le rôle des paramètres de

conception de la chambre. Nous avons constaté que les chambres statiques peuvent quantifier des débits de méthane allant de 1 à 500 g/h, ce qui représente la gamme inférieure des taux d'émission par rapport à d'autres sources de méthane telles que les puits de pétrole et de gaz en activité, avec une précision de ± 14

Dans le secteur du pétrole et du gaz, les puits de pétrole et de gaz abandonnés (PGA) représentent la plus grande partie des données d'activité, avec 4 millions de puits aux États-Unis et 370 000 au Canada. Les émissions de méthane provenant des puits PGA ont été incluses pour la première fois dans les rapports d'inventaire nationaux du Canada et des États-Unis en 2019, mais les estimations étaient basées sur un petit ensemble de 226 mesures directes réparties dans cinq États américains et sur aucune donnée de mesure provenant du Canada. Nous avons donc analysé les émissions de méthane à partir de 598 mesures publiées, y compris des mesures inédites d'émissions de méthane que nous avons effectuées sur 54 puits PGA en Oklahoma et 17 en Colombie-Britannique à l'aide d'une méthode de chambre statique. Nous avons élaboré des facteurs d'émission spécifiques aux attributs et aux régions des puits, allant de $1,8 \times 10^{-3}$ à 48 g/heure de méthane pour les puits PGA aux États-Unis et au Canada. Nous avons estimé qu'à partir de 2020, les émissions annuelles de méthane provenant des puits PGA sont supérieures de 20 % aux estimations de l'inventaire pour les États-Unis et de 150 % pour le Canada.

Il a été démontré que les inventaires municipaux de gaz à effet de serre sous-estiment leurs émissions annuelles de méthane par rapport aux études indépendantes. Cet écart peut être en partie attribué à l'absence de contribution des petites sources diffuses de méthane. Pour répondre à cette question, nous avons quantifié les émissions de méthane provenant des regards d'eaux usées (REU) et des décharges historiques de Montréal (Canada), deux sources qui comptent un grand nombre d'habitants et pour lesquelles les données de mesure directe sont rares, voire inexistantes. En outre, nous avons quantifié les émissions des systèmes de distribution de gaz naturel (GN) dans la ville, qui sont reconnus comme une source importante de méthane pour les villes. Nous avons extrapolé les émissions de méthane pour obtenir des estimations à l'échelle de la ville et effectué une analyse coûts-avantages des stratégies d'atténuation. Nous avons estimé que les décharges historiques et les REU, qui sont des sources de méthane non prises en compte dans les inventaires actuels de gaz

à effet de serre, émettaient respectivement 901 (452 - 1 541) et 786 (32 - 2 602) t/an de méthane, ce qui en fait les deuxième et troisième sources de méthane les plus importantes à Montréal. Nous avons constaté que les décharges historiques présentent un fort potentiel de réduction du méthane à des coûts d'atténuation élevés, que l'atténuation du méthane provenant des REU est peu coûteuse mais que les méthodes nécessitent des recherches supplémentaires, et que l'augmentation des taux de réparation des fuites de distribution de gaz naturel est une stratégie d'atténuation rentable.

Des études récentes, y compris notre étude sur les émissions de méthane à Montréal, ont montré que les sources biogéniques de méthane (par exemple, les REU et les plans d'eau urbains) étaient des sources importantes dans les villes, bien qu'elles ne soient pas incluses dans les inventaires de gaz à effet de serre. Pour combler cette lacune, nous avons mesuré directement les émissions de méthane provenant des REU et des plans d'eau urbains dans la région du Grand Toronto (GT), la plus grande agglomération urbaine du Canada. Nous avons constaté que les émissions annuelles de méthane provenant des masses d'eau urbaines s'élevaient à 2 737 t/an de méthane, soit 26,4 % des émissions provenant de l'agriculture et des zones humides, et que les émissions provenant des REU s'élevaient à 9 122 t/an de méthane, soit plus de 10 % du budget total de méthane de la région du GT.

Nos résultats comblent plusieurs lacunes dans la quantification des émissions de méthane des sources nécessitant des mesures directes sur site, qui sont nécessaires pour améliorer les inventaires de gaz à effet de serre et guider l'élaboration de stratégies d'atténuation. Dans l'ensemble, des mesures à plusieurs échelles, y compris des mesures directes, sont nécessaires pour combler les lacunes des inventaires actuels et un meilleur partage des données peut réduire les limitations et les incertitudes actuelles.

Acknowledgements

I would like to express my sincere gratitude to my supervisor, Prof. Mary Kang, for her guidance and support. I am also grateful to Dr. Felix Vogel from Environment and Climate Change Canada and Dr. Peter Douglas of McGill University for their valuable assistance and collaboration in field research campaigns and the geochemical analysis of gas samples. I would like to thank my colleagues from the Subsurface Hydrology and Environmental Impact Analysis Research Group, especially Khalil El Hachem, Amara Regehr, and Louise Klotz for their assistance and guidance during field research, laboratory trials, and in writing research articles. My heartfelt thanks to Pinar Ozcer, Manager of the Environmental Engineering Laboratory, and John Bartczak, for their help in laboratory experiments, guidance on method development and logistics, and their valuable advice. I also wish to extend my thanks to the administrative staff of the Department of Civil Engineering who have guided me through this process. I am also indebted to my family and friends in the Maritimes for their constant support and understanding. Finally, I would like to deeply acknowledge the following funding agencies for supporting my research and without which this thesis would not have been possible: McGill Engineering Doctoral Award (MEDA), McGill Graduate Excellence Award, Natural Sciences and Engineering Research Council of Canada (NSERC), and Mitacs Accelerate programs.

Preface

In accordance with the “Guidelines for Thesis Preparation”, this thesis is presented in a manuscript-based format. A general introduction and literature review are presented in Chapters 1 and 2. Chapters 3-6 comprise of three published articles and one article currently under review in *Environmental Science & Technology*. The author of this thesis is the primary author of all the manuscripts. In the final Chapter 7, we present a general discussion of each of the research-based chapters in addition to the inherent limitations of this research and provide recommendations for both policy-makers and researchers. Below is a description of the efforts of each contributing author.

Williams, J. P., el Hachem, K., & Kang, M. (2023). Controlled release testing of the static chamber methodology for direct measurements of methane emissions. *Atmospheric Measurement Techniques Discussions*, 1-18.

Authors’ contributions: James P. Williams: Designed the study, conducted the experimental procedures, analyzed the results, and wrote the manuscript. Khalil El Hachem: Assisted with experimental procedure, helped with study design, and revised the manuscript. Mary Kang: Supervised the research, helped with the study design, and revised the manuscript.

Williams, J. P., Regehr, A., & Kang, M. (2020). Methane emissions from abandoned oil and gas wells in Canada and the United States. *Environmental science & technology*, 55(1), 563-570.

Authors' contributions: James P. Williams: Designed the study, organized and performed the field work, analyzed the results, and wrote the manuscript. Amara Regehr: Assisted with field work organization, performed field work in British Columbia, and revised the manuscript. Mary Kang: Supervised the research, helped with the study design, and revised the manuscript.

Williams, J. P., Ars, S., Vogel, F., Regehr, A., & Kang, M. (2022). Differentiating and Mitigating Methane Emissions from Fugitive Leaks from Natural Gas Distribution, Historic Landfills, and Manholes in Montréal, Canada. *Environmental Science & Technology*, 56(23), 16686-16694.

Authors' contributions: James P. Williams: Designed the study, organized and performed the field work, performed the geochemical analysis, analyzed the results, and wrote the manuscript. Sebastien Ars: Organized and performed mobile surveys in Montreal, helped edit the manuscript. Felix Vogel: Organized and performed mobile surveys in Montreal, helped edit the manuscript. Amara Regehr: Assisted with field work organization, performed field work in Montreal, and revised the manuscript. Mary Kang: Supervised the research, helped with the study design, and revised the manuscript.

Williams, J. P., Ars, S., Vogel, F., Gillespie, L., Klotz, L., Wunch, D., Fabien, A., and & Kang, M. (2023). Characterizing and quantifying methane emissions from wastewater collection systems and urban water bodies. To be submitted to the journal of *Science of the Total Environment* (in preparation)

Authors' contributions: James P. Williams: Designed the study, organized and performed the field work, performed the geochemical analysis, analyzed the results, and wrote the manuscript. Sebastien Ars: Organized and performed extensive mobile surveys in Montreal and Toronto, oversaw floating chamber sampling of urban water bodies in Toronto. Felix Vogel: Organized and performed extensive mobile surveys in Montreal and Toronto, oversaw floating chamber sampling of urban water bodies in Toronto. Lawson Gillespie: Assisted with field work organization, helped

organize controlled release testing in Toronto, and revised the manuscript. Louise Klotz: Assisted with field work organization, performed field work in Toronto, assisted with geochemical analysis and laboratory work, revised the manuscript. Mary Kang: Supervised the research, helped with the study design, and revised the manuscript.

Chapter 1

Introduction

1.1 Introduction

Anthropogenic methane emissions have been identified as a strategically integral mitigation target to meet both long-term and short-term climate neutrality goals such as those outlined in the Paris Agreement. Methane is a potent greenhouse gas (GHG) with a global warming potential 84-87 times stronger than CO₂ over a 20-year period (IPCC, 2022). Global concentrations of methane have been rising (Nisbet et al., 2019) without a clear consensus on the relative contributions from specific anthropogenic sources and/or sectors (Turner et al., 2019). Generally, methane measurement data is used to calculate annual methane emissions by multiplying average methane emission rates (i.e., emission factors) by total site counts (i.e., activity data) (Calvo Buendia et al., 2019). Furthermore, the methodological guidelines provided by the Intergovernmental Panel on Climate Change highlight the importance of using country-specific emission factors for emissions estimates. Even within a country, substantial regional variations have been observed. In an effort to quantify methane emissions and identify targets for mitigation, there have been multiple studies published in the past few decades that have quantified methane emissions from different sectors, across a wide range of spatio-temporal scales, and using a variety of different methodologies (National Academies of Sciences, Engineering, and Medicine and others, 2018). These methodologies

all offer their own strengths and disadvantages, which depend on the characteristics of the methane sources.

Methane emissions are quantified using a range of different methods which can be classified, in general, as either indirect or direct measurement methods (National Academies of Sciences, Engineering, and Medicine and others, 2018). Most recent published literature has focused on testing indirect measurement methods (e.g., Robertson et al. (2017); Heltzel et al. (2020); Aubrey et al. (2013); Fox et al. (2019, 2021)). Fewer studies have tested and quantified the accuracy of direct measurement methods such as the static chamber method (Riddick et al., 2022; Pihlatie et al., 2013; Christiansen et al., 2011; Ravikumar et al., 2017). Indirect methods involve the quantification of methane emissions away from the source(s) of emissions, whereas direct methodologies involve the direct measurement of methane emissions from a source and then the extrapolation of those measurements over a larger population of sites (Vaughn et al., 2018). The advantages of indirect methods are that all methane emissions within the sampling footprint are measured giving a high probability of capturing super-emitting sites, that indirect methods have few logistical constraints such as site access requirements, and that a large number of sites can be measured rapidly relative to direct methods. The disadvantages of indirect measurements are higher limits of detection (≥ 10 g/hour) when compared to direct methods, lower accuracy in terms of quantification, and challenges in source attribution at the component/equipment (i.e., individual source) level (Fox et al., 2019). Alternatively, direct methane quantification methods are labour-intensive which restricts the amount of sites that can be measured, suffer logistical constraints such as site access requirements, and risk missing sources. However, direct measurement techniques offer higher quantification accuracy when compared to indirect methods, the ability to attribute methane emissions at the equipment/component level, and lower limits of detection. Accurate source attribution at the equipment/component level can be especially important for identifying specific discrepancies between measurements and greenhouse gas inventories (Rutherford et al., 2021). In addition, the lower limits of detection of direct methods is necessary for quantifying methane sources with relatively low emission factors.

There are two common findings throughout methane measurement studies; that methane inventories at municipal, regional, and national levels often underestimate methane emissions when compared to independent studies (de Foy et al., 2023; MacKay et al., 2021; Alvarez et al., 2018); and that methane emission rate distributions are heavily skewed, with a few high-emitting sources contributing the majority of cumulative methane emissions (Brandt et al., 2016). These high-emitting sites, often labeled as "super-emitters" (Zavala-Araiza et al., 2015) can emit methane at rates well above 10 kg/hour (Duren et al., 2019; Sherwin et al., 2023), making them well-suited for indirect measurement methods that cover large areas and have higher limits of detection. However, the emission rate threshold that defines a super-emitter will ultimately be constrained to the limit of detection of the measurement method, meaning that the contributions from diffuse lower-emitting sites can be overlooked despite contributing a significant percentage of cumulative methane emissions (Kunkel et al., 2023). As such, there is a need for measurements of methane emissions with higher sensitivities to low methane emission rates (i.e., ≤ 10 g/hour) to address the contributions of smaller diffuse methane sources.

The largest source of methane emissions in the United States (U.S.) and Canada is the energy sector, from which the majority of methane originates from fugitive leaks from oil and gas (O&G) systems (United States Environmental Protection Agency, 2021; Environment and Climate Change Canada, 2021). The importance of methane emissions from the O&G sector has been recognized through international commitments such as those made by Canada, the United States, and Mexico, towards methane reductions of 40-45% from the O&G sector from baseline 2012 levels to 2025 (Konschnik and Jordaan, 2018). As such, there have been multiple studies that have focused on quantifying methane emissions from the O&G sector, from production to distribution (MacKay et al., 2021; Alvarez et al., 2018; Weller et al., 2020; Zimmerle et al., 2015). Methane emissions from O&G production have been studied extensively (Alvarez et al., 2018; Festa-Bianchet et al., 2023; MacKay et al., 2021; Shen et al., 2022; Johnson et al., 2023; Omara et al., 2022) due to their high overall emissions relative to other parts of the O&G sector. However, recent studies have highlighted the substantial methane contributions of non-production-related sources in the O&G sector such as natural gas (NG) distribution systems (Weller et al., 2019, 2020; McKain et al.,

2015; Brandt et al., 2014). Another understudied source in the O&G sector is abandoned oil and gas (AOG) wells. Sites from both sources emit methane at relatively low levels compared to the O&G production sector, with emission factors ranging from 5-250 g/hour (Lamb et al., 2016; Kang et al., 2016; Townsend-Small et al., 2016). Despite lower emission factors, high activity counts in terms of the number of AOG wells, kilometers of primary and secondary distribution pipelines, and the number of NG meter-sets lead to substantial methane contributions from these sources.

Methane emissions from AOG wells were first included in the Canadian and U.S. GHG inventories in 2019 (United States Environmental Protection Agency, 2021; Environment and Climate Change Canada, 2021), and since their inclusion there have been multiple studies that have quantified methane emissions from AOG wells (Lebel et al., 2020; Riddick et al., 2019; Townsend-Small and Hoschouer, 2021; Williams et al., 2019; El Hachem and Kang, 2022; Bowman et al., 2022). For the Canadian inventory, several recent studies (Bowman et al., 2022; El Hachem and Kang, 2022) have been used to update the emission factors used for AOG wells (Environment and Climate Change Canada, 2023). However, the latest GHG inventory for the U.S. still uses data from two publications (Kang et al., 2016; Townsend-Small et al., 2016) to calculate their emission factors for AOG wells.

Methane emissions from NG distribution have long been included in national GHG inventories. However, there are multiple studies that have highlighted that inventories are likely underestimating methane emissions from this source category (Weller et al., 2020; McKain et al., 2015; Lamb et al., 2016; Ren et al., 2018; Plant et al., 2019). Notably, most of these studies have focused on NG distribution systems in the U.S., while few studies have targeted NG infrastructure in Canada (Hugenholtz et al., 2021; Ars et al., 2020; Brandt et al., 2014).

While methane emissions from O&G systems are major contributors of methane emissions in the U.S. and Canada, in cities and other regions, biogenic methane emissions from non-O&G sources in urban areas are increasingly being identified as major sources of methane emissions (Marcotullio et al., 2013; Floerchinger et al., 2021; Ars et al., 2020; Defratyka et al., 2021; Fernandez et al., 2022). Several urban measurement studies found that urban methane emissions were underestimated when compared to the respective cities methane inventories (Plant et al., 2022,

2019; McKain et al., 2015). Cambaliza et al. (2015) proposed that either poorly characterized emission sources or unidentified methane sources in urban centers are responsible for these observed discrepancies. A recent study using satellite remote sensing data by de Foy et al. (2023) found that methane emissions in urban areas across the world are underestimated by a factor of 3-4, with emission estimates from the study showing correlation with rates of untreated wastewater, a biogenic source. The contribution of methane emissions from wastewater collection systems has been highlighted in several studies as a dominant biogenic methane source in cities (Fernandez et al., 2022; Defratyka et al., 2021), but their methane emissions are not included in any GHG inventory. Furthermore, previous to Chapter 5 of this thesis, there has only been one study that has directly measured methane emissions from wastewater collection systems by directly measuring wastewater utility holes (WUHs) (Fries et al., 2018).

Another major biogenic methane source identified in cities are municipal solid waste landfills (Lamb et al., 2016; Ars et al., 2020; Cambaliza et al., 2015). While methane emissions from active landfill sites are well documented (Lohila et al., 2007; Ars et al., 2020; Mønster et al., 2019), methane emissions from historic landfills (i.e., landfills abandoned before adopting environmental regulations) are not included in any GHG inventory. There have been few studies in the past decades that have quantified methane emissions from historic landfills (Christophersen et al., 2001; Rachor et al., 2013; Whalen et al., 1990), and it is likely that the lack of environmental protection measures such as gas recovery systems and impermeable cover materials would lead to methane emissions (Lohila et al., 2007), despite the age of the waste material.

A final biogenic methane source that has been identified in cities is urban water bodies, and several studies have quantified their presence as a source of elevated methane emissions compared to natural water bodies (Herrero Ortega et al., 2019; Martinez-Cruz et al., 2017; Peacock et al., 2021). In North America, people residing in urban areas live on average 3.8 kilometers from a fresh water body (Kummu et al., 2011), implying that most cities contain urban water bodies. While the areal coverage and types of urban water bodies will differ among cities, it is important to assess whether their cumulative methane emissions are significant so that appropriate mitigation steps

can be considered. Notably, there are no direct measurement studies on urban water body methane emissions that have been conducted in Canada.

In order to properly plan and implement methane mitigation strategies, it is important that the methane emission contributions from different sources are well understood. The ability to resolve methane emissions data at the component/equipment level is important for mitigation, allowing for the calculation of cost-benefit analyses and aiding industries in identifying the exact sources of their methane emissions (Nisbet et al., 2020). The primary focus of this thesis is the quantification of methane emissions from low-emitting diffuse sources using direct measurement methods. Many of the methane sources we've highlighted contain little to no direct measurement data, and some are not included in any GHG inventory (i.e., historic landfills, WUHs, urban water bodies). Ultimately, this research will provide a better understanding of the exact source and methane emissions contributions for these low-emitting diffuse methane sources, which contributes to the international effort to measure, monitor, mitigate methane emissions, and complement indirect measurements.

1.2 Problem statement and hypotheses

Atmospheric concentrations of methane have been rising around the world, and methane inventories are consistently shown to underestimate methane emissions relative to measurement based studies. We hypothesized that a portion of the discrepancies observed in methane inventories and studies is due to contributions from low emitting methane sources with high activity data values, such as AOG wells, residential/customer NG meter-sets, WUHs, historic landfills, and urban water bodies. In this context, we tested the accuracy of the static chamber method (i.e. direct measurement method) for individual source measurements of methane emissions to quantify methane emission rates from low emitting sites. For these tests, we hypothesized that the overall accuracy of the static chamber method would be higher compared to other methods with appropriate selection of design parameters. All of the methane sources investigated here are either recent inclusions to GHG inventories that do not rely on the latest data (i.e. AOG wells), potential methane sources that have been identified but not included in GHG inventories (i.e., WUHs, historic landfills, urban

water bodies), or known methane sources that have been shown to be underestimated at municipal levels (i.e., NG distribution systems).

We hypothesized that direct measurements of methane emissions from AOG wells, WUHs, historic landfills, NG distribution networks, and urban water bodies, would all have low emission factors (i.e., ≤ 10 g/hour) but that their annual methane emissions will be significant at their respective spatial scales (i.e., national or municipal) due to high activity data values. We also hypothesized that the component/equipment level resolution offered by direct/individual source measurements would benefit methane mitigation efforts by revealing the specific sources of methane emissions.

1.3 Research objectives

The objectives of this research project were as follows:

a) To evaluate design parameters of the static chamber method as a direct methane quantification technique to accurately quantify methane emissions.

b) To compile published measurement data on methane emissions from AOG wells, and conduct new direct measurements from Oklahoma (U.S.) and British Columbia (Canada), determine AOG well counts for the U.S. and Canada, and estimate annual methane emissions from AOG wells for both countries.

c) To perform direct measurements of methane emissions from WUHs, historic, landfills, and NG distribution systems in Montreal (Canada), estimate annual contributions of methane from all three sources, geochemically characterize all three sources at the individual source level, and to perform cost-benefit analyses of methane mitigation strategies.

d) To conduct direct measurements of methane emissions from WUHs and urban water bodies in the Greater Toronto Area (Canada), analyze the temporal intermittence of high-emitting sites from both methane sources using mobile surveying data, and to estimate their annual methane emissions for the Greater Toronto Area.

1.4 Thesis organization

Following the introduction and literature review chapters, this thesis is structured into four chapters that describe novel research in the field of methane emissions quantification, followed by a discussion/conclusions chapter where the findings of this thesis are discussed further.

Chapter 3 analyzes the static chamber methodology we used for the direct measurements of component-level methane emissions performed during field campaigns presented in Chapters 4, 5, and 6. The research questions we sought to answer in this work were: (1) What are the current methane emission factor ranges for component-level sources and what methods (i.e., indirect and direct) have previously been tested through controlled releases of methane? (2) What is the overall methane flowrate quantification accuracy of the static chamber method? (3) How do physical factors (i.e., chamber shape, chamber volume) and leak properties (i.e., mass and volumetric flowrates) affect the accuracy of the static chamber method? To answer these questions, we compiled prior research articles that tested methane quantification methods using controlled releases of methane and categorized them by the tested flowrate ranges and by measurement platform. We analysed data on methane emission factors from the IPCC emission factor database and converted them to component-level emission factors across the waste, energy, and agriculture sectors. Finally, we performed a series of 64 controlled release experiments testing the static chamber method and varied the physical properties of the chamber and also the leak properties and analyzed their impacts on measurement accuracy.

Chapter 4 details the results of a compilation of individual source measurements of methane emissions and well counts from AOG wells across the U.S. and Canada, which includes our own measurements made from AOG wells in Oklahoma and British Columbia. The research questions we posed for this work were: (1) What are the methane emission factors for AOG wells in the U.S. and how do they vary by region, fluid type, and plugging status? (2) How many AOG wells are there in the U.S. and Canada? (3) How much methane do AOG wells emit annually in the U.S. and Canada? (4) How do those estimates of annual methane emissions compare with what is currently reported in national GHG inventories? We addressed these questions by gathering

data from research articles detailing individual source measurements of methane emissions from AOG wells and well counts from regional databases across the U.S. and Canada. We analyzed all individual source measurements, including our own, developed region-specific and attribute-specific emission factors across the U.S. and Canada, and estimated annual emissions under five different emission factor distribution scenarios.

Chapter 5 begins our analysis of methane emissions from urban areas in Canada and summarizes the results of multiple individual source measurement campaigns conducted in Montreal, Canada. Extending measurement and database analysis and emission estimation approaches from Chapters 3 and 4, we investigate the following research questions: (1) What are the methane emission rate characteristics for historic landfills, WUHs, and NG distribution systems in Montreal, Canada? (2) Are we able to geochemically distinguish between the different source types using ethane to methane ($C_2:C_1$) ratios, CO_2 concentrations, and/or $\delta^{13}C-CH_4$ signatures? (3) How do annual methane emissions from all three sources compare to Montreal's municipal GHG inventory? (4) How do mitigation options for all three methane sources compare in terms of costs, methane reductions, and mitigation technology readiness? We answered these questions by performing individual source measurements of methane emissions from all three sources over several years to gather both emission rate and geochemical data. We combined these measurements with activity data provided by the City of Montreal to determine annual estimates of methane emissions, analyzed geochemical data gathered from all sites, and used our annual emissions estimates to perform cost-benefit analyses of mitigation technologies.

Chapter 6 studies biogenic methane sources in urban areas in Canada that are not included in GHG inventories. The research questions we posed for this work were: (1) What are the methane emission rate profiles of WUHs and urban water bodies in the GTA? (2) Do methane emissions from high-emitting sites for each source category show seasonal intermittence? (3) What are annual methane emissions from each source and what are the relative contributions from source subcategories? (4) How do annual methane emissions from each source compare to inventoried methane sources in the GTA? To address these questions, we performed individual source measurements of methane emissions from WUHs and urban water bodies within the GTA using and

adapting methods developed in Chapters 3, 4, and 5. We estimated WUHs counts for the GTA from an empirical relationship between population counts and number of WUHs, and we found the total areal extent covered by urban water bodies within the GTA through geospatial data provided by Statistics Canada and the National Hydro Network. We analyzed data from repeat mobile surveys conducted over 4-5 years in the vicinity of two high-emitting sites to determine whether methane emissions persisted over seasons. We calculated annual methane emissions from WUHs and urban water bodies and further categorized them by source subcategories and compared their emissions to a bottom-up inventory for the GTA.

Chapter 7 provides a general discussion of the important findings of this thesis along with the associated limitations of this work, recommendations for policy-makers and researchers, and concluding remarks.

1.5 Contribution to original knowledge

Much of the recent published literature on anthropogenic methane emissions in the past decade has focused on indirect measurements and top-down inventory development with the majority of studies finding that methane inventories are underestimated at municipal, regional, and national levels (de Foy et al., 2023; McKain et al., 2015; Lamb et al., 2016; Gorchoy Negron et al., 2023; MacKay et al., 2021; Zavala-Araiza et al., 2018; Pétron et al., 2014; Alvarez et al., 2018). Despite this focus on methane quantification in literature, there have been a lack of direct methane measurement studies that offer the ability to quantify methane emission rates from low emitting sites at high spatial resolutions. At the inception of this work, we hypothesized individual source measurements would show that emissions from AOG wells, historic landfills, WUHs, NG distribution, and urban water bodies are all significant methane sources at their respective municipal or national levels despite all having relatively low methane emission factors. These hypotheses were investigated through field trials, measurement campaigns, and laboratory analysis which ultimately produced the following contributions to original knowledge.

a) We demonstrated the accuracy of the static chamber methodology in the direct quantification of methane emissions. The static chamber method has traditionally been tested and used for the quantification of trace gas emissions from soils, with few studies testing its ability to quantify methane emissions from more complex sources (e.g., O&G wells, NG distribution stations, landfill gas wells, etc) where the physical factors of the chamber and leakage properties of the source would differ from soil gas emissions. We quantified the accuracy of the static chamber method for these new settings and identified factors that influence accuracy.

b) We showed that annual methane emissions from AOG wells in Canada and the U.S. are underestimated in national inventories. Methane emissions from AOG wells were first included in national GHG inventories in the U.S. and Canada in 2019. However, only two studies were used to determine methane emission factors from AOG wells, with no measurements from Canada. We compiled available direct measurement studies on AOG well methane emissions and well counts, and conducted new measurements to fill gaps in Canada and the U.S. These data were used to estimate to provide annual emissions at national scales.

c) We found that methane emissions from historic landfills and WUHs are major methane sources in Montreal, and identified several potential low-cost mitigation options. Urban areas have been identified as significant methane sources in literature, however there have been no direct methane measurements conducted from cities in Canada. We quantified methane emissions from historic landfills and WUHs which are not included in any GHG inventory, and utilized data gathered from our individual source measurements to perform a cost-benefit analysis of methane emissions from NG distribution, historic landfills, and WUHs.

d) We showed that emissions from high-emitting WUHs and urban water bodies were persistent throughout multiple seasons, and found that methane emissions from both sources are significant contributors to total methane emissions in the GTA. Methane emissions from WUHs and urban water bodies have been identified as potential methane sources in several studies despite not being included in any greenhouse gas inventory. We directly measured methane emissions from both sources in the GTA, we assessed their emissions intermittence using extensive

mobile surveying data spanning 4-5 years, and we estimated their annual contributions to methane emissions from the GTA.

Bibliography

- Alvarez, R. A., Zavala-Araiza, D., Lyon, D. R., Allen, D. T., Barkley, Z. R., Brandt, A. R., Davis, K. J., Herndon, S. C., Jacob, D. J., Karion, A., et al.: Assessment of methane emissions from the US oil and gas supply chain, *Science*, 361, 186–188, 2018.
- Ars, S., Vogel, F., Arrowsmith, C., Heerah, S., Knuckey, E., Lavoie, J., Lee, C., Pak, N. M., Phillips, J. L., and Wunch, D.: Investigation of the spatial distribution of methane sources in the Greater Toronto Area using mobile gas monitoring systems, *Environmental Science & Technology*, 54, 15 671–15 679, 2020.
- Aubrey, A., Thorpe, A., Christensen, L., Dinardo, S., Frankenberg, C., Rahn, T., and Dubey, M.: Demonstration of Technologies for Remote and in Situ Sensing of Atmospheric Methane Abundances-a Controlled Release Experiment, in: *AGU Fall Meeting Abstracts*, vol. 2013, pp. A44E–05, 2013.
- Bowman, L. V., El Hachem, K., Aljabre, O., and Kang, M.: Methane Emissions from Abandoned and Suspended Oil and Gas Wells in Alberta and Saskatchewan, *GeoConvention*, pp. p–4, 2022.
- Brandt, A. R., Heath, G., Kort, E., O’Sullivan, F., Pétron, G., Jordaan, S. M., Tans, P., Wilcox, J., Gopstein, A., Arent, D., and Wofsy, S.: Methane leaks from North American natural gas systems, *Science*, 343, 733–735, 2014.
- Brandt, A. R., Heath, G. A., and Cooley, D.: Methane leaks from natural gas systems follow extreme distributions, *Environmental science & technology*, 50, 12 512–12 520, 2016.
- Calvo Buendia, E., Tanabe, K., Kranjc, A., Jamsranjav, B., Fukuda, M., Ngarize, S., Osako, A., Pyrozhenko, Y., Shermanau, P., and Federici, S.: 2019 Refinement to the 2006 IPCC Guidelines for National Greenhouse Gas Inventories, 2019.
- Cambaliza, M. O., Shepson, P., Bogner, J., Caulton, D., Stirm, B., Sweeney, C., Montzka, S., Gurney, K., Spokas, K., Salmon, O., et al.: Quantification and source apportionment of the methane emission flux from the city of IndianapolisMethane emission flux from the city of Indianapolis, *Elementa: Science of the Anthropocene*, 3, 2015.
- Christiansen, J. R., Korhonen, J. F., Juszczak, R., Giebels, M., and Pihlatie, M.: Assessing the effects of chamber placement, manual sampling and headspace mixing on CH₄ fluxes in a laboratory experiment, *Plant and soil*, 343, 171–185, 2011.
- Christophersen, M., Kjeldsen, P., Holst, H., and Chanton, J.: Lateral gas transport in soil adjacent to an old landfill: factors governing emissions and methane oxidation, *Waste Management & Research*, 19, 595–612, 2001.
- de Foy, B., Schauer, J. J., Lorente, A., and Borsdorff, T.: Investigating high methane emissions from urban areas detected by TROPOMI and their association with untreated wastewater, *Environmental Research Letters*, 2023.

- Defratyka, S. M., Paris, J.-D., Yver-Kwok, C., Fernandez, J. M., Korben, P., and Bousquet, P.: Mapping urban methane sources in Paris, France, *Environmental science & technology*, 55, 8583–8591, 2021.
- Duren, R. M., Thorpe, A. K., Foster, K. T., Rafiq, T., Hopkins, F. M., Yadav, V., Bue, B. D., Thompson, D. R., Conley, S., Colombi, N. K., et al.: California’s methane super-emitters, *Nature*, 575, 180–184, 2019.
- El Hachem, K. and Kang, M.: Methane and hydrogen sulfide emissions from abandoned, active, and marginally producing oil and gas wells in Ontario, Canada, *Science of The Total Environment*, 823, 153 491, 2022.
- Environment and Climate Change Canada: National Inventory Report 1990-2019: Greenhouse Gas Sources and Sinks in Canada, 2021.
- Environment and Climate Change Canada: National Inventory Report 1990-2021: Greenhouse Gas Sources and Sinks in Canada, 2023.
- Fernandez, J., Maazallahi, H., France, J., Menoud, M., Corbu, M., Ardelean, M., Calcan, A., Townsend-Small, A., van der Veen, C., Fisher, R., et al.: Street-level methane emissions of Bucharest, Romania and the dominance of urban wastewater., *Atmospheric Environment: X*, 13, 100 153, 2022.
- Festa-Bianchet, S. A., Tyner, D. R., Seymour, S. P., and Johnson, M. R.: Methane Venting at Cold Heavy Oil Production with Sand (CHOPS) Facilities Is Significantly Underreported and Led by High-Emitting Wells with Low or Negative Value, *Environmental Science & Technology*, 57, 3021–3030, 2023.
- Floerchinger, C., Shepson, P. B., Hajny, K., Daube, B. C., Stirm, B. H., Sweeney, C., and Wofsy, S. C.: Relative flux measurements of biogenic and natural gas-derived methane for seven US cities, *Elementa: Science of the Anthropocene*, 9, 2021.
- Fox, T. A., Barchyn, T. E., Risk, D., Ravikumar, A. P., and Hugenholtz, C. H.: A review of close-range and screening technologies for mitigating fugitive methane emissions in upstream oil and gas, *Environmental Research Letters*, 14, 053 002, 2019.
- Fox, T. A., Hugenholtz, C. H., Barchyn, T. E., Gough, T. R., Gao, M., and Staples, M.: Can new mobile technologies enable fugitive methane reductions from the oil and gas industry?, *Environmental Research Letters*, 16, 064 077, 2021.
- Fries, A. E., Schiffman, L. A., Shuster, W. D., and Townsend-Small, A.: Street-level emissions of methane and nitrous oxide from the wastewater collection system in Cincinnati, Ohio, *Environmental Pollution*, 236, 247–256, 2018.
- Gorchov Negron, A. M., Kort, E. A., Chen, Y., Brandt, A. R., Smith, M. L., Plant, G., Ayasse, A. K., Schwietzke, S., Zavala-Araiza, D., Hausman, C., et al.: Excess methane emissions from shallow water platforms elevate the carbon intensity of US Gulf of Mexico oil and gas production, *Proceedings of the National Academy of Sciences*, 120, e2215275 120, 2023.

- Heltzel, R. S., Zaki, M. T., Gebreslase, A. K., Abdul-Aziz, O. I., and Johnson, D. R.: Continuous OTM 33A analysis of controlled releases of methane with various time periods, data rates and wind filters, *Environments*, 7, 65, 2020.
- Herrero Ortega, S., Romero González-Quijano, C., Casper, P., Singer, G. A., and Gessner, M. O.: Methane emissions from contrasting urban freshwaters: Rates, drivers, and a whole-city footprint, *Global change biology*, 25, 4234–4243, 2019.
- Hugenholtz, C. H., Vollrath, C., Gough, T., Wearmouth, C., Fox, T., Barchyn, T., and Billingham, C.: Methane emissions from above-ground natural gas distribution facilities in the urban environment: A fence line methodology and case study in Calgary, Alberta, Canada, *Journal of the Air & Waste Management Association*, 71, 1319–1332, 2021.
- IPCC: Climate Change 2022: Mitigation of Climate Change. Contribution of Working Group III to the Sixth Assessment Report of the Intergovernmental Panel on Climate Change, Cambridge University Press, Cambridge, UK and New York, NY, USA, <https://doi.org/10.1017/9781009157926>, https://www.ipcc.ch/report/ar6/wg3/downloads/report/IPCC_AR6_WGIII_FullReport.pdf, 2022.
- Johnson, M. R., Tyner, D. R., and Conrad, B. M.: Origins of Oil and Gas Sector Methane Emissions: On-Site Investigations of Aerial Measured Sources, *Environmental Science & Technology*, 57, 2484–2494, 2023.
- Kang, M., Christian, S., Celia, M. A., Mauzerall, D. L., Bill, M., Miller, A. R., Chen, Y., Conrad, M. E., Darrah, T. H., and Jackson, R. B.: Identification and characterization of high methane-emitting abandoned oil and gas wells, *Proceedings of the National Academy of Sciences*, 113, 13 636–13 641, 2016.
- Konschnik, K. and Jordaan, S. M.: Reducing fugitive methane emissions from the North American oil and gas sector: a proposed science-policy framework, *Climate Policy*, 18, 1133–1151, 2018.
- Kummu, M., De Moel, H., Ward, P. J., and Varis, O.: How close do we live to water? A global analysis of population distance to freshwater bodies, *PloS one*, 6, e20 578, 2011.
- Kunkel, W., Thorpe, M., Carre-Burritt, A., Aivazian, G., Snow, N., Harris, J., Mueller, T., and Roos, P.: Extension of Methane Emission Rate Distribution for Permian Basin Oil and Gas Production Infrastructure by Aerial LiDAR, 2023.
- Lamb, B. K., Cambaliza, M. O., Davis, K. J., Edburg, S. L., Ferrara, T. W., Floerchinger, C., Heimburger, A. M., Herndon, S., Lauvaux, T., Lavoie, T., and Lyon, D.: Direct and indirect measurements and modeling of methane emissions in Indianapolis, Indiana, *Environmental Science & Technology*, 50, 8910–8917, 2016.
- Lebel, E. D., Lu, H. S., Vielstadte, L., Kang, M., Banner, P., Fischer, M. L., and Jackson, R. B.: Methane emissions from abandoned oil and gas wells in California, *Environmental Science & Technology*, 54, 14 617–14 626, 2020.

- Lohila, A., Laurila, T., Tuovinen, J.-P., Aurela, M., Hatakka, J., Thum, T., Pihlatie, M., Rinne, J., and Vesala, T.: Micrometeorological measurements of methane and carbon dioxide fluxes at a municipal landfill, *Environmental science & technology*, 41, 2717–2722, 2007.
- MacKay, K., Lavoie, M., Bourlon, E., Atherton, E., O’Connell, E., Baillie, J., Fougère, C., and Risk, D.: Methane emissions from upstream oil and gas production in Canada are underestimated, *Scientific reports*, 11, 1–8, 2021.
- Marcotullio, P. J., Sarzynski, A., Albrecht, J., Schulz, N., and Garcia, J.: The geography of global urban greenhouse gas emissions: An exploratory analysis, *Climatic Change*, 121, 621–634, 2013.
- Martinez-Cruz, K., Gonzalez-Valencia, R., Sepulveda-Jauregui, A., Plascencia-Hernandez, F., Belmonte-Izquierdo, Y., and Thalasso, F.: Methane emission from aquatic ecosystems of Mexico City, *Aquatic Sciences*, 79, 159–169, 2017.
- McKain, K., Down, A., Raciti, S. M., Budney, J., Hutyra, L. R., Floerchinger, C., Herndon, S. C., Nehr Korn, T., Zahniser, M. S., Jackson, R. B., and Phillips, N.: Methane emissions from natural gas infrastructure and use in the urban region of Boston, Massachusetts, *Proceedings of the National Academy of Sciences*, 112, 1941–1946, 2015.
- Mønster, J., Kjeldsen, P., and Scheutz, C.: Methodologies for measuring fugitive methane emissions from landfills—A review, *Waste Management*, 87, 835–859, 2019.
- National Academies of Sciences, Engineering, and Medicine and others: Improving characterization of anthropogenic methane emissions in the United States, National Academies Press, 2018.
- Nisbet, E., Fisher, R., Lowry, D., France, J., Allen, G., Bakkaloglu, S., Broderick, T., Cain, M., Coleman, M., Fernandez, J., and Forster, G.: Methane mitigation: Methods to reduce emissions, on the path to the Paris Agreement, *Reviews of Geophysics*, 58, e2019RG000675, 2020.
- Nisbet, E. G., Manning, M., Dlugokencky, E., Fisher, R., Lowry, D., Michel, S., Myhre, C. L., Platt, S. M., Allen, G., Bousquet, P., et al.: Very strong atmospheric methane growth in the 4 years 2014–2017: Implications for the Paris Agreement, *Global Biogeochemical Cycles*, 33, 318–342, 2019.
- Omara, M., Zavala-Araiza, D., Lyon, D. R., Hmiel, B., Roberts, K. A., and Hamburg, S. P.: Methane emissions from US low production oil and natural gas well sites, *Nature Communications*, 13, 2085, 2022.
- Peacock, M., Audet, J., Bastviken, D., Cook, S., Evans, C., Grinham, A., Holgerson, M., Högbom, L., Pickard, A., Zieliński, P., et al.: Small artificial waterbodies are widespread and persistent emitters of methane and carbon dioxide, *Global Change Biology*, 27, 5109–5123, 2021.
- Pétron, G., Karion, A., Sweeney, C., Miller, B. R., Montzka, S. A., Frost, G. J., Trainer, M., Tans, P., Andrews, A., Kofler, J., et al.: A new look at methane and nonmethane hydrocarbon emissions from oil and natural gas operations in the Colorado Denver-Julesburg Basin, *Journal of Geophysical Research: Atmospheres*, 119, 6836–6852, 2014.

- Pihlatie, M. K., Christiansen, J. R., Aaltonen, H., Korhonen, J. F., Nordbo, A., Rasilo, T., Benanti, G., Giebels, M., Helmy, M., Sheehy, J., et al.: Comparison of static chambers to measure CH₄ emissions from soils, *Agricultural and forest meteorology*, 171, 124–136, 2013.
- Plant, G., Kort, E. A., Floerchinger, C., Gvakharia, A., Vimont, I., and Sweeney, C.: Large fugitive methane emissions from urban centers along the US East Coast, *Geophysical research letters*, 46, 8500–8507, 2019.
- Plant, G., Kort, E. A., Murray, L. T., Maasackers, J. D., and Aben, I.: Evaluating urban methane emissions from space using TROPOMI methane and carbon monoxide observations, *Remote Sensing of Environment*, 268, 112756, 2022.
- Rachor, I., Gebert, J., Gröngroft, A., and Pfeiffer, E.-M.: Variability of methane emissions from an old landfill over different time-scales, *European Journal of Soil Science*, 64, 16–26, 2013.
- Ravikumar, A. P., Wang, J., and Brandt, A. R.: Are optical gas imaging technologies effective for methane leak detection?, *Environmental science & technology*, 51, 718–724, 2017.
- Ren, X., Salmon, O. E., Hansford, J. R., Ahn, D., Hall, D., Benish, S. E., Stratton, P. R., He, H., Sahu, S., Grimes, C., et al.: Methane emissions from the Baltimore-Washington area based on airborne observations: Comparison to emissions inventories, *Journal of Geophysical Research: Atmospheres*, 123, 8869–8882, 2018.
- Riddick, S. N., Mauzerall, D. L., Celia, M. A., Kang, M., Bressler, K., Chu, C., and Gum, C. D.: Measuring methane emissions from abandoned and active oil and gas wells in West Virginia, *Science of the Total Environment*, 651, 1849–1856, 2019.
- Riddick, S. N., Ancona, R., Mbua, M., Bell, C. S., Duggan, A., Vaughn, T. L., Bennett, K., and Zimmerle, D. J.: A quantitative comparison of methods used to measure smaller methane emissions typically observed from superannuated oil and gas infrastructure, *Atmospheric Measurement Techniques*, 15, 6285–6296, 2022.
- Robertson, A. M., Edie, R., Snare, D., Soltis, J., Field, R. A., Burkhart, M. D., Bell, C. S., Zimmerle, D., and Murphy, S. M.: Variation in methane emission rates from well pads in four oil and gas basins with contrasting production volumes and compositions, *Environmental science & technology*, 51, 8832–8840, 2017.
- Rutherford, J. S., Sherwin, E. D., Ravikumar, A. P., Heath, G. A., Englander, J., Cooley, D., Lyon, D., Omara, M., Langfitt, Q., and Brandt, A. R.: Closing the methane gap in US oil and natural gas production emissions inventories, *Nature communications*, 12, 4715, 2021.
- Shen, L., Gautam, R., Omara, M., Zavala-Araiza, D., Maasackers, J. D., Scarpelli, T. R., Lorente, A., Lyon, D., Sheng, J., Varon, D. J., et al.: Satellite quantification of oil and natural gas methane emissions in the US and Canada including contributions from individual basins, *Atmospheric Chemistry and Physics*, 22, 11203–11215, 2022.
- Sherwin, E., Rutherford, J., Zhang, Z., Chen, Y., Wetherley, E., Yakovlev, P., Berman, E., Jones, B., Thorpe, A., Ayasse, A., et al.: Quantifying oil and natural gas system emissions using one million aerial site measurements, 2023.

- Townsend-Small, A. and Hoschouer, J.: Direct measurements from shut-in and other abandoned wells in the Permian Basin of Texas indicate some wells are a major source of methane emissions and produced water, *Environmental Research Letters*, 16, 054 081, 2021.
- Townsend-Small, A., Ferrara, T. W., Lyon, D. R., Fries, A. E., and Lamb, B. K.: Emissions of coalbed and natural gas methane from abandoned oil and gas wells in the United States, *Geophysical Research Letters*, 43, 2283–2290, 2016.
- Turner, A. J., Frankenberg, C., and Kort, E. A.: Interpreting contemporary trends in atmospheric methane, *Proceedings of the National Academy of Sciences*, 116, 2805–2813, 2019.
- United States Environmental Protection Agency: Inventory of U.S. Greenhouse Gas Emissions and Sinks 1990-2019, 2021.
- Vaughn, T. L., Bell, C. S., Pickering, C. K., Schwietzke, S., Heath, G. A., Pétron, G., Zimmerle, D. J., Schnell, R. C., and Nummedal, D.: Temporal variability largely explains top-down/bottom-up difference in methane emission estimates from a natural gas production region, *Proceedings of the National Academy of Sciences*, 115, 11 712–11 717, 2018.
- Weller, Z. D., Yang, D. K., and von Fischer, J. C.: An open source algorithm to detect natural gas leaks from mobile methane survey data, *PLoS One*, 14, e0212 287, 2019.
- Weller, Z. D., Hamburg, S. P., and von Fischer, J. C.: A national estimate of methane leakage from pipeline mains in natural gas local distribution systems, *Environmental science & technology*, 54, 8958–8967, 2020.
- Whalen, S., Reeburgh, W., and Sandbeck, K.: Rapid methane oxidation in a landfill cover soil, *Applied and environmental microbiology*, 56, 3405–3411, 1990.
- Williams, J. P., Risk, D., Marshall, A., Nickerson, N., Martell, A., Creelman, C., Grace, M., and Wach, G.: Methane emissions from abandoned coal and oil and gas developments in New Brunswick and Nova Scotia, *Environmental monitoring and assessment*, 191, 1–12, 2019.
- Zavala-Araiza, D., Lyon, D., Alvarez, R. A., Palacios, V., Harriss, R., Lan, X., Talbot, R., and Hamburg, S. P.: Toward a functional definition of methane super-emitters: Application to natural gas production sites, *Environmental science & technology*, 49, 8167–8174, 2015.
- Zavala-Araiza, D., Herndon, S. C., Roscioli, J. R., Yacovitch, T. I., Johnson, M. R., Tyner, D. R., Omara, M., and Knighton, B.: Methane emissions from oil and gas production sites in Alberta, Canada, *Elementa: Science of the Anthropocene*, 6, 2018.
- Zimmerle, D. J., Williams, L. L., Vaughn, T. L., Quinn, C., Subramanian, R., Duggan, G. P., Willson, B., Opsomer, J. D., Marchese, A. J., Martinez, D. M., et al.: Methane emissions from the natural gas transmission and storage system in the United States, *Environmental science & technology*, 49, 9374–9383, 2015.

Chapter 2

Literature Review

2.1 Methane measurement methods

To track progress towards meeting these national methane reduction targets, many countries catalog and categorize their methane emissions on an annual basis in their respective national greenhouse gas inventory reports (United States Environmental Protection Agency, 2021; Environment and Climate Change Canada, 2021). Methane inventories are ultimately based on measurements of methane emissions, which can take a variety of different forms that span different spatial and temporal scales. It is important that these different methods are well understood in terms of quantification accuracy, limits of detection, and applications so that the appropriate method, or combinations of methods (Fox et al., 2019), can be selected.

Currently, the technologies utilized by different quantification methods measure methane emissions either through imaging spectrometry or through laser spectroscopy (Fox et al., 2019). Both technologies provide methane concentration data that can either be used directly to quantify methane emission rates (e.g., static chamber method, optical gas imaging cameras), or indirectly (e.g., mass-balance aircraft surveys, Light detection and ranging). The definitions of what constitutes a direct or indirect measurement method can vary depending on the source and environment being measured, so for the sake of consistency we will define all direct methods as measurements taking

place within 5 meters of the methane source, and all indirect methods as measurements taking place at distance greater than 5 meters from the source.

2.1.1 Indirect methods

Different methane measurement platforms quantify emissions over a range of different spatial scales. In order of ascending scale, methane measurement platforms quantify emissions at: component, equipment, site, facility, continental, or global level resolutions. Indirect measurement platforms quantify methane emissions using measurements performed away from the source of emissions, and are generally restricted to site-level scales at the lowest (Johnson et al., 2023; MacKay et al., 2021; Allen, 2014). In general, indirect measurement methane measurement platforms include satellite retrievals (de Foy et al., 2023; Ayasse et al., 2019; Sherwin et al., 2023), crewed aircraft-based measurements (Johnson et al., 2023), uncrewed aircraft-based (UAV) measurements (Barchyn et al., 2017), tower-based observations (Peltola et al., 2019; Lamb et al., 2016), and vehicle-based measurement platforms (MacKay et al., 2021; Ars et al., 2020).

Satellite retrievals can be classified into two general groups: area flux mappers and point source imagers (Jacob et al., 2022). Nearly all satellite platforms measure spectrally resolved backscattered solar radiation in the shortwave infrared (SWIR) to quantify methane emissions in air columns. Pixel sizes (i.e., resolution) for area flux mappers range from 130 x 400 m² (i.e., MethaneSAT, expected 2023 launch) to 7.5 x 7.5 km² (i.e., TROPOMI), whereas the resolution for point source imagers ranges from 3.7 x 3.7 m² (i.e., WorldView-3) to 30 x 30 m² (i.e., Landsat 8). Currently, the minimum detection limit for point source imagers is around 100 kg/hour of methane (Gauthier, 2021). The most recent study on the quantification accuracy of satellite retrievals found that GHGSat's targeted system (i.e., point source imager) quantified a controlled leak of 200 kg/hour with an accuracy of $\pm 13\%$ (Sherwin et al., 2023).

Aircraft-based measurement platforms utilize either on-board greenhouse gas analyzers to measure methane concentrations within the air and calculate methane emissions using techniques such as mass balance methods (Lavoie et al., 2015; Baray et al., 2018), and/or gas mapping systems

such as Gas Mapping LiDAR (Johnson et al., 2023; Conrad et al., 2023) or Airborne Visible Infrared Imaging Spectrometer - Next Generation (AVIRIS-NG) (Thorpe et al., 2016) to visualize and quantify methane emissions. The minimum methane emission rate detection threshold for aircraft-based platforms is roughly 0.6-2.3 kg/hour (Thorpe et al., 2016; Johnson et al., 2023). Johnson et al. (2023) list the quantification accuracy of the Gas Mapping LiDAR after multiple passes to be -46/+54% (or roughly $\pm 50\%$).

UAV-based sampling platforms typically utilize embedded or suspended laser methane detectors (Iwaszenko et al., 2021) to measure the density of methane concentrations within a column of air (e.g., ppm per meter), but there are also applications with optical gas imaging (OGI) systems as well (Titchener et al., 2022). Currently, the minimum detection threshold for UAV-based sampling platforms is around 50-100 g/hour (Smith et al., 2017; Fox et al., 2019). In a controlled release blind trial performed in Cardington (United Kingdom), Allen et al. (2017) found that for methane flowrates of 5 and 10 kg/hour, the standard error of quantification for a UAV-based sampling platform was $\pm 6\%$. A broader quantification accuracy was reported by Fox et al. (2019) to be 25-55% for a distance of 10 meters from the source.

Stationary tower measurement platforms vary from systems such as eddy covariance towers (Peltola et al., 2019) to tower networks spanning entire regions (Lamb et al., 2016; Barkley et al., 2022). In principle, stationary tower measurements utilize point-in-space measurements with detailed weather data to perform inversions of ambient methane concentrations to the measured footprint of the tower, which can range from m^2 (Lohila et al., 2007) to 100's of km^2 (Monteiro et al., 2022; Barkley et al., 2022). A controlled release study by Titchener et al. (2022) found that a stationary single photon LiDAR gas imager was able to detect methane emissions as low as 42 g/hour with a quantification accuracy of $\pm 50\%$.

Vehicle-based measurement platforms utilize on-board GHG analyzers to measure methane concentrations while traversing through methane plumes emitted from upwind sources (Ars et al., 2020; Fernandez et al., 2022; von Fischer et al., 2017), or by parking downwind of a source and utilizing detailed wind direction data to estimate the methane flowrates. Methane emission rates

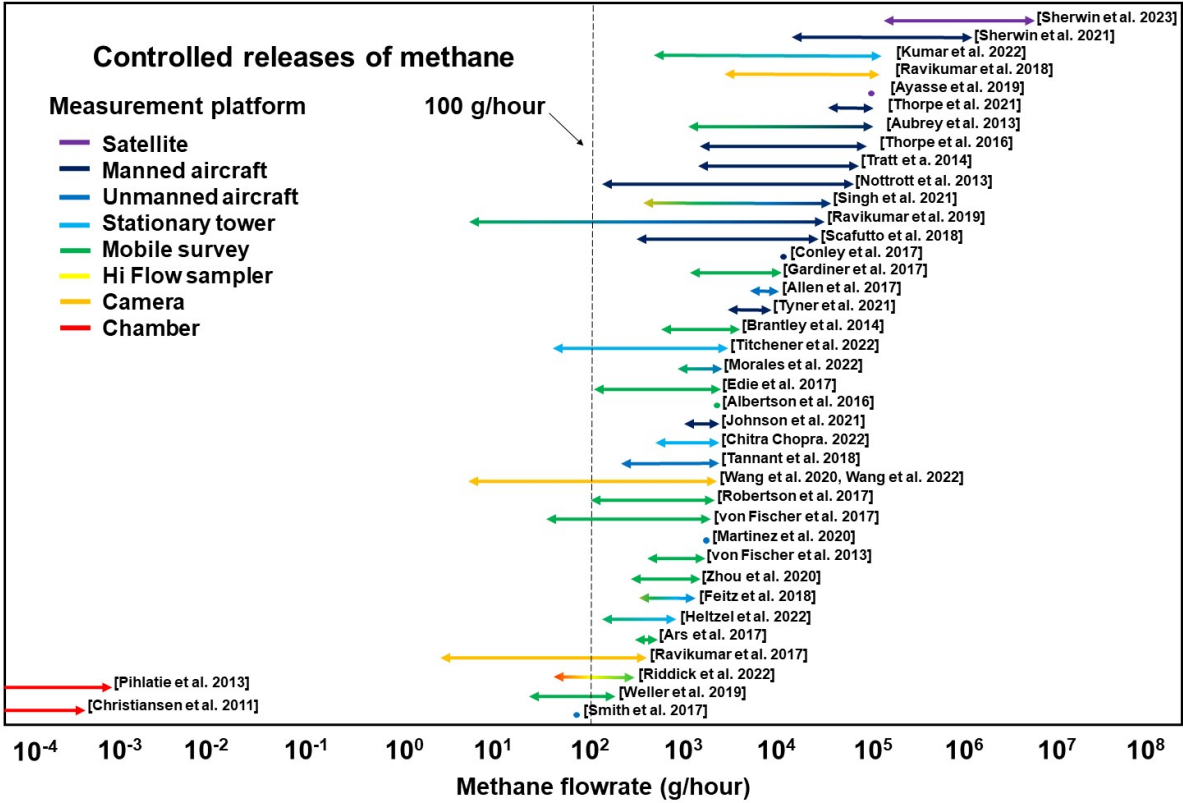


Figure 2.1: Summary of methane controlled release tests showing the range of methane flowrates tested and the type of measurement platform.

are typically quantified using inverse modelling approaches such as the inverse Gaussian approach (Ars et al., 2020), but can also be quantified from empirical equations developed through controlled release testing by von Fischer et al. (2017) and Weller et al. (2019) for proximal (i.e., ≤ 100 meters) on-road methane sources, or by tracer releases (Fox et al., 2019). The minimum detection limit for mobile survey based platforms rests at around 5-50 g/hour, albeit the detection limits vary depending on proximity to the methane source and weather conditions. Based on several controlled release experiments that have been conducted to quantify the accuracy of the mobile surveying method (Figure 2.1) (Kumar et al., 2022; von Fischer et al., 2017; Weller et al., 2019; Atherton et al., 2017) the quantification accuracy of the mobile surveying method after multiple passes is around $\pm 20-40\%$ but varies depending on multiple factors such as the emission rate, distance from the source, wind speed, among others.

2.1.2 Direct methods

Direct measurement methodologies quantify methane emissions directly from the source of emissions, which greatly reduces the uncertainty related to source attribution (Allen, 2014). Whereas indirect measurement platforms are restricted to site/facility/regional level resolution, direct methods are able to resolve methane emissions at the component/equipment level. Direct methods include point-source measurements using mass flow meters (Allen et al., 2015), OGI cameras (Ravikumar et al., 2018), direct methane measurement devices such as the Hi-Flow sampler (Connolly et al., 2019), or chamber-based methodologies (Pihlatie et al., 2013; Christiansen et al., 2011; Kang et al., 2014; Lebel et al., 2020).

Point-source measurements through mass flow meters involve attaching the instrument inlet directly to an emitting component, usually related to the O&G sector (Howard, 2015). There are challenges with using instruments such as mass flow meters to quantify methane emissions from sources other than NG-related infrastructure. Methane emissions can be dispersed over areas in many cases (Lohila et al., 2007; Herrero Ortega et al., 2019), or emitted from a component not easily connected to a flow-measuring device.

Optical gas imaging (OGI) cameras such as Forward Looking InfraRed (FLIR) produce two-dimensional thermal images of methane emissions which can then be used as either a leak versus no-leak qualification, or translated to methane emission rates in post processing using techniques such as machine learning (Wang et al., 2022, 2020). The current limit of detection for FLIR-camera based OGI cameras is around 20 g/hour (Ravikumar et al., 2018), and the quantification accuracy of OGI cameras varies from $\pm 3\%$ to $\pm 15\%$ depending on the distance from the source (Wang et al., 2020; Fox et al., 2019).

The Hi-Flow sampler has been available commercially (e.g., Bacharach Hi Flow Sampler, HETEK Flow Sampler), and functions by utilizing an intake with a high volumetric flow to sample a suspected leak enclosed by analyzer attachments to quantify emissions (Connolly et al., 2019). All models of the Hi-Flow sampler perform repeat measurements of methane flowrates using a two-stage measurement process by drawing in sample air to the methane detection sensor at two

different volumetric flowrates (Connolly et al., 2019). Notably, multiple studies have highlighted malfunctions within earlier versions of the instrument, primarily leading towards the underestimation of methane flowrates (Connolly et al., 2019; Howard et al., 2015; Howard, 2015). The limit of detection of the HETEK Hi-Flow sampler is listed as 18.3 g/hour of methane (Klotz, 2023). Recent studies on the measurement accuracy of Hi-Flow samplers found the accuracy of the Bacharach Hi Flow Sampler to be -18% and the HETEK Flow Sampler to be -27%.

Chamber-based methodologies can be classified into two categories: dynamic chambers and static chambers (Heinemeyer and McNamara, 2011). Both methods are based on physically enclosing a potential methane source within a known chamber volume and measuring methane concentrations or other trace gases within the chamber either continuously or intermittently. For the dynamic chamber method, pumps are used to provide a constant inflow and an outflow at equal volumetric rates through the chamber (Riddick et al., 2022). For the static chamber method, no pumps are used but a vent tube is installed on the chamber to prevent pressure build-up within the chamber. The lower detection limit of chamber-based methods is below 1 mg/hour, which is low compared to other methods. Chamber-based methods are routinely used to measure trace gas emissions from various land-cover types (Heinemeyer and McNamara, 2011; Rochette et al., 1992; Moore and Roulet, 1991) where emission rates are often much lower than those encountered in anthropogenic settings.

2.1.3 Methane source attribution and geochemistry

The ability to distinguish the source of methane emissions is a factor that compliments all methane measurement methods. While most direct methods facilitate source identification through visually identifying the emitting source, indirect methods face more challenges when it comes to source attribution. For some aerial-based measurement platforms, sources can be identified by observing the origin of a plume with complimentary site-level imagery and follow-up ground-based observations (Johnson et al., 2023). For mobile surveys, the source of emissions can be inferred from repeated survey passes in different weather conditions which allows for the triangulation of a source lo-

cation (Ars et al., 2020). These types of visual attribution methods are effective when potential methane sources are isolated, but are challenging in more logistically complex environments with multiple co-located sources such as urban environments.

Geochemical attribution involves the measurement of gases or gas signatures to infer the source of methane emissions, either through the elimination or confirmation of potential sources. Common gases used for the geochemical attribution of methane emissions are CO₂, CO, and ethane. Ratios of CO₂ to methane are used to identify sources emitting methane without corresponding CO₂ emissions (Atherton et al., 2017; Ars et al., 2020), and are useful for identifying NG-related sources unrelated to combustion emissions. Biogenic sources produce methane through anaerobic digestion, which is a process that produces methane and carbon dioxide simultaneously (Yu and Schanbacher, 2010). In contrast, leaks from NG distribution systems contain little CO₂, although NG combustion is an important CO₂ source (Balcombe et al., 2018). The presence, or lack of, CO allows for the identification of whether a methane source is attributable to pyrogenic sources related to fuel combustion (Ars et al., 2020) or biomass burning (Koppmann et al., 2005). Ethane is a widely-used gas for the identification of fossil fuel related methane emissions (Sherwood et al., 2017), and is used in several top-down studies (Zimmerle et al., 2022; McKain et al., 2015; Yacovitch et al., 2015; Schwietzke et al., 2014; Plant et al., 2019). Stable and radioactive isotopes are also a common method used for geochemical attribution (Lowry et al., 2001; Townsend-Small et al., 2012; Chamberlain et al., 2016). Both the stable isotope of carbon and hydrogen in methane (i.e., $\delta C^{13}\text{-CH}_4$, $\delta H^2\text{-CH}_4$) are used either individually, or in tandem, to infer whether a methane source is biogenic (i.e., bacterial), thermogenic, atmospheric, pyrogenic, or a mixture of multiple sources (Whiticar, 1999; Schoell, 1980, 1988). In addition, "clumped" isotopes in methane (i.e., the presence of one or more H² substitutions and C¹³ in a methane molecule) are also used in some cases and are posited to provide more detailed source attribution information (Douglas et al., 2017). Finally, radiocarbon (C¹⁴) measurements of methane can also provide information on the source of emissions by carbon dating the emitted methane to determine whether it originated from an older (e.g., fossil fuel related) or younger (e.g., bacterial) source.

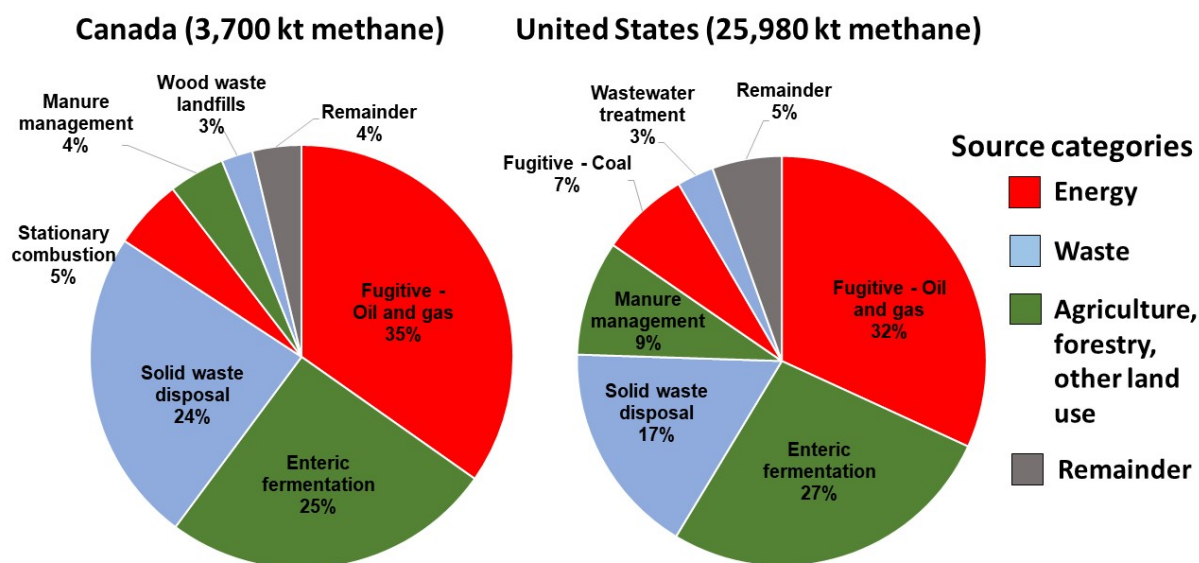


Figure 2.2: Pie charts of annual methane emissions from Canada and the U.S. in 2021 categorized according to the major sectors and sub-sectors in each countries inventory (United States Environmental Protection Agency, 2021; Environment and Climate Change Canada, 2023).

2.2 Methane sources: emission inventories

In Canada and the U.S., the three largest methane sources are the energy, waste, and the agriculture, forestry, and other land-use (AFOLU) sector, which collectively account for 96% and 95% of the countries annual methane emissions in 2021 (Figure 2.2) (United States Environmental Protection Agency, 2021; Environment and Climate Change Canada, 2021). In order to materialize these methane reductions, it is critical that the specific sources in all of these sectors are well-documented and quantified so that targets for mitigation can be identified.

2.2.1 Energy

The energy sector is the main source of methane emissions in both the Canadian and U.S. national inventories, being responsible for 41% and 42% of the countries' methane inventories, respectively (Environment and Climate Change Canada, 2021; United States Environmental Protection

Agency, 2021). The energy sector has several categories and subcategories of methane emissions sources, but all methane emissions from the energy sector can be broadly categorized as either transportation (e.g., gas powered heavy duty vehicles Clark et al. (2017)), stationary combustion (e.g., petrochemical industries (Ragothaman and Anderson, 2017)), and fugitive emissions (e.g., leaks from natural gas infrastructure (Schwietzke et al., 2014)). While both the transportation and stationary combustion sectors are major contributors of greenhouse gases to the atmosphere through emissions of CO₂, fugitive emissions are the major source of methane emissions for both Canada and the U.S. and are the primary focus in this thesis for methane emissions from the energy sector.

The term "fugitive" in fugitive emissions is generally meant to encompass all released methane from the O&G supply chain, whether the releases are intentional (e.g., liquid unloadings from storage tanks (Johnson et al., 2023)) or unintentional (e.g., leaking AOG wells (Kang et al., 2014, 2016; Townsend-Small et al., 2016; Townsend-Small and Hoschouer, 2021; El Hachem and Kang, 2022)), although the specific definition varies depending on the country (United States Environmental Protection Agency, 2021; Environment and Climate Change Canada, 2023). Fugitive emissions occur at all stages of the O&G sector which comprise exploration, production, transmission, processing, storage, refining, distribution, and beyond-the-meter emissions. The production sector in particular has been identified as an area with large discrepancies between what is reported in national inventories and measurement-based studies. Multiple indirect measurement studies based in the U.S. have estimated that methane emissions from the production sector are more than double what is currently reported (Alvarez et al., 2018; Shen et al., 2022), with similar results in Canada (MacKay et al., 2021; Johnson et al., 2023; Shen et al., 2022; Festa-Bianchet et al., 2023). Other categories such as methane emissions from AOG wells and NG distribution systems are also potentially large methane sources given their larger activity data counts and likely to be underestimated.

There are millions of AOG wells in Canada and the U.S. (Kang et al., 2016), much higher than the $\geq 100,000$ and $\geq 800,000$ active production sites in Canada and the U.S respectively (MacKay et al., 2021; Omara et al., 2022). Since the initial study that quantified methane emissions from

AOG wells by Kang et al. (2014), there have been multiple measurement studies conducted in Canada and the U.S. that have measured methane emissions from AOG wells (El Hachem and Kang, 2022; Lebel et al., 2020; Townsend-Small and Hoschouer, 2021; Townsend-Small et al., 2016; Pekney et al., 2018; Riddick et al., 2019; Bowman et al., 2022; Williams et al., 2019). With the exception of Lebel et al. (2020), all of these measurement studies utilized direct measurement methods, likely due to the low emission rates encountered from AOG well sites. Emission factors for different AOG well classifications varied from 0 g/hour for plugged wells in the eastern U.S. (Townsend-Small et al., 2016) to 75 g/hour for unplugged gas wells in non-coal regions (Kang et al., 2016). Almost all studies identified two key attributes that influenced methane emission rates: well plugging status and geographic area. A recent literature review study on factors that affect AOG well leakage by El Hachem and Kang (2023) supported the findings of these measurement studies. In terms of mitigation, Kang et al. (2019) performed a cost-benefit analysis of five mitigation options for AOG wells, three of which involve well plugging, and two that either flare or capture and utilize emitted gas. The costs in Kang et al. (2019) rely on methane emission rates derived from available data, which can change with new measurements.

Methane emissions from NG distribution systems have also been shown to emit methane at greater levels than what is currently reported in GHG inventories (Weller et al., 2020; McKain et al., 2015; Brandt et al., 2014). The NG distribution sector comprises all of equipment/facilities related to the distribution of NG, and is considerably larger, more complex, and logistically difficult to measure when compared to any other sector of the NG supply chain (Weller et al., 2020). Most of the studies that have measured methane emissions from NG distribution have been conducted in the U.S. (Lamb et al., 2015; Weller et al., 2020; Hendrick et al., 2016; McKain et al., 2015; Phillips et al., 2013), with only one in Canada (Ars et al., 2020). Among these studies, most utilized indirect measurement methods through mobile ground-based measurements (Weller et al., 2020; Ars et al., 2020; Phillips et al., 2013) or stationary tower observations (McKain et al., 2015), with two utilizing direct measurement methods (Lamb et al., 2015; Hendrick et al., 2016). The primary focus for most of these studies has been methane emissions from NG distribution pipelines

(Weller et al., 2020; Ars et al., 2020; Phillips et al., 2013), with the exception of Lamb et al. (2015) who also quantified leaks from metering and regulating stations. NG distribution infrastructure is complex, with multiple sites present in cities that regulate, monitor, and meter NG flow through extensive networks of primary and secondary distribution pipelines (Clearstone Engineering Ltd., 2020). An omission from all studies are methane emissions from consumer meters, or residential NG meters-sets (McKain et al., 2015). Furthermore, large leaks from distribution pipelines are often repaired within days of being reported by local NG distribution companies (Clearstone Engineering Ltd., 2020), meaning that measurement based studies that present a snapshot of methane emissions in time (Ars et al., 2020; Phillips et al., 2013; Hendrick et al., 2016; Lamb et al., 2015; Weller et al., 2020) could potentially miss these sporadic, but large, methane emissions sources. A notable exception in literature would be McKain et al. (2015) who note this limitation and address it through long-term monitoring using stationary tower networks in Boston, MA. Some mitigation options for NG distribution emissions are the implementation of leak detection and repair (LDAR) programs, where technicians visit sites at a regular frequency and perform methane screening to determine the location of leaks from the site and then perform repairs on the leaking components. Other mitigation options include the replacement of pneumatic devices to either low-bleed devices or air-based pneumatics through the installation of air compressors on-site (Limits, 2014; Methane Guiding Principles, 2019).

2.2.2 Waste

The waste sector is the third largest source of methane emissions in both Canada and the U.S., and is responsible for 20% and 27% of total methane emissions, respectively (Figure 2.1) (United States Environmental Protection Agency, 2021; Environment and Climate Change Canada, 2023). Solid waste disposal landfills are the main source of methane emissions from the waste sector in both countries. Methane is produced at solid waste landfills through the decomposition of organic matter through methanogenesis, and emitted from the areal cover of the landfill (Bogner et al., 1997; Lohila et al., 2007), and/or from biogas recovery systems (Themelis and Ulloa, 2007). The

majority of methane emissions from landfills in Canada and the U.S. occur from municipal solid waste landfills (Scarpelli et al., 2022; Maasackers et al., 2016), and the dominant materials contributing to methane formation are the decomposition of paper, food, and yard and garden waste. Municipal solid waste landfills have been measured in multiple studies in Canada and the U.S. (Ars et al., 2020; Mohsen et al., 2020; Mosher et al., 1999; Goldsmith Jr et al., 2012), with the majority focusing on active and managed landfills. In contrast, there have been few studies that have quantified methane emissions from older landfill sites (Christophersen et al., 2001; Rachor et al., 2013) despite the potential risks caused by poorer landfill management practices in the past (Brand et al., 2018) (e.g., lack of leachate and gas collection systems). Methane emissions from historical landfill sites are not included in any GHG inventory, and given the large contributions of methane emissions observed from active landfill sites, the emissions from historical landfill sites are likely significant as well.

Among the challenges associated with measuring historical landfill sites, one of the largest would be locating and defining both the waste material and areal extents of these sites (Reynolds and Taylor, 1996). The City of Montreal is unique in that it has developed open-access maps of historical landfill sites within the city (Ville de Montréal, 2022). The siting of historical landfill sites in Montreal presents a key opportunity to gather measurement data to address the lack of measurements from historical landfill sites in Canada, and more broadly the lack of any measurement data.

After solid waste landfills, methane emissions from wastewater treatment are the next highest methane source from the waste sector. Methane emissions from wastewater treatment originate from various stages of the wastewater treatment process such as anaerobic digesters, stabilization ponds, activated sludge systems, and wastewater collection systems (Song et al., 2023). Notably, the IPCC guidelines list the methane correction factors for closed flowing sewers as zero (Calvo Buendia et al., 2019), meaning that no methane emissions are assumed to originate from closed flowing sewers. For methane emissions from the wastewater treatment sector, almost all studies have focused on emissions from the wastewater treatment plant itself (Daelman et al., 2012;

Wang et al., 2011; Czepiel et al., 1993; Hwang et al., 2016), with few measurements from wastewater collection systems (Fries et al., 2018; Defratyka et al., 2021; Fernandez et al., 2022). Among the studies that have measured methane emissions from wastewater collection systems, the only study utilizing direct measurements (Fries et al., 2018) found relatively small methane emission rates from 80 WUHs in Indianapolis (U.S.) ranging from 0 to 12 mg/hour of methane per WUH. A study based in Bucharest, Romania, by Fernandez et al. (2022) utilizing mobile surveys estimated that methane emissions from WUHs accounted 58-63% of the cities total methane budget, and another mobile survey based study by Defratyka et al. (2021) in Paris estimated that methane from the municipal wastewater network accounted for 33% of the cities methane budget. In addition, a recent study utilizing satellite retrievals by de Foy et al. (2023) found that cities across the world underestimate their methane inventories, and that the observed discrepancies positively correlate with levels of untreated wastewater.

Wastewater collection networks are complex systems in urban environments that can be categorized by industrial or domestic wastewater, separated or combined sewer systems, storm water versus sanitary sewers, and by rising mains or gravity drains (El-Fadel and Massoud, 2001; Song et al., 2023). Among the few studies that have measured methane emissions from wastewater collection systems, only Fries et al. (2018) was able to separate different types of WUHs in their measured emission rate data, but none distinguished different types of WUHs in their activity data. With the high counts of WUHs in most cities (e.g., 84,000 estimated for the city of Indianapolis by Fries et al. (2018)), it is important that both emission factors and activity data reflect the heterogeneity of wastewater collection systems and are considered in order to develop realistic methane emissions estimates.

2.2.3 Agriculture, forestry, and other land-use

Methane emissions from the AFOLU sector are the second highest methane source in Canada and the U.S. accounting for 29% and 36% of the countries respective total methane budget (United States Environmental Protection Agency, 2021; Environment and Climate Change Canada, 2021).

Methane emissions from the AFOLU sector occur primarily from enteric fermentation, with a smaller percentage attributed to manure management (Figure 2.3). For enteric fermentation, methane is generated in the intestinal system of ruminants and released primarily through exhalation and eructation (Fong et al., 2014). For manure management, methane emissions are released from containment units for large quantities of manure, with higher methane emissions from poorly aerated management systems (Environment and Climate Change Canada, 2023; Lopez-Real and Baptista, 1996). Over 95% of methane emissions from enteric fermentation and manure management in the U.S. and Canada originate from dairy and non-dairy cattle (Boadi et al., 2004). Aside from agriculture, smaller levels of methane are emitted from forestry and other land-use. Methane emissions from forestry and other-land use are highest for forest lands which occurs primarily in the form of forest fires (United States Environmental Protection Agency, 2021; Environment and Climate Change Canada, 2021). Methane emissions from the AFOLU sector are one of the most uncertain sources in GHG inventories (National Academies of Sciences, Engineering, and Medicine and others, 2018).

In addition to the inherent uncertainty in the recognized methane sources within the AFOLU sector, there are also methane sources that are not currently included in GHG inventories. Multiple studies have flagged inland water bodies, especially in urban areas, as significant sources of methane to the atmosphere (Herrero Ortega et al., 2019; Peacock et al., 2021; Martinez-Cruz et al., 2017; Aben et al., 2017). Methane emissions from urban water bodies occur as either diffusion through the water-to-air interface, or in the form of ebullition where bubbles of gas generated at the bottom of the water body travel to the surface (Herrero Ortega et al., 2019). Several factors unique to urban water bodies can lead to increased methane emissions which include shallower depths that limit methane oxidation through the water column (Herrero Ortega et al., 2019; Holgerson, 2015), increased catchment and retention of organic material from modified geomorphologies (Walsh et al., 2005), and increased influx of organic material from sources such as wastewater overflows and storm water drainage (Walsh et al., 2005; Ars et al., 2020). Among the studies that have quantified methane emissions from urban water bodies, most have utilized some form of direct

measurements in the form of floating chambers to directly quantify fluxes from urban water bodies (Herrero Ortega et al., 2019; Wang et al., 2022; Martinez-Cruz et al., 2017; Peacock et al., 2021). In terms of the differences in total flux contributions from ebullition and diffusion, ebullition appears to be the main contributor representing roughly 3-5 times the fluxes contributed by diffusion (Herrero Ortega et al., 2019). With regards to flux rates among water body types in boreal or temperate climates, ponds have the highest emission factors ranging from 100-500 mg CH₄ m⁻² day⁻¹ (Herrero Ortega et al., 2019) with the exception of more heavily modified water bodies such as a dammed section of river in China which had an emission factor of over 2,000 mg CH₄ m⁻² day⁻¹ (He et al., 2018). Despite higher emission factors, total methane emissions from ponds and heavily modified urban water bodies are generally lower than urban water body types that have large areal covers, such as lakes (Herrero Ortega et al., 2019).

Bibliography

- Aben, R. C., Barros, N., Van Donk, E., Frenken, T., Hilt, S., Kazanjian, G., Lamers, L. P., Peeters, E. T., Roelofs, J. G., de Senerpont Domis, L. N., et al.: Cross continental increase in methane ebullition under climate change, *Nature communications*, 8, 1682, 2017.
- Allen, D. T.: Methane emissions from natural gas production and use: reconciling bottom-up and top-down measurements, *Current Opinion in Chemical Engineering*, 5, 78–83, 2014.
- Allen, D. T., Pacsi, A. P., Sullivan, D. W., Zavala-Araiza, D., Harrison, M., Keen, K., Fraser, M. P., Daniel Hill, A., Sawyer, R. F., and Seinfeld, J. H.: Methane emissions from process equipment at natural gas production sites in the United States: Pneumatic controllers, *Environmental science & technology*, 49, 633–640, 2015.
- Allen, G., Shah, A., Williams, P. I., Ricketts, H., Hollingsworth, P., Kabbabe, K., Bourn, M., Pitt, J. R., Helmore, J., Lowry, D., et al.: The development and validation of an unmanned aerial system (UAS) for the measurement of methane flux, in: *AGU Fall Meeting Abstracts*, vol. 2017, pp. A44F–05, 2017.
- Alvarez, R. A., Zavala-Araiza, D., Lyon, D. R., Allen, D. T., Barkley, Z. R., Brandt, A. R., Davis, K. J., Herndon, S. C., Jacob, D. J., Karion, A., et al.: Assessment of methane emissions from the US oil and gas supply chain, *Science*, 361, 186–188, 2018.
- Ars, S., Vogel, F., Arrowsmith, C., Heerah, S., Knuckey, E., Lavoie, J., Lee, C., Pak, N. M., Phillips, J. L., and Wunch, D.: Investigation of the spatial distribution of methane sources in the Greater Toronto Area using mobile gas monitoring systems, *Environmental Science & Technology*, 54, 15 671–15 679, 2020.
- Atherton, E., Risk, D., Fougère, C., Lavoie, M., Marshall, A., Werring, J., Williams, J. P., and Minions, C.: Mobile measurement of methane emissions from natural gas developments in north-eastern British Columbia, Canada, *Atmospheric Chemistry and Physics*, 17, 12 405–12 420, 2017.
- Ayasse, A. K., Dennison, P. E., Foote, M., Thorpe, A. K., Joshi, S., Green, R. O., Duren, R. M., Thompson, D. R., and Roberts, D. A.: Methane mapping with future satellite imaging spectrometers, *Remote Sensing*, 11, 3054, 2019.
- Balcombe, P., Brandon, N., and Hawkes, A.: Characterising the distribution of methane and carbon dioxide emissions from the natural gas supply chain, *Journal of Cleaner Production*, 172, 2019–2032, 2018.
- Baray, S., Darlington, A., Gordon, M., Hayden, K. L., Leithead, A., Li, S.-M., Liu, P. S., Mittermeier, R. L., Moussa, S. G., O'Brien, J., et al.: Quantification of methane sources in the Athabasca Oil Sands Region of Alberta by aircraft mass balance, *Atmospheric Chemistry and Physics*, 18, 7361–7378, 2018.
- Barchyn, T. E., Hugenholtz, C. H., Myshak, S., and Bauer, J.: A UAV-based system for detecting natural gas leaks, *Journal of Unmanned Vehicle Systems*, 6, 18–30, 2017.

- Barkley, Z., Davis, K., Miles, N., Richardson, S., Deng, A., Hmiel, B., Lyon, D., and Lauvaux, T.: Quantification of Oil and Gas Methane Emissions in the Delaware and Marcellus Basins Using a Network of Continuous Tower-Based Measurements, *Atmospheric Chemistry and Physics Discussions*, pp. 1–25, 2022.
- Boadi, D., Wittenberg, K., Scott, S., Burton, D., Buckley, K., Small, J., and Ominski, K.: Effect of low and high forage diet on enteric and manure pack greenhouse gas emissions from a feedlot, *Canadian Journal of Animal Science*, 84, 445–453, 2004.
- Bogner, J., Meadows, M., and Czepiel, P.: Fluxes of methane between landfills and the atmosphere: natural and engineered controls, *Soil use and management*, 13, 268–277, 1997.
- Bowman, L. V., El Hachem, K., Aljabre, O., and Kang, M.: Methane Emissions from Abandoned and Suspended Oil and Gas Wells in Alberta and Saskatchewan, *GeoConvention*, pp. p–4, 2022.
- Brand, J. H., Spencer, K. L., O’shea, F. T., and Lindsay, J. E.: Potential pollution risks of historic landfills on low-lying coasts and estuaries, *Wiley Interdisciplinary Reviews: Water*, 5, e1264, 2018.
- Brandt, A. R., Heath, G., Kort, E., O’Sullivan, F., Pétron, G., Jordaan, S. M., Tans, P., Wilcox, J., Gopstein, A., Arent, D., and Wofsy, S.: Methane leaks from North American natural gas systems, *Science*, 343, 733–735, 2014.
- Calvo Buendia, E., Tanabe, K., Kranjc, A., Jamsranjav, B., Fukuda, M., Ngarize, S., Osako, A., Pyrozhenko, Y., Shermanau, P., and Federici, S.: 2019 Refinement to the 2006 IPCC Guidelines for National Greenhouse Gas Inventories, 2019.
- Chamberlain, S. D., Ingraffea, A. R., and Sparks, J. P.: Sourcing methane and carbon dioxide emissions from a small city: Influence of natural gas leakage and combustion, *Environmental pollution*, 218, 102–110, 2016.
- Christiansen, J. R., Korhonen, J. F., Juszczak, R., Giebels, M., and Pihlatie, M.: Assessing the effects of chamber placement, manual sampling and headspace mixing on CH₄ fluxes in a laboratory experiment, *Plant and soil*, 343, 171–185, 2011.
- Christophersen, M., Kjeldsen, P., Holst, H., and Chanton, J.: Lateral gas transport in soil adjacent to an old landfill: factors governing emissions and methane oxidation, *Waste Management & Research*, 19, 595–612, 2001.
- Clark, N. N., McKain, D. L., Johnson, D. R., Wayne, W. S., Li, H., Akkerman, V., Sandoval, C., Covington, A. N., Mongold, R. A., Hailer, J. T., et al.: Pump-to-wheels methane emissions from the heavy-duty transportation sector, *Environmental science & technology*, 51, 968–976, 2017.
- Clearstone Engineering Ltd.: Estimation of Air Emissions from the Canadian Natural Gas Transmission, Storage and Distribution System, 2020.
- Connolly, J., Robinson, R., and Gardiner, T.: Assessment of the Bacharach Hi Flow® Sampler characteristics and potential failure modes when measuring methane emissions, *Measurement*, 145, 226–233, 2019.

- Conrad, B. M., Tyner, D. R., and Johnson, M. R.: Robust probabilities of detection and quantification uncertainty for aerial methane detection: Examples for three airborne technologies, *Remote Sensing of Environment*, 288, 113 499, 2023.
- Czepiel, P. M., Crill, P. M., and Harriss, R. C.: Methane emissions from municipal wastewater treatment processes, *Environmental science & technology*, 27, 2472–2477, 1993.
- Daelman, M. R., van Voorthuizen, E. M., van Dongen, U. G., Volcke, E. I., and van Loosdrecht, M. C.: Methane emission during municipal wastewater treatment, *Water research*, 46, 3657–3670, 2012.
- de Foy, B., Schauer, J. J., Lorente, A., and Borsdorff, T.: Investigating high methane emissions from urban areas detected by TROPOMI and their association with untreated wastewater, *Environmental Research Letters*, 2023.
- Defratyka, S. M., Paris, J.-D., Yver-Kwok, C., Fernandez, J. M., Korben, P., and Bousquet, P.: Mapping urban methane sources in Paris, France, *Environmental science & technology*, 55, 8583–8591, 2021.
- Douglas, P. M., Stolper, D. A., Eiler, J. M., Sessions, A. L., Lawson, M., Shuai, Y., Bishop, A., Podlaha, O. G., Ferreira, A. A., Neto, E. V. S., et al.: Methane clumped isotopes: Progress and potential for a new isotopic tracer, *Organic Geochemistry*, 113, 262–282, 2017.
- El-Fadel, M. and Massoud, M.: Methane emissions from wastewater management, *Environmental pollution*, 114, 177–185, 2001.
- El Hachem, K. and Kang, M.: Methane and hydrogen sulfide emissions from abandoned, active, and marginally producing oil and gas wells in Ontario, Canada, *Science of The Total Environment*, 823, 153 491, 2022.
- El Hachem, K. and Kang, M.: Reducing oil and gas well leakage: a review of leakage drivers, methane detection and repair options., *Environmental Research: Infrastructure and Sustainability*, 2023.
- Environment and Climate Change Canada: National Inventory Report 1990-2019: Greenhouse Gas Sources and Sinks in Canada, 2021.
- Environment and Climate Change Canada: National Inventory Report 1990-2021: Greenhouse Gas Sources and Sinks in Canada, 2023.
- Fernandez, J., Maazallahi, H., France, J., Menoud, M., Corbu, M., Ardelean, M., Calcan, A., Townsend-Small, A., van der Veen, C., Fisher, R., et al.: Street-level methane emissions of Bucharest, Romania and the dominance of urban wastewater., *Atmospheric Environment: X*, 13, 100 153, 2022.
- Festa-Bianchet, S. A., Tyner, D. R., Seymour, S. P., and Johnson, M. R.: Methane Venting at Cold Heavy Oil Production with Sand (CHOPS) Facilities Is Significantly Underreported and Led by High-Emitting Wells with Low or Negative Value, *Environmental Science & Technology*, 57, 3021–3030, 2023.

- Fong, Wee Kean Sotos, M., Schultz, S., Deng-Beck, C., Marques, A., and Doust, M.: Global protocol for community-scale greenhouse gas emission inventories, 2014.
- Fox, T. A., Barchyn, T. E., Risk, D., Ravikumar, A. P., and Hugenholtz, C. H.: A review of close-range and screening technologies for mitigating fugitive methane emissions in upstream oil and gas, *Environmental Research Letters*, 14, 053 002, 2019.
- Fries, A. E., Schifman, L. A., Shuster, W. D., and Townsend-Small, A.: Street-level emissions of methane and nitrous oxide from the wastewater collection system in Cincinnati, Ohio, *Environmental Pollution*, 236, 247–256, 2018.
- Gauthier, J.-F.: The Importance of Matching Needs to Satellite System Capability when Monitoring Methane Emissions from Space, in: 2021 IEEE International Geoscience and Remote Sensing Symposium IGARSS, pp. 687–690, IEEE, 2021.
- Goldsmith Jr, C. D., Chanton, J., Abichou, T., Swan, N., Green, R., and Hater, G.: Methane emissions from 20 landfills across the United States using vertical radial plume mapping, *Journal of the Air & Waste Management Association*, 62, 183–197, 2012.
- He, B., He, J., Wang, J., Li, J., and Wang, F.: Characteristics of GHG flux from water-air interface along a reclaimed water intake area of the Chaobai River in Shunyi, Beijing, *Atmospheric Environment*, 172, 102–108, 2018.
- Heinemeyer, A. and McNamara, N. P.: Comparing the closed static versus the closed dynamic chamber flux methodology: Implications for soil respiration studies, *Plant and soil*, 346, 145–151, 2011.
- Hendrick, M. F., Ackley, R., Sanaie-Movahed, B., Tang, X., and Phillips, N. G.: Fugitive methane emissions from leak-prone natural gas distribution infrastructure in urban environments, *Environmental Pollution*, 213, 710–716, 2016.
- Herrero Ortega, S., Romero González-Quijano, C., Casper, P., Singer, G. A., and Gessner, M. O.: Methane emissions from contrasting urban freshwaters: Rates, drivers, and a whole-city footprint, *Global change biology*, 25, 4234–4243, 2019.
- Holgerson, M. A.: Drivers of carbon dioxide and methane supersaturation in small, temporary ponds, *Biogeochemistry*, 124, 305–318, 2015.
- Howard, T.: Comment on “Methane emissions from process equipment at natural gas production sites in the United States: Pneumatic controllers”, *Environmental Science & Technology*, 49, 3981–3982, 2015.
- Howard, T., Ferrara, T. W., and Townsend-Small, A.: Sensor transition failure in the high flow sampler: Implications for methane emission inventories of natural gas infrastructure, *Journal of the Air & Waste Management Association*, 65, 856–862, 2015.
- Hwang, K.-L., Bang, C.-H., and Zoh, K.-D.: Characteristics of methane and nitrous oxide emissions from the wastewater treatment plant, *Bioresource Technology*, 214, 881–884, 2016.

- Iwaszenko, S., Kalisz, P., Słota, M., and Rudzki, A.: Detection of natural gas leakages using a laser-based methane sensor and uav, *Remote Sensing*, 13, 510, 2021.
- Jacob, D. J., Varon, D. J., Cusworth, D. H., Dennison, P. E., Frankenberg, C., Gautam, R., Guanter, L., Kelley, J., McKeever, J., Ott, L. E., et al.: Quantifying methane emissions from the global scale down to point sources using satellite observations of atmospheric methane, *Atmospheric Chemistry and Physics*, 22, 9617–9646, 2022.
- Johnson, M. R., Tyner, D. R., and Conrad, B. M.: Origins of Oil and Gas Sector Methane Emissions: On-Site Investigations of Aerial Measured Sources, *Environmental Science & Technology*, 57, 2484–2494, 2023.
- Kang, M., Kanno, C. M., Reid, M. C., Zhang, X., Mauzerall, D. L., Celia, M. A., Chen, Y., and Onstott, T. C.: Direct measurements of methane emissions from abandoned oil and gas wells in Pennsylvania, *Proceedings of the National Academy of Sciences*, 111, 18 173–18 177, 2014.
- Kang, M., Christian, S., Celia, M. A., Mauzerall, D. L., Bill, M., Miller, A. R., Chen, Y., Conrad, M. E., Darrah, T. H., and Jackson, R. B.: Identification and characterization of high methane-emitting abandoned oil and gas wells, *Proceedings of the National Academy of Sciences*, 113, 13 636–13 641, 2016.
- Kang, M., Dong, Y., Liu, Y., Williams, J. P., Douglas, P. M., and McKenzie, J. M.: Potential increase in oil and gas well leakage due to earthquakes, *Environmental Research Communications*, 1, 121 004, 2019.
- Klotz, L.: Methane Emissions and Environmental Impacts of Oil and Gas Systems: Post-meter natural gas systems and well sites in northern regions, 2023.
- Koppmann, R., Von Czapiewski, K., and Reid, J.: A review of biomass burning emissions, part I: gaseous emissions of carbon monoxide, methane, volatile organic compounds, and nitrogen containing compounds, *Atmospheric chemistry and physics discussions*, 5, 10 455–10 516, 2005.
- Kumar, P., Broquet, G., Caldow, C., Laurent, O., Gichuki, S., Cropley, F., Yver-Kwok, C., Fontanier, B., Lauvaux, T., Ramonet, M., et al.: Near-field atmospheric inversions for the localization and quantification of controlled methane releases using stationary and mobile measurements, *Quarterly Journal of the Royal Meteorological Society*, 148, 1886–1912, 2022.
- Lamb, B. K., Edburg, S. L., Ferrara, T. W., Howard, T., Harrison, M. R., Kolb, C. E., Townsend-Small, A., Dyck, W., Possolo, A., and Whetstone, J. R.: Direct measurements show decreasing methane emissions from natural gas local distribution systems in the United States, *Environmental Science & Technology*, 49, 5161–5169, 2015.
- Lamb, B. K., Cambaliza, M. O., Davis, K. J., Edburg, S. L., Ferrara, T. W., Floerchinger, C., Heimbürger, A. M., Herndon, S., Lauvaux, T., Lavoie, T., and Lyon, D.: Direct and indirect measurements and modeling of methane emissions in Indianapolis, Indiana, *Environmental Science & Technology*, 50, 8910–8917, 2016.

- Lavoie, T. N., Shepson, P. B., Cambaliza, M. O., Stirr, B. H., Karion, A., Sweeney, C., Yacovitch, T. I., Herndon, S. C., Lan, X., and Lyon, D.: Aircraft-based measurements of point source methane emissions in the Barnett Shale basin, *Environmental science & technology*, 49, 7904–7913, 2015.
- Lebel, E. D., Lu, H. S., Vielstadte, L., Kang, M., Banner, P., Fischer, M. L., and Jackson, R. B.: Methane emissions from abandoned oil and gas wells in California, *Environmental Science & Technology*, 54, 14 617–14 626, 2020.
- Limits, C.: Quantifying Cost-effectiveness of Systematic Leak Detection and Repair Programs Using Infrared Cameras - CL report CL-13-27, Tech. rep., https://www.carbonlimits.no/wp-content/uploads/2015/06/Carbon_Limits_LDAR.pdf, 2014.
- Lohila, A., Laurila, T., Tuovinen, J.-P., Aurela, M., Hatakka, J., Thum, T., Pihlatie, M., Rinne, J., and Vesala, T.: Micrometeorological measurements of methane and carbon dioxide fluxes at a municipal landfill, *Environmental science & technology*, 41, 2717–2722, 2007.
- Lopez-Real, J. and Baptista, M.: A preliminary comparative study of three manure composting systems and their influence on process parameters and methane emissions, *Compost Science & Utilization*, 4, 71–82, 1996.
- Lowry, D., Holmes, C. W., Rata, N. D., O'Brien, P., and Nisbet, E. G.: London methane emissions: Use of diurnal changes in concentration and $\delta^{13}\text{C}$ to identify urban sources and verify inventories, *Journal of Geophysical Research: Atmospheres*, 106, 7427–7448, 2001.
- Maasackers, J. D., Jacob, D. J., Sulprizio, M. P., Turner, A. J., Weitz, M., Wirth, T., Hight, C., DeFigueiredo, M., Desai, M., Schmeltz, R., et al.: Gridded national inventory of US methane emissions, *Environmental science & technology*, 50, 13 123–13 133, 2016.
- MacKay, K., Lavoie, M., Bourlon, E., Atherton, E., O'Connell, E., Baillie, J., Fougère, C., and Risk, D.: Methane emissions from upstream oil and gas production in Canada are underestimated, *Scientific reports*, 11, 1–8, 2021.
- Martinez-Cruz, K., Gonzalez-Valencia, R., Sepulveda-Jauregui, A., Plascencia-Hernandez, F., Belmonte-Izquierdo, Y., and Thalasso, F.: Methane emission from aquatic ecosystems of Mexico City, *Aquatic Sciences*, 79, 159–169, 2017.
- McKain, K., Down, A., Raciti, S. M., Budney, J., Hutyra, L. R., Floerchinger, C., Herndon, S. C., Nehr Korn, T., Zahniser, M. S., Jackson, R. B., and Phillips, N.: Methane emissions from natural gas infrastructure and use in the urban region of Boston, Massachusetts, *Proceedings of the National Academy of Sciences*, 112, 1941–1946, 2015.
- Methane Guiding Principles: Reducing Methane Emissions: Best Practice Guide - Pneumatic Devices, 2019.
- Mohsen, R. A., Abbassi, B., and Zytner, R.: Investigation of fugitive methane and gas collection efficiency in Halton landfill in Ontario, Canada, *Environmental Monitoring and Assessment*, 192, 1–12, 2020.

- Monteiro, V. C., Miles, N. L., Richardson, S. J., Barkley, Z., Haupt, B. J., Lyon, D., Hmiel, B., and Davis, K. J.: Methane, carbon dioxide, hydrogen sulfide, and isotopic ratios of methane observations from the Permian Basin tower network, *Earth System Science Data*, 14, 2401–2417, 2022.
- Moore, T. and Roulet, N.: A comparison of dynamic and static chambers for methane emission measurements from subarctic fens, *Atmosphere-Ocean*, 29, 102–109, 1991.
- Mosher, B. W., Czepiel, P. M., Harriss, R. C., Shorter, J. H., Kolb, C. E., McManus, J. B., Allwine, E., and Lamb, B. K.: Methane emissions at nine landfill sites in the northeastern United States, *Environmental science & technology*, 33, 2088–2094, 1999.
- National Academies of Sciences, Engineering, and Medicine and others: Improving characterization of anthropogenic methane emissions in the United States, National Academies Press, 2018.
- Omara, M., Zavala-Araiza, D., Lyon, D. R., Hmiel, B., Roberts, K. A., and Hamburg, S. P.: Methane emissions from US low production oil and natural gas well sites, *Nature Communications*, 13, 2085, 2022.
- Peacock, M., Audet, J., Bastviken, D., Cook, S., Evans, C., Grinham, A., Holgerson, M., Högbom, L., Pickard, A., Zieliński, P., et al.: Small artificial waterbodies are widespread and persistent emitters of methane and carbon dioxide, *Global Change Biology*, 27, 5109–5123, 2021.
- Pekney, N. J., Diehl, J. R., Ruehl, D., Sams, J., Veloski, G., Patel, A., Schmidt, C., and Card, T.: Measurement of methane emissions from abandoned oil and gas wells in Hillman State Park, Pennsylvania, *Carbon Management*, 9, 165–175, 2018.
- Peltola, O., Vesala, T., Gao, Y., Rätty, O., Alekseychik, P., Aurela, M., Chojnicki, B., Desai, A. R., Dolman, A. J., Euskirchen, E. S., et al.: Monthly gridded data product of northern wetland methane emissions based on upscaling eddy covariance observations, *Earth System Science Data*, 11, 1263–1289, 2019.
- Phillips, N. G., Ackley, R., Crosson, E. R., Down, A., Hutyra, L. R., Brondfield, M., Karr, J. D., Zhao, K., and Jackson, R. B.: Mapping urban pipeline leaks: Methane leaks across Boston, *Environmental pollution*, 173, 1–4, 2013.
- Pihlatie, M. K., Christiansen, J. R., Aaltonen, H., Korhonen, J. F., Nordbo, A., Rasilo, T., Benanti, G., Giebels, M., Helmy, M., Sheehy, J., et al.: Comparison of static chambers to measure CH₄ emissions from soils, *Agricultural and forest meteorology*, 171, 124–136, 2013.
- Plant, G., Kort, E. A., Floerchinger, C., Gvakharia, A., Vimont, I., and Sweeney, C.: Large fugitive methane emissions from urban centers along the US East Coast, *Geophysical research letters*, 46, 8500–8507, 2019.
- Rachor, I., Gebert, J., Gröngröft, A., and Pfeiffer, E.-M.: Variability of methane emissions from an old landfill over different time-scales, *European Journal of Soil Science*, 64, 16–26, 2013.
- Ragothaman, A. and Anderson, W. A.: Air quality impacts of petroleum refining and petrochemical industries, *Environments*, 4, 66, 2017.

- Ravikumar, A. P., Wang, J., McGuire, M., Bell, C. S., Zimmerle, D., and Brandt, A. R.: “Good versus good enough?” Empirical tests of methane leak detection sensitivity of a commercial infrared camera, *Environmental science & technology*, 52, 2368–2374, 2018.
- Reynolds, J. M. and Taylor, D. I.: Use of geophysical surveys during the planning, construction and remediation of landfills, Geological Society, London, *Engineering Geology Special Publications*, 11, 93–98, 1996.
- Riddick, S. N., Mauzerall, D. L., Celia, M. A., Kang, M., Bressler, K., Chu, C., and Gum, C. D.: Measuring methane emissions from abandoned and active oil and gas wells in West Virginia, *Science of the Total Environment*, 651, 1849–1856, 2019.
- Riddick, S. N., Ancona, R., Mbuja, M., Bell, C. S., Duggan, A., Vaughn, T. L., Bennett, K., and Zimmerle, D. J.: A quantitative comparison of methods used to measure smaller methane emissions typically observed from superannuated oil and gas infrastructure, *Atmospheric Measurement Techniques*, 15, 6285–6296, 2022.
- Rochette, P., Gregorich, E., and Desjardins, R.: Comparison of static and dynamic closed chambers for measurement of soil respiration under field conditions, *Canadian Journal of Soil Science*, 72, 605–609, 1992.
- Scarpelli, T. R., Jacob, D. J., Moran, M., Reuland, F., and Gordon, D.: A gridded inventory of Canada’s anthropogenic methane emissions, *Environmental Research Letters*, 17, 014007, 2022.
- Schoell, M.: The hydrogen and carbon isotopic composition of methane from natural gases of various origins, *Geochimica et Cosmochimica Acta*, 44, 649–661, 1980.
- Schoell, M.: Multiple origins of methane in the Earth, *Chemical geology*, 71, 1–10, 1988.
- Schwietzke, S., Griffin, W. M., Matthews, H. S., and Bruhwiler, L. M.: Natural gas fugitive emissions rates constrained by global atmospheric methane and ethane, *Environmental science & technology*, 48, 7714–7722, 2014.
- Shen, L., Gautam, R., Omara, M., Zavala-Araiza, D., Maasackers, J. D., Scarpelli, T. R., Lorente, A., Lyon, D., Sheng, J., Varon, D. J., et al.: Satellite quantification of oil and natural gas methane emissions in the US and Canada including contributions from individual basins, *Atmospheric Chemistry and Physics*, 22, 11 203–11 215, 2022.
- Sherwin, E., Rutherford, J., Zhang, Z., Chen, Y., Wetherley, E., Yakovlev, P., Berman, E., Jones, B., Thorpe, A., Ayasse, A., et al.: Quantifying oil and natural gas system emissions using one million aerial site measurements, 2023.
- Sherwood, O. A., Schwietzke, S., Arling, V. A., and Etiope, G.: Global inventory of gas geochemistry data from fossil fuel, microbial and burning sources, version 2017, *Earth System Science Data*, 9, 639–656, 2017.

- Smith, B. J., John, G., Christensen, L. E., and Chen, Y.: Fugitive methane leak detection using sUAS and miniature laser spectrometer payload: System, application and groundtruthing tests, in: 2017 International Conference on Unmanned Aircraft Systems (ICUAS), pp. 369–374, IEEE, 2017.
- Song, C., Zhu, J.-J., Willis, J. L., Moore, D. P., Zondlo, M. A., and Ren, Z. J.: Methane Emissions from Municipal Wastewater Collection and Treatment Systems, *Environmental Science & Technology*, 57, 2248–2261, 2023.
- Themelis, N. J. and Ulloa, P. A.: Methane generation in landfills, *Renewable energy*, 32, 1243–1257, 2007.
- Thorpe, A. K., Frankenberg, C., Aubrey, A., Roberts, D., Nottrott, A., Rahn, T., Sauer, J., Dubey, M., Costigan, K., Arata, C., et al.: Mapping methane concentrations from a controlled release experiment using the next generation airborne visible/infrared imaging spectrometer (AVIRIS-NG), *Remote Sensing of Environment*, 179, 104–115, 2016.
- Titchener, J., Millington-Smith, D., Goldsack, C., Harrison, G., Dunning, A., Ai, X., and Reed, M.: Single photon Lidar gas imagers for practical and widespread continuous methane monitoring, *Applied Energy*, 306, 118 086, 2022.
- Townsend-Small, A. and Hoschouer, J.: Direct measurements from shut-in and other abandoned wells in the Permian Basin of Texas indicate some wells are a major source of methane emissions and produced water, *Environmental Research Letters*, 16, 054 081, 2021.
- Townsend-Small, A., Tyler, S. C., Pataki, D. E., Xu, X., and Christensen, L. E.: Isotopic measurements of atmospheric methane in Los Angeles, California, USA: Influence of “fugitive” fossil fuel emissions, *Journal of Geophysical Research: Atmospheres*, 117, 2012.
- Townsend-Small, A., Ferrara, T. W., Lyon, D. R., Fries, A. E., and Lamb, B. K.: Emissions of coalbed and natural gas methane from abandoned oil and gas wells in the United States, *Geophysical Research Letters*, 43, 2283–2290, 2016.
- United States Environmental Protection Agency: Inventory of U.S. Greenhouse Gas Emissions and Sinks 1990-2019, 2021.
- Ville de Montréal: Carte de localisation des anciennes carrières et des dépôts de surface de la Ville de Montréal, Tech. rep., <https://environnementmtl.maps.arcgis.com/apps/webappviewer/index.html?id=eddf22f7ef54982a6545e8eb3c86a9a>, 2022.
- von Fischer, J. C., Cooley, D., Chamberlain, S., Gaylord, A., Griebenow, C. J., Hamburg, S. P., Salo, J., Schumacher, R., Theobald, D., and Ham, J.: Rapid, vehicle-based identification of location and magnitude of urban natural gas pipeline leaks, *Environmental Science & Technology*, 51, 4091–4099, 2017.
- Walsh, C. J., Roy, A. H., Feminella, J. W., Cottingham, P. D., Groffman, P. M., and Morgan, R. P.: The urban stream syndrome: current knowledge and the search for a cure, *Journal of the North American Benthological Society*, 24, 706–723, 2005.

- Wang, J., Zhang, J., Xie, H., Qi, P., Ren, Y., and Hu, Z.: Methane emissions from a full-scale A/A/O wastewater treatment plant, *Bioresource technology*, 102, 5479–5485, 2011.
- Wang, J., Tchapmi, L. P., Ravikumar, A. P., McGuire, M., Bell, C. S., Zimmerle, D., Savarese, S., and Brandt, A. R.: Machine vision for natural gas methane emissions detection using an infrared camera, *Applied Energy*, 257, 113 998, 2020.
- Wang, J., Ji, J., Ravikumar, A. P., Savarese, S., and Brandt, A. R.: VideoGasNet: Deep learning for natural gas methane leak classification using an infrared camera, *Energy*, 238, 121 516, 2022.
- Weller, Z. D., Yang, D. K., and von Fischer, J. C.: An open source algorithm to detect natural gas leaks from mobile methane survey data, *PLoS One*, 14, e0212 287, 2019.
- Weller, Z. D., Hamburg, S. P., and von Fischer, J. C.: A national estimate of methane leakage from pipeline mains in natural gas local distribution systems, *Environmental science & technology*, 54, 8958–8967, 2020.
- Whiticar, M. J.: Carbon and hydrogen isotope systematics of bacterial formation and oxidation of methane, *Chemical Geology*, 161, 291–314, 1999.
- Williams, J. P., Risk, D., Marshall, A., Nickerson, N., Martell, A., Creelman, C., Grace, M., and Wach, G.: Methane emissions from abandoned coal and oil and gas developments in New Brunswick and Nova Scotia, *Environmental monitoring and assessment*, 191, 1–12, 2019.
- Yacovitch, T. I., Herndon, S. C., Pétron, G., Kofler, J., Lyon, D., Zahniser, M. S., and Kolb, C. E.: Mobile laboratory observations of methane emissions in the Barnett Shale region, *Environmental Science & Technology*, 49, 7889–7895, 2015.
- Yu, Z. and Schanbacher, F. L.: Production of methane biogas as fuel through anaerobic digestion, *Sustainable Biotechnology: Sources of Renewable Energy*, pp. 105–127, 2010.
- Zimmerle, D., Duggan, G., Vaughn, T., Bell, C., Lute, C., Bennett, K., Kimura, Y., Cardoso-Saldana, F. J., and Allen, D. T.: Modeling air emissions from complex facilities at detailed temporal and spatial resolution: The Methane Emission Estimation Tool (MEET), *Science of The Total Environment*, 824, 153 653, 2022.

Chapter 3

Controlled release testing of the static chamber methodology for direct measurements of methane emissions

Connecting text: This chapter presents a study on the accuracy of the static chamber method which is the principal measurement methodology used in this thesis. In this chapter, we reviewed published literature on component level methane emission rates and controlled release tests of methane from different measurement platforms. We also performed multiple controlled release tests of methane emissions for the static chamber method to test the impacts of physical chamber factors and leak properties on measurement accuracy. We showed that methane emission factors from component level sources are generally lower than 100 g/hour which is lower than the lower limits of tested emission rate ranges in other work but falls within the methane emission rate ranges we measure from the sources presented in Chapters 4, 5, and 6 of this thesis.

The results of this research have been accepted for publication as:

Williams, J. P., El Hachem, K., & Kang, M. (2023). Controlled release testing of the static chamber methodology for direct measurements of methane emissions. *Atmospheric Measurement*

Techniques Discussions, 1-18.

3.1 Introduction

Methane is a potent greenhouse gas, and international initiatives such as the Global Methane Pledge (European Commission, United States of America, 2021) have motivated national commitments towards reducing emissions of methane from a variety of sectors from waste to energy to agriculture. In order to materialize methane reductions through actionable mitigation strategies, accurate methane inventories that quantify methane from different sectors and sources are needed. Methane emission sources can be broadly classified as either site or component level emissions, where site level emissions are the sum of multiple emitting components. There are also additional classifications such as facility, regional, continental, and global level (?) which encompass each preceding classification within a larger agglomeration of methane emission sources. Understanding methane emissions at the component level (i.e., the smallest tier of methane emissions sources) is particularly important for developing actionable methane reduction strategies as these data can be used to directly analyze the cost-benefits of mitigation options which allows policy makers and project developers to make informed decisions (Kang et al., 2019; International Energy Agency, 2021). Therefore, it is important that we test and develop methane quantification methods that are capable of measuring methane emissions accurately at the component level.

To select the optimal methane measurement methods, there is a need to understand the expected magnitude of methane emission rates from different component level sources. Some data sources such as the IPCC emission factor database (Intergovernmental Panel on Climate Change, 2022) have compiled emission factors for different greenhouse gas sources around the world. However, some emission factors within this database are provided at the site level, and some are provided in alternative forms to methane emission rates (e.g., mass of methane emitted per ton of waste) which makes it difficult to determine the magnitude of expected component level emission rates. As such, our goal is to determine the approximate magnitude of methane emission rates at the component level so that we can conduct tests at appropriate methane flowrates.

There are multiple methods that are used to quantify methane emissions, which we classify here as either indirect or direct methods. Indirect methane quantification methods are based on

measurements made away from the source of emissions and can often be conducted without site access. These methods include mobile surveying, stationary tower (e.g., eddy covariance tower) measurements, aerial based surveys, and satellite measurements (Cusworth et al., 2022; Edie et al., 2020; Robertson et al., 2017; Kumar et al., 2022; Riddick et al., 2022; Ravikumar et al., 2017; Ayasse et al., 2019; ?; Varon et al., 2018; de Foy et al., 2023). Direct methane quantification methods are based on quantifying methane emissions directly at the source of emissions and generally require site access. The most common direct measurement methods include optical gas imaging cameras, Hi-Flow samplers, and chamber based methodologies.

Methane sources can be classified as component, site, facility, regional, and global level sources in order of increasing spatial scales (?). As an example, a valve on an oil and gas well would constitute a component level source whereas all oil and gas wells in the Appalachian basin would comprise a regional methane source. The advantages of methane inventories created from component level measurements are high resolution and easy comparisons to regional inventories, which are predominantly made using component level data (??), where specific discrepancies can be identified (Rutherford et al., 2021). Indirect measurements can be used to measure methane emissions at site/facility/regional levels. On the other hand, direct measurement methods are labour intensive and can omit methane sources when scaling up measurements to facility/regional/global levels, but can quantify and attribute methane emissions at the component level. In terms of testing methane measurement methods for accuracy, the majority of published literature has focused on indirect methods (e.g., Robertson et al. (2017); Edie et al. (2020); Sherwin et al. (2021); Aubrey et al. (2013)), whereas few studies have tested and quantified the accuracy of direct measurement methods (Riddick et al., 2022; Pihlatie et al., 2013; Christiansen et al., 2011).

Among the direct measurement methods, optical gas imaging cameras and Hi-Flow samplers both have limits of detection at roughly 20 g/hour (Ravikumar et al., 2017; Fox et al., 2019). However the stated uncertainties of optical gas imaging cameras in Fox et al. (2019) of 3-15% are noted as being complex and likely much higher, and there have been several studies that have highlighted measurement errors attributed to the Hi-Flow sampler (Connolly et al., 2019; Howard et al., 2015).

As an alternative, the static chamber methodology is a well-established direct methane measurement method (Riddick et al., 2022; Pihlatie et al., 2013) traditionally used in the measurement of methane and other trace gas emissions from soils (Conen and Smith, 1998; Raich et al., 1990; Smith and Cresser, 2003). In recent years, the static chamber method has been applied in a wide range of settings such as the quantification of methane emissions from oil and gas wells (Lebel et al., 2020; Williams et al., 2020; Kang et al., 2014; ?; Townsend-Small et al., 2016; Townsend-Small and Hoschouer, 2021; ?; Riddick et al., 2019), manholes (Fries et al., 2018; Williams et al., 2022), landfill vents and observation wells (Williams et al., 2022), and natural gas (NG) distribution infrastructure (Williams et al., 2022; Lamb et al., 2016, 2015). All of these sources vary in terms of their leakage properties and structural complexity with regards to the installation of chambers over leaking components. However, there are few studies that have quantified the measurement accuracy of the static chamber method, and even fewer (Riddick et al., 2022; Lebel et al., 2020) that have tested the static chamber method in conditions that mimic the wide range of settings in which they are now being used.

Different methane sources can emit methane at the same mass flowrates albeit at different volumetric flowrates depending on the methane concentration of the source. For example, biogas produced from landfills (~50% methane) will differ in its source methane concentration from NG from a distribution pipeline (~90% methane). To our knowledge, there have been no studies that have tested the effects of a varying volumetric flowrate of methane as a factor to be considered in measurement accuracy for any methane measurement method. In terms of the structural complexity of these sites, several studies have employed large chambers with sub-optimal shapes to accommodate more complex sites. For example, a study by Lebel et al. 2020 in California targeting oil and gas wells used three static chambers that ranged in size (i.e., 33.8 litres to 32,659 litres) and shape (i.e., cylindrical and rectangular configurations). A key assumption in the static chamber method is that the air/gas within the chamber is well mixed (Kang et al., 2014). If the emission rate is low and the chamber is large, it may be challenging to have the gases in the chamber be well-mixed. Chamber shapes such as rectangular have been shown to have "dead zones" where

gases are not well-mixed, thereby lowering the effective volume of the chamber (Christiansen et al., 2011).

In this work we: 1) compile component level methane emission factors and categorize them by source category; 2) investigate prior controlled release testing of direct and indirect methane measurement methods to identify gaps in testing; 3) test the impacts of physical factors such as the chamber shape, size, and usage of fans on the accuracy of methane flowrate estimates; and 4) test the effects of leak properties (i.e., mass flowrates, volumetric flowrates, concentration of methane in the leak) on the accuracy of chamber measurements. Our results highlight the applicability of the static chamber technique in direct measurements of methane emissions and provide the detail necessary to inform future measurement campaigns.

3.2 Methodology

We compiled a dataset of methane emission factors from the IPCC emission factor database (Intergovernmental Panel on Climate Change, 2022) and categorized them into three source categories: agriculture, forestry, and other land use (AFOLU), energy, and waste. We removed all emission factors that were not related to a direct mass flowrates of methane at the component level. We removed all emission factors presented as methane flux rates (i.e., mass of methane emitted over a given area), and where possible, converted all remaining methane emission factors to component level methane mass flowrate presented in grams of methane emitted per hour based on assumptions outlined in the SI - Table 3.3.

We performed a literature review of 40 controlled release experiments of methane using both indirect and direct methods to evaluate the range of methane flowrates tested and the methods Google Scholar. The criteria for the literature review included all studies where methane was released at known mass flowrates of methane from above-ground points and excludes studies related to methane released in the subsurface, laboratory experiments of methane plume transport through porous media, and studies where the tested mass flowrates of methane were not reported

(SI - Table 3.5). We also exclude studies where methane quantification methods were tested on in-situ methane sources for validation. We categorized the studies based on the tested measurement platform which we grouped into eight categories: satellite (indirect method), manned aerial vehicle (indirect method), unmanned aerial vehicle (indirect method), stationary tower (indirect method), mobile surveying (indirect method), Hi-Flow sampler (direct method), camera-based (direct method), chamber measurements (direct method), and/or a combination of all the above.

We performed controlled releases of methane for the static chamber method outdoors on the McGill University campus in Montréal, Canada on June 2nd, 8th, and 10th, 2021. The weather for these days was sunny with sparse clouds with an average temperature of 25°C and wind speeds ranging from 5-15 kph (World Meteorological Station ID: 71612). We designed the controlled release experiments to test a combination of six different factors: mass flowrate, volumetric flowrate, methane percentage of leaking gas, chamber shape (i.e., rectangular versus circular), chamber size (i.e., 14 L, 18 L, 322 L, and 2,265 L), and the usage of the fans within the chamber. For the 322 L and 2,265 L chambers we used four battery-powered equipment cooling fans (airflow: 40 ft³ of air per minute) installed at the top of the chamber framework and oriented at 45° angles downward into the chamber, and for the smaller chambers we used one fan. The tested chamber shapes were a 2,265 L rectangular chamber, a 322 L cylindrical chamber, a 18 L cylindrical chamber, and a 14 L rectangular chamber (Table 3.1). In addition, for a qualitative comparison between chamber sizes, we define ≤ 20 L chambers as small, and the 322 L and 2,265 L chambers as large. Other factors such as the aspect ratio of the chamber, the rigidity of the chamber material, and the type of chamber material are provided in Table 3.1.

We tested four different mass flowrates: 1.02 g/hour, 10.2 g/hour, 102 g/hour, and 512 g/hour. In order to provide a qualitative comparison between mass flowrates, we define the mass flowrates of 1.02 and 10.2 g/hour as small flowrates, and the 102 and 512 g/hour releases as high flowrates. At least two different volumetric flowrates and two different methane concentrations were used for each of the mass flowrates we tested. The volumetric flowrates ranged from 0.238 SLPM (standard litres per minute) to 23.8 SLPM for a total of ten unique leaks (Table 3.2). We controlled mass

Table 3.1: Physical descriptions of chambers used for the controlled release experiments. Qualitative descriptions of chamber volume are indicated in parenthesis in the first row.

Chamber ID	A	B	C	D
Chamber size (L)	2,265 (large)	322 (large)	18 (small)	14 (small)
Shape	Rectangular	Cylindrical	Cylindrical	Rectangular
Structure	Collapsible	Collapsible	Solid	Solid
Material	PE tarp	PE plastic	HDPE plastic	HDPE plastic
Aspect ratio	5:4	18:11	1:1	4:5

PE = polyethylene

HDPE = high density polyethylene

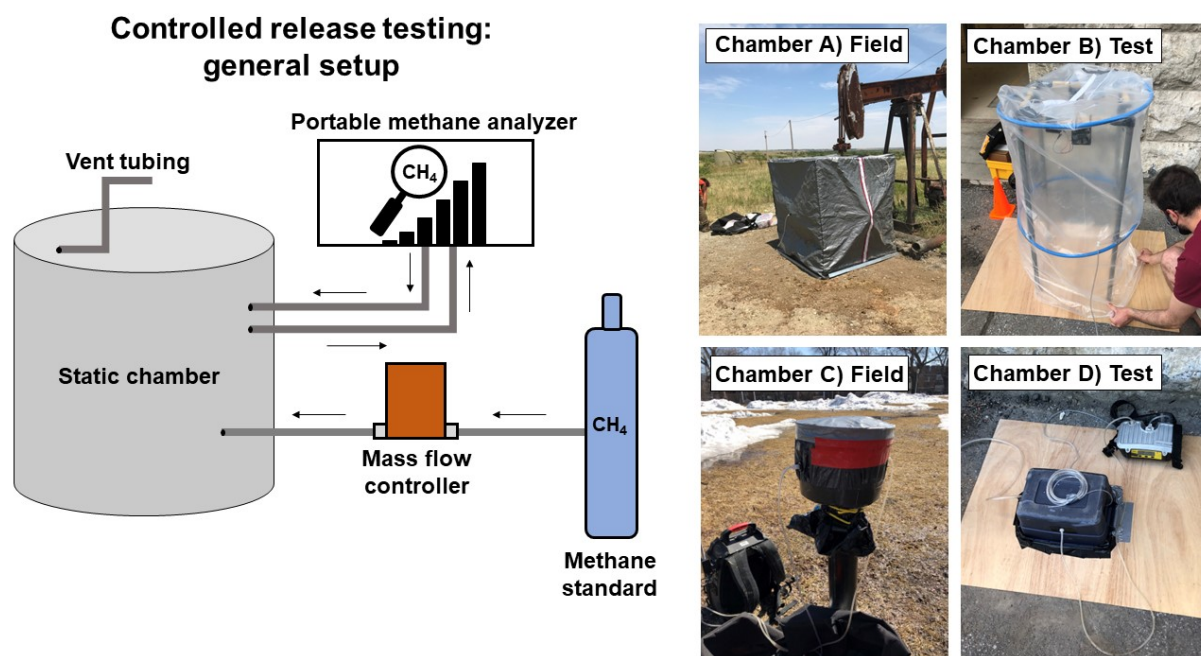


Figure 3.1: Diagram of the controlled release experiments for the static chamber method (left), with photos of chamber deployments in both field settings and during controlled release testing. The four chambers shown correspond to the four chambers we tested.

flowrates of methane using two mass flow controllers (Masterflex Mass Flowmeter Controller) with volumetric flow ranges of 50 to 0.5 SLPM and 1 to 0.01 SLPM (error of $\pm 0.8\%$ of reading and $\pm 0.2\%$ of full-scale range). Both mass flow controllers were factory calibrated prior to use for these experiments. Four different methane standards, prepared by Linde Canada, were used in our study: 100%, 50%, 10%, and 5% methane ($\pm 0.5\%$) all with a gas balance of air.

We performed the controlled release tests by releasing methane through Tygon tubing connected to the chamber (Figure 3.1). We oriented the tubing to the center of the chamber and secured it to the ground with tape to orient the flow upwards. We measured methane concentrations within the chamber continuously using a Sensit Portable Methane Detector which has a range of 0-100% methane, precision of 1 ppm, sampling frequency of 1 Hz, pump flow of 1 L per minute, and a reported accuracy of $\pm 10\%$. The analyzer was located outside the chambers with the analyzer inlets and outlets connected to the chamber ports in a closed loop with Tygon tubing of equal lengths for the inlet and outlet. Chambers were equipped with a 2 meter coil of 1/8" diameter Tygon tubing to allow for pressure equalisation between the chamber and the atmosphere (Christiansen et al., 2011). The duration of each controlled release was 5 minutes, with the exception of releases where fans were used within the chamber and methane concentrations were expected to reach the lower explosive limit of methane (i.e., 5% methane) before the 5 minute mark. Since the fans were not intrinsically safe, these experiments were terminated when the methane concentration within the chamber reached 35,000 ppm (i.e., 70% LEL). For this same reason, we did not test mass flowrates of 102 and 512 g/hour with the smaller chambers (i.e., ≤ 20 L) with fans present. When larger volume chambers were used, we were able to maintain methane levels within the chamber at safe limits.

Mass flowrates were calculated from the rate of methane build-up within the chamber over time multiplied by the volume of the chamber (5.1): where M is the mass flowrate of methane, dc/dt is the change in methane concentration over time, and V is the volume of the chamber.

$$M = \frac{dc}{dt}V \quad (3.1)$$

For some experiments, methane concentrations within the chamber were expected to rapidly reach steady-state. Steady-state is reached when methane concentrations no longer increase over time in the chamber and the concentration of methane within the chamber is equal to the concentration of the released gas. The residence time, or time to reach steady-state, is defined by (3.2): where

Table 3.2: Leak properties of ten different leaks used in controlled release experiments including percentage errors associated with mass flow controllers (MFC). Qualitative descriptions of the leak sizes are shown in parenthesis in the first column.

Methane mass flowrate (g/hour)	Volumetric flowrate (SLPM)	% methane	MFC error
1.02 (small flowrate)	0.238	10%	±1.64%
-	0.476	5%	±1.22%
10.2 (small flowrate)	0.476	50%	±1.64%
-	2.38	10%	±5.00%
-	4.76	5%	±2.90%
102 (large flowrate)	2.38	100%	±5.00%
-	4.76	50%	±2.90%
-	23.8	10%	±1.22%
512 (large flowrate)	11.9	100%	±1.64%
-	23.8	50%	±1.22%

SLPM = Standard litres per minute

MFC = Mass flow controller

τ is the residence time, V is the volume of the chamber, and Q is the volumetric flowrate of gas (i.e., methane and balance gas combined) into the chamber. For any controlled releases where the expected residence time was two minutes or shorter, we only used the initial ten data points for the linear regression to avoid the period of exponential decay as methane concentrations approach steady-state (Pihlatie et al., 2013).

$$\tau = \frac{V}{Q} \quad (3.2)$$

We summarized the results of the controlled release tests by calculating the percentage deviation of the true versus measured methane flowrate (3.3): where E is the error in (%), Q_i is the estimated methane flowrate and Q is the actual methane flowrate. For each factor being investigated, we grouped the results depending on whether the measurement was an under- or overestimate of the true methane flowrate. We calculated the accuracy of measurements as a range spanning from the median of the over- and underestimated methane flowrates, respectively. We determined the bias of measurements as the average of the raw percentage errors to determine whether tests were biased

more towards the under- or overestimation of methane flowrates.

$$E = \frac{Q_i - Q}{Q} * 100 \quad (3.3)$$

3.3 Results

3.3.1 Prior controlled methane releases and component level methane emissions

We compiled a total of 1,142 component level methane emission factors from the IPCC emission factor database (Intergovernmental Panel on Climate Change, 2022). A total of 718 emission factors were from the AFOLU sector, 291 were from the energy sector, and 133 were from the waste sector. The emission factors ranged from 9.8×10^5 to -1.1×10^{-2} g/hour. We found that 1% of emission factors were above 100 g/hour, 5% of emission factors were above 10 g/hour, and 45% of emission factors were above 1 g/hour. The remaining 55% of emission factors were below 1 g/hour. Within the energy sector the highest component level emission factors were associated with liquid unloadings of storage tanks, flowback events for unconventional oil and gas wells, and fugitive emissions from flaring and venting at oil and gas wells which ranged from 9.8×10^5 to 1.6×10^5 g/hour. For the waste sector, the highest component level emission factors were associated with leachate collections wells, pump stations, and sludge pits from landfills which ranged from 4.3×10^3 to 2.4×10^3 g/hour. For the AFOLU sector, no component level emission factors were above 100 g/hour, but the highest component level methane emissions we observed from the AFOLU sector were from enteric fermentation from dairy cattle which emitted in the range of 10 g/hour (Figure 3.2).

We analyzed a total of 40 controlled release studies spanning from 2011 to 2023 (Figure 3.3). We found that 32 of the 40 (i.e., 80%) controlled release tests had upper methane emission ranges that exceeded 1,000 g/hour, with the highest tested flowrate at 7.2×10^6 g/hour for a satellite based platform (Sherwin et al., 2023). We also saw that 31 of the 40 (i.e., 78%) controlled release tests

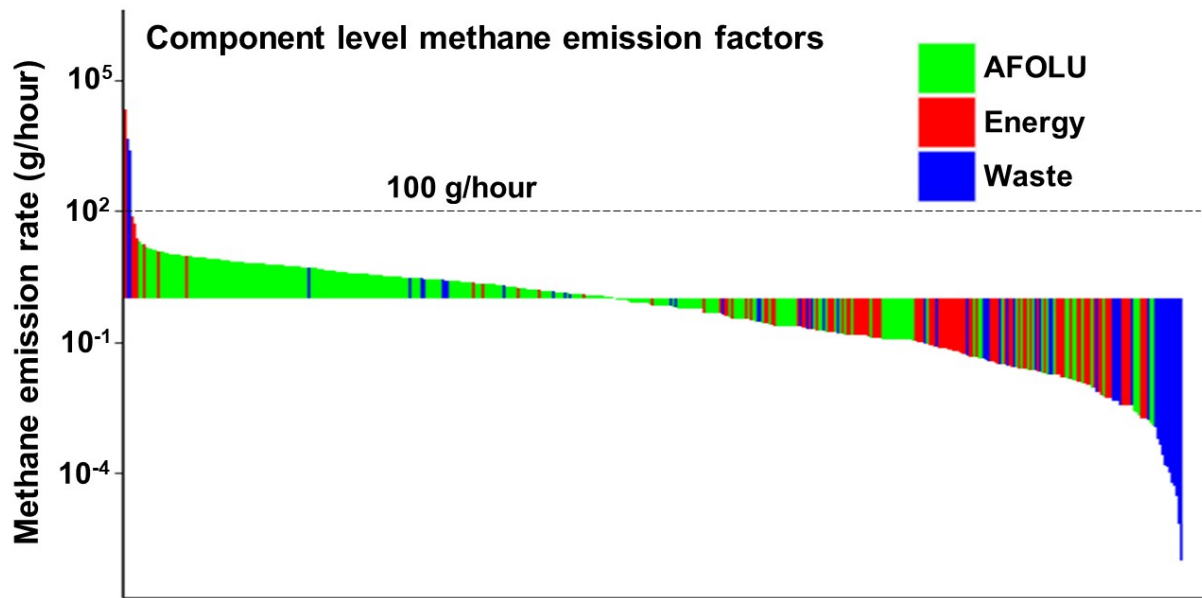


Figure 3.2: Component level methane emission factors from the IPCC emission factor database. Emission factors are categorized according to their respective IPCC source category. All emission factors were converted to methane mass flowrates based on assumptions outlined in the SI-Section 1.1.

had a lower methane emission range that exceeded 100 g/hour. The majority of controlled releases focused on indirect sampling methods, especially mobile surveying (i.e., 45%) and manned aircraft (i.e., 30%) based measurement platforms (Figure 3.2). Other indirect methods that were tested less frequently in our review were unmanned aircraft (i.e., 15%), stationary tower (i.e., 13%), and satellite (i.e., 5%) based methods. For direct measurement methods, we observed that camera-based methods were tested the most frequently (i.e., 10%). We only found three studies that conducted controlled methane releases for chamber based methodologies (Riddick et al., 2022; Pihlatie et al., 2013; Christiansen et al., 2011). We found that eight studies performed controlled releases using multiple measurement methods, with two studies (Singh et al., 2021; Riddick et al., 2022) employing five different methodologies. Overall, we found that the majority of controlled release tests we analyzed focused on indirect sampling methods, and tested methane emission ranges of

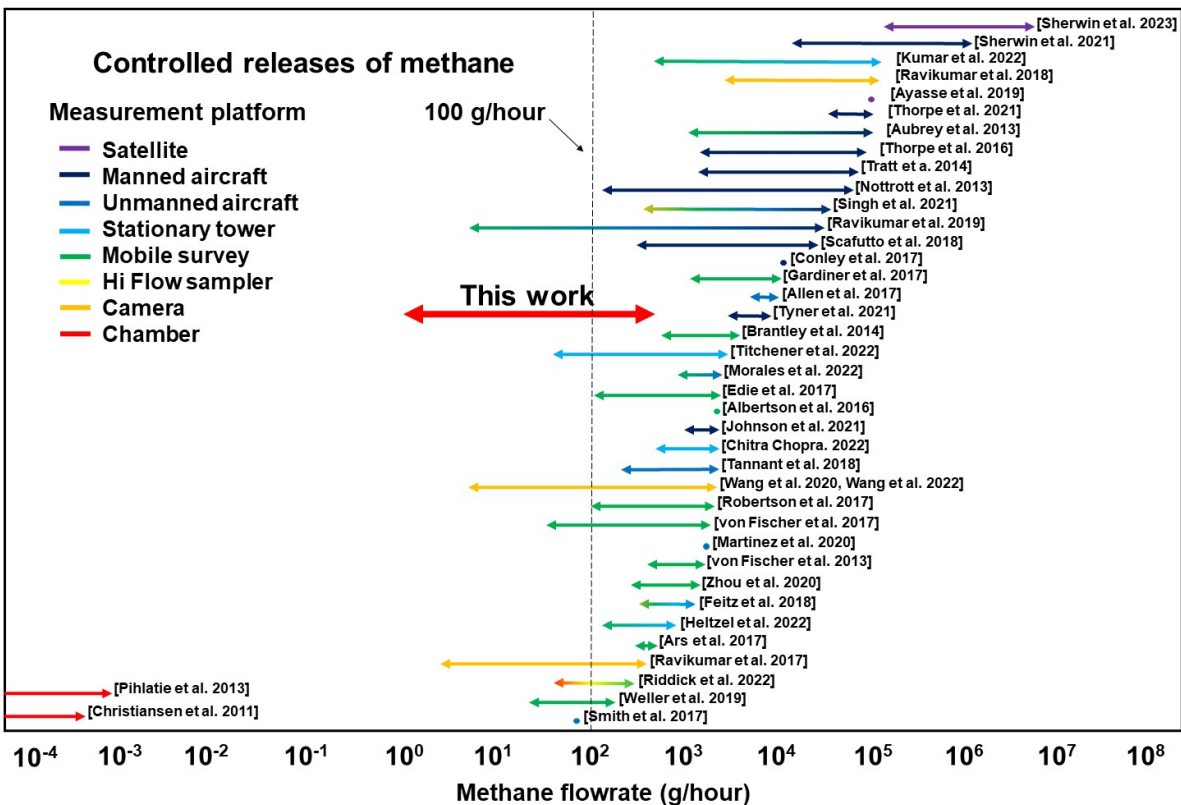


Figure 3.3: Summary of published literature of controlled releases of methane showing the range of methane emissions being tested and coloured according to the measurement platform used to quantify emissions.

≥ 100 g/hour. Therefore, the testing we present here (1.02 g/hour to 512 g/hour) fills this gap and provides guidance for measuring an appropriate range of component level methane sources.

3.3.2 Controlled releases of methane

The accuracy of our 64 controlled release experiments was +14/-14% with a standard deviation of 19%. The average absolute percentage error was $\pm 20\%$ and the median absolute percentage error was $\pm 14\%$. The lowest error we observed was 0.2%, and 25 of 64 controlled release tests (i.e., 39%) had percentage errors lower than $\pm 10\%$. Based on testing for bias, we found that the average percentage difference between actual and measured mass flowrates to be -3%, implying a small bias towards the underestimation of methane flowrates.

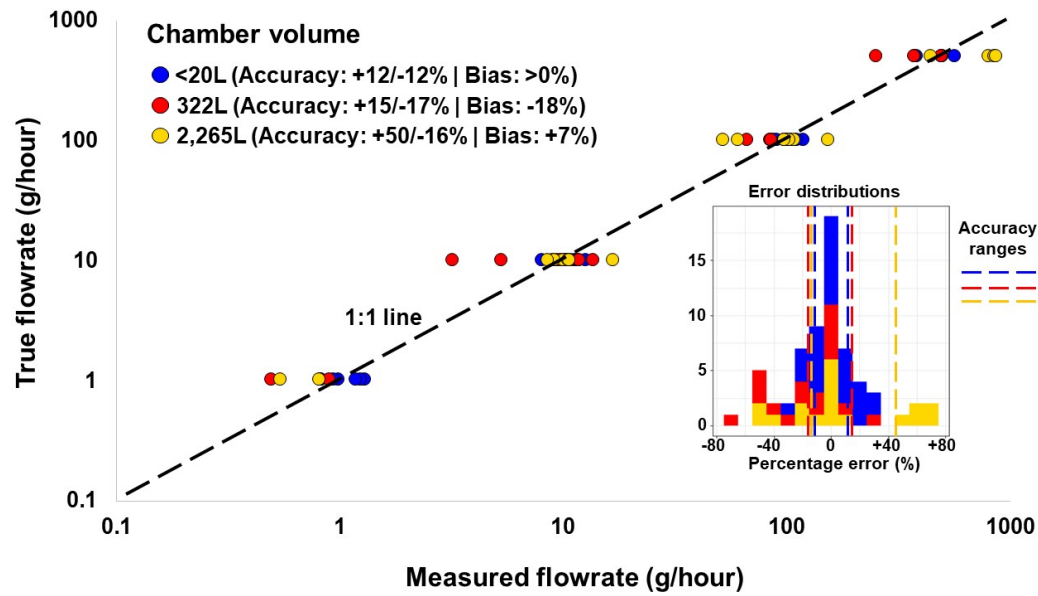


Figure 3.4: Parity plot showing the true versus measured measured methane flowrates for different chamber volumes. The distribution of actual percentage errors is shown in the right. Points and bars are coloured according to the different chamber volumes. The perfect fit line is shown by a dashed black line.

Chamber volume

Our analysis of chamber volume with respect to quantification accuracy showed that the accuracy of measurements increased with smaller chamber volumes (Figure 3.4). The ≤ 20 L chambers had the highest accuracy at +12/-12% with an error standard deviation of 12%. The 322 L chamber had a lower accuracy of +15/-17% with a standard deviation of 23%. Our highest errors were measured from the largest 2,265 L chamber with an accuracy of +50/-16% and a standard deviation of 26%. We analyzed all three chamber sizes for bias and found that the ≤ 20 L chambers showed a slight tendency for underestimation of flowrates with an average bias of $\geq 0\%$, the 322 L chamber showed a stronger tendency towards the underestimation of flowrates at -18%, and the 2,265 L chamber showed a slight bias towards overestimating flowrates at +7% (Figure 3.4).

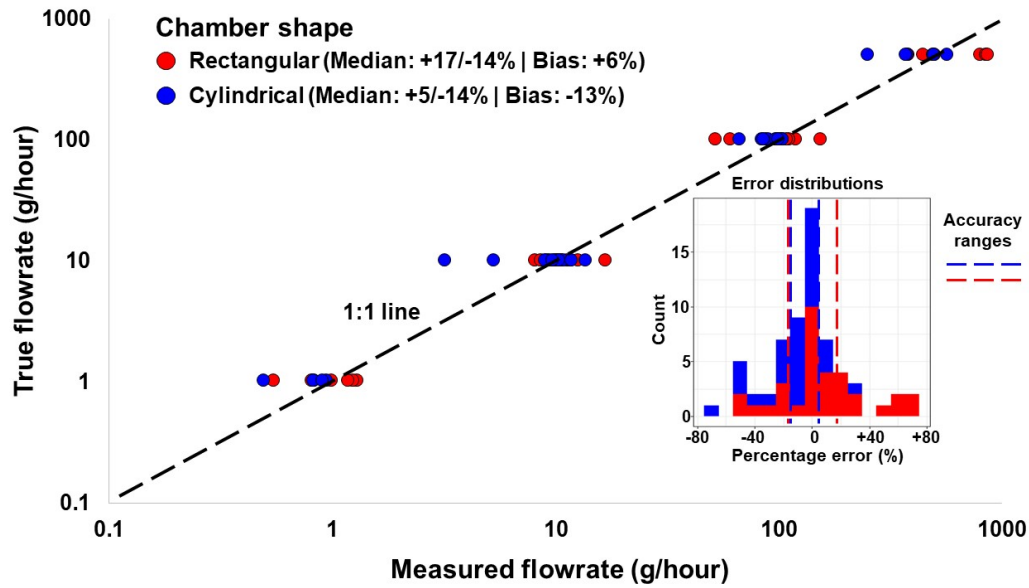


Figure 3.5: Parity plot showing the true versus measured measured methane flowrates for different chamber shapes. The distribution of actual percentage errors is shown in the right. Points and bars are coloured according to the different chamber shapes. The perfect fit line is shown by a dashed black line.

Chamber shape

Our comparisons of different chamber shapes showed that the cylindrical chambers were more accurate than the rectangular chambers, showing an accuracy of +5/-14% and a standard deviation of 18% (Figure 3.5). We found that the rectangular chambers showed a lower accuracy of +17/-14% with a standard deviation of 22%. Similar to the chamber volume, the median percentage error was smaller than the average error for both chamber shapes, which indicates an extreme distribution in percentage errors. We analyzed both chamber shapes for bias and found that the cylindrical chambers were biased towards the underestimation of methane flowrates with an average bias of -13% whereas the rectangular chambers showed a small bias towards the overestimation of methane flowrates with an average bias of +6% (Figure 3.5).

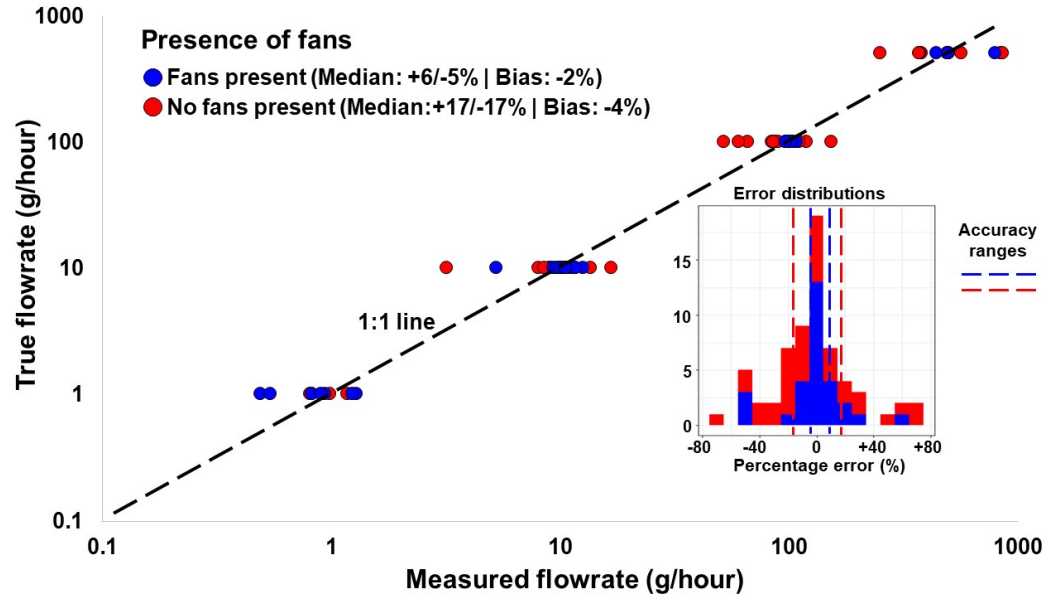


Figure 3.6: Parity plot showing the true versus measured measured methane flowrates for experiments with and without fans present. The distribution of actual percentage errors is shown in the right. Points and bars are coloured according to whether fans were present or not. The perfect fit line is shown by a dashed black line.

Usage of fans

The most impactful physical factor we observed on chamber measurement accuracy was the presence of fans, where chambers with fans present had a median percentage error of +6/-5% and a standard deviation of 17% (Figure 3.6), which was higher than chambers without fans which had an accuracy of +17/-17% and a standard deviation of 22%. For both data-sets we observed median values lower than the mean indicating a skewed data-set. We analyzed both data-sets for bias and found that both chambers with and without fans showed slight biases towards the underestimation of methane flowrates at -2% and -4% respectively (Figure 3.6).

3.3.3 Effects of leak properties

Mass flowrate

We tested four different mass flowrates for our controlled release tests: 1.02 g/hour, 10.2 g/hour, 102 g/hour, and 511 g/hour (Figure 3.7). The lowest errors were measured from the 10.2 and 102 g/hour mass flowrates each with accuracies of +8/-11% and +7/-13% respectively. The lowest accuracy of +56/-15% was attributed to the highest mass flowrate of 512 g/hour. We found that the 1.02, 10.2, and 102 g/hour mass flowrates all had negative biases of -11%, -1%, and -6% respectively. The mass flowrate of 512 g/hour had a slight bias of +4% towards the overestimation of mass flowrates, and also the highest upper accuracy estimate of +46% we observe among the different factors we analyzed.

Volumetric flowrate

We analyzed six different volumetric flowrates for the range of methane flowrates we tested: 0.238 L/min, 0.476 L/min, 2.38 L/min, 4.76 L/min, 11.9 L/min, and 23.8 L/min (Figure 3.7). We found that the lowest accuracies were attributed to both the highest and lowest volumetric flowrates with accuracies of +50/-15% and +21/-14% respectively, whereas higher accuracy was observed with the mid-level volumetric flowrates of 11.8, 4.76, 2.38, and 0.476 SLPM with accuracies ranging from +26/-3% to +9/-11%. Similar to the mass flowrates, we also found the highest accuracies were associated with the mid-level volumetric flowrates while the lowest accuracies were observed at the upper and lower volumetric flowrates.

Methane percentage of leaking gas

We analyzed four different percentages of methane in the leaking gas for the controlled releases (Figure 3.7). The lowest accuracies were associated with the 5% methane gas with an accuracy of +31/-16%, whereas the highest accuracies were observed with the 10% methane at +15/-8%. The

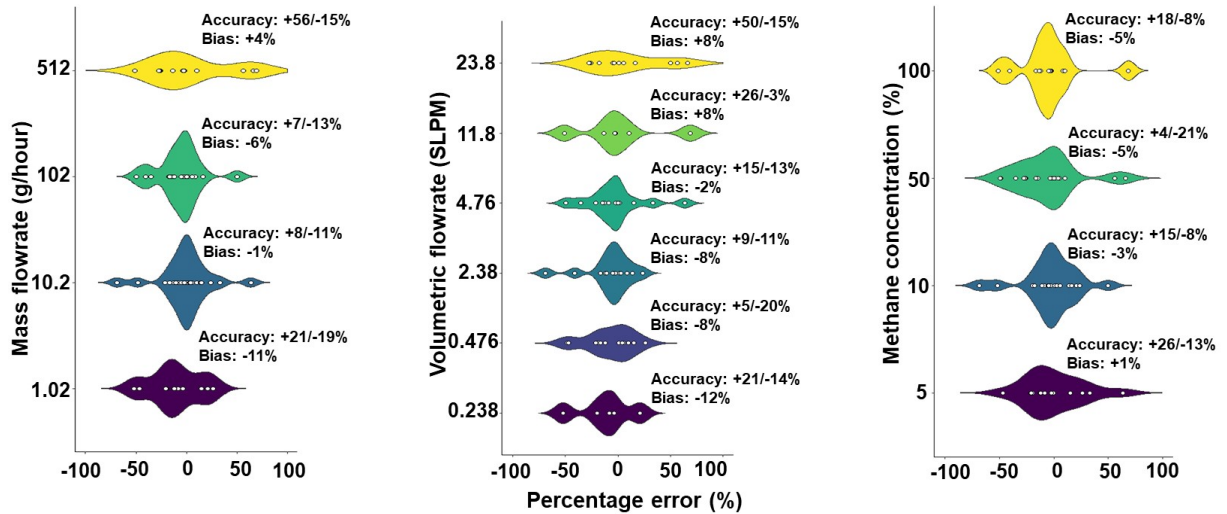


Figure 3.7: Violin plots of the percentage errors of true versus measured methane flowrates under varying mass flowrates (left), volumetric flowrates (middle), and gas concentrations (right) of methane. The points represent the measured percentage errors, and the shaded areas represent the relative density (on the y-axis) of the observed percentage errors. Uncertainty ranges and biases are displayed for each factor.

three highest percentages of methane in the leaking gas all had small negative biases ranging from -5% to -3%, whereas the 5% methane leak had a slight positive bias at +1%.

3.3.4 Optimizing the static chamber method for accuracy

For consistency, we define release rates of 1.02 and 10.2 g/hour as small flowrates, and releases of 102 and 512 g/hour as high flowrates. In addition, we define chamber volumes ≤ 20 L as small, and chamber volumes of 322 L and 2,265 L as large. We analyzed how chamber configurations (i.e., chamber volume, usage of fans, chamber shapes) can be optimized to increase the accuracy of methane flowrate estimates. In general, we found that smaller sized chambers produced the lowest errors. No measurements from a smaller sized chamber produced a percentage error above $\pm 30\%$. We also saw that smaller chambers performed similarly if fans were present or not, with smaller chambers with fans producing an accuracy of +16/-8% and smaller chambers without fans having an accuracy of +12/-13%. Smaller chambers performed slightly better if the chambers

were cylindrical, with an accuracy of $+3/-12\%$ compared to smaller rectangular chambers that had an accuracy of $+16/-3\%$. For larger sized chambers (i.e., $\geq 20\text{L}$), the usage of fans was critical for reducing measurement error. Larger chambers with fans produced an accuracy of $+4/-5\%$ compared to large chambers without fans which produced an accuracy of $+63/-27\%$. Therefore, although smaller chambers generally have lower errors than larger chambers, the errors in the larger chambers can be comparable to the smaller chambers when fans are used.

We found that chamber configurations could also be optimized according to the mass flowrate of methane. At low mass flowrates of methane (i.e., $\leq 100\text{ g/hour}$), we found that smaller sized chambers were more accurate than larger chambers with accuracies of $+12/-8\%$ and $+15/-19\%$ respectively. The usage of fans had little impact on the accuracy of smaller sized chambers at these low flowrates, with smaller chambers with fans producing an accuracy of $+16/-8\%$ and smaller chambers without fans having an accuracy of $+7/-13\%$. In contrast, the usage of fans was important for the accuracy of larger chambers at these lower mass flowrates. Larger chambers with fans had an accuracy of $+4/-30\%$ and larger chambers without fans had an accuracy of $+48/-19\%$. In terms of chamber shape, at low flowrates smaller cylindrical chambers had an accuracy of $+1/-11\%$ compared to small rectangular chambers which produced an accuracy of $+15/-3\%$. For larger chambers at low mass flowrates, we observed a contrasting result with large rectangular chambers producing an accuracy of $+6/-16\%$ and large cylindrical chambers producing a median percentage error of $+24/-48\%$.

We observed similar results for optimizing chamber configurations for high methane mass flowrates (i.e., $\geq 100\text{ g/hour}$). We found that smaller chambers ($\leq 20\text{ L}$) performed better than larger chambers with accuracies of $+14/-13\%$ and $+50/-16\%$ respectively. We found that the usage of fans was critical for measurement accuracy for larger sized chambers at these higher mass flowrates of methane. Larger chambers with fans had an accuracy of $+4/-4\%$ compared to larger chambers without fans which had an accuracy of $+66/-35\%$. For chamber shapes, cylindrical chambers were more accurate than rectangular chambers with an accuracy of $+6/-14\%$ compared to $+26/-15\%$

from rectangular chambers. At higher mass flowrates of methane, we found that large cylindrical chambers with fans were highly accurate at +2/-3% of the true methane flowrate.

From all of the controlled release experiments we performed, we saw that the median absolute error of $\pm 14\%$ was lower than the mean error of 20%, indicating a heavy-tailed distribution of measurement errors. As such, we analyzed all controlled release experiments where the resulting error exceeded 40% to assess the potential cause of these erroneous measurements. A total of 12 controlled releases had quantification errors that exceeded 40% (SI - Figure 3.9 - 3.10). All of these experiments were conducted on larger volume chambers (i.e., 322L and 2,265L), and 8 of the 12 had no fans present. Based on a comparison of the fit of the linear regressions, we found that these 12 experiments did have good correlation between methane concentrations and time with R^2 values averaging 0.91 when compared to the rest of the data-set (mean $R^2 = 0.96$). Notably, 3 of the 12 high-error measurements had very high R^2 values exceeding 0.99, with an example being shown in the bottom left of Figure 3.8. We observed a similar phenomena with a single controlled release performed with an “ideal” and “non-ideal” chamber seal which is shown in the SI - Section 3.6.1, where a “non-ideal” chamber seal produced a high R^2 value yet underestimated the methane flowrate by 43%.

3.4 Discussion

Our compilation of component level methane flowrates from the IPCC emission factor database showed that 99% of the component level emission rates fall below the 100 g/hour level. Therefore, it is important to develop and test methane quantification methods for these lower methane flowrates (i.e., ≤ 100 g/hour). Quantification of methane emissions at the component level provides a level of detail necessary to develop actionable mitigation strategies through the clear identification of emitting components. Most controlled release studies focus on indirect sampling methods which are effective in measuring methane emissions at the site and/or facility level scale. While these data are important for validating greenhouse gas inventories and quantifying emissions from

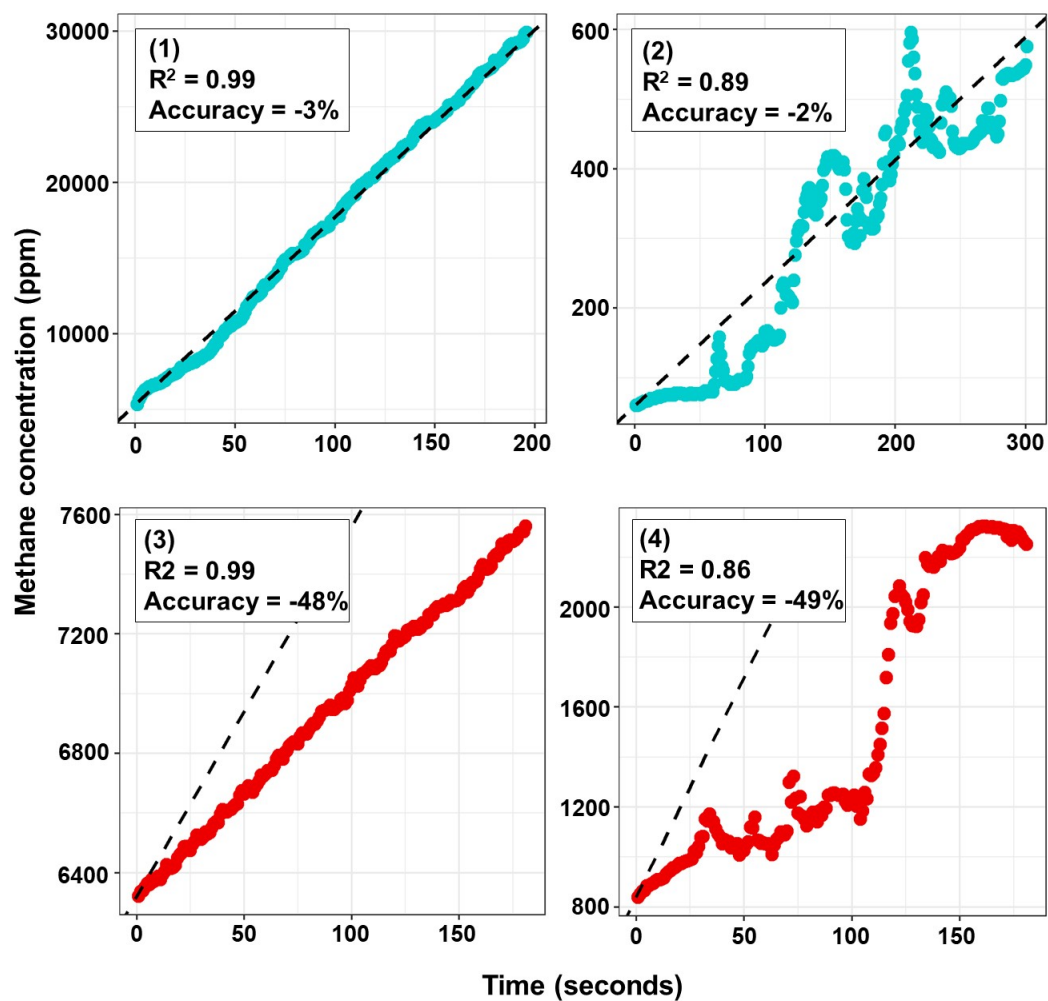


Figure 3.8: Four examples of raw controlled release data showing methane concentrations versus time. The measured concentrations within the chamber are shown by the coloured dots, and the true or expected concentrations are indicated by the dashed lines. Points coloured blue indicate a measurement error less than 40%, and the points coloured red indicate a measurement error greater than 40%. The examples shown are 1) high R^2 value and high quantification accuracy; 2) low R^2 value and high quantification accuracy; 3) high R^2 value and low quantification accuracy; 4) low R^2 value and low quantification accuracy.

super-emitting methane sources (Brandt et al., 2016; Ravikumar et al., 2017), emissions data at the component level are also needed to improve bottom-up greenhouse gas inventories and develop actionable mitigation strategies. Many of the component level sources we consider such as manholes, livestock, abandoned oil and gas wells, and NG pipeline leaks have all been shown to be signifi-

cant methane sources at municipal, provincial/state/territorial, and national levels (El Hachem and Kang, 2022; Seiler et al., 1983; Kang et al., 2016; Hendrick et al., 2016). These sources are all characterized by low methane emissions rates below 100 g/hour range on average, which are challenging to measure using indirect methods. Several studies have highlighted the super-emitting nature of methane emission sources, particularly from the NG sector (Brandt et al., 2016). However, the upper range of super-emitting methane sources varies depending on the source being measured. For example, a study of methane emissions from Montreal, Canada, found that both residential NG meter-sets and manholes were significant sources of methane for the city despite having maximum methane emission rates of 4.2 and 33 g/hour respectively (Chapter 5). While many controlled release studies focus on a higher range of methane emissions, it is still important that methods are developed and tested for lower methane emitting sources.

In addition to the factors we tested, there are several other sources of uncertainty in the static chamber method that we did not investigate. One factor that could impact measurement accuracy is the effectiveness of the chamber seal. An improper chamber seal could lead to intrusion from atmospheric air which dilutes the chamber headspace leading to an underestimation of the true methane flow rate (SI - Section 3.6.1). Typically in field settings, chambers are sealed to the ground (Kang et al., 2016; Lebel et al., 2020). In some cases, chambers can be sealed above-ground to an emitting component (Figure 3.1). A variety of different methods have been used to create these chamber-to-site seals, such as tape, bungie chords, chamber collars, sand, snow, etc (Lebel et al., 2020; Kang et al., 2016). In our experience, smaller chambers are easier to seal to an emitting component given the smaller size and ease in identifying potential breaches. Ensuring a proper chamber seal in larger chambers is more difficult due to the chamber size but the seal is achievable under stable environmental conditions. The methane concentration measurement method is one aspect of the static chamber method that will affect both the measurement accuracy and sensitivity of the static chamber method. In this work we use a portable greenhouse gas analyzer to continuously measure methane concentrations within the chamber. Uncertainty related to the frequency of methane concentration measurement and the accuracy and precision of the

greenhouse gas analyzer are all important factors related to uncertainty. Furthermore, portable greenhouse gas analyzers can generally be classified as either measuring a full range of methane concentrations at the cost of precision at lower methane concentrations (i.e., ≤ 10 ppm methane), or measuring methane with high precision at the cost of an upper measurement range (i.e., 1,000 ppm). Therefore, the selection of the greenhouse analyzer can also be optimized according to the methane source being measured to improve accuracy. Other factors such as the release point of the emitted gas; presence of multiple emission sources; environment; chamber rigidity; method and strength of interior chamber mixing; and position of the gas sampling points are all factors that could also impact measurement uncertainty. Further analysis of the impacts of these factors on measurement accuracy would be beneficial for guiding ideal deployment of the static chamber method for the quantification of component-level methane sources.

Our results showed that the static chamber methodology can quantify methane emissions ranging from 1.02 g/hour to 512 g/hour with an accuracy of +14/-14%. In comparison to indirect methods, Johnson et al. (2023) state that their aircraft-based method has a multi-pass uncertainty range of -46/+54%, which roughly corresponds to an absolute error of $\pm 50\%$. In von Fischer et al. (2017), they state an uncertainty range of -24/+32% after five mobile survey passes, which roughly corresponds to an absolute error of $\pm 28\%$. With regards to other controlled release tests on static chambers, we do find that our median uncertainty of +14/-14% falls within the 10-20% range reported by Lebel et al. (2020) and Pihlatie et al. (2013). For the larger chambers, we found that the usage of fans was critical for maximizing accuracy, which is expected given the larger volume of air that is required to be mixed. All of the 12 largest measurement errors occurred from large volume chambers, with 8 of those controlled releases having no fans present. The larger chambers we used were all collapsible chambers, which could have impacted measurement accuracy through pressure pumping in the chamber headspace through wind impacting the collapsible chamber walls and altering the chamber volumes throughout the experiment. The large volume chambers we used are designed to accommodate odd site shapes encountered in the field, such as abandoned oil and gas wells (Figure 3.1). Future controlled release studies that test larger volume rigid chambers

would help elucidate the cause of these high errors. We also noted that all of these large measurement error experiments showed high R^2 values above 0.80, meaning that they would be difficult to distinguish based on the goodness-of-fit of the measurement data alone. Furthermore, several experiments showed relatively poor R^2 values but good measurement accuracy (Figure 3.8), adding to this difficulty. We found that chamber shape is more important for larger chambers than smaller chambers, with the large cylindrical chamber performing better than the large rectangular chamber whereas we did not find any difference between the smaller sized chambers with respect to shape. Ideally static chambers should be constructed to minimize potential "dead zones" where gases can accumulate (Christiansen et al., 2011), and cylindrical, or even semi-spherical or spherical chambers, should facilitate easier mixing of the chamber headspace.

At higher methane flowrates (≥ 100 g/hour) we found that our large cylindrical chamber with fans quantified methane emissions with the highest accuracy (i.e., $\pm 2\text{-}3\%$) of any chamber combination we used throughout this study. In addition, a methane source such as an oil and gas well can have multiple emitting components (e.g., pipe flanges, valves, surface casing vents, soil gas migration) which could be missed if using smaller sized chambers. Methane concentrations within a smaller chamber can also rapidly reach explosive levels which can pose safety concerns if the environment is not intrinsically safe (Riddick et al., 2022), but these risks can be minimized at little cost to accuracy if fans are omitted. Furthermore, intrinsically safe methods of chamber mixing such as external pumps could be used to mix air within chambers, regardless of the size of chamber. Theoretically, there is no upper methane flowrate limitation of the static chamber method, and utilizing large chambers such as the 32,000 L chamber used in Lebel et al. (2020) could theoretically quantify methane flowrates in the 100-200 kg/hour range. However, there are practical limitations to directly measuring components emitting methane at these high levels, the most notable being safety concerns and access issues (e.g., measuring flare stacks and liquid storage tank unloadings). Another factor to consider is the time to reach steady-state. Enclosing a high methane emitting source within a smaller chamber causes methane concentrations within the chamber to rapidly reach steady-state, essentially creating a dynamic chamber, which we do not

test in this work (Pedersen et al., 2010; Levy et al., 2011). Overall, our findings indicate that small chambers (i.e., ≤ 20 L), regardless of the chamber shape and usage of fans, can be used to quantify component level methane flowrates with an accuracy of $\pm 11\%$ for methane flowrates ranging from 1.02 to 512 g/hour. If larger chambers are required/desired, optimal configurations (i.e., fans present and cylindrical shapes) will produce errors $\pm 3\%$ for high methane flowrates (i.e., ≥ 100 g/hour).

Our results have shown that the static chamber methodology can be an effective and accurate method for the quantification of component level methane flowrates. While indirect sampling methods have been tested extensively, there is a need to test direct sampling methods given their ability to quantify methane emissions at the component level, which is important for developing actionable mitigation strategies. The static chamber method is logistically simple to implement and adaptable to multiple methane sources, making it a viable measurement option for many component level emission sources. Going forward, there are opportunities to improve the static chamber design to reduce measurement uncertainties. Our work provides the testing and design information for the static chamber methodology, thereby contributing to the range of measurement tools needed to quantify methane emission rates from all sources.

3.5 Acknowledgements

We would like to acknowledge the members of the Kang Lab at McGill University for their valuable insights in organizing, performing, and summarizing the work in this manuscript.

3.6 Supplementary information

3.6.1 Effects of chamber seal

We performed an additional single controlled release test of the static chamber method in June 2019 to investigate the impacts of a chamber seal on measurement accuracy. One controlled release was performed outdoors of the MacDonald Engineering Building at McGill University (Canada) using the rectangular 2,265 L chamber with fans present in the interior. The chamber was installed over soft ground for this experiment. One single controlled release of methane (2.5% methane with a balance of air) at a rate of 160 mg/hour of methane. The controlled release test lasted 20 minutes in total. For the first 10 minutes, the chamber was sealed to the ground using metal collars to press the chamber material to the ground. For the second 10 minutes of the release, the metal collars were removed and the chamber material was allowed to rest over the ground. Wind speeds were low (i.e., ≤ 5 kph) for this experiment. The measured methane flowrate during the first 5 minutes of the experiment was 133 mg/hour ($R^2 = 0.9758$), and for the second 5 minutes the measured flowrate was 91 mg/hour ($R^2 = 0.9587$), meaning that the change in the chamber seal led to a decrease in accuracy from -17% for the proper chamber seal to -43% from the improper chamber seal.

Table 3.3: IPCC Emission factor database – summary of assumptions used for component level methane emission factor calculations.

Category	Assumption	Reasoning (if applicable)
Waste	5.12 L of wastewater per capita per hour	- 8,000,000,000 people globally - 359,000,000,000 m ³ /yr wastewater generation globally (Jones et al., 2021)
Waste	0.019 kg of waste per capita per hour	- 8,000,000,000 people globally - 1,300,000,000 tons/yr solid waste generation globally (Kawai and Tasaki, 2016)
Energy	1.12 hours per liquid unloading	- Average duration of liquid unloading (Allen et al., 2013)
Energy	9,301 km driven per year per capita	- Population based average from 12 countries (International Comparisons, 2023)
Energy	19.1 gram of methane per ft ³	
Energy	80.5 hours per flowback event	- Average flowback duration (Allen et al., 2013)
AFOLU	Component level = 1 head of cattle	
Other	16.04 grams per mol of methane	
Other	GWP of methane = 24	

Table 3.4: Physical chamber factors and leak properties of all 64 controlled release tests.

Leak ID	Mass flowrate (g/hour)	Methane percentage of leak (%)	Volumetric flowrate of leak (SLPM)	Chamber volume (L)	Chamber shape	Fans present
3	1.02	5	0.476	2,265	Rec.	Yes
4	10.2	5	4.76	2,265	Rec.	Yes
6	10.2	10	2.38	2,265	Rec.	Yes
7	102	10	23.8	2,265	Rec.	Yes
8	10.2	50	0.476	2,265	Rec.	Yes
9	102	50	4.76	2,265	Rec.	Yes
10	512	50	23.8	2,265	Rec.	Yes
11	102	100	2.38	2,265	Rec.	Yes
12	512	100	11.9	2,265	Rec.	Yes
14	1.02	5	0.476	2,265	Rec.	No
15	10.2	5	4.76	2,265	Rec.	No
18	10.2	10	2.38	2,265	Rec.	No
19	102	10	23.8	2,265	Rec.	No
20	10.2	50	0.476	2,265	Rec.	No
21	102	50	4.76	2,265	Rec.	No
22	512	50	23.8	2,265	Rec.	No
23	102	100	2.38	2,265	Rec.	No
24	512	100	11.9	2,265	Rec.	No
26	1.02	5	0.476	322	Cyl.	Yes
27	10.2	5	4.76	322	Cyl.	Yes
29	1.02	10	0.238	322	Cyl.	Yes

30	10.2	10	2.38	322	Cyl.	Yes
31	102	10	23.8	322	Cyl.	Yes
32	10.2	50	0.476	322	Cyl.	Yes
33	102	50	4.76	322	Cyl.	Yes
34	512	50	23.8	322	Cyl.	Yes
35	102	100	2.38	322	Cyl.	Yes
36	512	100	11.9	322	Cyl.	Yes
39	10.2	5	4.76	322	Cyl.	No
42	10.2	10	2.38	322	Cyl.	No
43	102	10	23.8	322	Cyl.	No
45	102	50	4.76	322	Cyl.	No
46	512	50	23.8	322	Cyl.	No
47	102	100	2.38	322	Cyl.	No
48	512	100	11.9	322	Cyl.	No
50	1.02	5	0.476	14	Rec.	Yes
51	10.2	5	4.76	14	Rec.	Yes
53	1.02	10	0.238	14	Rec.	Yes
54	10.2	10	2.38	14	Rec.	Yes
55	10.2	50	0.476	14	Rec.	Yes
57	1.02	5	0.476	14	Rec.	No
58	10.2	5	4.76	14	Rec.	No
60	1.02	10	0.238	14	Rec.	No
61	10.2	10	2.38	14	Rec.	No
62	102	10	23.8	14	Rec.	No
63	10.2	50	0.476	14	Rec.	No
64	102	50	4.76	14	Rec.	No

65	512	50	23.8	14	Rec.	No
66	102	100	2.38	14	Rec.	No
67	512	100	11.9	14	Rec.	No
69	1.02	5	0.476	18	Cyl.	Yes
70	10.2	5	4.76	18	Cyl.	Yes
72	1.02	10	0.238	18	Cyl.	Yes
73	10.2	10	2.38	18	Cyl.	Yes
74	10.2	50	0.476	18	Cyl.	Yes
77	10.2	5	4.76	18	Cyl.	No
79	1.02	10	0.238	18	Cyl.	No
80	10.2	10	2.38	18	Cyl.	No
81	102	10	23.8	18	Cyl.	No
82	10.2	50	0.476	18	Cyl.	No
83	102	50	4.76	18	Cyl.	No
84	512	50	23.8	18	Cyl.	No
85	102	100	2.38	18	Cyl.	No
86	512	100	11.9	18	Cyl.	No

Table 3.5: Summary of controlled release experiments examined for literature review.

Study	Method	Tested rates (g/h)	Accept/Reject
Riddick et al. 2022	Static chamber	40 - 200	Accept
	Dynamic chamber	40 - 200	-
	Hi Flow Sampler	40 - 200	-
	Inverse Gaussian	40 - 200	-
	bLs	40 - 200	-
Kumar et al. 2022	Stationary tower	576 - 108,000	Accept
	Mobile survey	576 - 108,000	-
Ravikumar et al. 2019	Mobile survey	5 - 26,000	Accept
	Uncrewed aerial	5 - 26,000	-
	Crewed aerial	5 - 26,000	-
Robertson et al. 2014	Mobile survey	108 - 2,016	Accept
Edie et al. 2017	Mobile survey	144 - 2,160	Accept
Sherwin et al. 2021	Crewed aerial	18,000 - 1,025,000	Accept
Aubrey et al. 2013	Crewed aerial	2,100 - 100,800	Accept
	Mobile survey	2,100 - 100,800	-
Ars et al. 2016	Mobile survey	360 - 482	Accept
Martinez et al. 2020	Uncrewed aerial	1800	Accept
Morales et al. 2022	Uncrewed aerial	936 - 2,448	Accept
	Mobile survey	936 - 2,448	-
Thorpe et al. 2016	Crewed aerial	2,282 - 99,082	Accept
Chitra Chopra, 2022	Stationary tower - eddy	525 - 2,100	Accept
Singh et al. 2021	Crewed aerial	470 - 29,810	Accept
	Uncrewed aerial	470 - 29,810	-
	Mobile survey	470 - 29,810	-

	Camera	470 - 29,810	-
	Handheld sensor	470 - 29,810	-
Smith et al. 2017	Uncrewed aerial	78.44	Accept
Ravikumar et al. 2018	Camera	3,600 - 104,400	Accept
Ravikumar et al. 2017	Camera	3.5 - 295	Accept
Zhou et al. 2020	Mobile survey	290 - 1,240	Accept
Johnson et al. 2021	Crewed aerial	1,260 - 2,100	Accept
Wang et al. 2020	Camera	5.3 - 2,051.6	Accept
Tannant et al. 2018	Uncrewed aerial	204 - 2,100	Accept
Gardiner et al. 2017	Mobile survey	1,400 - 11,000	Accept
Tratt et al. 2014	Crewed aerial	2,200 - 82,000	Accept
Thorpe et al. 2021	Crewed aerial	47,500 - 101,700	Accept
Albertson et al. 2016	Mobile survey	2,160	Accept
Brantley et al. 2014	Mobile survey	684 - 4,320	Accept
Weller et al. 2019	Mobile survey	21 - 172	Accept
Tyner et al. 2021	Crewed aerial	3,700 - 8,600	Accept
Scafutto et al. 2018	Crewed aerial	310 - 22,750	Accept
Von Fischer et al. 2013	Mobile survey	420 - 1,680	Accept
Allen et al. 2017	Uncrewed aerial	5,000 - 10,000	Accept
Nottrott et al. 2013	Crewed aerial	160 - 78,440	Accept
Conley et al. 2017	Crewed aerial	13,900	Accept
Ayasse et al. 2019	Satellite	103,710	Accept
Titchener et al. 2022	Camera	43.2 - 3,006	Accept
Heltzel et al. 2022	Mobile survey	144 - 864	Accept
Von Fisher et al. 2017	Mobile Survey	42 - 1,890	Accept
	Mobile survey	300 - 1,200	Accept

Feitz et al. 2018

	Stationary tower	300 - 1,200	-
	Uncrewed aerial	300 - 1,200	-
	Camera	300 - 1,200	-
Wang et al. 2022	OGI - Machine learning	3.4 - 2,051.6	Reject - results already presented
Sherwin et al., 2023	Satellite	200,000 - 7,200,000	Accept
Brewer et al. 1998	Remote vehicle	5	Reject - submarine release
Cahill et al. 2017	Discrete samples	5 - 125	Reject - groundwater release
Felice et al. 2018	Discrete samples	>0.02	Reject - subsurface release
Pihlatie et al. 2013	Chamber	>0.001	Accept
Christiansen et al. 2011	Chamber	>0.001	Accept

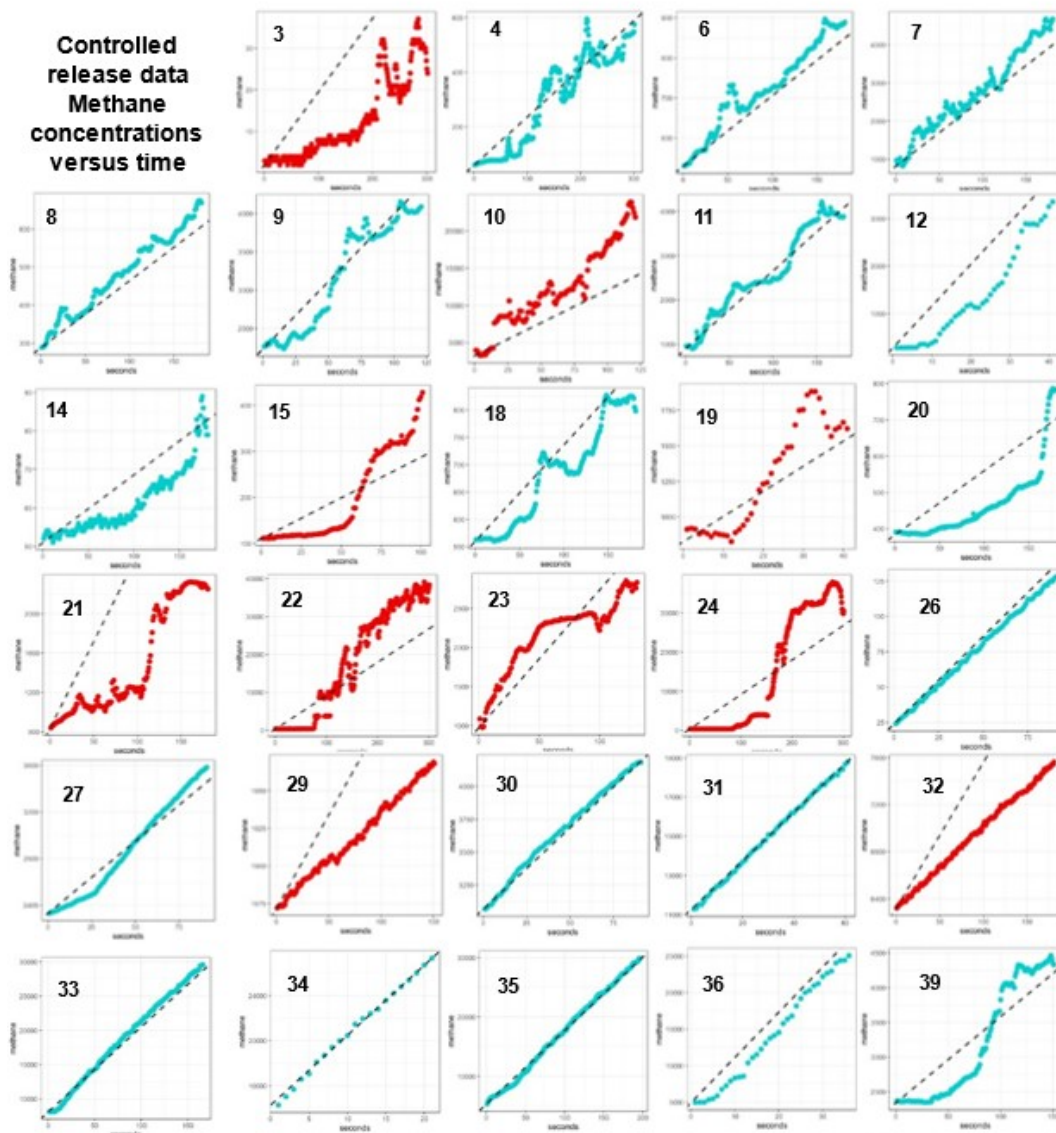


Figure 3.9: Scatter-plots of methane concentration over time for all 64 controlled release tests. Points coloured blue indicate a measurement accuracy of 40% or better. Points coloured red indicate a measurement accuracy of 40% or worse (1/2).

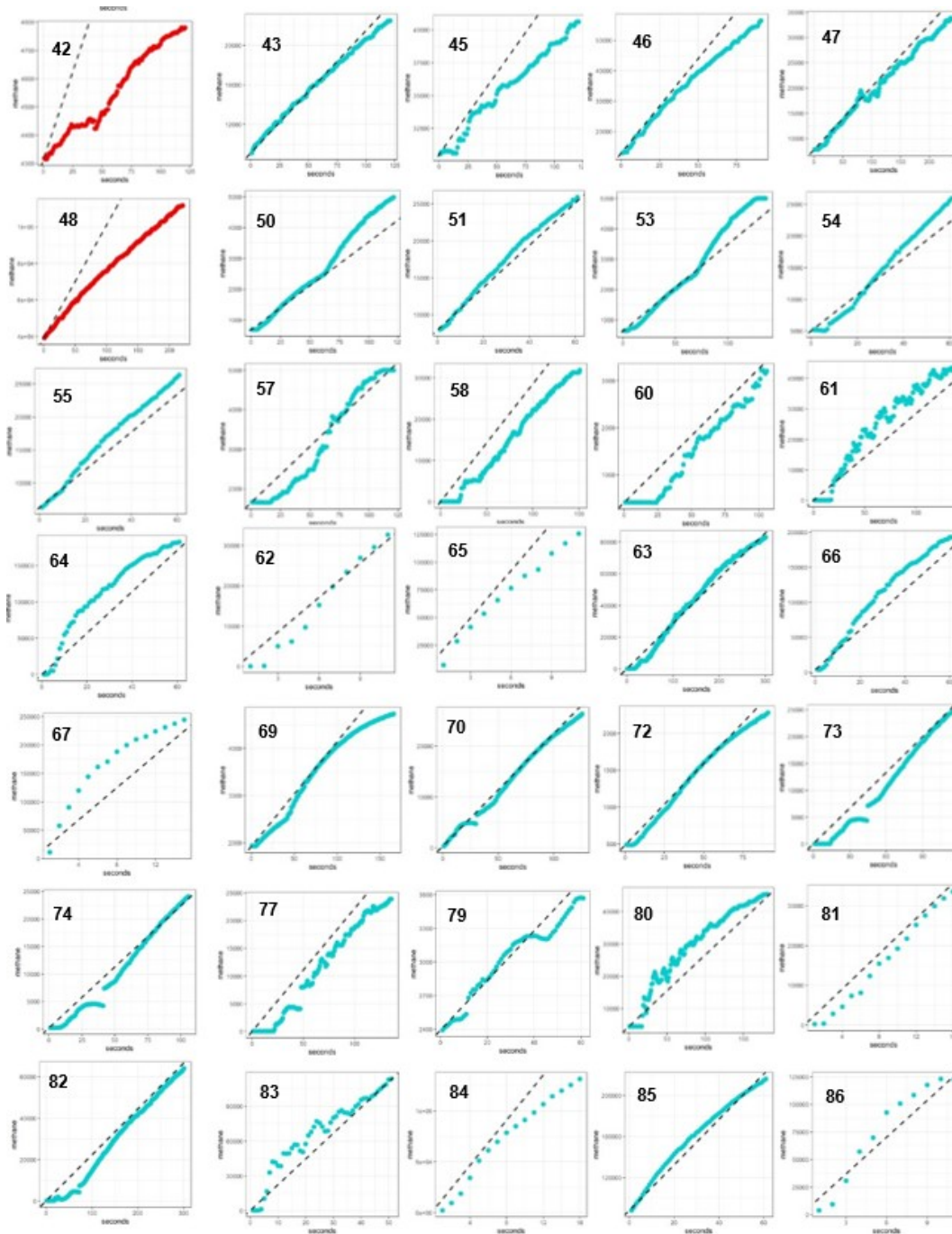


Figure 3.10: Scatter-plots of methane concentration over time for all 64 controlled release tests. Points coloured blue indicate a measurement accuracy of 40% or better. Points coloured red indicate a measurement accuracy of 40% or worse (2/2).

Bibliography

- Allen, D. T., Torres, V. M., Thomas, J., Sullivan, D. W., Harrison, M., Hendler, A., Herndon, S. C., Kolb, C. E., Fraser, M. P., Hill, A. D., et al.: Measurements of methane emissions at natural gas production sites in the United States, *Proceedings of the National Academy of Sciences*, 110, 17 768–17 773, 2013.
- Aubrey, A., Thorpe, A., Christensen, L., Dinardo, S., Frankenberg, C., Rahn, T., and Dubey, M.: Demonstration of Technologies for Remote and in Situ Sensing of Atmospheric Methane Abundances—a Controlled Release Experiment, in: *AGU Fall Meeting Abstracts*, vol. 2013, pp. A44E–05, 2013.
- Ayasse, A. K., Dennison, P. E., Foote, M., Thorpe, A. K., Joshi, S., Green, R. O., Duren, R. M., Thompson, D. R., and Roberts, D. A.: Methane mapping with future satellite imaging spectrometers, *Remote Sensing*, 11, 3054, 2019.
- Brandt, A. R., Heath, G. A., and Cooley, D.: Methane leaks from natural gas systems follow extreme distributions, *Environmental science & technology*, 50, 12 512–12 520, 2016.
- Christiansen, J. R., Korhonen, J. F., Juszczak, R., Giebels, M., and Pihlatie, M.: Assessing the effects of chamber placement, manual sampling and headspace mixing on CH₄ fluxes in a laboratory experiment, *Plant and soil*, 343, 171–185, 2011.
- Conen, F. and Smith, K.: A re-examination of closed flux chamber methods for the measurement of trace gas emissions from soils to the atmosphere, *European Journal of Soil Science*, 49, 701–707, 1998.
- Connolly, J., Robinson, R., and Gardiner, T.: Assessment of the Bacharach Hi Flow® Sampler characteristics and potential failure modes when measuring methane emissions, *Measurement*, 145, 226–233, 2019.
- Cusworth, D. H., Thorpe, A. K., Ayasse, A. K., Stepp, D., Heckler, J., Asner, G. P., Miller, C. E., Yadav, V., Chapman, J. W., Eastwood, M. L., et al.: Strong methane point sources contribute a disproportionate fraction of total emissions across multiple basins in the United States, *Proceedings of the National Academy of Sciences*, 119, e2202338 119, 2022.
- de Foy, B., Schauer, J. J., Lorente, A., and Borsdorff, T.: Investigating high methane emissions from urban areas detected by TROPOMI and their association with untreated wastewater, *Environmental Research Letters*, 2023.
- Edie, R., Robertson, A. M., Field, R. A., Soltis, J., Snare, D. A., Zimmerle, D., Bell, C. S., Vaughn, T. L., and Murphy, S. M.: Constraining the accuracy of flux estimates using OTM 33A, *Atmospheric Measurement Techniques*, 13, 341–353, 2020.
- El Hachem, K. and Kang, M.: Methane and hydrogen sulfide emissions from abandoned, active, and marginally producing oil and gas wells in Ontario, Canada, *Science of The Total Environment*, 823, 153 491, 2022.

- European Commission, United States of America: European-Commission, Joint EU-US Press Release on the Global Methane Pledge, 2021.
- Fox, T. A., Barchyn, T. E., Risk, D., Ravikumar, A. P., and Hugenholtz, C. H.: A review of close-range and screening technologies for mitigating fugitive methane emissions in upstream oil and gas, *Environmental Research Letters*, 14, 053 002, 2019.
- Fries, A. E., Schifman, L. A., Shuster, W. D., and Townsend-Small, A.: Street-level emissions of methane and nitrous oxide from the wastewater collection system in Cincinnati, Ohio, *Environmental Pollution*, 236, 247–256, 2018.
- Hendrick, M. F., Ackley, R., Sanaie-Movahed, B., Tang, X., and Phillips, N. G.: Fugitive methane emissions from leak-prone natural gas distribution infrastructure in urban environments, *Environmental Pollution*, 213, 710–716, 2016.
- Howard, T., Ferrara, T. W., and Townsend-Small, A.: Sensor transition failure in the high flow sampler: Implications for methane emission inventories of natural gas infrastructure, *Journal of the Air & Waste Management Association*, 65, 856–862, 2015.
- Intergovernmental Panel on Climate Change: IPCC Emission Factor Database., <https://www.ipcc-nggip.iges.or.jp/EFDB/main.php>, accessed 2022-12-14, 2022.
- International Comparisons: International Comparisons – Transportation, <https://internationalcomparisons.org/environmental/transportation/>, accessed 2023-02-09, 2023.
- International Energy Agency: Net Zero by 2050, IEA, Paris, <https://www.iea.org/reports/net-zero-by-2050>, accessed 2022-04-10, 2021.
- Johnson, M. R., Tyner, D. R., and Conrad, B. M.: Origins of Oil and Gas Sector Methane Emissions: On-Site Investigations of Aerial Measured Sources, *Environmental Science & Technology*, 57, 2484–2494, 2023.
- Jones, E. R., Van Vliet, M. T., Qadir, M., and Bierkens, M. F.: Country-level and gridded estimates of wastewater production, collection, treatment and reuse, *Earth System Science Data*, 13, 237–254, 2021.
- Kang, M., Kanno, C. M., Reid, M. C., Zhang, X., Mauzerall, D. L., Celia, M. A., Chen, Y., and Onstott, T. C.: Direct measurements of methane emissions from abandoned oil and gas wells in Pennsylvania, *Proceedings of the National Academy of Sciences*, 111, 18 173–18 177, 2014.
- Kang, M., Christian, S., Celia, M. A., Mauzerall, D. L., Bill, M., Miller, A. R., Chen, Y., Conrad, M. E., Darrah, T. H., and Jackson, R. B.: Identification and characterization of high methane-emitting abandoned oil and gas wells, *Proceedings of the National Academy of Sciences*, 113, 13 636–13 641, 2016.
- Kang, M., Dong, Y., Liu, Y., Williams, J. P., Douglas, P. M., and McKenzie, J. M.: Potential increase in oil and gas well leakage due to earthquakes, *Environmental Research Communications*, 1, 121 004, 2019.

- Kawai, K. and Tasaki, T.: Revisiting estimates of municipal solid waste generation per capita and their reliability, *Journal of Material Cycles and Waste Management*, 18, 1–13, 2016.
- Kumar, P., Broquet, G., Caldow, C., Laurent, O., Gichuki, S., Cropley, F., Yver-Kwok, C., Fontanier, B., Lauvaux, T., Ramonet, M., et al.: Near-field atmospheric inversions for the localization and quantification of controlled methane releases using stationary and mobile measurements, *Quarterly Journal of the Royal Meteorological Society*, 148, 1886–1912, 2022.
- Lamb, B. K., Edburg, S. L., Ferrara, T. W., Howard, T., Harrison, M. R., Kolb, C. E., Townsend-Small, A., Dyck, W., Possolo, A., and Whetstone, J. R.: Direct measurements show decreasing methane emissions from natural gas local distribution systems in the United States, *Environmental Science & Technology*, 49, 5161–5169, 2015.
- Lamb, B. K., Cambaliza, M. O., Davis, K. J., Edburg, S. L., Ferrara, T. W., Floerchinger, C., Heimburger, A. M., Herndon, S., Lauvaux, T., Lavoie, T., and Lyon, D.: Direct and indirect measurements and modeling of methane emissions in Indianapolis, Indiana, *Environmental Science & Technology*, 50, 8910–8917, 2016.
- Lebel, E. D., Lu, H. S., Vielstadte, L., Kang, M., Banner, P., Fischer, M. L., and Jackson, R. B.: Methane emissions from abandoned oil and gas wells in California, *Environmental Science & Technology*, 54, 14617–14626, 2020.
- Levy, P. E., Gray, A., Leeson, S., Gaiawyn, J., Kelly, M., Cooper, M., Dinsmore, K., Jones, S., and Sheppard, L.: Quantification of uncertainty in trace gas fluxes measured by the static chamber method, *European Journal of Soil Science*, 62, 811–821, 2011.
- Pedersen, A., Petersen, S., and Schelde, K.: A comprehensive approach to soil-atmosphere trace-gas flux estimation with static chambers, *European Journal of Soil Science*, 61, 888–902, 2010.
- Pihlatie, M. K., Christiansen, J. R., Aaltonen, H., Korhonen, J. F., Nordbo, A., Rasilo, T., Benanti, G., Giebels, M., Helmy, M., Sheehy, J., et al.: Comparison of static chambers to measure CH₄ emissions from soils, *Agricultural and forest meteorology*, 171, 124–136, 2013.
- Raich, J., Bowden, R., and Steudler, P. A.: Comparison of two static chamber techniques for determining carbon dioxide efflux from forest soils, *Soil science society of America Journal*, 54, 1754–1757, 1990.
- Ravikumar, A. P., Wang, J., and Brandt, A. R.: Are optical gas imaging technologies effective for methane leak detection?, *Environmental science & technology*, 51, 718–724, 2017.
- Riddick, S. N., Mauzerall, D. L., Celia, M. A., Kang, M., Bressler, K., Chu, C., and Gum, C. D.: Measuring methane emissions from abandoned and active oil and gas wells in West Virginia, *Science of the Total Environment*, 651, 1849–1856, 2019.
- Riddick, S. N., Ancona, R., Mbuja, M., Bell, C. S., Duggan, A., Vaughn, T. L., Bennett, K., and Zimmerle, D. J.: A quantitative comparison of methods used to measure smaller methane emissions typically observed from superannuated oil and gas infrastructure, *Atmospheric Measurement Techniques*, 15, 6285–6296, 2022.

- Robertson, A. M., Edie, R., Snare, D., Soltis, J., Field, R. A., Burkhart, M. D., Bell, C. S., Zimmerle, D., and Murphy, S. M.: Variation in methane emission rates from well pads in four oil and gas basins with contrasting production volumes and compositions, *Environmental science & technology*, 51, 8832–8840, 2017.
- Rutherford, J. S., Sherwin, E. D., Ravikumar, A. P., Heath, G. A., Englander, J., Cooley, D., Lyon, D., Omara, M., Langfitt, Q., and Brandt, A. R.: Closing the methane gap in US oil and natural gas production emissions inventories, *Nature communications*, 12, 4715, 2021.
- Seiler, W., Holzappel-Pschorn, A., Conrad, R., and Scharffe, D.: Methane emission from rice paddies, *Journal of Atmospheric Chemistry*, 1, 241–268, 1983.
- Sherwin, E., Rutherford, J., Zhang, Z., Chen, Y., Wetherley, E., Yakovlev, P., Berman, E., Jones, B., Thorpe, A., Ayasse, A., et al.: Quantifying oil and natural gas system emissions using one million aerial site measurements, 2023.
- Sherwin, E. D., Chen, Y., Ravikumar, A. P., and Brandt, A. R.: Single-blind test of airplane-based hyperspectral methane detection via controlled releases, *Elementa: Science of the Anthropocene*, 9, 2021.
- Singh, D., Barlow, B., Hugenholtz, C., Funk, W., Robinson, C., and Ravikumar, A. P.: Field Performance of New Methane Detection Technologies: Results from the Alberta Methane Field Challenge, 2021.
- Smith, K. A. and Cresser, M. S.: Measurement of trace gases, I: gas analysis, chamber methods, and related procedures, in: *Soil and Environmental Analysis*, pp. 394–433, CRC Press, 2003.
- Townsend-Small, A. and Hoschouer, J.: Direct measurements from shut-in and other abandoned wells in the Permian Basin of Texas indicate some wells are a major source of methane emissions and produced water, *Environmental Research Letters*, 16, 054 081, 2021.
- Townsend-Small, A., Ferrara, T. W., Lyon, D. R., Fries, A. E., and Lamb, B. K.: Emissions of coalbed and natural gas methane from abandoned oil and gas wells in the United States, *Geophysical Research Letters*, 43, 2283–2290, 2016.
- Varon, D. J., Jacob, D. J., McKeever, J., Jervis, D., Durak, B. O., Xia, Y., and Huang, Y.: Quantifying methane point sources from fine-scale satellite observations of atmospheric methane plumes, *Atmospheric Measurement Techniques*, 11, 5673–5686, 2018.
- von Fischer, J. C., Cooley, D., Chamberlain, S., Gaylord, A., Griebenow, C. J., Hamburg, S. P., Salo, J., Schumacher, R., Theobald, D., and Ham, J.: Rapid, vehicle-based identification of location and magnitude of urban natural gas pipeline leaks, *Environmental Science & Technology*, 51, 4091–4099, 2017.
- Williams, J. P., Regehr, A., and Kang, M.: Methane emissions from abandoned oil and gas wells in Canada and the United States, *Environmental science & technology*, 55, 563–570, 2020.
- Williams, J. P., Ars, S., Vogel, F., Regehr, A., and Kang, M.: Differentiating and Mitigating Methane Emissions from Fugitive Leaks from Natural Gas Distribution, Historic Landfills, and Manholes in Montréal, Canada, *Environmental Science & Technology*, 56, 16 686–16 694, 2022.

Chapter 4

Methane emissions from abandoned oil and gas wells in Canada and the United States

Connecting text: In this chapter, we present the results of a compilation of activity data and emission rate measurements of methane emissions from abandoned oil and gas (AOG) wells in Canada and the U.S., including new measurements we made from 17 AOG wells in British Columbia and 53 AOG wells in Oklahoma using the static chamber method tested in Chapter 3. We found that methane emissions from AOG wells were underestimated in both countries, and that the underestimation was more pronounced in Canada due to the difference in emission factors. This study presents the first of three chapters focused on field measurements of methane emissions using direct measurement techniques, particularly the chamber method presented in Chapter 3.

The results of this research are currently published as:

Williams, J. P., Regehr, A., & Kang, M. (2020). Methane emissions from abandoned oil and gas wells in Canada and the United States. *Environmental Science & Technology*, 55(1), 563-570.

4.1 Introduction

In 2019, methane emissions from abandoned oil and gas (AOG) wells were included for the first time in national greenhouse gas (GHG) inventories (United States Environmental Protection Agency, 2021a; Environment and Climate Change Canada, 2021). AOG wells can act as subsurface leakage pathways that connect oil and gas reservoirs to groundwater aquifers and the atmosphere, contributing to water and air quality degradation and climate change (Cahill et al., 2019). This is particularly true if the AOG well is left unplugged or the integrity of the well and/or plug is compromised. Methane is a potent GHG, with a global warming potential 28–36 times stronger than that of carbon dioxide over a 100 year timeframe and 84–86 times stronger over a 20 year timeframe (Stocker, 2014). Therefore, to curb warming, it is important to quantify and mitigate methane emissions. The U.S. GHG inventory shows that methane emissions from AOG wells represent 0.28 million metric tonnes (MMt) of methane per year and 1–13% of total methane emissions from the oil and natural gas sector (United States Environmental Protection Agency, 2021a). In Canada, the current national inventory estimates that AOG wells represent 1.0×10^{-2} MMt of methane emissions in 2018 and less than 1% of total methane emissions from the oil and natural gas sector (Environment and Climate Change Canada, 2021). Of the top 15 anthropogenic methane emission sources from all sectors, AOG wells are the most uncertain source in the U.S. and the fourth most uncertain in Canada (SI - Table 4.2). Therefore, a comprehensive analysis of available data and estimation approaches are needed to improve estimates for this new source category.

Measurements of methane emission rates at AOG wells are used to determine emission factors, which are multiplied with the number of AOG wells to estimate total emissions. Emission factors for AOG wells for the U.S. and Canada are calculated using the arithmetic mean of available direct methane measurements and are assumed to be representative of the population of wells that the emission factors are applied to. There have been a total of six published studies that have directly measured methane flow rates from AOG wells in the U.S. and Canada (Kang et al., 2014, 2016; Townsend-Small et al., 2016; Williams et al., 2019; Riddick et al., 2019b; Pekney et al.,

2018). Most of these measurements are focused on the eastern U.S., specifically the Appalachian region (Kang et al., 2014, 2016; Riddick et al., 2019b; Pekney et al., 2018) with the exceptions of Townsend-Small et al. (2016) who measured wells in Utah (U.S.), Colorado (U.S.), and Wyoming (U.S.) and Williams et al. (2019) who measured wells in New Brunswick (Canada). Emission factors based on available measurements vary from region to region, averaging as high as 17 g/h in Pennsylvania (from combining measurements of both Kang et al. (2016) and Pekney et al. (2018)) to as low as 2.4×10^{-3} g/h in Utah. (Townsend-Small et al., 2016) In addition, the flow rates vary depending on the attributes of the well such as the plugging status and whether the well produced gas and/or oil (Kang et al., 2016; Townsend-Small et al., 2016; Williams et al., 2019; Riddick et al., 2019b; Pekney et al., 2018; Boothroyd et al., 2016; Schout et al., 2019; Ingraffea et al., 2014). In general, it appears that plugged wells emit less methane than unplugged wells (Kang et al., 2016; Riddick et al., 2019b; Townsend-Small et al., 2016; Pekney et al., 2018). However, there are subcategories of plugged wells such as those that are in coal areas and vented by regulation that emit as much as unplugged wells (Kang et al., 2016). In terms of the well type, gas wells have been shown to emit more methane than oil or combined oil and gas wells. Overall, it is important to consider regional variations, the plugging status, and the well type in the development of emission factors for AOG wells.

There are many ways in which emission factors can be defined and applied. The latest national inventory reports for Canada and the U.S. estimate methane emissions from AOG wells using emission factors derived from two studies (Kang et al., 2016; Townsend-Small et al., 2016). Emission factors for both the U.S. and Canada are grouped according to the plugging status (i.e., unplugged or plugged). In the U.S., emission factors are divided into two regions: the Appalachian region and the rest of the U.S. No spatial division is applied for the Canadian emission factors, which implies that emissions per well are assumed to be similar throughout the country. However, studies such as Watson and Bachu (2009) highlight a geographic region as a factor with a major impact on the occurrence of gas migration and/or surface casing vent flow (indicators of well leakage) in wells. Furthermore, oil and gas basins have different properties and current/historical regulatory practices

vary among provinces/states/territories. (Saint-Vincent et al., 2020). To better estimate emissions and reduce uncertainties, there is a need to understand how the different estimation approaches impact methane emission estimates for AOG wells.

In addition to emission factors, methane emission estimates depend on the well count. Previous studies estimate the number of documented AOG wells in the U.S. at around 3,200,000 for 2018 (United States Environmental Protection Agency, 2021a). To the best of our knowledge, there are no published studies that estimate the total number of AOG wells in Canada. In both countries, thousands of wells, especially those drilled prior to the 1950s, are likely to be undocumented (Kang et al., 2016; Calvert and Smith, 1994; Dilmore et al., 2015). For example, a study by Kang et al. (2016) showed that AOG well counts in Pennsylvania are likely in the range of 470,000 to 750,000, more than ten times higher than the 48,144 recorded by the Pennsylvania Department of Environmental Protection. Similarly, the number of AOG wells in West Virginia is estimated in the range of 60,000 to 760,000 by Riddick et al. (2019b) which places the 70,000 reported by the West Virginia Department of Environmental Protection on the low end of this range. Given the large uncertainty in well counts, we consider them in evaluating uncertainties in methane emissions from AOG wells.

In this work, we estimate methane emissions from AOG wells in Canada and the U.S. and evaluate uncertainties considering all available measurement and well count data. We develop five scenarios to attribute emission factors to different regions with corresponding probability density functions to estimate annual emissions and uncertainties using Monte Carlo simulations. For the emission factor development, we include previously unavailable field measurement data from Oklahoma and British Columbia, which partially address the lack of measurements from the southern region of the U.S. and an overall lack of empirical data from Canada. We provide estimates of well counts grouped into the well type and plugging status and explore how AOG well counts have changed over time. Finally, we calculate annual emissions from AOG wells across Canada and the U.S. and discuss how future measurements and data analysis can reduce uncertainties and increase the representativeness of regional methane emission measurements at national scales.

4.2 Methods

4.2.1 Methane flow rate measurements and emission factors

We compile and analyze a total of 598 methane flow rate measurements across seven states and two provinces: Ohio (Townsend-Small et al., 2016), Wyoming (Townsend-Small et al., 2016), Utah (Townsend-Small et al., 2016), Colorado (Townsend-Small et al., 2016), Pennsylvania (Kang et al., 2016, 2014; Pekney et al., 2018), West Virginia (Riddick et al., 2019b), New Brunswick (Williams et al., 2019), Oklahoma, and British Columbia. Emission factors are calculated from all six published studies (Kang et al., 2014, 2016; Townsend-Small et al., 2016; Pekney et al., 2018; Riddick et al., 2019b; Williams et al., 2019) and data from 17 unplugged wells that we measured in British Columbia and 53 unplugged wells from Oklahoma. These measurements are grouped according to the plugging status (i.e., unplugged and plugged) and well type (i.e. gas, combined oil and gas, and unknown) and averaged to obtain emission factors. It should be noted that we use the term “well classification” to refer to a combination of the well type and plugging status. We group measurements from oil wells and combined oil and gas (O&G) wells to obtain one emission factor representing both types and hereafter referred them to as O&G wells, as many data sources do not distinguish between these two types. For unknown well types, we develop an emission factor based on all available measurements regardless of the well type. In total, there are 148 measurements from gas wells and 196 from combined oil and gas wells, with the remaining 254 measurements from wells with the unknown well type.

4.2.2 Number of AOG wells

We define AOG wells as wells with no recent production, which follows the definitions used by both the Canadian and U.S. inventories (United States Environmental Protection Agency, 2021a; Environment and Climate Change Canada, 2021) that include terms such as suspended, idle, orphaned, plugged, dormant, deserted, inactive, junked, temporarily abandoned, and shut-in.

We use two approaches to determine the number of AOG wells. First, we analyze AOG wells from 47 provincial, territorial, and state repositories. The source of each of these databases are provided in the SI - Table 4.3. Second, we estimate the number of AOG wells from historical documents and national agencies/organizations (Canadian Association of Petroleum Producers, 2020; U.S. Energy Information Administration, 2020). Using the data from provincial/state/territorial agencies, we categorize AOG wells based on the plugging status and well type depending on the data reported by regional agencies. If no plugging status is reported, we assign the dataset-wide percentage of unplugged and plugged wells based on the total number of unplugged and plugged wells gathered from state/provincial/territorial datasets for that country. If no well type is reported, we use the ratio of currently active well types in 2018 reported by the Canadian Association of Petroleum Producers (CAPP) or the Energy Information Agency (EIA). In Canada, 3% of wells do not report the plugging status and 23% do not report the well type. In the U.S., 23% of wells do not report the plugging status and 7% of wells do not report the well type. Using historical documents and data from the CAPP and EIA, we estimate the total nationwide number of AOG wells based on the number of active wells subtracted from the total number of drilled wells in each country up to 2018 (Canadian Association of Petroleum Producers, 2020; U.S. Energy Information Administration, 2020), similar to the methodology of Brandt et al. (2016) for AOG wells. For Canada, we scale the number of AOG wells for each well classification by the total number of AOG wells obtained from the CAPP (Canadian Association of Petroleum Producers, 2020). For the U.S., we scale the number of AOG wells for each well classification by the total number of AOG wells obtained using data from the EIA and Brandt et al. (2016) with the exception of Oklahoma, Pennsylvania, and West Virginia. For Pennsylvania and West Virginia, we use the midpoint well counts of Kang et al. (2016) and Riddick et al. (2019b) which are 610,000 for Pennsylvania and 410,000 for West Virginia. For Oklahoma, we use a count of 280,000, which is the midpoint between the state database total (140,283) and a well count from the Independent Petroleum Association of America (422,826) (Independent Petroleum Association of America, 2016). Total AOG well counts for each province and state are provided in the SI - Table 4.3.

4.2.3 Emission factor attribution scenarios

We develop five different scenarios to assign emission factors for AOG wells to regions in the U.S. and Canada (Table 4.1 and SI - Figure 4.5). In the first scenario (1), we develop six nationwide emission factors for each country corresponding to the two plugging statuses and three well types. For the second scenario (2), we apply 17 emission factors provided in region-specific studies for four states and one province and apply nationwide emission factors to remaining regions. In the third scenario (3), we divide the U.S. and Canada broadly into the eastern and western regions, resulting in 24 emission factors. The western U.S. is determined to be all states west of the Texas–Louisiana and Minnesota–North Dakota state boundaries, while western Canada represents provinces/territories to the west of the Saskatchewan–Manitoba and Northwest Territories and Nunavut boundaries. These divisions are chosen to evenly distribute measurement data. In the fourth scenario (4), we divide the U.S. into northern and southern regions by the state boundary closest to the 35° latitude, which reflects the distributions of measurement data. In the fifth and final scenario (5), we use 15 emission factors to regions based on oil and gas basins (SI - Figure 4.5). The basin-specific emission factors can capture impacts of geological factors, operators, policies, and the history of oil and gas development. Because of the lack of empirical data from Canada, we use all available measurement data from the U.S. and Canada to develop emission factors for the first three scenarios for Canada. We do not make estimates for Canada using the fourth and fifth scenarios. We use the five different attribution scenarios to show how different approaches can affect annual emission estimates rather than identify a single scenario as the most representative or “best” estimate. As new data are gathered, the representativity of emission estimates for AOG wells will improve and other emission factor attribution scenarios may be appropriate.

Following the emission factor attribution scenarios, we determine emission factors based on measurement data for each state/province (Table 4.1). In cases where data from multiple studies are used to calculate emission factors, we use 4.1:

$$EF_{X,a} = \frac{\sum_{i=1} M_{X,i} \times N_{X,i}}{\sum_{i=1} N_{X,i}} \quad (4.1)$$

Table 4.1: Emission factor spatial attribution scenarios in the U.S. and Canada as described in the Methods section.^a

		Emission factors (g/h)					
United States		Unplugged			Plugged		
Scenario	Region	O&G	Gas	All	O&G	Gas	All
1	U.S.	13 (101)	23 (60)	11 (293)	5.1×10^{-2} (80)	4.8 (84)	1.6 (276)
2	Oklahoma	14 (34)	22 (19)	17 (53)	5.1×10^{-2} (80)	4.8 (84)	1.6 (276)
	Pennsylvania	12 (56)	48 (19)	21 (75)	0.17 (22)	18 (22)	9.6 (44)
	Utah	13 (101)	23 (60)	11 (293)	5.1×10^{-2b} (80)	4.1×10^{-3} (51)	2.4×10^{-3} (88)
	West Virginia	13 (101)	23 (60)	3.2 (147)	5.1×10^{-2} (80)	4.8 (84)	0.10 (112)
	Colorado	13 (101)	23 (60)	11 (293)	5.1×10^{-2} (80)	4.8 (84)	1.6 (276) ^b
	Remainder	13 (101)	23 (60)	11 (293)	5.1×10^{-2} (80)	4.8 (84)	1.6 (276)
3	East	14 (62)	28 (34)	9.6 (228)	0.13 (28)	18 (22)	2.8 (162)
	West	13 (39)	17 (26)	15 (65)	5.1×10^{-2} (80)	4.8 (84)	1.8×10^{-3} (114)
4	North	12 (56)	24 (41)	8.8 (257)	6.2×10^{-2} (59)	4.8 (84)	1.6 (276)
	South	14 (34)	22 (19)	17 (53)	5.1×10^{-2} (80)	4.8 (84)	1.6 (276)
5	AP ^c	14 (62)	28 (34)	9.6 (228)	0.13 (28)	18 (22)	2.8 (162)
	AN ^c	13 (101)	22 (19)	16 (26)	5.1×10^{-2} (80)	4.8 (84)	1.6 (276)
	UI ^c	13 (101)	23 (60)	11 (293)	5.1×10^{-2} (80) ^b	4.1×10^{-3} (51)	2.4×10^{-3}
	DE ^c	13 (101)	23 (60)	11 (293)	5.1×10^{-2} (80)	4.8 (84)	1.6 (276) ^b
	PR/DE ^c	13 (101)	23 (60)	11 (293)	5.1×10^{-2} (80)	4.8 (84)	1.6 (276) ^b
	AN/UI/DE ^c	13 (101)	17 (25)	12 (38)	5.1×10^{-2} (80) ^b	3.7×10^{-3} (57)	2.0×10^{-3} (104)
	Remainder	13 (101)	23 (60)	11 (293)	5.1×10^{-2} (80)	4.8 (84)	1.6 (276)
		Emission factors (g/h)					
Canada		Unplugged			Plugged		
Scenario	Region	O&G	Gas	All	O&G	Gas	All
1	Canada	12 (113)	22 (65)	10 (310)	4.6×10^{-2} (92)	4.8 (84)	1.5 (288)
2	British Columbia	12 (113)	22 (65)	0.15 (17)	4.6×10^{-2} (92)	4.8 (84)	1.5 (288)
	Remainder	12 (113)	22 (65)	10 (310)	4.6×10^{-2} (92)	4.8 (84)	1.5 (288)
3	East	14 (62)	28 (34)	9.6 (228)	0.12 (40)	18 (22)	2.5 (174)
	West	14 (51)	15 (31)	12 (82)	5.1×10^{-2} (80)	4.8 (84)	1.8×10^{-3} (114)

^aThe number of measurements used to calculate each emission factor is shown in parenthesis. “Remainder” refers to the states/provinces not specifically identified in the scenario. Maps of spatial attribution scenarios are provided in the SI - Figure 4.5.

^bEmission factor based on the total dataset average based on the reasoning outlined in the SI - Section 4.6.1.

^cAbbreviations for basin types: AP = Appalachian, AN = Anadarko, UI = Uintah, DE = Denver, PR = Powder River.

, where $EF_{X,a}$ is the emission factor for well classification X and area a , $M_{X,i}$ is the mean methane flow rate from study i and well classification X , $N_{X,i}$ is the number of measurements for the well classification X from study i , and i represents a study associated with region a .

4.2.4 Uncertainty analysis

We evaluate uncertainties in annual methane emissions from AOG wells using Monte Carlo simulations of the emission factors and well counts following approach 2 of the IPCC guidelines (Calvo Buendia et al., 2019). First, methane emissions are aggregated for a region and well classification following the emission factor attribution scenarios. We use bootstrapping with 2000 iterations with replacement to resample our methane flow rate data to obtain a distribution of emission factors. The bootstrapped distribution of emission factors is fitted to a probability density function using the “fitdistrplus” package in R (Delignette-Muller and Dutang, 2015) to obtain parameters to be used in the Monte Carlo simulations. We assume an asymmetrical triangle distribution for well counts ranging from the state/provincial/territorial database well number to an upper range determined either from a secondary source (e.g., research articles, ?) or a default of +100% (SI - Section 4.6.2). Using these distributions, we obtain a set of 1,000,000 estimates of annual methane emissions. We determine the lower and upper limit in methane emission estimates from the 2.5th and 97.5th percentile values of the simulated annual methane emissions. These steps are repeated for each emission factor attribution scenario.

4.3 Results

4.3.1 Methane flow rates and emission factors

Available measurements of methane flow rates are from seven states and two provinces and cover the two plugging types (unplugged and plugged) and three well types (O&G, gas-only, and unknown) that we use in our analysis. In terms of regions, most measurements are from West Vir-

ginia (n = 259) and Pennsylvania (n = 119), with the smallest number of measurements being from Ohio (n = 12), New Brunswick (n = 12), and Wyoming (n = 12). There are 288 measurements from plugged wells, with 85 of those measurements being from plugged gas wells, 92 from O&G wells, and 112 from an unknown well type. A total of 310 unplugged wells have been measured, of which 65 are unplugged gas wells, 113 are O&G wells, and 132 are from an unknown well type.

Empirical cumulative distributions from all well types and statuses exhibit heavy-tailed distributions (Figure 4.1). For plugged wells, we find that 99% of emissions are attributed to 10% of plugged wells. Unplugged wells show slightly lower percentages, with unplugged gas wells having 84% of cumulative methane emissions attributed to 10% of wells. Overall, the top 10% of AOG wells are responsible for 96% of cumulative methane emissions.

Based on our synthesis of all available methane emission data from AOG wells, average methane flow rates range from 1.8×10^{-3} g/h to 48 g/h based on the plugging status, well type, and region (Table 4.1). In terms of the plugging status, unplugged gas wells are the highest methane emitters overall, averaging 11 g/h, compared to 1.6 g/h from plugged wells. In terms of the well type, abandoned gas wells emit on average 12 g/h methane, which is almost double the emissions from abandoned O&G wells at 6.6 g/h. In addition to dependence on well classifications, emission factors also vary regionally. Notably, unplugged O&G wells in Ohio (i.e., 34 g/h) emit more methane than unplugged O&G wells in Oklahoma (i.e., 14 g/h), Pennsylvania (i.e., 12 g/h), Colorado (i.e., 3.2 g/h), and British Columbia (i.e., 0.14 g/h) (Table 4.1). Plugged gas wells also show regional variability, with plugged gas wells in Pennsylvania averaging 18 g/h compared to 4.1×10^{-3} g/h in Utah.

4.3.2 Number of AOG wells

We estimate the total number of AOG wells to be 4,047,809 for the U.S. based on our compilation of state/provincial/territorial databases, research articles, and national repositories of drilled and active wells. In the U.S., compiling regional databases alone gives a total of 2,485,445 AOG wells, leaving 1,562,364 AOG wells undocumented by the relevant state agencies. For Canada,

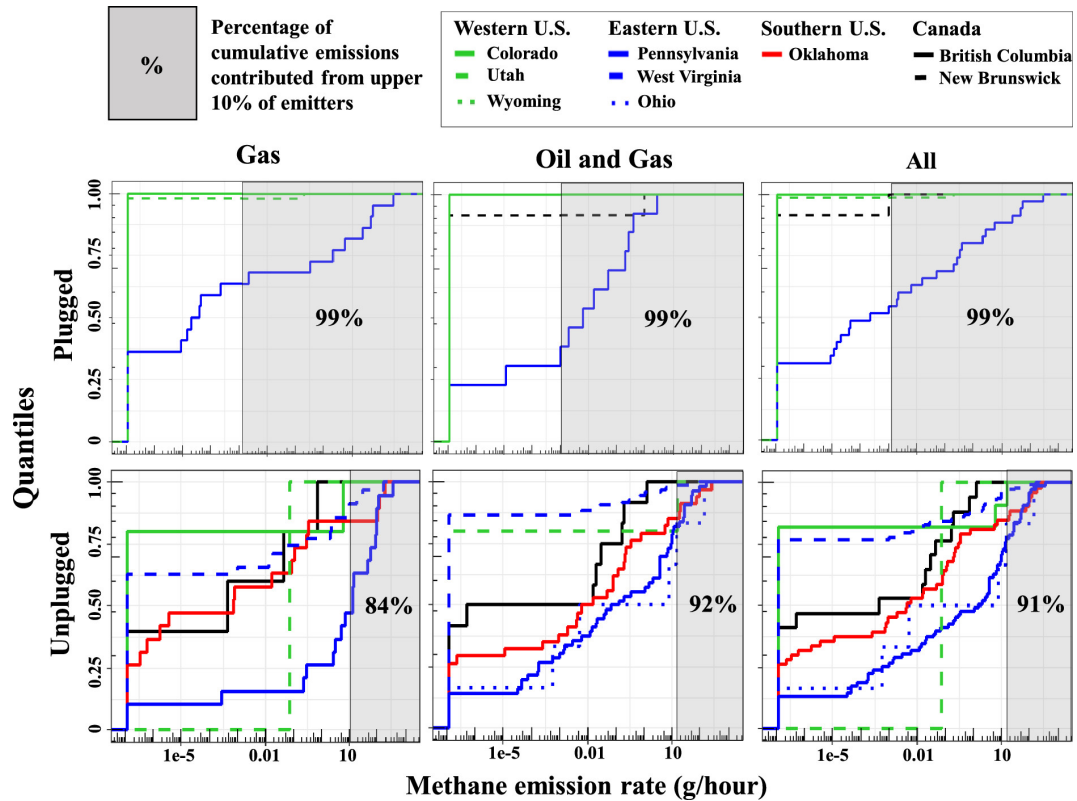


Figure 4.1: Empirical cumulative distributions of measured methane flow rate from unplugged (top) and plugged (bottom) AOG wells in the U.S. and Canada. Each curve represents a state/province. Blue and green curves represent eastern and western states in the U.S., respectively. Red curves represent Oklahoma, which is in the southern U.S. Black curves represent Canadian provinces. Shaded regions in each plot represent the 90–100th percentile of methane emission rates for that group, with the annotation showing the percentage of cumulative emissions, the top 10% of AOG wells.

a compilation of regional databases gives a total of 312,445 AOG wells. Based on the difference in cumulative drilled wells and active wells provided by the CAPP (Canadian Association of Petroleum Producers, 2020), we estimate 372,925 AOG wells in Canada, meaning at least 60,483 wells are not included in databases of provincial/territorial agencies. The figure 372,925 is likely an underestimation of the total number of AOG wells in Canada because the total number of drilled wells provided by CAPP is limited to those drilled from 1955 onward and there are historical documents confirming that oil and gas activity in Canada began in the 1850s (Brownsey, 2015; Howie, 1968).

Most wells in the U.S. are unplugged wells with an unknown type (1,044,976 wells). This is followed by 836,850 plugged O&G wells, 693,921 unplugged O&G wells, 558,019 unplugged gas wells, 488,751 plugged wells of unknown type, and 425,291 plugged gas wells. In Canada, the well classification with the largest number of wells is plugged wells with an unknown type at 74,113 wells, followed by 65,316 unplugged O&G wells, 63,377 unplugged wells with an unknown type, 61,773 unplugged gas wells, 55,067 plugged O&G wells, and 53,279 plugged gas wells. Although we assign 37% of AOG wells in Canada and the U.S. to the unknown well type, they are still assigned an emission factor based on the reported plugging statuses of all AOG wells, which is the current approach used in the Canadian and U.S. inventories. A total of 37% of wells are assigned an unknown well type.

States with the highest AOG well counts in the U.S. are Texas, Pennsylvania, Kansas, West Virginia, and Oklahoma, which collectively account for 65% of the total AOG well count in the U.S. In Canada, Alberta and Saskatchewan contain 87% of AOG wells in the nation, with the majority of the remaining wells located in British Columbia, Ontario, and Manitoba. Of these ten states/provinces across Canada and the U.S., there are direct methane flow rate measurements for only three states (Pennsylvania, West Virginia, and Oklahoma) and one province (British Columbia). These measurements collectively represent less than 0.01% of all AOG wells in Canada and the U.S. (Figure 4.2).

The number of AOG wells is increasing in Canada and the U.S. (Figure 4.3). In Canada, the largest year-to-year increase in AOG wells since 1956 was in 2015 with an increase of 27,000 wells, whereas the smallest was in 2012 with 100 wells. A linear regression shows an average of 5800 wells abandoned per year from 1956 to 2012. In Canada, both the variability and annual growth rate of wells have increased since the mid 1950's, averaging 3200 wells abandoned per year from 1956 to 1986 and 8800 wells abandoned per year from 1987 to 2017. In the U.S. from 2000 to 2013, an average of 18,600 wells were abandoned per year, with a maximum of 35,500 in 2008 and a minimum of 4000 in 2009. The negative numbers of AOG wells drilled per year, represent a decrease in total AOG well numbers, and is likely a result of idle/inactive wells being re-entered

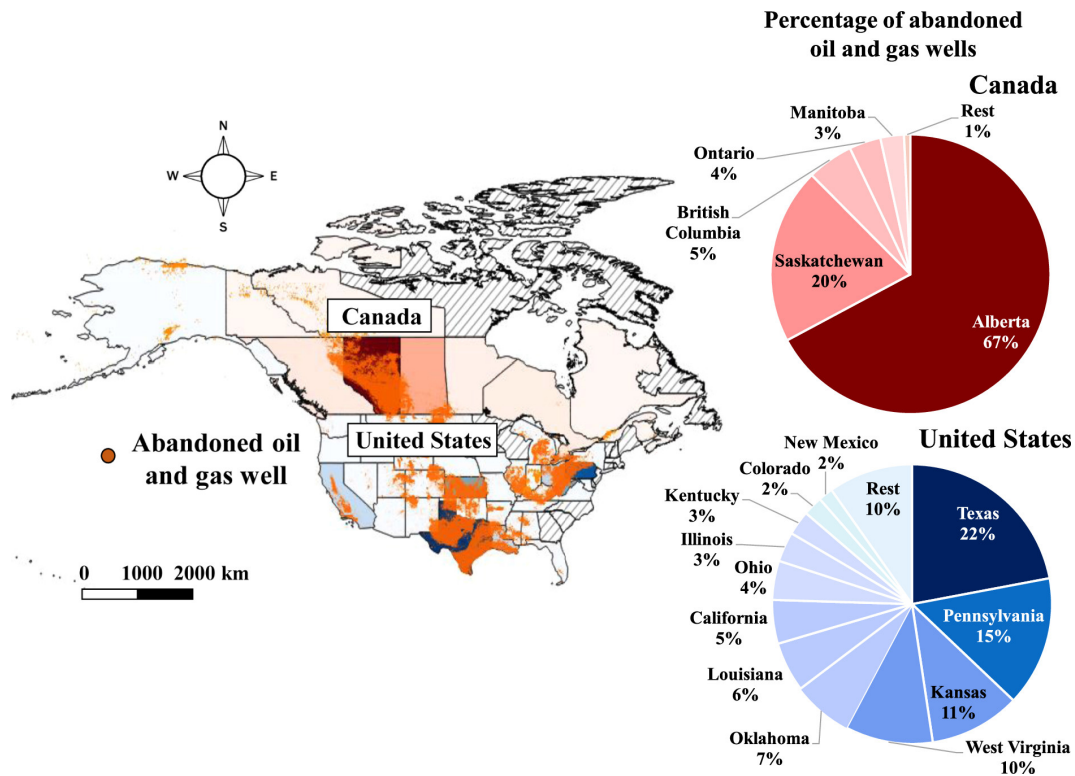


Figure 4.2: Map of all active and AOG onshore well locations (left) gathered from publicly available databases for the U.S. and Canada. Pie charts (right) show percentages of AOG wells in each state/province/territory relative to those across the country. States/provinces/territories in the map and the pie charts are presented using the same color scheme.

into the production life cycle. Overall, the growing number of AOG wells implies that methane emissions from AOG wells are likely to be increasing.

4.3.3 National methane emission estimates

We estimate annual methane emissions from AOG wells across the U.S. to be 0.32 (1—Total) to 0.36 (3—east/west) MMt of methane emitted annually (Figure 4.4). All five scenarios show higher methane emissions than the U.S. EPA’s estimate for 2018 of 0.28 MMt of methane per year. The states with the most methane emitted annually, on average, are Pennsylvania (0.088 MMt of methane), Texas (0.086 MMt of methane), West Virginia (0.051 MMt of methane), and Kansas

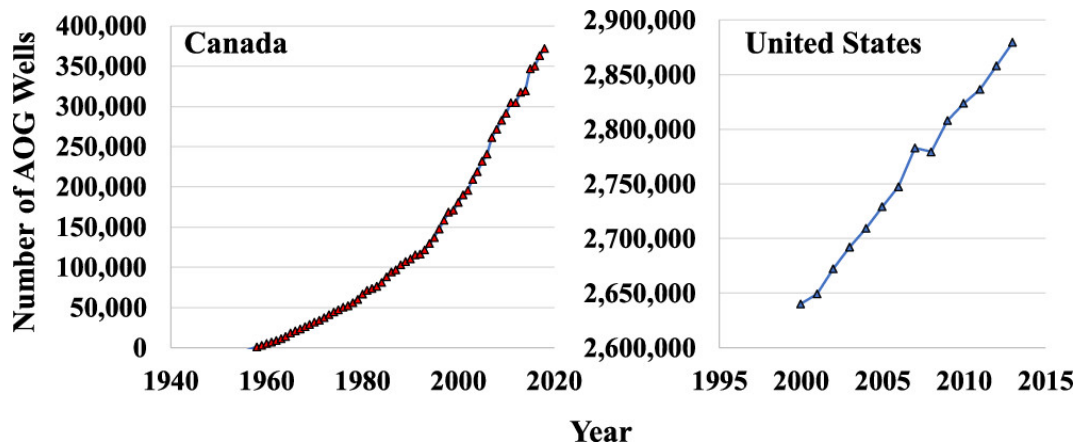


Figure 4.3: Annual growth rates of AOG well counts in Canada from 1956 to 2017 and the U.S. from 2000 to 2013. The count of AOG wells calculated from the difference between active and cumulative drilled wells for that year.

(0.027 MMt of methane). Breakdowns of emissions by the well type and plugging status for all five scenarios are shown in the SI - Figure 4.6.

Annual methane emissions from AOG wells in Canada average at 0.026 MMt of methane (Figure 4.4) and range between 0.027 MMt of methane (1—total, 2—region) and 0.024 MMt of methane (3—east/west). All three scenarios indicate that emissions are nearly three times the 10×10^{-2} MMt of methane estimated by Environment and Climate Change Canada for 2018. (2) The primary region contributing to methane emissions from AOG wells is Alberta (0.022 MMt of methane), followed by Saskatchewan (4.7×10^{-3} MMt of methane) and British Columbia (1.8×10^{-3} MMt of methane) (SI - Figure 4.7).

The results of our uncertainty analysis show upper uncertainty bounds ranging from +100 to +140% and lower bounds of 60 to 70% for the U.S. We find that the upper uncertainty bounds are roughly half of the +218% reported by the U.S. EPA (United States Environmental Protection Agency, 2021b). For Canada, the upper uncertainty bounds of +160 to +190% are higher than the +69.9% reported by ECCC (Environment and Climate Change Canada, 2021), with lower uncertainty bounds of 50% on average, which are similar to the 47% reported by ECCC (Environment and Climate Change Canada, 2021). However, these ranges do not account for uncertainties arising from differences between emission factor attribution scenarios, meaning that uncertainties are

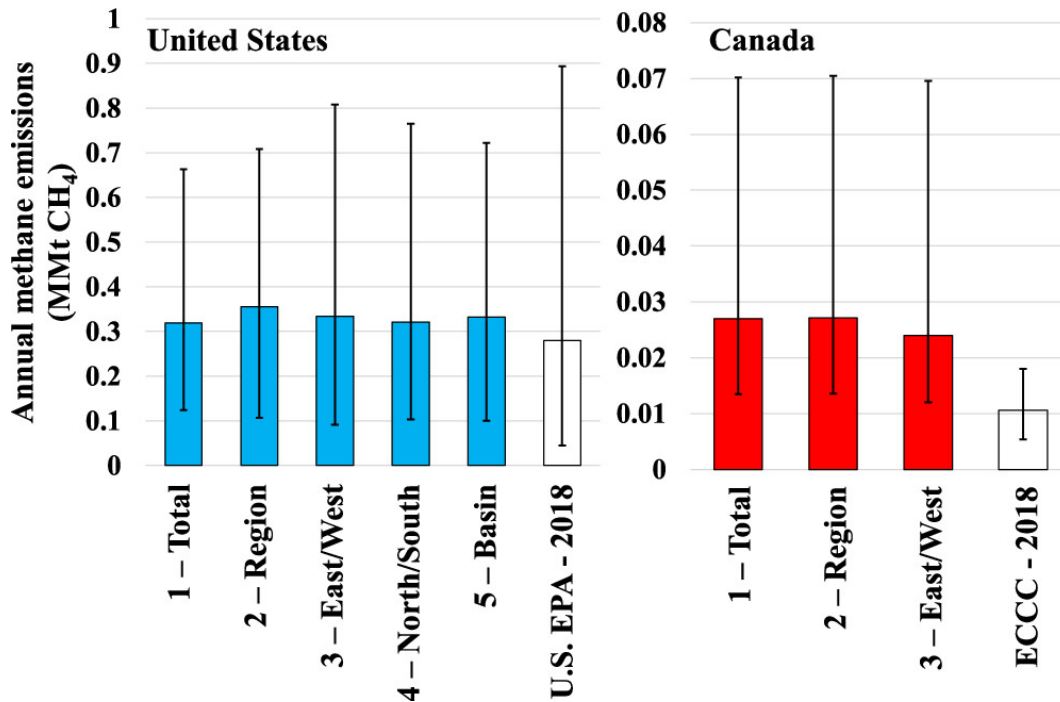


Figure 4.4: Bar plot of annual methane emissions (expressed in million metric tonnes of methane) from AOG wells from the U.S. (blue bars), Canada (red bars), and the most recent national inventory estimates (white bars). The 95% uncertainties are shown in black lines.

likely to be higher than those reported. In short, compared to previous national inventories, we find that uncertainties in methane emissions from AOG wells are higher in Canada and lower in the U.S.

4.4 Discussion

Our estimates for annual methane emissions from AOG wells are consistently higher than those reported in the latest inventory report by 150% (Environment and Climate Change Canada, 2021) for Canada and by 20% for the U.S. (United States Environmental Protection Agency, 2021a). The reasons for the larger degree of underestimation in the Canadian inventory are due to our use of a larger number of wells and higher emission factors. In contrast, the difference in the U.S. inventory is primarily due to our use of a larger number of wells. Nevertheless, emissions factors for the “entire U.S.” relied on data that were not distributed throughout the country but focused on

western states, Wyoming, Utah, and Colorado and missing data from major oil- and gas-producing states such as Texas, Oklahoma, and California.

We find uncertainty ranges for methane emissions from AOG wells to be lower than those of the latest national inventory report for the U.S. but higher than those in the Canadian inventory. Methane emissions from AOG wells remain the most uncertain anthropogenic methane source in the U.S. and increase to the most uncertain anthropogenic methane source in the Canadian national GHG inventory. Methane emissions from AOG wells correspond to 1–4% of methane emissions from the energy sector in the Canadian inventory and 1–13% in the U.S. inventory. Overall, methane emissions from AOG wells are higher than previous estimates and remain one of the most uncertain anthropogenic methane emission sources.

There is an overall lack of measurement data in Canada and the U.S., with less than 0.01% of AOG wells in the U.S. and Canada measured to date. The few available emission measurements are not in the states/provinces where the majority of emissions from AOG wells are found such as Texas and Alberta. Therefore, to reduce the high uncertainties, these regions should be targeted in future measurement studies.

All available measurements show statistically heavy-tailed distributions, similar to active operations (Ingraffea et al., 2014; Brandt et al., 2016). Unplugged gas wells show the least-skewed distribution in methane flow rates with 84% of cumulative emissions attributed to the top 10% of emitters, compared to the remaining well types and plugging statuses which range from 91–99% (Figure 4.1). Moreover, unplugged gas wells have the highest emission factor among any of the well classifications.

Only 10 high-emitting wells with over 100 g/h have been measured to date, yet they contribute roughly 65% of cumulative emissions (i.e., superemitters) from all studies. Although mitigating a small number of sites can reduce a large percentage of methane emissions, it also means that AOG wells with methane flow rates much higher than those measured to date may exist. Gathering new measurements from regions without prior data may greatly enhance the representativeness of emission factors, help characterize and identify the highest emitters that heavily influence emission

factors, and provide information on how these emissions are distributed regionally and across well classifications.

Emission factors are shown to vary regionally and across well classifications for the five scenarios we employ. Unplugged oil wells in West Virginia emit less methane than those in Pennsylvania and Oklahoma, and plugged gas wells in Pennsylvania emit an order of magnitude more methane than those in other regions. This difference can be explained by the fact that plugged wells in coal areas in Pennsylvania are vented, highlighting how regional practices can influence emission factors. In other regions, plugged wells emit much less methane than unplugged wells, which highlights the general effectiveness of plugging procedures in preventing methane migration to the atmosphere. In addition, there are a number of factors that could influence methane emissions from AOG wells that are not investigated in this work. Well-specific factors such as the well age (Watson and Bachu, 2009), abandonment date (Watson and Bachu, 2009), well bore deviation (Watson and Bachu, 2009), well platform (i.e., onshore vs offshore) (Yacovitch et al., 2020; Riddick et al., 2019a; Gorchoy Negron et al., 2020), and external factors (e.g., earthquakes) (Kang et al., 2019) could control methane emissions from AOG wells, meaning that emission factors may need to reflect these relationships.

A large source of uncertainty in current methane emission inventories is the number of wells. Both Kang et al. (2016) and Riddick et al. (2019b) show that regional databases are likely underestimating well counts by a factor of ten for Pennsylvania and West Virginia. If undocumented wells for all states/provinces/territories follow the same trends as observed in Pennsylvania and West Virginia, the uncertainty ranges we employ to well counts may still be underestimating the uncertainty in well numbers. Historical analyses of the many oil- and gas-producing regions could help narrow these ranges in AOG well numbers. Alternative approaches such as helicopters, unmanned aerial vehicles, and ground-based magnetic surveys could also provide reasonable approximations of undocumented well numbers (Pekney et al., 2018; Saint-Vincent et al., 2020; ?). Overall, the number of AOG wells remains an uncertain input in the estimation of annual methane emissions.

A 60-year analysis of wells abandoned annually in Canada shows that the growth rate and variability of AOG wells drilled per year have almost tripled from 1956–1986 compared to 1987–2018 (Figure 4.3). Therefore, it is important to evaluate mitigation strategies such as well plugging, re-entering unplugged wells into the production life cycle or for alternative uses (e.g., geothermal), or reducing the number of new wells drilled. In order to lower methane emissions from AOG wells, it is critical that AOG wells be plugged according to modern standards, that idle/suspended/dormant wells be either plugged or mitigated without remaining unplugged and inactive for extended periods of time, and that undocumented wells are located and characterized (Saint-Vincent et al., 2020; Pekney et al., 2018; Hammack et al., 2016).

Methane emissions from AOG wells are currently the 10th and 11th largest anthropogenic methane emission sources in the U.S. and Canada, respectively. The emissions are highly uncertain and are expected to increase in the future. Therefore, it is important to accurately estimate methane emissions from AOG wells. To do this, efforts are needed to ensure that (a) emission factors represent the wide range of regions and well classifications, (b) well counts are accurate, and (c) both emission factors and well counts are applied in a way that best represents methane emissions from the millions of AOG wells across the U.S., Canada, and elsewhere.

4.5 Acknowledgements

This research was supported by funding from the Fonds de Recherche du Quebec—Nature et Technologie Support for New Academics grant to M.K., the McGill Engineering Doctoral Award to J.P.W., the McGill Graduate Mobility Award to J.P.W., and McGill University. We thank Ziming Wang for his help in data collection and ArcGIS data analysis.

4.6 Supplementary information

4.6.1 Treatment of zeroes

The detection limit for flow rates varies between the studies. All studies used some form of well screening using portable gas detectors to measure atmospheric methane concentrations on the well sites (Kang et al., 2014, 2016; Williams et al., 2019; Pekney et al., 2018; Riddick et al., 2019b) followed by direct methane flow rate measurements using chambers. Townsend-Small et al. (2016) used the screening step to select wells at which chambers are deployed to measure methane emission rates. If methane concentrations above background are not detected during the screening step, Townsend-Small et al. (2016) present the methane flow rate as zero. In contrast, Kang et al. (2016), Riddick et al. (2019b), Pekney et al. (2018), and Williams et al. (2019) deployed chambers at all wells. Therefore, zeros in Townsend-Small et al. (2016) are different from those in other studies presented in this work. While emissions may be minimal (i.e. ≤ 0.1 g/hour) from these wells showing no atmospheric methane enhancements, the true methane flow rates from these sites are not likely to be 0 g/hour as reported. In the interest of preserving data and not skewing results, we keep all measurements from Townsend-Small et al. (2016), but in instances where emission factors are calculated solely from 0 ppmv methane screening results from their study (e.g. plugged O&G wells in Utah in Scenario 2), we assign the total dataset average of methane flow rate data for that well classification and region.

4.6.2 Uncertainties in the number of AOG wells

We use an asymmetrical triangular distribution based on two main assumptions: that the number of AOG wells in our study can be an underestimate and that the likelihood of the number of AOG wells being near the upper and lower bounds is lower. We select lower bounds based on the percent difference between our final well counts and the results of the state/provincial/territorial database compilation of well numbers which we assume to be all documented AOG wells. We estimate a default upper bound of +100% based on the upper range of undocumented wells from Okla-

homa, Pennsylvania, and West Virginia, including data on the estimated number of undocumented orphan wells from the Interstate Oil and Gas Compact Commission, compared to the number of documented wells for the respective states/provinces/territories (1,233,144).

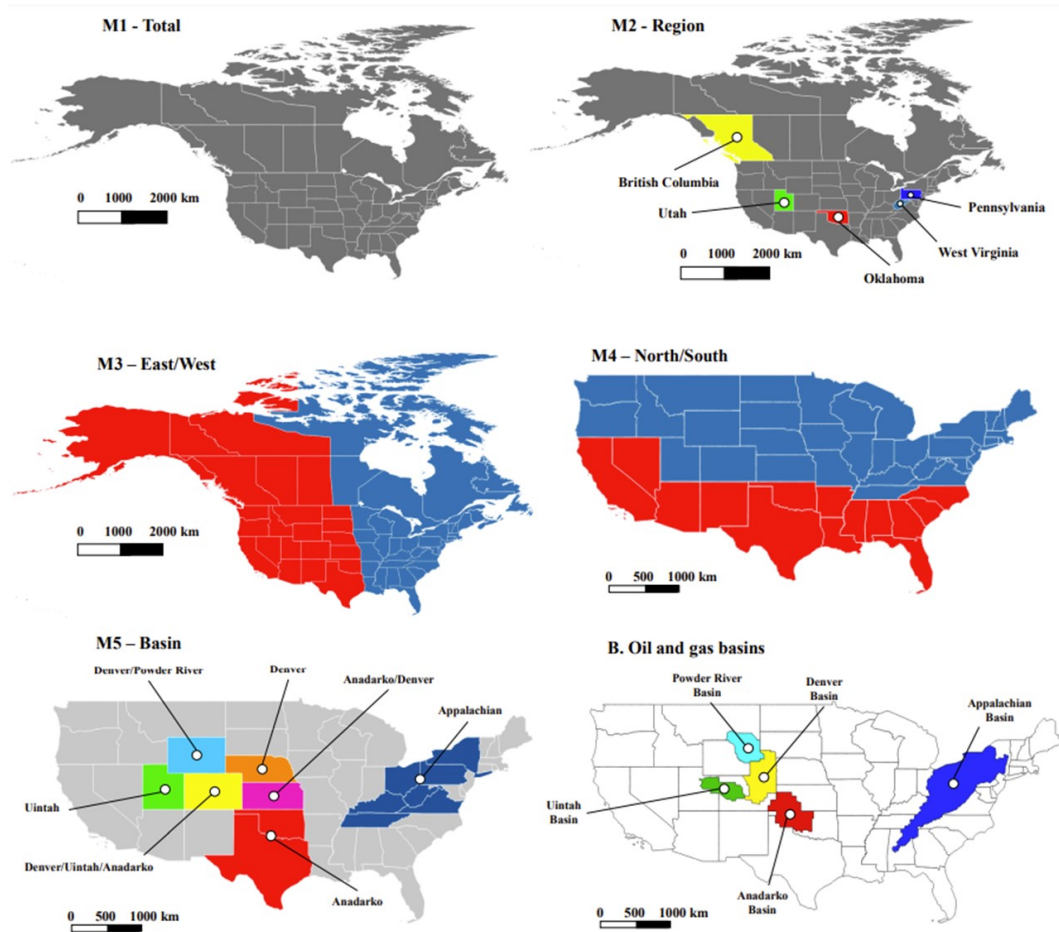


Figure 4.5: Maps of five emission factor attribution scenarios as summarized in Table 4.1 (M1 to M5), and map of oil and gas basins (bottom-right - B. Oil and gas basins) used to obtain emission factors for scenario M5. Oil and gas basin shapefiles are obtained from the United States Geological Survey: Central Energy Resources Science Center. Regions coloured grey represent the “U.S.” and “Canada” in M1 or “Remainder” in M2 and M5.

Table 4.2: Annual anthropogenic methane emissions and associated uncertainties for Canada and the U.S. All data is taken from the national greenhouse gas inventory reports for Canada (Environment and Climate Change Canada, 2021) and the U.S. (United States Environmental Protection Agency, 2021a).

Canada				
Rank - Emissions	Anthropogenic Emissions Source	2018 Methane Emissions (kt/yr)	Combined Uncertainty (%)	
1	Agriculture - Enteric Fermentation	966	22	
2	Fugitive Sources - Venting and Flaring	852	10	
3	Fugitive Sources - Oil and Gas	683	22	
4	Managed Waste Disposal Sites	491	40	
5	Agriculture - Manure Management	154	32	
6	Unmanaged Waste Disposal - Wood Waste Landfills	136	190	
7	Fuel Combustion - Other Sectors	129	15	
8	Manufacture of Solid Fuels and Other Energy Industries	100	140	
9	Fugitive Sources - Coal Mining and Handling	53.2	57	
10	Wastewater Treatment and Discharge	26.2	45	
11	Fuel Combustion - Off-Road	21.2	11	
12-13	Biological Treatment of Solid Waste - Composting	10.4	170	
12-13	Abandoned Oil and Gas Wells*	10.4	117	
14	Road Transportation (Gas, Diesel, Natural Gas, Propane)	9.84	110	
15	Fuel Combustion	8.04	15	
United States				
Rank - Emissions	Anthropogenic Emissions Source	2018 Methane Emissions (kt/yr)	Combined Uncertainty (%)	
1	Enteric Fermentation	7,100	29	
2	Natural Gas Systems	5,600	29	
3	Landfills	4,420	45	
4	Manure Management	2,470	38	
5	Coal Mining	2,110	29	
6	Petroleum Systems	1,450	65	
7	Wastewater Treatment	568	51	
8	Rice Cultivation	532	93	
9	Stationary Combustion	344	165	
10	Abandoned Oil and Gas Wells	280	302	
11	Abandoned Underground Coal Mines	248	35	
12	Mobile Combustion	124	35	
13	Composting	100	100	
14	Field Burning of Agricultural Residues	16.0	32	
15	Petrochemical Products	12.0	103	

*Abandoned Oil and Gas Wells are a sub-category of Fugitive Sources - Oil and Gas.

Table 4.3: Counts of unplugged and plugged AOG wells assigned to each state/province/territory in the U.S. and Canada with the corresponding data sources.

United States		
Region	AOG Wells	Source
Alabama	25,913	Geological Survey of Alabama O&G Board
Alaska	6,338	Alaska Oil and Gas Conservation Commission
Arizona	1,622	Arizona Oil and Gas Conservation Commission
Arkansas	13,696	Arkansas Oil and Gas Commission
California	204,769	California's Division of Oil, Gas, and Geothermal Resources
Colorado	91,075	Colorado Oil and Gas Conservation Commission
Florida	1,331	Florida Department of Environmental Protection
Idaho	25	Idaho Geological Survey and/or Idaho Department of Lands
Illinois	139,611	Illinois Natural Resources Geospatial Data Clearinghouse
Indiana	67,159	Indiana Department of Natural Resources
Iowa	334	Iowa Department of Natural Resources
Kansas	426,142	Kansas Geological Survey
Kentucky	114,643	Kentucky Geological Survey/University of Kentucky
Louisiana	232,917	Louisiana Department of Natural Resources
Maryland	24	Maryland Oil and Gas Viewer
Michigan	36,818	Michigan Department of Environmental Quality
Mississippi	30,286	Mississippi Oil and Gas Board
Missouri	5,694	Missouri Department of Natural Resources
Montana	50,086	Montana Board of Oil and Gas Conservation
Nebraska	6,349	Nebraska Oil and Gas Commission
Nevada	1,587	Nevada Commission on Mineral Resources
New Mexico	68,229	New Mexico Oil Conservation Division
New York	28,056	New York State Department of Environmental Conservation
North Dakota	30,341	North Dakota Department of Mineral Resources
Ohio	183,090	Ohio Department of Natural Resources
Oklahoma	280,034	Oklahoma Corporation Commission, IPAA
Oregon	968	State of Oregon Department of Geology and Mineral Industries
Pennsylvania	610,000	Pennsylvania Department of Environmental Protection, Kang et al. 2016
South Dakota	1,312	South Dakota Geological Survey
Tennessee	15,066	Tennessee Department of Environment and Conservation
Texas	891,718	Texas Railroad Commission
Utah	41,504	Utah Department of Natural Resources
Virginia	10,321	Virginia Department of Mines, Minerals, and Energy
Washington	1,295	Washington State Department of Natural Resources
West Virginia	410,000	West Virginia Department of Environmental Protection, Riddick et al. 2019
Wyoming	20,175	Wyoming Oil and Gas Conservation Commission
Canada		
Alberta	250,513	Alberta Energy Regulator - ST37: List of Wells in Alberta
British Columbia	19,930	British Columbia Oil and Gas Commission
Manitoba	10,139	Manitoba Petroleum: Interactive GIS Gallery
New Brunswick	346	Government of New Brunswick - Natural Resources and Energy Development
Nova Scotia	156	Geoscience Data and Maps - Nova Scotia Department of Energy
Ontario	13,626	Ontario Oil, Gas, and Salt Resources Library
Quebec	970	ArcGIS Home: Quebec Wells
Saskatchewan	75,955	Saskatchewan Mining and Petroleum GeoAtlas
Yukon	90	Yukon Government - Energy, Mines and Resources
Northwest Territories	1,168	NWT Government - Office of the Regulator of Oil and Gas Operations
Prince Edward Island	27	PEI - Transportation, Infrastructure, and Energy

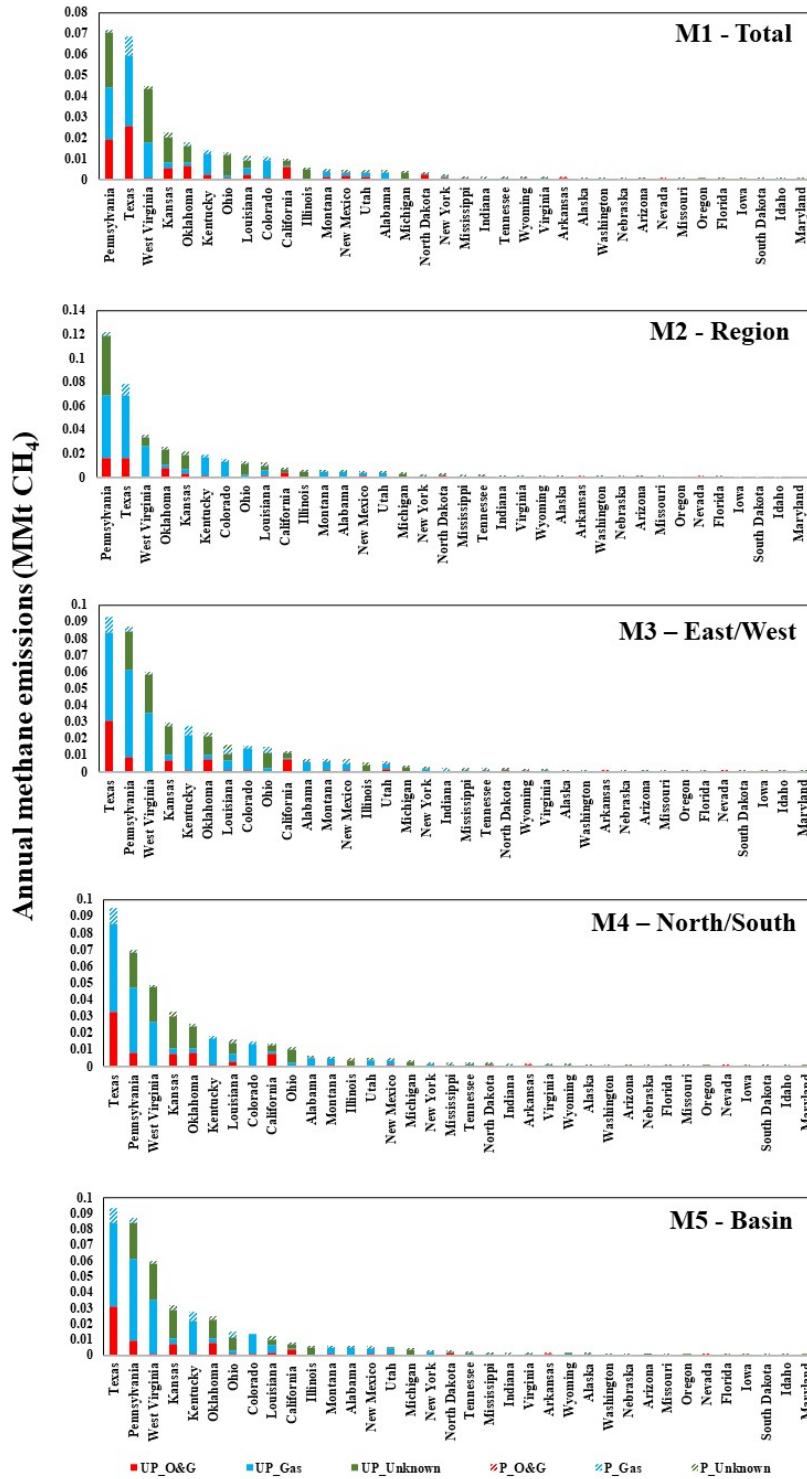


Figure 4.6: Barplots of methane emissions from each state in the U.S. based on well type and plugging status for all five emission factor attribution scenarios. Note: UP = Unplugged, P = Plugged, O&G = Oil and gas.

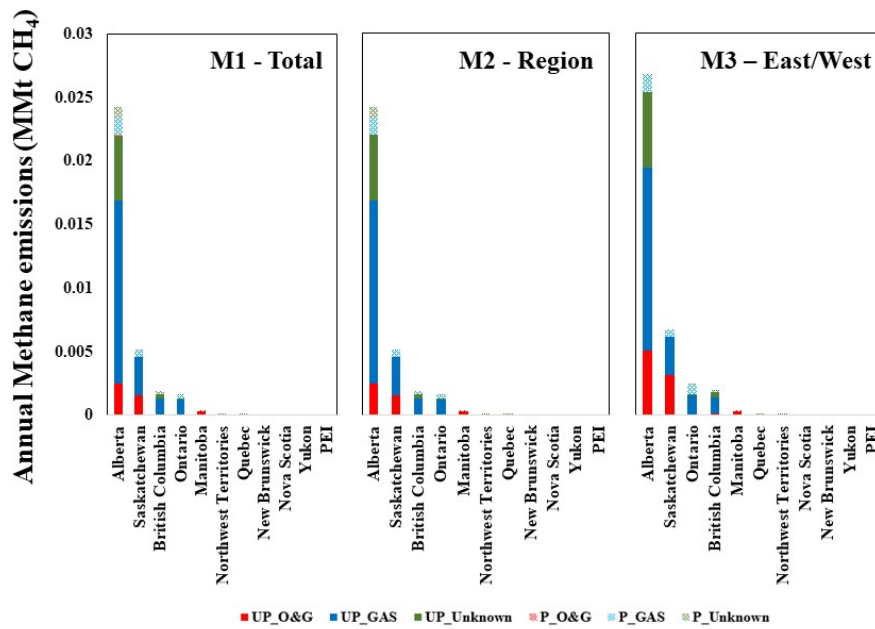


Figure 4.7: Barplots of methane emissions from each province/territory in Canada based on well type and plugging status for all three emission factor attribution scenarios. Note: UP = Unplugged, P = Plugged, O&G = Oil and gas.

Bibliography

- Boothroyd, I. M., Almond, S., Qassim, S., Worrall, F., and Davies, R. J.: Fugitive emissions of methane from abandoned, decommissioned oil and gas wells, *Science of the Total Environment*, 547, 461–469, 2016.
- Brandt, A. R., Heath, G. A., and Cooley, D.: Methane leaks from natural gas systems follow extreme distributions, *Environmental science & technology*, 50, 12 512–12 520, 2016.
- Brownsey, K.: *Cities of Oil: Municipalities and Petroleum Manufacturing in Southern Ontario, 1860–1969*, 2015.
- Cahill, A. G., Beckie, R., Ladd, B., Sandl, E., Goetz, M., Chao, J., Soares, J., Manning, C., Chopra, C., Finke, N., et al.: Advancing knowledge of gas migration and fugitive gas from energy wells in northeast British Columbia, Canada, *Greenhouse Gases: Science and Technology*, 9, 134–151, 2019.
- Calvert, D. and Smith, D. K.: Issues and techniques of plugging and abandonment of oil and gas wells, in: *SPE Annual Technical Conference and Exhibition, OnePetro*, 1994.
- Calvo Buendia, E., Tanabe, K., Kranjc, A., Jamsranjav, B., Fukuda, M., Ngarize, S., Osako, A., Pyrozhenko, Y., Shermanau, P., and Federici, S.: *2019 Refinement to the 2006 IPCC Guidelines for National Greenhouse Gas Inventories*, 2019.
- Canadian Association of Petroleum Producers: *CAPP Statistical Handbook—Production*, <https://www.capp.ca/resources/statistics/>, accessed 2020-04-27, 2020.
- Delignette-Muller, M. L. and Dutang, C.: *fitdistrplus: An R Package for Fitting Distributions*, *Journal of Statistical Software*, 64, 1–34, <https://doi.org/10.18637/jss.v064.i04>, 2015.
- Dilmore, R. M., Sams III, J. I., Glosser, D., Carter, K. M., and Bain, D. J.: Spatial and temporal characteristics of historical oil and gas wells in Pennsylvania: Implications for new shale gas resources, *Environmental science & technology*, 49, 12 015–12 023, 2015.
- Environment and Climate Change Canada: *National Inventory Report 1990-2019: Greenhouse Gas Sources and Sinks in Canada*, 2021.
- Gorchov Negron, A. M., Kort, E. A., Conley, S. A., and Smith, M. L.: Airborne assessment of methane emissions from offshore platforms in the US Gulf of Mexico, *Environmental science & technology*, 54, 5112–5120, 2020.
- Hammack, R., Veloski, G., Hodges, D. G., and White Jr, C. E.: *Methods for finding legacy wells in large areas*, Tech. rep., National Energy Technology Lab.(NETL), Pittsburgh, PA,(United States), 2016.
- Howie, R.: *Stony Creek gas and oil field*, New Brunswick, 1968.
- Independent Petroleum Association of America: *2015–2016: IPAA—The Oil and Gas Producing Industry in Your State*, <http://www.ipaa.org/wp-content/uploads/2017/09/2015-2016OPI.pdf>, accessed 2020-04-10, 2016.

- Ingraffea, A. R., Wells, M. T., Santoro, R. L., and Shonkoff, S. B.: Assessment and risk analysis of casing and cement impairment in oil and gas wells in Pennsylvania, 2000–2012, *Proceedings of the National Academy of Sciences*, 111, 10 955–10 960, 2014.
- Kang, M., Kanno, C. M., Reid, M. C., Zhang, X., Mauzerall, D. L., Celia, M. A., Chen, Y., and Onstott, T. C.: Direct measurements of methane emissions from abandoned oil and gas wells in Pennsylvania, *Proceedings of the National Academy of Sciences*, 111, 18 173–18 177, 2014.
- Kang, M., Christian, S., Celia, M. A., Mauzerall, D. L., Bill, M., Miller, A. R., Chen, Y., Conrad, M. E., Darrah, T. H., and Jackson, R. B.: Identification and characterization of high methane-emitting abandoned oil and gas wells, *Proceedings of the National Academy of Sciences*, 113, 13 636–13 641, 2016.
- Kang, M., Dong, Y., Liu, Y., Williams, J. P., Douglas, P. M., and McKenzie, J. M.: Potential increase in oil and gas well leakage due to earthquakes, *Environmental Research Communications*, 1, 121 004, 2019.
- Pekney, N. J., Diehl, J. R., Ruehl, D., Sams, J., Veloski, G., Patel, A., Schmidt, C., and Card, T.: Measurement of methane emissions from abandoned oil and gas wells in Hillman State Park, Pennsylvania, *Carbon Management*, 9, 165–175, 2018.
- Riddick, S. N., Mauzerall, D. L., Celia, M., Harris, N. R., Allen, G., Pitt, J., Staunton-Sykes, J., Forster, G. L., Kang, M., Lowry, D., et al.: Methane emissions from oil and gas platforms in the North Sea, *Atmospheric Chemistry and Physics*, 19, 9787–9796, 2019a.
- Riddick, S. N., Mauzerall, D. L., Celia, M. A., Kang, M., Bressler, K., Chu, C., and Gum, C. D.: Measuring methane emissions from abandoned and active oil and gas wells in West Virginia, *Science of the Total Environment*, 651, 1849–1856, 2019b.
- Saint-Vincent, P. M., Sams III, J. I., Hammack, R. W., Veloski, G. A., and Pekney, N. J.: Identifying abandoned well sites using database records and aeromagnetic surveys, *Environmental Science & Technology*, 54, 8300–8309, 2020.
- Schout, G., Griffioen, J., Hassanizadeh, S. M., de Lichtbuer, G. C., and Hartog, N.: Occurrence and fate of methane leakage from cut and buried abandoned gas wells in the Netherlands, *Science of the Total Environment*, 659, 773–782, 2019.
- Stocker, T.: *Climate change 2013: the physical science basis: Working Group I contribution to the Fifth assessment report of the Intergovernmental Panel on Climate Change*, Cambridge university press, 2014.
- Townsend-Small, A., Ferrara, T. W., Lyon, D. R., Fries, A. E., and Lamb, B. K.: Emissions of coalbed and natural gas methane from abandoned oil and gas wells in the United States, *Geophysical Research Letters*, 43, 2283–2290, 2016.
- United States Environmental Protection Agency: *Inventory of U.S. Greenhouse Gas Emissions and Sinks 1990-2019*, 2021a.

United States Environmental Protection Agency: Inventory of U.S. Greenhouse Gas Emissions and Sinks 1990-2019, 2021b.

U.S. Energy Information Administration: U.S. Oil and Natural Gas Wells by Production Rate, <https://www.eia.gov/petroleum/wells/>, accessed 2020-01-22, 2020.

Watson, T. L. and Bachu, S.: Evaluation of the potential for gas and CO₂ leakage along wellbores, *SPE Drilling & Completion*, 24, 115–126, 2009.

Williams, J. P., Risk, D., Marshall, A., Nickerson, N., Martell, A., Creelman, C., Grace, M., and Wach, G.: Methane emissions from abandoned coal and oil and gas developments in New Brunswick and Nova Scotia, *Environmental monitoring and assessment*, 191, 1–12, 2019.

Yacovitch, T. I., Daube, C., and Herndon, S. C.: Methane emissions from offshore oil and gas platforms in the Gulf of Mexico, *Environmental science & technology*, 54, 3530–3538, 2020.

Chapter 5

Differentiating and mitigating methane emissions from fugitive leaks from natural gas distribution, historic landfills, and WUH in Montréal, Canada

Connecting text: In this chapter, we detail the results of 615 individual source measurements we made in Montréal, Canada, to quantify CH₄ emissions from urban methane sources using the same static chamber method we tested in Chapter 3 and utilized in Chapter 4. We demonstrated that historic landfills, WUH, and natural gas (NG) distribution systems were all among the top four methane sources in Montréal by geospatially distributing emission factors informed by our activity data, following and expanding on methods used in Chapter 4. Methane emissions from both historic landfills and WUH are not accounted for in any greenhouse gas inventory. We found that geochemistry alone cannot positively identify source subcategories (e.g., type of WUH or NG infrastructure) in almost all cases, although C₂:C₁ ratios were effective in identifying thermogenic sources. Furthermore, we quantified the cost-benefits of mitigation for multiple source subcategories for all of the three sources we measured. This study provides the justification for the

research performed in the following chapter on biogenic urban methane emissions and builds on the methods presented in Chapters 3 and 4.

The results of this research have been published as:

Williams, J. P., Ars, S., Vogel, F., Regehr, A., & Kang, M. (2022). Differentiating and Mitigating Methane Emissions from Fugitive Leaks from Natural Gas Distribution, Historic Landfills, and manholes in Montréal, Canada. *Environmental Science & Technology*, 56(23), 16686-16694.

5.1 Introduction

Cities are responsible for 19% of global anthropogenic methane (CH₄) emissions, and 35% of anthropogenic CH₄ emissions in North America, according to Marcotullio et al. (Marcotullio et al., 2013). CH₄ is a potent greenhouse gas (GHG) with an atmospheric lifetime of 11.8 years and a global warming potential 83-times stronger than carbon dioxide (CO₂) over 20 years (IPCC, 2022). Therefore, new international commitments such as the Global Methane Pledge are focusing on CH₄ emissions from a wide range of sources. Cities are uniquely positioned to mitigate CH₄ emissions as they face fewer political challenges compared to provinces/states/territories and countries (Hopkins et al., 2016). However, municipal GHG inventories often underestimate emissions and are not sufficiently detailed to develop actionable mitigation strategies, often omitting details such as gas species or identifying the specific type of source emitting CH₄ (Lamb et al., 2016; Plant et al., 2019; Weller et al., 2020; McKain et al., 2015; Brandt et al., 2014). Understanding the magnitude of emissions at the source subcategory level (e.g., separated sanitary wastewater utility holes vs. storm drain) is important as mitigation costs and options vary among source subcategories based on multiple factors such as emission rate (i.e., emission factor), number of sites (i.e., activity data), and type of site. Individual source measurements in cities can provide the level of detail required to improve municipal GHG inventories, create monitoring best practices, and reduce CH₄ emissions through identifying the source of leaking urban infrastructure.

Given the abundance of co-located CH₄ sources, cities pose unique challenges to determining the origin of emissions (Hopkins et al., 2016; Ars et al., 2020; Phillips et al., 2013; Williams et al., 2018), which is critical for developing actionable mitigation strategies. Individual source measurements, such as chamber measurements (Kang et al., 2014), offer the advantage of directly quantifying CH₄ emissions while limiting inter-source mixing with other co-located sources. Individual source measurements also compliment vehicle-based mobile surveying, where measurements are made downwind from sources, and other top-down measurements. Furthermore, geochemical data such as stable isotopic ratios (e.g., $\delta^{13}\text{C-CH}_4$) and gas ratios (e.g., ethane to methane) collected

from individual sources help establish source signatures that can better inform top-down measurement campaigns (Plant et al., 2019; Floerchinger et al., 2021).

Multiple urban CH₄ emission studies have focused on natural gas (NG) distribution systems (von Fischer et al., 2017; Plant et al., 2019; Hendrick et al., 2016; Phillips et al., 2013; McKain et al., 2015; Lamb et al., 2016; Floerchinger et al., 2021; Weller et al., 2020, 2018) with the majority concluding that CH₄ emissions from NG distribution in municipal inventories are underestimated and are a significant contributor to urban CH₄ emissions (Brandt et al., 2014; Fong et al., 2014). The primary sources of CH₄ emissions from NG distribution are fugitive equipment leaks, venting, and accidental losses caused by either equipment malfunctions or from damage caused by a third party (i.e., third party breaks) (Nisbet et al., 2020; Fong et al., 2014). These emissions are termed fugitive NG distribution emissions in greenhouse gas inventories (Fong et al., 2014). While many studies have measured CH₄ emissions from NG distribution systems in the U.S. (Wunch et al., 2016; Peischl et al., 2013; Weller et al., 2018, 2020; Floerchinger et al., 2021; Fries et al., 2018; Phillips et al., 2013; McKain et al., 2015; Plant et al., 2019; Lamb et al., 2016), few have targeted Canadian cities (Ars et al., 2020; Hugenholtz et al., 2021) and none have been conducted in Montréal, Canada.

The waste sector is a major source of CH₄ emissions in cities, particularly from municipal solid waste landfills (IPCC, 2022). The magnitude of CH₄ emissions from landfills is influenced by a city's waste management practices, both current and historical (IPCC, 2022). CH₄ emissions from engineered and managed active landfill sites are well-documented, have been directly measured in previous work (Lohila et al., 2007; Babilotte et al., 2010), and have commercially-available and widely implemented mitigation strategies (Themelis and Ulloa, 2005). In Canada, regulations for waste management were defined in 1999 through the Canadian Environmental Protection Act (CEPA). The City of Montréal (Québec, Canada) has 94 historic landfills that were abandoned before the introduction of the CEPA. However, few studies have directly measured CH₄ emissions from historic landfills (Christophersen et al., 2001; Rachor et al., 2013; Whalen et al., 1990), which we define as landfills closed before the implementation of modern environmental regulations.

Wastewater utility holes (WUHs) have been flagged in several urban emission measurement studies as a CH₄ emission source (Williams et al., 2018; Chamberlain et al., 2016; Fries et al., 2018; Fernandez et al., 2022; Defratyka et al., 2021). WUHs are subsurface conduits with environments primed for the production of CH₄ through anaerobic digestion (i.e., low oxygen, abundance of organic matter) (Guisasola et al., 2009). Millions of WUHs can be found across cities, and can easily be found near NG distribution infrastructure and historic and active landfills. Because WUHs are often co-located with NG distribution sites and they may be an important CH₄ source, there is a need to quantify their potential CH₄ emissions, evaluate the impact/viability of mitigation strategies, and to establish their geochemical source signatures.

In this work, we (1) provide detailed individual source CH₄ emission rate measurements from three types of sources: fugitive emissions from NG distribution, historic landfills, and WUHs; (2) estimate annual CH₄ emissions from these three sources across the City of Montréal in Canada; (3) geochemically characterize the emitted CH₄ to improve source attribution; and (4) evaluate mitigation potential and costs for each source subcategory we directly measure.

5.2 Methods

Our study site is the City of Montréal (Canada) (Figure 5.1). In 2018, cumulative GHG emissions from Montréal were estimated to be 10.4 MMt of CO_{2eq} (0.35 MMt CO_{2eq} from CH₄) (SI - Table 5.1).

We performed individual source measurements over seven sampling campaigns spanning from August 2019 to March 2021. Site selection was partially guided by a 1,200 km mobile surveying campaign that identified super-ambient atmospheric CH₄ plumes (SI - Section 5.5.1). Three sampling campaigns targeted random sites throughout the entire city, two campaigns focused on areas (i.e., 2 km²) where a high density of super-ambient CH₄ plumes were located, and two campaigns targeted larger NG distribution stations (i.e., not residential meter-sets) which required Énergir (i.e., one of the principal energy provider in Québec) technicians to provide direct access

to the stations (Figure 5.1). CH₄ Flowrates were quantified using a chamber-based methodology similar to previous studies (Kang et al., 2014, 2016) which is detailed in the SI - Section 5.5.2. We categorized all individual source measurements by their source and source subcategory. We define the emission source as the group to which a number of different source subcategories belong. The source subcategories we used for fugitive NG distribution emissions were gate stations, branch stations, residential meter sets, industrial meter sets, block valve stations, telemetry stations, and district regulator station. For fugitive NG distribution emissions we also analyzed 81 third party breaks that occurred in Montréal in the year 2020 and were documented by Énergir. The source subcategories for historic landfills were soil gas fluxes, landfill gas (LFG) vents, and observation wells. The source subcategories for WUHs were sewers, storm drains, and other WUH types (SI - Section 5.5.3).

We obtained the locations of historic landfill sites from shapefiles provided by the City of Montréal data portal (Ville de Montréal, 2022b). We obtained NG station locations and types, main and secondary pipelines, material types, and a list of third party breaks (i.e., ruptures to NG pipelines caused by a third party) for 2020 directly from Énergir. WUHs are access points for underground structures such as wastewater networks, electrical cables, and NG stations. We acquired shapefiles containing the locations of sewers and storm drains for Montréal from the City of Montréal data portal (Ville de Montréal, 2022c). We estimated the locations and count of "other" WUH types assuming that sewers are co-located in equal numbers (SI - Section 5.5.4). We identified WUH types using a combination of markings on the WUH, the structure, and/or the geospatial information provided by the City of Montréal. We categorized all WUHs that could not be positively identified as sewers, storm drains, NG distribution access WUHs, or underground fiber optic cable access as "other" WUHs. It is important to note that we did not have an extensive network of wastewater infrastructure for Montréal, and therefore we could not identify whether the WUHs were connected to unitary or separated lines, or whether the infrastructure was gravity drain, rising mains, or pump stations. However, we do know that the majority of WUHs we measured were from the central or eastern portions of the city, which are unitary wastewater lines

with a combination of sanitary and storm water. Based on personal communications with experts in the field, there are no pump stations in Montréal.

We estimated annual CH₄ emissions for Montréal from historic landfills, WUHs, and NG distribution by summing source subcategory emission estimates, which are based on our individual source measurements and activity data from the city and Énergir. We mapped annual CH₄ emissions from these sources in a gridded 500 x 500 meter inventory by aggregating CH₄ emission sources within each grid cell (Figure 1). Uncertainty ranges for annual CH₄ emissions (95% c.i.) were calculated using a Monte Carlo simulation with 1,000,000 iterations. We used bootstrapping with re-sampling (2,000 iterations) using the “boot” package in R-Studio to develop a distribution of emission factors. The bootstrapped distribution was fitted to a gamma distribution using the “fitdistrplus” package in R-Studio. For activity data, we assumed a uniform distribution over specified ranges (SI - Table 5.2). Samples were pulled from both the emission factor and activity data distributions and multiplied to obtain a set of 1,000,000 estimates of annual CH₄ emissions. We used the 97.5th and 2.5th percentiles as the upper and lower confidence intervals (SI - Figure 5.6). We repeated these steps for each source subcategory. We estimated the uncertainty ranges of annual CH₄ emissions for pipeline leaks and third party breaks based on the ranges presented in the Clearstone Manual (Clearstone Engineering Ltd., 2020).

Gas samples were taken during chamber measurements for analysis of $\delta^{13}\text{C-CH}_4$, CO₂:CH₄ ratios (i.e., the ratio of CO₂ to CH₄), and C₂:C₁ ratios (i.e., the ratio of C₂H₆ to CH₄) on a Picarro G2210-i analyzer. We selected samples with a minimum CH₄ enhancement of 1.0 ppm above the extra dry air baseline CH₄ concentration. We calculated the source C₂:C₁ ratios, CO₂:CH₄ ratios, and $\delta^{13}\text{C-CH}_4$ signatures using Keeling plots (SI - Section 5.5.5). Using the selected samples we evaluated whether the geochemical signatures of the different source subcategories overlapped.

We estimated CH₄ emission mitigation potential from all three sources by comparing mitigation options and costs versus the potential reductions in CH₄ emissions based on our individual source measurements averaged over a period of 15 years. For WUHs we considered the costs of installing and maintaining wastewater dosing stations throughout the city, for historic landfills

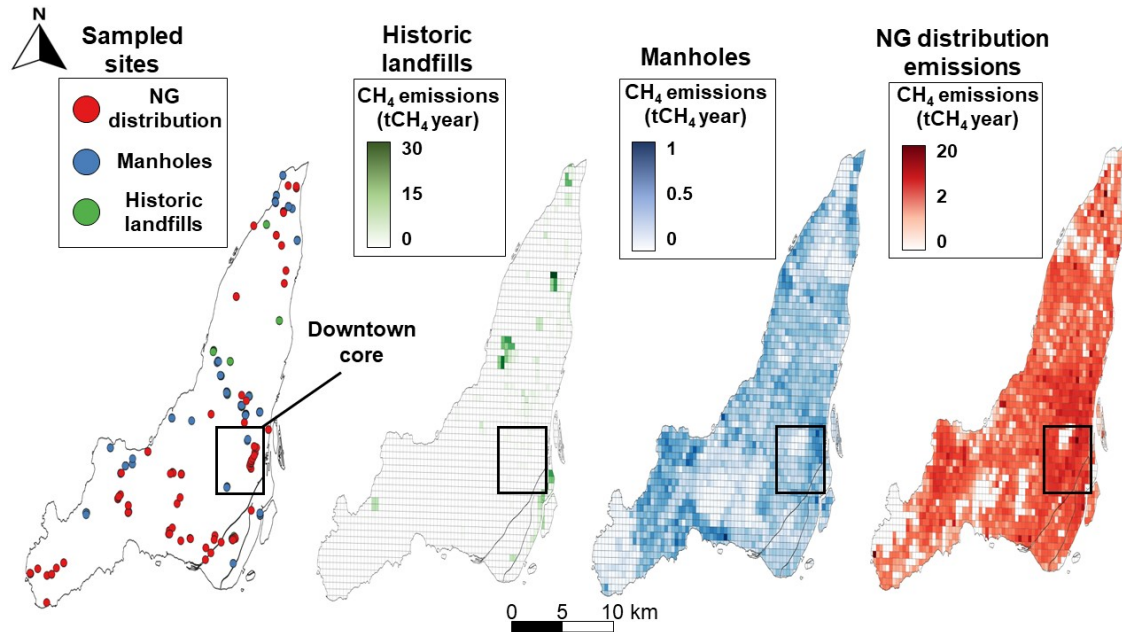


Figure 5.1: Map of sampled sites (far left panel) and gridded inventories (500m by 500m) of CH₄ emissions from historic landfills (middle left panel), WUH (middle right panel), and NG distribution (right panel) emissions in the Island of Montréal for 2020 created from our direct CH₄ measurements and activity data.

we considered the installation of LFG recovery systems and maintenance including offsets from selling recovered gas, and for fugitive NG distribution emissions we considered the effects of leak detection and repair surveys and increasing repair rates while including offsets from selling recovered gas. We also included a social cost of CH₄ (SCM) of USD \$-1,024 (Environment and Climate Change Canada, 2016) which quantifies the economic loss of welfare of emitting one ton of CH₄ into the atmosphere. The specific costs are outlined in detail in the SI - Section 5.5.6.

5.3 Results

5.3.1 Methane emissions by source

We made a total of 615 individual source measurements from August 2019 to March 2021. Of the individual source measurements, 124 were from NG distribution sites, 136 were from WUHs,

and 355 were from historic landfills (Figure 5.2). We assigned measurements from fugitive NG distribution (i.e., CH₄ emissions caused by equipment leaks, venting, and accidental losses to the NG distribution stream), historic landfills, and WUH to source subcategories.

Annual CH₄ emissions for Montréal from the three sources we measured totaled 2,130 (660 to 4,986, 95% c.i.) tons of CH₄ in 2020. Annual CH₄ emissions from historic landfills were 901 (452 to 1,541, 95% c.i.) tons of CH₄, which is the highest among the three source types we measured (Figure 5.3). When compared to other sources in the Montréal inventory, including those we did not measure, the 901 tons of CH₄ per year places historic landfills as the second highest CH₄ source in Montréal, preceded only by municipal solid waste emissions (Figure 5.3). Annual CH₄ emissions from WUHs totaled 786 (32 to 2,602, 95% c.i.) tons of CH₄, of which 577 tons originated from sewer WUHs, 183 tons from other WUH types, and 26 tons from storm drains (Figure 5.3). This places CH₄ emissions from WUH anywhere from the largest to the tenth largest CH₄ source in Montréal (SI – Table S11), closely following emissions from historic landfills. We calculated annual CH₄ emissions from fugitive NG distribution to be 451 (176 to 843, 95% c.i.) tons of CH₄ which is comparable to the 590 tons of CH₄ from fugitive emissions estimated in Montréal's 2018 inventory (Figure 5.3). On average, our estimates of fugitive NG distribution emissions places them as the fourth highest CH₄ source in Montréal.

Fugitive emissions from natural gas distribution

We found the average CH₄ emission rate from the 124 measurements from NG distribution sites ranged from $2.30 \cdot 10^{-1}$ ($0.70 \cdot 10^{-1}$ to $3.85 \cdot 10^{-1}$, 95% c.i.) g/hour for residential meter-sets to $2.44 \cdot 10^3$ (0.74^3 to $4.90 \cdot 10^3$, 95% c.i.) g/hour for gate stations. Of the different NG distribution site types (SI - Section 5.5.3), we directly measured 100% of branch stations (n=1), 67% of gate stations (n=2), 50% of pre-detention stations (n=1), 16% of district regulating stations (n=12), 15% of block valve stations (n=10), 6% of telemetry stations (n=1), 2% of industrial meter sets (n=4), and 0.1% of residential meter sets in the city (n=71) for a total of 102 unique sites. We found that the mean mass of CH₄ released from third party breaks (i.e, damages caused by construction

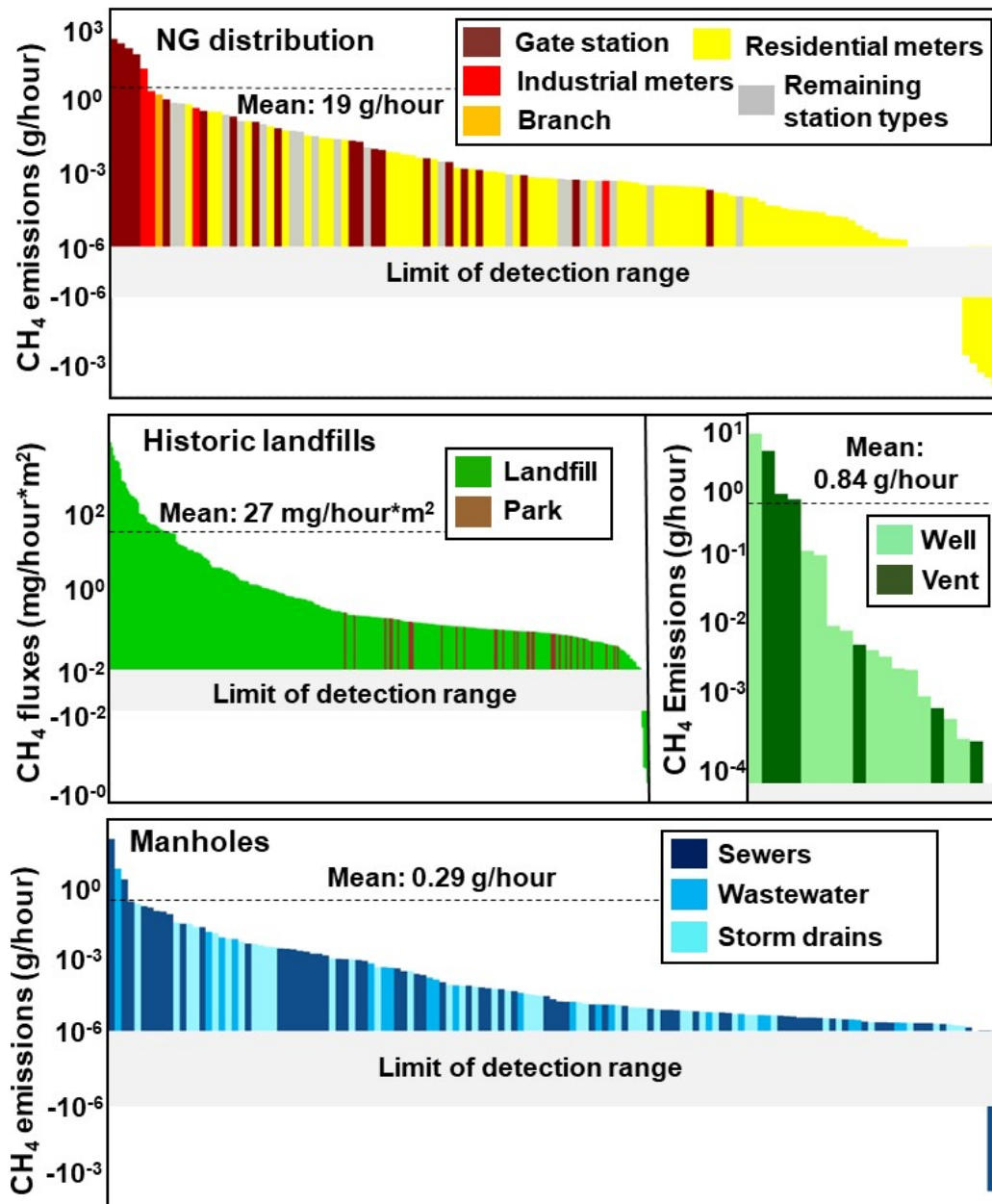


Figure 5.2: Distributions of direct measurements of CH₄ emissions released from NG stations (top), soil gas fluxes from historic landfills (middle left), above-ground infrastructure (LFG vents and observation wells) at historic landfill sites (middle right), and WUH (bottom). The measurements are sorted by CH₄ emission rate with the highest emission rate on the left. Repeat measurements from the same sites are also displayed.

companies) was 1.79 (1.26 to 2.43, 95% c.i.) tons of CH₄ per break, with a maximum release of 20.9 tons of CH₄.

Historic landfills

We sampled a total of 15 historic landfill sites and three control sites (i.e., public parks without known underlying historic landfills) and conducted a total of 340 individual flux measurements (Figure 5.2). The flux measurements covered 0.56 km² of ground and 8% of the total surface extent of documented historic landfills in Montréal. An additional 15 CH₄ flowrate measurements were made from above-ground infrastructure such as vents and observation wells (SI - Figure 5.7). The average CH₄ flux rate from landfills was 26.7 (15.5 to 49.0, 95% c.i.) mg/hour·m² with a maximum flux rate of 1.39·10³ mg/hour·m² (Figure 5.2). Control fluxes measured from public parks outside of known historic landfill boundaries were minor CH₄ sources averaging 0.18 (0.16 to 0.21, 95% c.i.) mg/hour·m². The average CH₄ flowrate from above-ground infrastructure was 0.84 (0.13 to 2.15, 95% c.i.) g/hour with a maximum flowrate from an observation well at 10.4 g/hour.

Wastewater utility holes

Of the 136 WUHs that we measured, 67 were sewers, 46 were storm drains, and 23 were from other WUH types, which is the largest sample set of direct measurements from WUHs conducted to date, to our knowledge. Our sample set represents 0.03% of all WUHs in Montréal. The average CH₄ flowrate from all sampled WUHs was 2.93·10⁻¹ (0.17·10⁻² to 9.49·10⁻¹, 95% c.i.) g/hour with a maximum flowrate of 33.4 g/hour from a sewer (Figure 5.2). Overall, sewers emitted CH₄ at an average rate of 5.40·10⁻¹ (2.49·10⁻¹ to 1.95, 95% c.i.) g/hour compared to 1.44·10⁻¹ (5.08·10⁻³ to 5.04·10⁻¹, 95% c.i.) g/hour from other WUH types and 8.53·10⁻³ (2.14·10⁻³ to 1.95·10⁻², 95% c.i.) g/hour from storm drains. The distribution of CH₄ flowrates from WUHs was highly skewed with a mean value four orders of magnitude higher than the median flowrate of 1.16·10⁻⁴ g/hour, resulting in large uncertainty ranges in annual CH₄ emissions estimates for WUHs that ranged

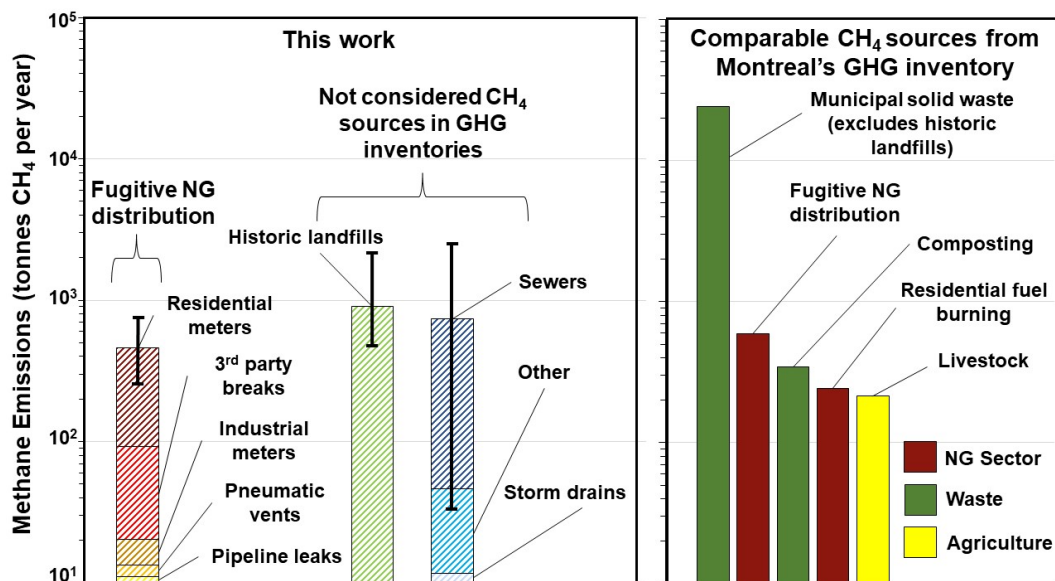


Figure 5.3: Annual CH₄ emission estimates from fugitive NG distribution systems, historic landfills, and WUWs. Other CH₄ sources in Montréal’s 2018 municipal inventory are shown for comparison Ville de Montréal (2022a).

from 2,602 to 32 tons of CH₄. The three highest emitting WUWs (i.e. 2% of sample set) were responsible for 96% of cumulative CH₄ emissions from this source. Two of these high emitting WUWs were characterized by a strong odour, and two were located within, or close to historic landfill sites.

5.3.2 Geochemical analysis

We analyzed a total of 214 gas samples and grouped them based on their respective source subcategories and analyzed them for CO₂:CH₄ ratios, $\delta^{13}\text{C-CH}_4$ signatures, and C₂:C₁ ratios. A total of 98 samples were excluded based on our 1.0 ppm CH₄ enhancement threshold, leaving a total of 116 samples. Based on our analysis of geochemical indicators, we find that only observation wells at historic landfills and other WUH types can be distinguished from all other source subcategories due to their light $\delta^{13}\text{C-CH}_4$ signatures of -69‰ ($\pm 3\text{‰}$, 95% c.i.) and -57‰ ($\pm 2\text{‰}$, 95% c.i.) respectively (Figure 5.4). The remaining source subcategories all have overlapping CO₂:CH₄ ratios, $\delta^{13}\text{C-CH}_4$ signatures, C₂:C₁ ratios, or a combination of all three. At the source level, we find that

that $C_2:C_1$ ratios are the most effective indicator for positively identifying fugitive NG distribution emissions (Figure 5.4), but cannot discriminate between WUH and historic landfill source subcategories. We find that $CO_2:CH_4$ ratios and $\delta^{13}C-CH_4$ signatures can sometimes differentiate between WUH and historic landfill source subcategories, but that most WUHs and historic landfill source subcategories show overlapping fingerprints.

We observe that in some cases source subcategories from the same source can show differing geochemical signatures. From WUHs, we see that $CO_2:CH_4$ ratios for sewers and other WUH types average 23 (± 5 , 95% c.i.) and 0.2 (± 0.1 , 95% c.i.) respectively, whereas storm drains average much higher at 43 (± 46 , 95% c.i.) with statistical overlap. Sewers and other WUH types both show lighter $\delta^{13}C-CH_4$ signatures of -51‰ ($\pm 3\text{‰}$, 95% c.i.) and -57‰ ($\pm 2\text{‰}$, 95% c.i.) respectively when compared to storm drains which average -46‰ ($\pm 3\text{‰}$, 95% c.i.). For historic landfills, we see that soil gas fluxes have $CO_2:CH_4$ ratios that average 20 (± 12 , 95% c.i.) when compared to vents and observation wells which average 4 (± 5 , 95% c.i.) and 6 (± 9 , 95% c.i.) respectively. In terms of $\delta^{13}C-CH_4$ signatures, all three historic landfill source subcategories showed varying signatures where observation wells have light signatures of -69‰ ($\pm 3\text{‰}$, 95% c.i.), soil gas fluxes have slightly light signatures of -50‰ ($\pm 1\text{‰}$, 95% c.i.), and vents show heavier signatures averaging -41‰ ($\pm 7\text{‰}$, 95% c.i.). All fugitive NG distribution gas samples show the same signatures with low $CO_2:CH_4$ ratios at 13 or lower, elevated $C_2:C_1$ ratios around 0.04, and heavy $\delta^{13}C-CH_4$ signatures ranging from -39‰ to -44‰ .

5.3.3 Mitigation options: costs, technology readiness, and potential CH_4 reductions

We evaluated the CH_4 mitigation potential (i.e., the mass of CH_4 that can be reduced), the cost per tonne of CH_4 reduced, and the readiness of the mitigation technology (i.e., the qualitative level to which the technology can be implemented successfully at city-wide scales) for the urban sources we measured: fugitive NG distribution, historic landfills, and WUHs (Figure 5.5). We also included a social cost of CH_4 (SCM) emissions of USD -1,027 per tonne of CH_4 which quantifies

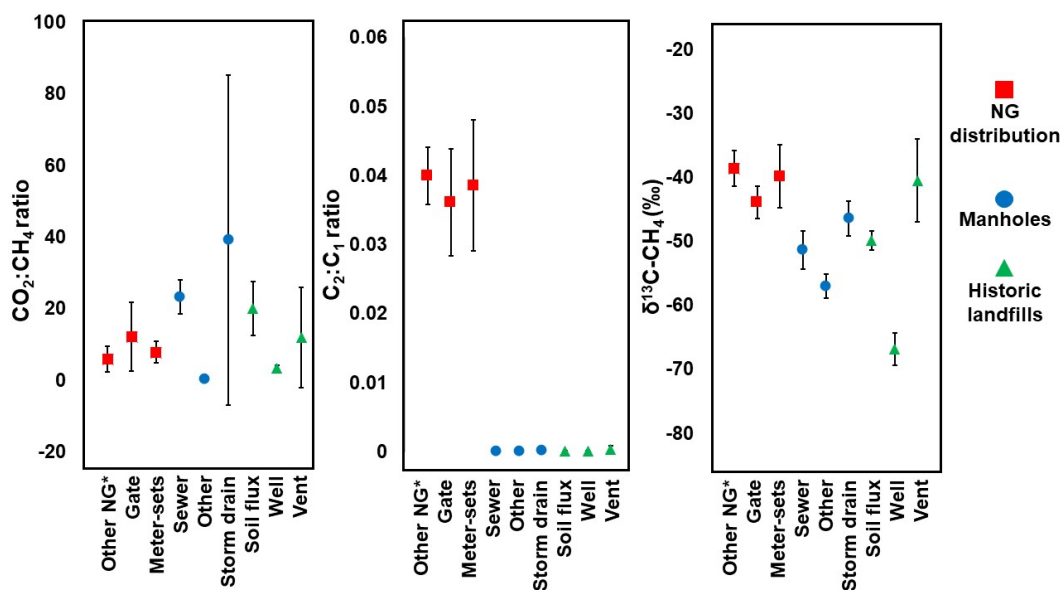


Figure 5.4: Average CO₂:CH₄ ratios, C₂:C₁ ratios, and δ¹³C-CH₄ signatures of historic landfill, WUH, and NG distribution source groups. Confidence intervals (95% CI) are shown as black capped bars.

the expected economic and socioeconomic impacts of emitting one ton of CH₄ (Environment and Climate Change Canada, 2016). We found large potential CH₄ reductions from the installation of LFG recovery systems at all historic landfill locations with expected CH₄ reductions of 585 tons, albeit with potentially high costs of USD \$7,000 to \$12,000 per tonne of CH₄ reduced (Figure 5.5). We found that mitigation options for WUHs, which involve dosing wastewater networks with chemicals to reduce the growth of CH₄ generating archaea (Jiang et al., 2013; Mohanakrishnan et al., 2009; Zhang et al., 2009; Jiang et al., 2011a; Ganigué and Yuan, 2014; Gutierrez et al., 2014, 2009; Jiang et al., 2011b), are all generally low cost, ranging from USD \$20 to \$400 per ton of CH₄ reduced. However, the technology is untested at city-wide scales and varies depending on the dosage schemes and potential reductions in CH₄ production. We found that several mitigation methods for fugitive NG distribution emissions produce net savings with the price of captured NG exceeding the mitigation costs. Mitigation methods for fugitive NG distribution include increasing repair rates to capture the top 10% of leaking components from industrial meter-sets (i.e., USD \$-130 per tonne CH₄), and the enforcement of underground pipe checks during excavation activities

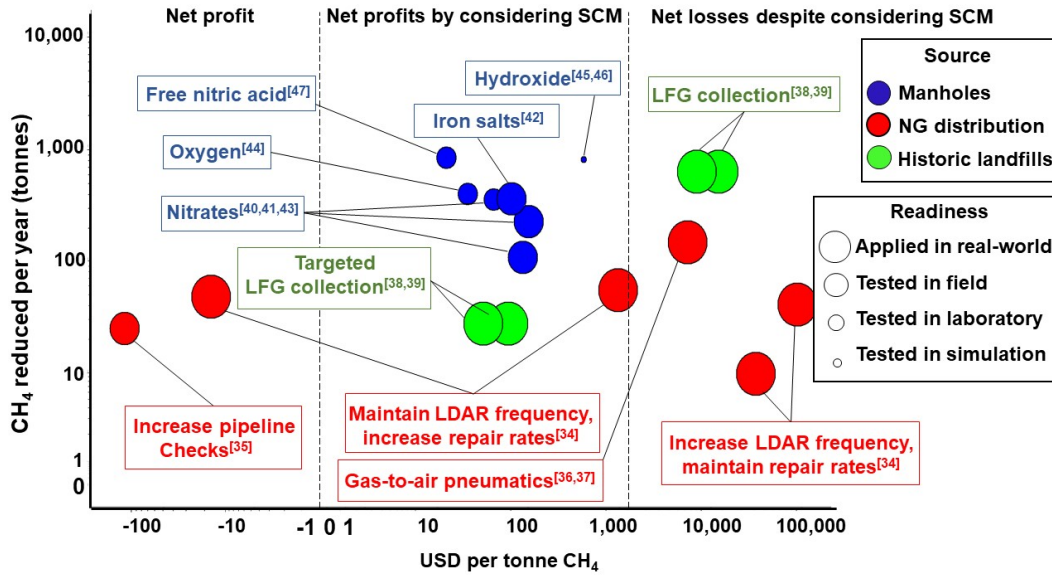


Figure 5.5: Mitigation options are categorized by whether the resulting methods produce net profits, net profits by including the social cost of CH₄, and net losses despite including the social cost of CH₄. Mitigation costs (USD) per tonne of CH₄ versus the potential CH₄ emissions reductions for Montréal for fugitive NG distribution (Limits, 2014; Clearstone Engineering Ltd., 2020; Magder, 2018; Methane Guiding Principles, 2019; Petroleum Technology Alliance Canada, 2017), historic landfills (Agency, 2021; Duffy, 2019), and WUHs (Jiang et al., 2013; Mohanakrishnan et al., 2009; Zhang et al., 2009; Jiang et al., 2011a; Ganigué and Yuan, 2014; Gutierrez et al., 2014, 2009; Jiang et al., 2011b). The potential annual CH₄ emissions reductions and mitigation costs are presented in log 10 scale. Mitigation options are categorized by whether the resulting methods produce net profits, net profits by including the social cost of CH₄ (SCM), and net losses despite including the social cost of CH₄ (SCM). Other references for costs are shown in SI - Section 5.5.6

to reduce the occurrence of third party breaks (i.e., USD \$-270 per tonne CH₄). When including the SCM, we found that ten of the mitigation options we consider become net savings, with only five options having net costs (Figure 5.5).

5.4 Discussion

5.4.1 Wastewater utility holes and historic landfills: larger CH₄ sources than previously thought

Of the three source types considered in this study, we find that historic landfills contribute the majority of CH₄ emissions among the sources we measured (Figure 5.3). Over 99% of CH₄ emissions from historic landfills originate from soil gas fluxes as opposed to the above-ground infrastructure we measured (e.g. observation wells and vents) which is due to the small number of historic landfill vents and wells in Montréal. Our observed range of CH₄ fluxes from historic landfills was 0 to 1.4 g/hour·m² with an average of $2.7 \cdot 10^{-2}$ g/hour·m², which is an order of magnitude lower than the 0 to 54 g/hour·m² observed by Rachor et al. (Rachor et al., 2013) from an old landfill site in Germany, but comparable to the 0 to 3.0 g/hour·m² and averages ranging from 0 to 0.4 g/hour·m² observed from an old landfill at a site in Denmark (Christophersen et al., 2001). The differences are likely attributable to many factors, such as the type of waste, local climate, cover material and depth, and age. Many cities in Canada, the United States, and elsewhere, likely contain historic landfills given the less stringent regulations on waste management in the past (Pichtel, 2014). In addition to environmental risks, landfills pose additional risks to human health through water and air pollution, the exposure to pathogens, and explosion risks in buildings (Lisk, 1991). Historic landfills are likely also present in developing countries where LFG recovery systems or soil covers are not commonplace (Guerrero et al., 2013). In order to better understand emissions from historic landfill sites, additional measurements must be made.

We find that the second highest source of CH₄ emissions observed in our study are WUHs, primarily sewers. A comparable study by Fries et al. (2018) utilized a chamber-based technique to directly measure 43 WUHs in Cincinnati, Ohio, and found CH₄ flowrates ranging from 0.00 to 0.01 g/hour, which are lower than our estimates. However, we measured 136 WUHs, and given the heavy-tailed emission distribution we observed, it could be that the sample set from Fries et al. (2018) missed potential super-emitting sites leading to their low observed emission rates. Other

relevant studies focused on detailed measurements from a small number of sites (n=1-5) (Liu et al., 2015) or measured them as a by-product of targeting other sources such as NG emissions (Williams et al., 2018; Hendrick et al., 2016; Chamberlain et al., 2016). None of these studies captured any super-emitting WUHs such as the three (i.e., above 1 g/hour) we measured in this work, which dramatically increases average emission rates. We observed that the three highest CH₄ emitting WUHs that contributed most to overall CH₄ emissions were characterized by a strong odour, were closely located or within historical landfills, or both. In addition, two of the three high emitting WUHs were sewers, including the highest emitting WUH.

Understanding the attributes of the highest CH₄ emitting WUHs can help guide measurement efforts to locate them and better understand the upper limit of CH₄ emissions from WUHs. Despite gathering one of the largest sample sets of direct measurements from WUHs to date, we measured only 0.03% of all WUHs in Montréal, meaning that there may be sites emitting at higher rates than we observed, and that the upper range of CH₄ emissions from WUHs remains unknown. Our findings show that CH₄ emissions from WUHs are very uncertain but can be a significant CH₄ source in cities, and that additional individual source measurements are needed to better understand their magnitude and behavior and to better constrain these uncertainties so that the accuracy of annual CH₄ emission estimates from WUHs are improved and that they are included in greenhouse gas inventories.

Both historic landfills and WUHs are CH₄ sources that are not accounted for in any GHG inventory, despite being significant sources of CH₄. There are also likely other CH₄ sources in urban environments that are yet to be quantified and documented. For example, a study by Ars et al. (2020) showed that urban waterways and wetlands are CH₄ sources in cities but are not documented as CH₄ sources in any GHG inventory. Going forward, it is important that these undocumented sources are quantified and characterized so that proper mitigation options can be explored and implemented.

5.4.2 CH₄ source subcategories are generally not identifiable using geochemistry alone

Of all the source subcategories we measured, we could only positively identify observation wells at historic landfills and other WUH types using the geochemical indicators we employed. We found that observation wells in historic landfills were a small contributor of CH₄ emissions in this work whereas other WUH types were the second largest contributor of CH₄ from WUHs. The ability to positively identify source subcategories using geochemistry increases in value depending on the overall CH₄ contributions from that source subcategory. Source subcategory identification is critical for developing actionable mitigation strategies since the mitigation options and costs vary by source subcategory, even within the same source (e.g., transitioning to air-based pneumatics cannot mitigate leaks from residential meter-sets). Individual source measurements, by design, produce measurements with low uncertainties in source attribution meaning that they can be an alternative to relying on geochemistry alone for identifying a CH₄ source subcategory.

While we find that the geochemical indicators we utilize are largely ineffective at identifying source subcategories, we do see that broader distinctions can be made, such as differentiating between thermogenic (i.e., fugitive NG distribution) and biogenic (i.e., WUHs and historic landfills) sources. We find that C₂:C₁ ratios are especially effective in our work in differentiating between thermogenic and biogenic sources, which has also been observed in previous work (Peischl et al., 2013; Wunch et al., 2016). Similar distinctions have been made by previous work such as Fries et al. (Fries et al., 2018) who distinguished sources as biogenic, thermogenic, or mixed using $\delta^2\text{H-CH}_4$ and $\delta^{13}\text{C-CH}_4$ signatures. Identifying a CH₄ source can be useful in guiding individual source measurements by eliminating potential targets and focusing measurements. We find that the easiest source to identify is fugitive NG distribution emissions through positive C₂:C₁ ratios, and that distinguishing between different biogenic sources remains a challenge. The only way we were able to distinguish between different sources and source subcategories was through the use of individual source measurements. It is likely that we would need to utilize additional geochemical

indicators (e.g., H₂S, Ne, He, $\delta^2\text{H-CH}_4$) or accept that geochemistry can not effectively partition the full range of CH₄ source subcategories encountered in urban environments.

5.4.3 Mitigation options vary in readiness, impact, and cost effectiveness

We observed that only 2% of WUHs were responsible for 96% of cumulative CH₄ emissions, meaning that the identification of these high-emitting WUHs is a priority for mitigation. The mitigation options for WUHs emissions we consider involve altering the biochemistry of wastewater networks (Liu et al., 2015; Jiang et al., 2013; Mohanakrishnan et al., 2009; Zhang et al., 2009; Jiang et al., 2011a; Ganigué and Yuan, 2014; Gutierrez et al., 2014, 2009; Jiang et al., 2011b). There are potential drawbacks of chemical dosing such as the production of nitrous oxide and negative impacts on downstream nutrient removal in wastewater treatment plants (Liu et al., 2015). All of the mitigation options we analyze for reducing CH₄ emissions from WUHs show relatively low mitigation costs per tonne of CH₄ reduced (Figure 5.5). Furthermore, by focusing on the sewers emitting the most CH₄ it is likely that costs would be lower and the quantity of CH₄ emissions mitigated would increase, which highlights the importance of individual source measurements in the identification of these sites.

Some of the highest potential CH₄ reductions from the sources we consider in Montréal are from historic landfills (Figure 5.5). The production and use of biogas from gas recovery wells at historic landfills would limit the CH₄ released to the atmosphere while simultaneously providing a renewable energy source (Nastev et al., 2001). However, mitigation costs for historic landfills are high due to the costs of installing and maintaining LFG recovery systems and the lower quantity of expected biogas production when compared to an active landfill (Figure 5.4). CH₄ production from landfills peaks within the first year after waste deposition (Themelis and Ulloa, 2005), and historic landfills are not fed any new waste. The overall costs drop if LFG recovery systems are targeted to the two highest emitting historic landfills. By targeting the two highest emitting historic landfill sites, the quantity of recovered gas per unit area increases leading to higher profits, and the risks of investing in these systems at sites with little/no emissions are reduced, highlighting that

cost-effective mitigation of emissions from historic landfills can be informed through individual source measurements.

Our breakdown of fugitive NG distribution emissions shows that mitigation efforts should prioritize reducing the occurrences of third party breaks and increasing repair rates for industrial meter sets (Petroleum Technology Alliance Canada, 2017). Leak detection plays a key role for mitigation in the NG distribution sector since repair options are generally low-cost and commercially available. Other options are expensive, such as increasing the frequency of LDAR surveys at residential and industrial meter sets, where the high number of sites and low emission factors lead to high mitigation costs (Figure 5.5). We see that increasing the repair rates while maintaining a biannual LDAR survey frequency results in lower costs compared to increasing the frequency of LDAR surveys. Currently, leak detection from NG distribution in Montréal (and many other cities) involves qualitative site screening (Clearstone Engineering Ltd., 2020) and the decision to repair a leak is based on arbitrarily defined CH₄ concentration thresholds (e.g., screening of 500 ppm CH₄ or higher). Lowering this arbitrary CH₄ screening threshold would be one avenue to increase repair rates and cost-effectively lower CH₄ emissions from NG distribution systems.

Understanding CH₄ emissions at the source subcategory level is critical for developing actionable mitigation strategies. Most of the mitigation options we propose here rely on identifying the exact source subcategory responsible for the CH₄ emissions and the expected mass of CH₄ being released from that source subcategory. Broadly identifying an emission source as thermogenic or biogenic, where we find C₂:C₁ ratios are effective, provides valuable information regarding the general source of CH₄ emissions. Ultimately follow-up investigation is required to identify the specific source subcategory responsible for emissions. In urban environments, where sources are not easily distinguished due to the co-location of multiple potential emitters, understanding the exact source subcategory responsible for CH₄ emissions is even more important to identify the appropriate mitigation option. For example, a biogenic CH₄ plume detected via mobile surveying in a city would require further investigation to determine whether the source of said plume was a super-emitting WUH, historic or active landfill, another source not considered in this work (e.g.,

urban water body (Ars et al., 2020)), or a combination of all of the above. The mitigation options for all sources and source subcategories vary in both cost, technology readiness, and expected CH₄ reductions. Individual source measurements offer the advantage of high accuracy in both CH₄ emission rate quantification and source subcategory identification but are labour intensive. Therefore, it is important to effectively couple other methods such as mobile surveying with individual source measurements, geochemistry, and geospatial database analysis to better quantify and reduce CH₄ emissions from urban sources.

5.5 Acknowledgements

We would like to thank AF, SC, and PL of Énergir for sharing data, guidance and aid in preparation of field work. We also thank McGill Sustainability Systems Initiative New Opportunities Award - Adapting Urban Environments for the Future awarded to MK, Natural Sciences and Engineering Research Council CGS-D awarded to JPW (reference ID: CGS-D 559246-2021), Mitacs Accelerate Grant awarded to MK and JPW, and McGill Engineering Doctoral Award to JPW for providing funding.

5.6 Supplementary information

5.6.1 Mobile surveying and site selection

Individual source measurements were partially guided by a 1,200 km mobile surveying campaign that identified on-road CH₄ plumes. The mobile surveys in Montréal were performed over a span of six days from November 18-24th, 2019 using a vehicle mounted Picarro G2401 analyzer that measured CH₄, CO₂, CO, and H₂O concentrations at a 0.5 Hz frequency. We separated super-ambient CH₄ plumes from background gas concentrations using the methods described in Ars et al. (2020). Background gas concentrations are calculated using a two step approach: first the fifth percentile is applied through a moving window optimized to the driving speed, and second the standard deviation of the first background estimate is calculated to identify areas where wide plumes were encountered which is then adjusted to interpolated values.

We categorized CH₄ plumes measured during mobile surveying as small (height of 0.04-0.2 ppm, width of 50-500 ppm/m²), medium (height of 0.2-1 ppm, width of 500-1000 ppm/m²), and large (height over 1 ppm, width greater than 1000 ppm/m²) according to the plume height and width (Table S2) (Ars et al., 2020). Sites were selected qualitatively for two direct measurement campaigns by visually identifying areas (2 km²) in Montréal with a higher density of CH₄ enhancements observed during the mobile surveys. The specific locations of the plumes were not targeted, but rather the general area of the plumes. The sampled sites that were guided by mobile surveys were primarily WUHs, residential meter-sets, and historic landfill sites. Larger NG distribution stations were sampled based on advice provided by Energir, where sites in high-traffic areas or on roads were avoided and sites in quieter low traffic areas were prioritized. These sites were measured over two direct measurement campaigns where these larger NG distribution sites were specifically targeted.

5.6.2 Static chamber measurements

We measured CH₄ concentration build-up continuously over a period of 1 to 10 minutes within pre-constructed static chamber using either a Sensit Portable Methane Detector for higher methane concentrations (i.e., above 400 ppm) or a Picarro G4301 Gas Scouter for lower concentrations (i.e., below 400 ppm). The use of the Picarro G4301 allowed for the simultaneous measurement of carbon dioxide (CO₂) concentrations within the chamber. Mass flow rates of CH₄ were calculated using 5.1:

$$M = \frac{dc}{dt}V \quad (5.1)$$

where M is the mass flow rate, dc is the change in concentration, dt is the change in time, and V_e is the effective volume of the chamber, assuming that the initial concentration of CH₄ in the chamber is negligible. A minimum R² of 0.80 was required for a flowrate estimate to be used as the given emission rate for that site. Chamber sizes and dimensions varied depending on the source being measured. For NG systems, chambers were built in-situ depending on the location and type of leaking component and varied from 10 to 30 Litres in volume. For WUH covers and landfills a 20 Litre plastic chamber or the Picarro Mobile Soil Flux System was used (9.4 Litres). At landfills the chamber or mobile soil flux system was set up directly on the soil surface of the landfill. For wastewater covers a rubber mat was placed over the cover to isolate gas transport to the chamber. At the terminus of all flowrate measurements a sample of air was withdrawn from the chamber to a vacuumed and N₂-purged 35mL or 125mL glass vial for further geochemical analysis. Pictures of static chamber setups from all three source types are shown in Figure S5.3.

5.6.3 Description of source subcategories

Eight different NG station types were considered for our study. A branch station links the distribution lines in Montréal to the TransCanada pipeline. There is only one branch station in the region of Montréal. Gate stations are complex sites making up several units that clean NG, regulate pressure

and temperature, and odorize the NG through the injection of mercaptan before delivery into the main distribution lines. District regulator stations are secondary regulating facilities located downstream of the main gate stations and further regulate the gas pressure. Industrial, commercial, and residential meter sets are stations that regulate gas pressure to the desired pressure of the customer and measure the amount of gas consumed. A valve station is used to isolate a segment of the main transmission line for maintenance or tie-in purposes. Telemetry stations are used to monitor gas pressures through remote sensing. Third party breaks were classified in three groups: calculated volume released (i.e., volume is estimated), negligible (i.e., break occurred but presence of a leak limiter in the system prevented any fugitive release), and incalculable (i.e., leak was shut-off by third party making it impossible to estimate the volume released).

Static chamber measurements from landfills were conducted predominantly on the ground surface which we defined as soil gas fluxes. We also measured above-ground sources which we classify as either vents/stacks or wells (Figure S5.2). Seven vents/stacks were measured at LF-36 which surrounded an Astroturf outdoor recreation facility, and 12 observation wells were sampled at two different historic landfill sites. Three types of WUHs were sampled throughout this study. Sewer covers are connected to the underground sewage lines which transport wastewater to a treatment and disposal site (i.e., wastewater treatment plant). Storm drains are open channels that collect rainwater, floodwater, and melted snow/ice and convey wastewater to a wastewater treatment and disposal site. They also collect aboveground debris (e.g., vegetation and garbage) that passes through the grated covers. Other WUH types are a category we assign to the remaining WUH covers where we could not positively identify the cover as sewer or storm drain. This category was created as we observed several sites we measured in the field did not correlate with the mapped WUHs meaning that the maps of WUHs for Montréal do not contain every WUH in Montréal. Common markings on these covers include conduit, interceptor, and aqueduct.

5.6.4 Annual methane emissions calculations

Emission factors used in the calculation of annual CH₄ emissions from Montréal were calculated for each of the source types used in this study (Table S5.3). The highest emission factor was attributed to the NG gate stations, more specifically from pneumatic vents located on site. Emission factors for historic landfills that were not directly measured were calculated from the spatially weighted fluxes from all other measured historic landfill sites (Table S5.3).

All emission factors were multiplied with their corresponding activity data (Table S5.2) to obtain an estimate of annual emissions for Montréal in 2020. Activity data for residential meter sets was estimated by counting the sum of secondary NG distribution lines. The secondary NG distribution lines branch from the main distribution lines to deliver NG to customers. This method of calculating activity data for the residential meter sets was chosen based on expert input from Energir. The areal cover of historic landfills was calculated based on the shapefiles of known historic landfill sites provided by the City of Montréal data portal. Activity data for WUHs was the number of sewers and storm drains contained in Montréal's geospatial database. No activity data was available for wastewater covers so it was assumed that have the same activity data as sewer WUH. Based on a report by the EPA, they estimate a total distribution of WUHs to be one per 400 ft² of pavement in the U.S., which equates to a total of roughly 453,000 WUHs in Montréal. Based on the number of storm drains and sewer covers in Montréal, a remaining 155,000 WUHs are unaccounted for, which means our estimate for wastewater covers may be an underestimate. Geospatial information on the number of historic landfill observation wells and vents is unknown but based on historical map data from the City of Montréal data portal we can assume the total number is low (i.e., less than 1000), and therefore their inclusion would not increase overall CH₄ emissions estimates by more than 0.1%. For the gridded inventory of CH₄ emissions in Montréal, a shapefile representing Montréal was divided into equal 250m by 250m cells. Within each cell the activity data for each source and subcategory was counted and multiplied by their respective emission factor.

5.6.5 Geochemical analysis and Keeling plot regressions

Glass vial samples gathered in the field were analyzed on a Picarro G2210-i benchtop analyzer using Tedlar bag dilutions to accommodate the allowed methane concentration ranges of the analyzer. We diluted the gas samples with extra dry air in Tedlar bags to accommodate the CH₄ threshold of the Picarro analyzer. Samples were analyzed on the Picarro for CH₄, CO₂, δ¹³C-CH₄, H₂O, and C₂:C₁ ratios (i.e., ratio of CH₄ to C₂H₆) using the averaged values over a five minute interval after one minute was allowed for the readings to stabilise. Vial samples were injected into 1-Litre Tedlar bags using 60 mL syringes. The vial samples were further diluted using extra-dry zero air (Linde Canada) using a 500 mL syringe which was injected directly into the Tedlar bag. Volumes of both the sample and zero air were determined using the estimated CH₄ concentration in the vial sample to ensure that the diluted CH₄ concentration within the Tedlar did not exceed the analyzer specifications. At the beginning of each analysis, a Tedlar bag sample of pure extra dry air was analyzed to determine the corresponding concentration values. During each day of analysis, one CH₄ concentration standard (i.e., 49.9, 502, 1005, 15,000, 25,000 ppm) and one C₂H₆ standard (i.e., 10.4, 100 ppm) were analyzed. The measured discrepancies averaged at 5% for CH₄ and 1% for C₂H₆.

Source δ¹³C-CH₄ signatures, C₂:C₁ ratios, and CO₂:CH₄ ratios were all calculated using a Keeling plot regression of the extra dry air values versus the values measured from the Tedlar diluted samples. In some cases we observed that CH₄ sources were sinks of CO₂ which yielded a negative CO₂:CH₄ ratio which we observe in samples from all three source types. In all instances we are assuming that the geochemical fingerprint of the extra dry air is similar to the background gas fingerprints of the measured sites in order for the Keeling plot regression to hold true. We performed a sensitivity analysis while varying the background δ¹³C-CH₄ signatures, C₂:C₁ ratios, and CO₂:CH₄ ratios to observe differences from our calculated source signatures versus the source signatures that would be calculated under these different background ranges (Figure S5.4).

From our sensitivity analysis we found that selecting an excess CH₄ concentration threshold of 1.0 ppm minimizes the calculated differences between the Keeling plot regression values while

retaining at least 50% of samples. The selected background ranges for CO₂ concentrations were 375 and 500 ppm which corresponds to the range of ambient CO₂ concentrations measured by the Picarro G4301 while on site. The selected background ranges for C₂:C₁ ratios were 0.0001 and 0.0005 which were selected based on the highest ranges observed from sampling lab air by the Picarro G2210-i at McGill University. The selected background ranges for δ¹³C-CH₄ signatures were -48‰ and -43‰ which were also selected based on the highest ranges observed from sampling lab air by the Picarro G2210-i at McGill University.

5.6.6 Methane mitigation costs

Methane abatement costs were calculated using the estimated reduction in CH₄ emissions and the anticipated costs. Estimated reductions in CH₄ emissions were based on the reported reductions from scientific studies in all cases except for third party breaks. In addition, the social cost of CH₄ was also included in the abatement calculations at a rate of USD \$1,027 per tonne of CH₄ based on the 2020 value provided by Environment and Climate Change Canada. The conversion of \$CAD to \$USD was listed as 1.252:1 (USD:CAD). The cost of natural gas was based on the monthly average of the natural gas prices provided by the Energy Information Agency from 2000 to 2021 (Henry Hub Natural Gas Spot Price) at USD 4.42 \$ per MMBtu. Electricity costs were estimated at USD \$0.1042 per kWh. The potential CH₄ reductions and relative costs of abatement are outlined in Table S5.4. The specific abatement costs for each source type are discussed below.

Methane mitigation costs – NG distribution

Abatement costs were estimated for the major CH₄ sources we found from our measurements: residential and industrial meter-sets, pneumatic systems at NG gate stations, and third party breaks. Leak detection and repair (LDAR) costs were estimated from the Carbon Limits report (Limits, 2014) which was created using data primarily gathered from Canadian upstream and midstream oil and gas facilities. We assumed a cost per LDAR survey for an industrial meter set to be USD \$400, which is the value cited in the Carbon Limits report for a well site. We assumed the LDAR costs

for residential meter sets based on a linear relationship between the number of components for an industrial meter set (i.e., 59 components) compared to a residential meter-set (i.e., 13 components) taken from the 2019 Air Emissions Methodology Manual (Clearstone Engineering Ltd., 2020), which was USD \$85 per LDAR survey. Average repair costs were calculated from a weighted average of the average component repair costs from the Carbon Limits report and the number of datapoints for each component, which was USD \$72 (Limits, 2014). For third party breaks, we base our estimated CH₄ reductions on a theoretical scenario in which half of the 33% of third party breaks involving a lack of underground pipeline checks, which are offered at no cost in Montréal, are negated through more stringent regulations enforced at the municipal level.

Methane mitigation costs – wastewater utility holes

The mitigation options for WUHs we consider involve the chemical dosage of wastewater networks to impede the production of CH₄. Nitrate and ferric iron dosages promote the growth of nitrate reducing bacteria which compete with methanogenic archaea (Jiang et al., 2013; Mohanakrishnan et al., 2009; Zhang et al., 2009). Free nitric acid is biocidal to methanogenic archaea (Jiang et al., 2011a). Oxygen injections (Ganigué and Yuan, 2014) and pH control through hydroxide dosages (Gutierrez et al., 2014, 2009) suppress the development of methanogenic populations in sewer biofilms. Abatement costs for WUHs were estimated using the observed or simulated reductions in CH₄ production in sewer systems from a variety of studies (Table S5.4). We found no studies that quantified the expected reductions in atmospheric CH₄ emissions, and therefore assumed that the expected reductions in CH₄ production would manifest equally in reductions to atmospheric CH₄ emissions. The costs of abatement were calculated from the bulk costs of chemicals/supplied needed for the dosage of wastewater and scaled to the City of Montréal, including the capital costs of installing a chemical dosing system which include a dosing pump, container, NIST calibrated flowmeter, piping, concrete padding, and fencing. Annual wastewater produced by Montréal was estimated to be 1,825 million tonnes based on a daily estimated wastewater production of 5 million tonnes. The annual electricity costs for a dosing system were estimated at \$110 per station. The

potential CH₄ reductions and relative costs of abatement are described in Table S5.4. No costs were estimated for the hiring of technicians or companies to implement wastewater dosages.

Methane mitigation costs – Historic landfills

Abatement costs for historic landfills were based on the installation costs of landfill gas (LFG) collection systems estimated by a Waste Management report (Duffy, 2019). We applied a range of costs for the installation and maintenance of LFG extraction and storage equipment based on the ranges stated in the Waste Management report (Duffy, 2019). These costs are comparable on a per-acre level to those used in the EPA's LFGcostV3.5 model. We did not use the LFGcostV3.5 model directly since the model requires an estimate of the total quantity of waste deposited which is unknown, or highly uncertain in the case of these historical landfill sites. We applied these costs to a scenario where all historic landfills in Montréal are targeted, and to the two highest emitting historic landfills we measured to illustrate the impacts of a targeted installation of LFG equipment. We estimated the costs based on a project life of 15 years, which is the default timeline used in the LFGcostV3.5 model. The expected reductions in atmospheric CH₄ emissions were estimated to be 85% which is equal to the extraction efficiency of the LFG recovery system. We employed a CH₄ production decay rate of 4% per year, and an LFG to compressed natural gas conversion rate of 65%. Our abatement cost estimates for historic landfills do not include the fact that some historic landfill sites already have some LFG monitoring equipment installed (e.g., observation wells), which would offset overall costs.

Table 5.1: Ranking of CH₄ emission sources from Montréal’s 2018 greenhouse gas inventory.

Sector	GPC Scope*	Category	Description	CH ₄ emissions (tons per year)
Waste	3	Solid waste disposal	All waste	10,627
Stationary	1	Fugitive emission from O&G systems	Emissions from NG distribution	590
Waste	1	Solid waste disposal	All waste	570
Waste	3	Biological treatment of waste	Composting	241
Stationary	1	Residential building	Wood combustion	172
AFOLU	1	Livestock	Enteric fermentation and manure management	134
Stationary	1	Energy industries	Petroleum refining and combined heat and power	80
Waste	1	Biological treatment of waste	Composting	74
Transportation	1	Off-road transportation	Motor gasoline (petrol)	47
Stationary	1	Commercial/institutional building and facilities	NG combustion	23
Transportation	1	Aviation	Fuel combustion from domestic air transport	22
Transportation	1	Waterborne navigation	Domestic maritime transport weighted to Port of Montreal	22
Waste	1	Wastewater treatment and discharge	Fugitive emissions from wastewater treatment and septic tanks	20

*GPC scope: Global Protocol for Cities guidelines on emission source classification where Scope 1 emissions are emissions produced within the city boundary and Scope 3 emissions are emissions originating from the activity inside the city boundaries but where emissions occur outside of the city boundary.

Table 5.2: Activity data used for all source types and sub-types considered in this study. Units for each source are unique to the type of emissions present. The associated uncertainty in activity data assuming a uniform distribution is shown in parenthesis.

NG distribution	Activity data (% uncertainty) [# sites]
Branch station	1 ($\pm 0\%$)
Gate station	2.5* ($\pm 5\%$)
District regulator stations	85 ($\pm 0\%$)
Industrial/commercial meter-sets	298 ($\pm 0\%$)
Residential meter-sets	85,977 ($\pm 20\%$)
Valve station	64 ($\pm 0\%$)
Telemetry station	17 ($\pm 0\%$)
Pre-detention station	1 ($\pm 0\%$)
WUH	Activity data (% uncertainty) [# sites]
Water distribution	116,304 ($\pm 20\%$)
Sewer	116,304 ($\pm 20\%$)
Storm drains	182,231 ($\pm 20\%$)
Historic landfills	Activity data (% uncertainty) [m²]
Historic landfills	7,027,116 ($\pm 20\%$)
Historic landfills - above-ground	Activity data (% uncertainty) [# per m²]
Observation wells	152 ($\pm 50\%$)
Vents	88 ($\pm 50\%$)

*One NG gate station does not operate for six months out of the year which is interpreted as an activity data value of 0.5 (i.e., annual CH₄ emissions are 50% of station operating for entire year).

Table 5.3: Classification of methane plumes measured during mobile surveys. Classification criteria follows that outlined in Ars et al. (2020).

Enhancement classification	Enhancement height (ppm)	Enhancement width (ppm/m ²)
Large	≥ 1	$\geq 1,000$
Medium	0.2 to 1	500 to 1,000
Small	0.04 to 0.2	50 to 500
Negligeable*	≤ 0.04	≤ 50

*Considered to have a likely chance of being caused by analyzer noise and therefore excluded from analysis.

Table 5.4: Source category and mitigation activity, potential reduction in methane emissions and reasoning, and source of costs.

Category	Methane reductions (%)	Cost of implementation (\$USD) and other considerations
WUH - Nitrate	42% (Jiang et al., 2013)	\$210 per ton CaNO ₃ ^a 5 dosing stations capital costs per station \$8,500 ^b \$110 per year electricity cost per dosing station 15-year timeframe
WUH - Oxygen	47 % (Ganigué and Yuan, 2014)	\$125 per ton CaO ₂ ^a 5 dosing stations capital costs per station 8,500 ^b \$110 per year electricity cost per dosing station 15-year timeframe
WUH - Nitrate	13% (Jiang et al., 2011a)	\$210 per ton CaNO ₃ ^a 5 dosing stations capital costs per station \$8,500 ^b \$110 per year electricity cost per dosing station 15-year timeframe
WUH - Nitrate	27% (Jiang et al., 2011a)	\$210 per ton CaNO ₃ ^a 5 dosing stations capital costs per station \$8,500 ^b \$110 per year electricity cost per dosing station 15-year timeframe
WUH - Hydroxide	97% (Gutierrez et al., 2009)	\$470 per ton NaOH ^a 5 dosing stations capital costs per station \$8,500 ^b \$110 per year electricity cost per dosing station 15-year timeframe
WUH - Iron salts	43% (Zhang et al., 2009)	\$125 per ton CaO ₂ 5 dosing stations capital costs per station \$8,500 ^b \$110 per year electricity cost per dosing station 15-year timeframe
WUH - Free nitric acid	99% (Jiang et al., 2011a)	\$700 per ton NaNO ₂ and HCl combined ^a 5 dosing stations capital costs per station \$8,500 ^b \$110 per year electricity cost per dosing station 15-year timeframe
NG distribution - LDAR residential meters repair top 10% emitters	89% (Methane Guiding Principles, 2019)	\$72 per repair top 10% of emitters repaired 1 repairs per site \$85 per LDAR survey annual LDAR survey \$245 per ton natural gas (Methane Guiding Principles, 2019)
NG distribution - Transition from pneumatics to air	100% (Limits, 2014)	\$60,000 for initial installation \$1,000 per year for maintenance \$13,000 per year electricity 15-year timeframe \$245 per ton natural gas (Limits, 2014)
NG distribution - LDAR industrial meters repair top 10% emitters	91% (Limits, 2014)	\$72 per repair top 10% of emitters repaired 2 repairs per site \$85 per LDAR survey maintain LDAR frequency \$245 per ton natural gas (Limits, 2014)
NG distribution - Mandatory pipeline checks	17%	No cost as pipeline checks are free \$245 per ton natural gas
NG distribution - LDAR residential meters semi-annual frequency	75% (Limits, 2014)	\$85 per LDAR survey \$72 per repair 1 repair per leaking site \$245 per ton natural gas (Limits, 2014)
NG distribution - LDAR industrial meters increase frequency from semi-annual to quarterly	25% (Limits, 2014)	\$400 per LDAR survey \$72 per repair 2 repairs per leaking site \$245 per ton natural gas (Limits, 2014)
Landfills - Installation of gas recovery system	85%	Cost range of \$30,000-54,000 per acre installation \$800-1,100 per acre maintenance 65% LFG to CNG conversion \$245 per ton natural gas (Duffy, 2019)
Landfills - Installation of gas recovery systems: targeted to high emitting landfills	4%	Cost range of \$30,000-54,000 per acre installation \$800-1,100 per acre maintenance 65% LFG to CNG conversion \$245 per ton natural gas (Duffy, 2019)

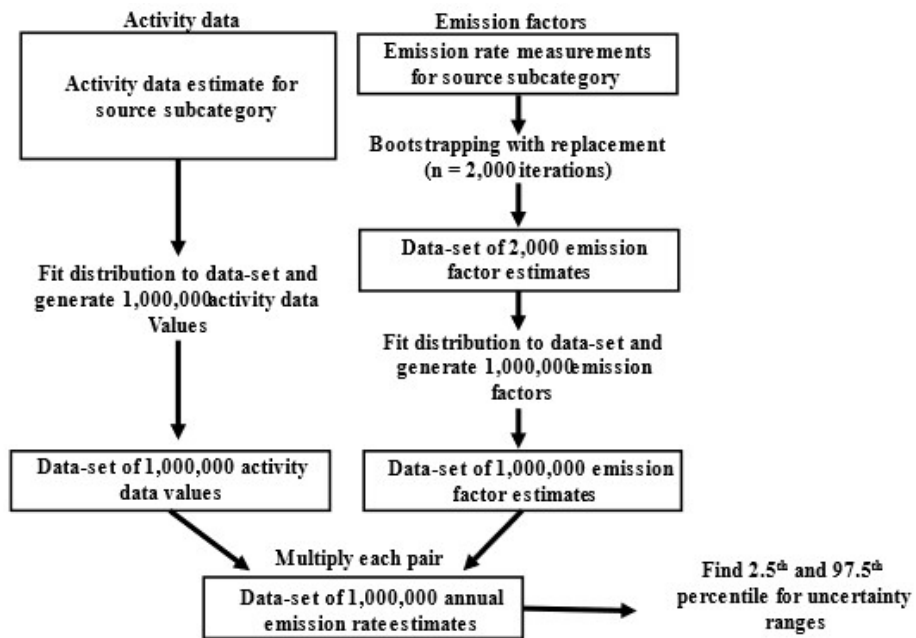


Figure 5.6: Stepwise methodology of uncertainty range calculations for CH₄ source subcategories in this work.



Figure 5.7: Photos of two CH₄ source types encountered at some historic landfill locations: A) observation well with locked cap; B) J-shaped metal vent surrounding an Astroturf outdoor recreation facility built over a historic landfill site.

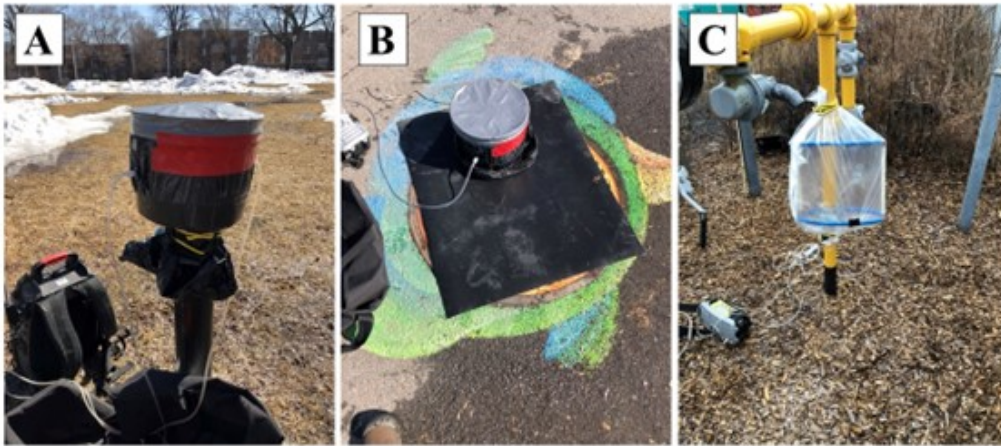


Figure 5.8: Static chambers installed over three different source types: A) observation well located on a historic landfill site; B) wastewater cover with rubber mat installed (opening located underneath chamber); C) leaking valve on a NG station.

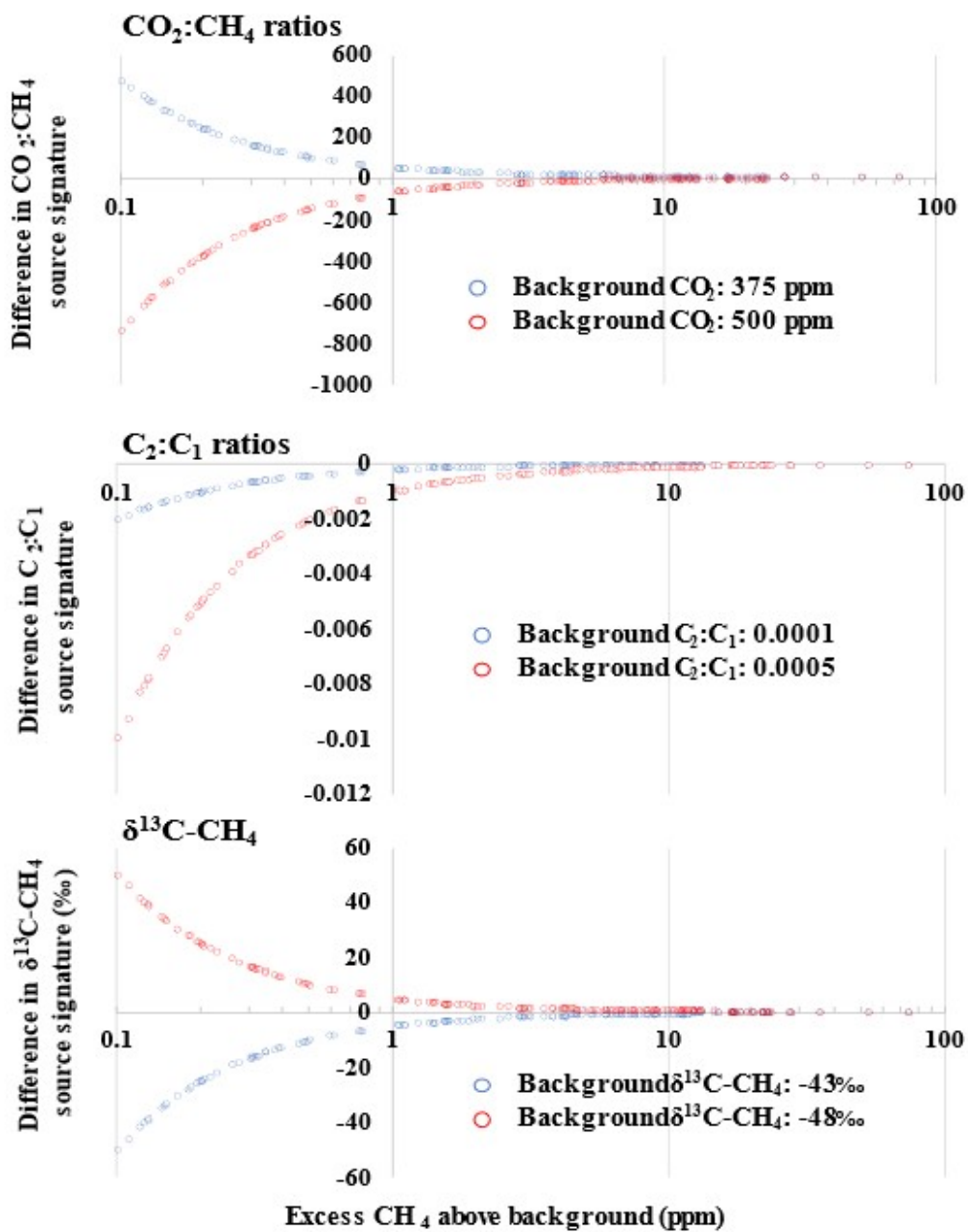


Figure 5.9: Sensitivity analysis of Keeling plot regressions of source signatures assuming different background levels of $\delta^{13}\text{C-CH}_4$ signatures, $\text{CO}_2:\text{CH}_4$ ratios, and $\text{C}_2:\text{C}_1$ ratios.

Bibliography

- Agency, U. S. E. P.: LFGcost-Web — Landfill Gas Energy Cost Model, Washington, DC, USA, <https://www.epa.gov/lmop/lfgcost-web-landfill-gas-energy-cost-model>, 2021.
- Ars, S., Vogel, F., Arrowsmith, C., Heerah, S., Knuckey, E., Lavoie, J., Lee, C., Pak, N. M., Phillips, J. L., and Wunch, D.: Investigation of the spatial distribution of methane sources in the Greater Toronto Area using mobile gas monitoring systems, *Environmental Science & Technology*, 54, 15 671–15 679, 2020.
- Babilotte, A., Lagier, T., Fiani, E., and Taramini, V.: Fugitive methane emissions from landfills: field comparison of five methods on a French landfill, *Journal of Environmental Engineering*, 136, 777–784, 2010.
- Brandt, A. R., Heath, G., Kort, E., O’Sullivan, F., Pétron, G., Jordaan, S. M., Tans, P., Wilcox, J., Gopstein, A., Arent, D., and Wofsy, S.: Methane leaks from North American natural gas systems, *Science*, 343, 733–735, 2014.
- Chamberlain, S. D., Ingraffea, A. R., and Sparks, J. P.: Sourcing methane and carbon dioxide emissions from a small city: Influence of natural gas leakage and combustion, *Environmental pollution*, 218, 102–110, 2016.
- Christophersen, M., Kjeldsen, P., Holst, H., and Chanton, J.: Lateral gas transport in soil adjacent to an old landfill: factors governing emissions and methane oxidation, *Waste Management & Research*, 19, 595–612, 2001.
- Clearstone Engineering Ltd.: Estimation of Air Emissions from the Canadian Natural Gas Transmission, Storage and Distribution System, 2020.
- Defratyka, S. M., Paris, J.-D., Yver-Kwok, C., Fernandez, J. M., Korben, P., and Bousquet, P.: Mapping urban methane sources in Paris, France, *Environmental science & technology*, 55, 8583–8591, 2021.
- Duffy, D.: Day to Day, <https://www.mswmanagement.com/landfills/article/13036124/day-to-day>, accessed 2022-09-20, 2019.
- Environment and Climate Change Canada: Technical Update to Environment and Climate Change Canada’s Social Cost of Greenhouse Gas Estimates, 2016.
- Fernandez, J., Maazallahi, H., France, J., Menoud, M., Corbu, M., Ardelean, M., Calcan, A., Townsend-Small, A., van der Veen, C., Fisher, R., et al.: Street-level methane emissions of Bucharest, Romania and the dominance of urban wastewater., *Atmospheric Environment: X*, 13, 100 153, 2022.
- Floerchinger, C., Shepson, P. B., Hajny, K., Daube, B. C., Stirm, B. H., Sweeney, C., and Wofsy, S. C.: Relative flux measurements of biogenic and natural gas-derived methane for seven US cities, *Elementa: Science of the Anthropocene*, 9, 2021.
- Fong, Wee Kean Sotos, M., Schultz, S., Deng-Beck, C., Marques, A., and Doust, M.: Global protocol for community-scale greenhouse gas emission inventories, 2014.

- Fries, A. E., Schifman, L. A., Shuster, W. D., and Townsend-Small, A.: Street-level emissions of methane and nitrous oxide from the wastewater collection system in Cincinnati, Ohio, *Environmental Pollution*, 236, 247–256, 2018.
- Ganigué, R. and Yuan, Z.: Impact of oxygen injection on CH₄ and N₂O emissions from rising main sewers, *Journal of environmental management*, 144, 279–285, 2014.
- Guerrero, L. A., Maas, G., and Hogland, W.: Solid waste management challenges for cities in developing countries, *Waste management*, 33, 220–232, 2013.
- Guisasola, A., Sharma, K. R., Keller, J., and Yuan, Z.: Development of a model for assessing methane formation in rising main sewers, *Water Research*, 43, 2874–2884, 2009.
- Gutierrez, O., Park, D., Sharma, K. R., and Yuan, Z.: Effects of long-term pH elevation on the sulfate-reducing and methanogenic activities of anaerobic sewer biofilms, *Water research*, 43, 2549–2557, 2009.
- Gutierrez, O., Sudarjanto, G., Ren, G., Ganigué, R., Jiang, G., and Yuan, Z.: Assessment of pH shock as a method for controlling sulfide and methane formation in pressure main sewer systems, *Water research*, 48, 569–578, 2014.
- Hendrick, M. F., Ackley, R., Sanaie-Movahed, B., Tang, X., and Phillips, N. G.: Fugitive methane emissions from leak-prone natural gas distribution infrastructure in urban environments, *Environmental Pollution*, 213, 710–716, 2016.
- Hopkins, F. M., Ehleringer, J. R., Bush, S. E., Duren, R. M., Miller, C. E., Lai, C.-T., Hsu, Y.-K., Carranza, V., and Randerson, J. T.: Mitigation of methane emissions in cities: How new measurements and partnerships can contribute to emissions reduction strategies, *Earth's Future*, 4, 408–425, 2016.
- Hugenholtz, C. H., Vollrath, C., Gough, T., Wearmouth, C., Fox, T., Barchyn, T., and Billingham, C.: Methane emissions from above-ground natural gas distribution facilities in the urban environment: A fence line methodology and case study in Calgary, Alberta, Canada, *Journal of the Air & Waste Management Association*, 71, 1319–1332, 2021.
- IPCC: *Climate Change 2022: Mitigation of Climate Change. Contribution of Working Group III to the Sixth Assessment Report of the Intergovernmental Panel on Climate Change*, Cambridge University Press, Cambridge, UK and New York, NY, USA, <https://doi.org/10.1017/9781009157926>, 2022.
- Jiang, G., Gutierrez, O., Sharma, K. R., Keller, J., and Yuan, Z.: Optimization of intermittent, simultaneous dosage of nitrite and hydrochloric acid to control sulfide and methane productions in sewers, *Water research*, 45, 6163–6172, 2011a.
- Jiang, G., Gutierrez, O., and Yuan, Z.: The strong biocidal effect of free nitrous acid on anaerobic sewer biofilms, *Water research*, 45, 3735–3743, 2011b.
- Jiang, G., Sharma, K. R., and Yuan, Z.: Effects of nitrate dosing on methanogenic activity in a sulfide-producing sewer biofilm reactor, *Water research*, 47, 1783–1792, 2013.

- Kang, M., Kanno, C. M., Reid, M. C., Zhang, X., Mauzerall, D. L., Celia, M. A., Chen, Y., and Onstott, T. C.: Direct measurements of methane emissions from abandoned oil and gas wells in Pennsylvania, *Proceedings of the National Academy of Sciences*, 111, 18 173–18 177, 2014.
- Kang, M., Christian, S., Celia, M. A., Mauzerall, D. L., Bill, M., Miller, A. R., Chen, Y., Conrad, M. E., Darrah, T. H., and Jackson, R. B.: Identification and characterization of high methane-emitting abandoned oil and gas wells, *Proceedings of the National Academy of Sciences*, 113, 13 636–13 641, 2016.
- Lamb, B. K., Cambaliza, M. O., Davis, K. J., Edburg, S. L., Ferrara, T. W., Floerchinger, C., Heimburger, A. M., Herndon, S., Lauvaux, T., Lavoie, T., and Lyon, D.: Direct and indirect measurements and modeling of methane emissions in Indianapolis, Indiana, *Environmental Science & Technology*, 50, 8910–8917, 2016.
- Limits, C.: Quantifying Cost-effectiveness of Systematic Leak Detection and Repair Programs Using Infrared Cameras - CL report CL-13-27, Tech. rep., https://www.carbonlimits.no/wp-content/uploads/2015/06/Carbon_Limits_LDAR.pdf, 2014.
- Lisk, D. J.: Environmental effects of landfills, *Science of the total environment*, 100, 415–468, 1991.
- Liu, Y., Ni, B.-J., Sharma, K. R., and Yuan, Z.: Methane emission from sewers, *Science of the Total Environment*, 524, 40–51, 2015.
- Lohila, A., Laurila, T., Tuovinen, J.-P., Aurela, M., Hatakka, J., Thum, T., Pihlatie, M., Rinne, J., and Vesala, T.: Micrometeorological measurements of methane and carbon dioxide fluxes at a municipal landfill, *Environmental science & technology*, 41, 2717–2722, 2007.
- Magder, J.: Increased number of gas leaks in Montreal probably tied to construction boom, <https://montrealgazette.com/news/local-news/increased-number-of-gas-leaks-likely-tied-to-construction-boom>, accessed 2022-08-15, 2018.
- Marcotullio, P. J., Sarzynski, A., Albrecht, J., Schulz, N., and Garcia, J.: The geography of global urban greenhouse gas emissions: An exploratory analysis, *Climatic Change*, 121, 621–634, 2013.
- McKain, K., Down, A., Raciti, S. M., Budney, J., Hutyra, L. R., Floerchinger, C., Herndon, S. C., Nehrkorn, T., Zahniser, M. S., Jackson, R. B., and Phillips, N.: Methane emissions from natural gas infrastructure and use in the urban region of Boston, Massachusetts, *Proceedings of the National Academy of Sciences*, 112, 1941–1946, 2015.
- Methane Guiding Principles: Reducing Methane Emissions: Best Practice Guide - Pneumatic Devices, 2019.
- Mohanakrishnan, J., Gutierrez, O., Sharma, K., Guisasola, A., Werner, U., Meyer, R., Keller, J., and Yuan, Z.: Impact of nitrate addition on biofilm properties and activities in rising main sewers, *Water research*, 43, 4225–4237, 2009.

- Nastev, M., Therrien, R., Lefebvre, R., and Gelinas, P.: Gas production and migration in landfills and geological materials, *Journal of contaminant hydrology*, 52, 187–211, 2001.
- Nisbet, E., Fisher, R., Lowry, D., France, J., Allen, G., Bakkaloglu, S., Broderick, T., Cain, M., Coleman, M., Fernandez, J., and Forster, G.: Methane mitigation: Methods to reduce emissions, on the path to the Paris Agreement, *Reviews of Geophysics*, 58, e2019RG000675, 2020.
- Peischl, J., Ryerson, T., Brioude, J., Aikin, K., Andrews, A., Atlas, E., Blake, D., Daube, B., De Gouw, J., Dlugokencky, E., and Frost, G.: Quantifying sources of methane using light alkanes in the Los Angeles basin, California, *Journal of Geophysical Research: Atmospheres*, 118, 4974–4990, 2013.
- Petroleum Technology Alliance Canada: Canadian Upstream Oil and Gas Eco-Efficiency Equipment and Operations Handbook - 3.2.3. Instrument Gas to Instrument Air (IGIA) Conversion Projects for Pneumatic Control Systems, 2017.
- Phillips, N. G., Ackley, R., Crosson, E. R., Down, A., Hutyra, L. R., Brondfield, M., Karr, J. D., Zhao, K., and Jackson, R. B.: Mapping urban pipeline leaks: Methane leaks across Boston, *Environmental pollution*, 173, 1–4, 2013.
- Pichtel, J.: Waste management practices, CRC press, 2014.
- Plant, G., Kort, E. A., Floerchinger, C., Gvakharia, A., Vimont, I., and Sweeney, C.: Large fugitive methane emissions from urban centers along the US East Coast, *Geophysical research letters*, 46, 8500–8507, 2019.
- Rachor, I., Gebert, J., Gröngroft, A., and Pfeiffer, E.-M.: Variability of methane emissions from an old landfill over different time-scales, *European Journal of Soil Science*, 64, 16–26, 2013.
- Themelis, N. and Ulloa, P.: Capture and utilization of landfill gas, 2005.
- Ville de Montréal: Émissions de gaz à effet de serre de la collectivité montréalaise, Tech. rep., <https://donnees.montreal.ca/ville-de-montreal/emissions-ges-collectivite-montrealaise>, 2022a.
- Ville de Montréal: Carte de localisation des anciennes carrières et des dépôts de surface de la Ville de Montréal, Tech. rep., <https://environnementmtl.maps.arcgis.com/apps/webappviewer/index.html?id=eddf22f7ef54982a6545e8eb3c86a9a>, 2022b.
- Ville de Montréal: Regards d'égouts, Tech. rep., <https://donnees.montreal.ca/ville-de-montreal/regards-egouts>, 2022c.
- von Fischer, J. C., Cooley, D., Chamberlain, S., Gaylord, A., Griebenow, C. J., Hamburg, S. P., Salo, J., Schumacher, R., Theobald, D., and Ham, J.: Rapid, vehicle-based identification of location and magnitude of urban natural gas pipeline leaks, *Environmental Science & Technology*, 51, 4091–4099, 2017.
- Weller, Z. D., Roscioli, J. R., Daube, W. C., Lamb, B. K., Ferrara, T. W., Brewer, P. E., and von Fischer, J. C.: Vehicle-based methane surveys for finding natural gas leaks and estimating their size: Validation and uncertainty, *Environmental science & technology*, 52, 11922–11930, 2018.

- Weller, Z. D., Hamburg, S. P., and von Fischer, J. C.: A national estimate of methane leakage from pipeline mains in natural gas local distribution systems, *Environmental science & technology*, 54, 8958–8967, 2020.
- Whalen, S., Reeburgh, W., and Sandbeck, K.: Rapid methane oxidation in a landfill cover soil, *Applied and environmental microbiology*, 56, 3405–3411, 1990.
- Williams, P. J., Reeder, M., Pekney, N. J., Risk, D., Osborne, J., and McCawley, M.: Atmospheric impacts of a natural gas development within the urban context of Morgantown, West Virginia, *Science of the Total Environment*, 639, 406–416, 2018.
- Wunch, D., Toon, G. C., Hedelius, J. K., Vizenor, N., Roehl, C. M., Saad, K. M., Blavier, J.-F. L., Blake, D. R., and Wennberg, P. O.: Quantifying the loss of processed natural gas within California’s South Coast Air Basin using long-term measurements of ethane and methane, *Atmospheric Chemistry and Physics*, 16, 14 091–14 105, 2016.
- Zhang, L., Keller, J., and Yuan, Z.: Inhibition of sulfate-reducing and methanogenic activities of anaerobic sewer biofilms by ferric iron dosing, *Water research*, 43, 4123–4132, 2009.

Chapter 6

Characterizing and quantifying methane emissions from wastewater collection systems and urban water bodies

Connecting text: In this chapter, we present the results of direct measurements of methane emissions from biogenic urban sources in the Greater Toronto Area (GTA). We showed that annual methane emissions from urban water bodies and wastewater collection manholes (WUHs) are significant with respect to the most recent greenhouse gas (GHG) inventory for the GTA. We found that methane emissions from two high emitting methane sources were persistent throughout multiple years and seasons, which helps characterize the intermittence of their emissions. This study builds upon the research on urban methane sources presented in Chapter 5 and uses chamber-based methods presented in Chapters 3, 4, and 5.

The results of this research will be submitted to *Science of the Total Environment* under the title "Characterizing and quantifying methane emissions from wastewater collection manholes and urban water bodies". The authors will be listed as James P. Williams, Sebastien Ars, Felix Vogel, Lawson Gillespie, Debra Wunch, Louise Klotz, Anthony Fabien, and Mary Kang.

6.1 Introduction

Urban areas (i.e., cities) are a major source of methane emissions globally, and are expected to account for roughly 22% of global methane emissions (de Foy et al., 2023), and 35% of methane emissions in North America (Marcotullio et al., 2013). Multiple studies have found that annual methane emissions from cities in the United States as reported by the Environmental Protection Agency are underestimated by a factor of 2-4 (Anderson et al., 2021; Pitt et al., 2022), and that the underestimation could be widespread across sectors and geographies (Plant et al., 2022; de Foy et al., 2023; Fernandez et al., 2022; Whiting et al., 2022). A recent study by de Foy et al. (de Foy et al., 2023) found that top-down satellite estimates of methane emissions from the TROPospheric Monitoring Instrument from 61 cities across the world did not correlate to sectoral inventories, but did correlate with rates of untreated wastewater. Urban water bodies, which are another biogenic methane source, have been shown to account for over 10% of Berlin's total methane budget (Klausner et al., 2020; Herrero Ortega et al., 2019). These two sources of methane, wastewater utility holes (WUHs) and urban water bodies, are not included in greenhouse gas inventories (Fries et al., 2018; Fernandez et al., 2022; Ars et al., 2020; Defratyka et al., 2021; Herrero Ortega et al., 2019). Methane emissions from wastewater collection systems and urban water bodies may explain the observed discrepancies between municipal methane inventories and top-down and bottom-up measurement studies.

Methane emissions from wastewater collection systems have recently been highlighted as a potential significant source of methane in cities (Fernandez et al., 2022; Song et al., 2023; Defratyka et al., 2021). Fernandez et al. (2022) found that 58-63% of methane emissions in Bucharest, Romania, were attributed to urban wastewater emissions originating primarily from venting storm grates and sewer utility holes (i.e., also known as "manholes"). In Chapter 5 of this thesis, annual methane emissions from WUHs were estimated to emit 786 tons of methane in Montreal, Canada, which would be the third highest methane source in the city. A study based in Paris by Defratyka et al. (2021) found that 33% of methane leaks in the city were attributable to sewage. Despite these recent findings, methane emissions from WUHs are not included in municipal, provin-

cial/territorial/state, and national greenhouse gas inventories. In the wastewater treatment sector, methane correction factors, or multipliers, that translate biological/chemical oxygen demand to methane emissions from various stages of the wastewater treatment process are used (Eggleston et al., 2006). Notably, the IPCC Guidelines for National Greenhouse Gas Inventories (Calvo Buendia et al., 2019) for the waste sector list default methane correction factors for flowing sewers as zero, implying that methane emissions from closed underground wastewater collection systems are negligible or non-existent. To our knowledge, there has been only been Fries et al. (2018) and our research from Chapter 5 that has directly quantified methane emissions from WUHs. As such, there is a need for additional direct measurements from WUHs to better understand their emission rates and inform national inventories.

Urban water bodies are a second biogenic methane source that is not included in any form of greenhouse gas inventory despite being identified as a notable methane source in cities (Ars et al., 2020; Wang et al., 2021). Ars et al. (2020) found that methane emissions from a single urban water channel in Toronto, Canada, ranged from 100 to 400 kg/day (i.e., 36 to 146 tons of methane per year), although these emissions were not confirmed to be solely of biogenic origin (Ars et al., 2020). Another study by Wang et al. (2021) found that methane fluxes from lakes and ponds adjacent to Beijing, China were more than three times higher than the global average, with ebullitive fluxes more than six times higher than the global average (Wang et al., 2021). Most studies on methane emissions from urban water bodies highlight the fact that methane emissions from these sources occur either through ebullition events where methane produced in organic-rich anoxic sediment bubbles to the surface (Wang et al., 2021), or through diffusion at the water-to-air interface (Herrero Ortega et al., 2019). Urban water bodies are not considered to be an anthropogenic source of greenhouse emissions, despite having several characteristics that are influenced by human activity. The factors that lead to increased methane production from urban water bodies as opposed to natural water bodies include shallower depths that limit methane oxidation through the water column during ebullition (Herrero Ortega et al., 2019; Holgerson, 2015), heavily modified geomorphology which leads to increased catchment and retention of organic material (Walsh

et al., 2005), and increased influx of organic material from sources such as wastewater overflows and storm water drainage (Walsh et al., 2005; Ars et al., 2020). To our knowledge, there is only one study based in Canada that has quantified methane fluxes from one urban pond in Saskatchewan as part of a larger sample set (Baron et al., 2022), which highlights a need for additional direct measurements from urban water bodies in Canada, and elsewhere in the world (Walsh et al., 2005; DelSontro et al., 2018).

In this work, we (1) performed direct measurements of methane emissions from WUHs and urban water bodies in Toronto, Canada, and categorized them by source subcategory; (2) used empirical data on WUH counts from other cities in the U.S. and Canada to estimate the WUH counts in the GTA; (3) determined the areal extents of urban water bodies in the GTA; (4) analyzed mobile surveying data near a cluster of high emitting WUHs and an urban channel to assess the intermittency of methane emissions from these biogenic sources; and (5) performed estimates of annual methane emissions from WUHs and urban water bodies for the GTA.

6.2 Methods

6.2.1 Defining urban extents and site description

Our study focuses on methane emissions from the GTA, although we do incorporate data from other cities in Canada and the U.S. to develop our emission factor distributions or activity data. We acquired geospatial data from Statistics Canada to outline the geographic extent of the Greater Toronto Area (GTA) (Figure 6.1). We measured methane emissions from WUHs the GTA, and also used measurements from a prior study based on Montreal (Chapter 5). Both cities are considered to be warm-summer continental climates according to the Köppen-Geiger classification scheme. Additionally, we compiled WUH measurements from a prior study based in Indianapolis, U.S. (Fries et al., 2018), which is considered a humid subtropical climate (SI - Section 6.6.1). For urban water bodies, we measured methane fluxes from sites in the GTA.

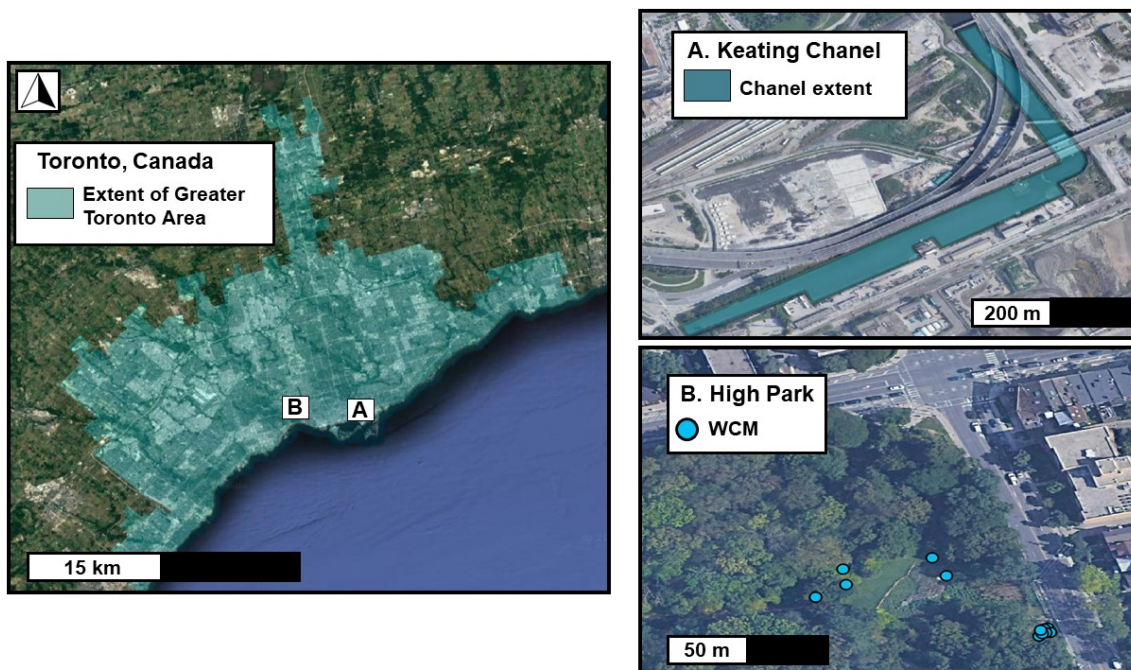


Figure 6.1: Maps of Toronto, Canada, with the Keating Channel and northeastern corner of High Park highlighted. High methane emitting wastewater utility holes in High Park are shown by blue dots.

We focused on the analysis of additional measurements from mobile surveys (described later in this section) to two specific locations in the GTA, the Keating Channel and a cluster of WUHS in a corner of High Park (Figure 6.1). Both locations were selected because they were identified as high methane emitting sites in extensive proximal (i.e., within 500 meters) mobile surveying data (i.e., n surveys above 10). Emissions from the Keating Channel had already been quantified from mobile surveying data in a previous study by Ars et al. (2020), although this analysis focused on warmer months from May to June, 2019. The Keating Channel is dredged annually over a period of three months with the removed material transported to a containment cell south of the city. Ars et al. (2020) also identified the northeastern corner of High Park but the source could not be determined using mobile surveying alone.

6.2.2 Emission factors

We performed individual source measurements of methane emissions from manholes and urban water bodies in the GTA from November 2021 to December 2022 using a static chamber methodology (Kang et al., 2014). We measured methane concentrations within the chamber head spaces using a Sensit Portable Methane Detector (0-100% methane range, 1 ppm sensitivity), Picarro G4301 Gas Scouter (0-800 ppm methane range, 1 ppb sensitivity), Los Gatos Research UGGA (0-1,000 ppm methane, 1 ppb sensitivity), and/or Li-Cor 7810 (0-100 ppm methane, 0.6 ppb sensitivity). We calculated methane flux rates using a linear regression of the rate of linear build-up of methane multiplied by the known chamber headspace volume and areas over time (Chapter 3). We used a rectangular 16.2 L and cylindrical 8.2 L floating chambers for measurements from urban water bodies, and a cylindrical 30 L chamber for measurements from WUHs. We used a single linear regression for methane flowrate measurements from WUHs with a minimum R^2 requirement of 0.80 for a measurement to be used and a typical measurement duration ranging from 3-5 minutes. For urban water bodies, we applied a similar approach to quantify methane flux rates over longer duration chamber deployments which ranged from 5 to 180 minutes (SI - Section 6.6.2). Longer deployments were used to capture the temporally sporadic methane emissions occurring from ebullition events. Methane emissions from urban water bodies occurred either as steady diffusive fluxes, or as intermittent ebullition events. Emission factors for diffusive fluxes were calculated as an average, similar to WUHs. For ebullition, we calculated emission factors for the different water body types by the total mass of methane per unit area emitted from ebullition divided by the total duration of time the chamber was measuring in that water body type. During longer chamber deployments (i.e., ≥ 20 minutes), the chamber would be manually vented every ~ 5 minutes either by pumping in atmospheric air, or lifting the chamber above the surface of the water to allow methane concentrations to drop back to atmospheric levels.

Emission factors were calculated for every type of urban water body and WUH through bootstrapping with replacement of the methane measurement data ($n = 10,000$). For urban water bodies, we used all measurements we gathered from our field work and divided the measurements into four

categories: ponds, bays, rivers, and canals. Additionally, we added lakes as a classification and used our pooled measurement data for bays, rivers, and ponds for the calculation of emission factors for lakes. For WUHs, we gathered direct measurement data from Chapter 5 and from Fries et al. (2018), including our own measurements from the GTA.

6.2.3 Activity data

We categorized WUHs as two subcategories, sewer WUHs and other WUHs based on the limited availability of categorized emission rate estimates data and activity data (i.e., WUH counts). Few cities in Canada and the U.S. provide data on the counts and types of WUHs within city boundaries. The GTA is an agglomeration of the city of Toronto and the four regional municipalities of York, Durham, Peel, and Halton. Publicly available data on WUH counts is not available for any of these urban regions. In order to estimate the number and types of WUHs in the GTA, we collected municipal data of total WUH counts from fifteen cities in Canada and three cities in the United States, and municipal data of sewer WUH counts from fourteen cities in Canada and one from the United States (Figure 6.2). We estimated the number of WUHs in the GTA using this linear model relating the population of the city to the WUH count (SI - Figure 6.8). We used two linear relationships: one to estimate the number of sewer manholes which were the most common type of reported WUH, and one to estimate the total number of WUHs which includes additional types to sewers such as storm drains, combined sewer/storm manholes, abandoned/inactive manholes (i.e., connected to abandoned or inactive wastewater collection system), and wet wells (i.e., manholes located at the terminus of a rising main wastewater system). We calculated the number of "other" WUH types other than sewers by subtracting the estimated number of sewer WUHs from the estimated total number of WUHs.

We obtained geospatial data for urban water bodies from the National Hydro Network (NHN) for all of Canada (Natural Resources Canada, 2022) and the Government of Canada census data (Statistics Canada, 2011b). We used the NHN geospatial data to map water bodies throughout the GTA and geospatially clipped all water bodies within the GTA boundaries using QGIS (v3.16.4).

Since the NHN data does not categorize water bodies by type, we used the Government of Canada census data to determine the relative percentages of each water body type within the GTA and applied those percentages to the NHN data. Water body subcategories are classified in the Government of Canada census data as "channels", "lakes", "bays", and "rivers", but we added an additional subcategory of "ponds" based on their importance highlighted in previous work (Herrero Ortega et al., 2019; Martinez-Cruz et al., 2017; Gonzalez-Valencia et al., 2014). We assigned a water body subcategory for any unclassified water body in the Statistics Canada data by evaluating Google Earth imagery.

6.2.4 Temporal analysis and mobile surveys

We analyzed mobile surveying data from the GTA to qualitatively assess the temporal variability and intermittence of the cluster of sewer WUHs in High Park and the Keating Channel (Figure 6.1). Mobile surveying data was collected using both a vehicle- and bike-based sampling platform in the GTA from early-2018 to late-2022 (Wunch et al., 2016; Ars et al., 2020). On-board trace gas analyzers utilized during mobile surveys to measure methane concentrations included a Los Gatos Research Ultra-Portable Greenhouse Gas Analyzer, Picarro G2401, Picarro G1301, and/or Li-Cor 7810. We geospatially clipped all measurement data within a 1 km radius of the areal extent of the cluster of WUHs and the Keating Channel. Next, we estimated the excess methane above ambient concentrations for all surveys within that 1 km boundary by calculating the 5th percentile of methane concentrations for each survey, and subtracting that value from the measured methane concentrations to obtain excess methane values. Then, we performed an additional geospatial clip of all mobile survey measurements to 500 meters from the cluster of WUHs and the Keating Channel. Finally, we identified methane plumes using the R package "IDPmisc" with a minimum plume height of 0.04 ppm, a minimum plume width at half plume height of five data-points aside, and categorized the plumes following Ars et al. (2020) (i.e., small plumes = plume height of 0.04 - 0.2 ppm excess methane, medium plumes = plume height of 0.2 - 1.0 ppm excess methane, large plumes = plume height of over 1.0 ppm excess methane).

6.2.5 Annual methane emissions estimates

We estimated annual methane emissions from both WUHs and urban water bodies by multiplying source subcategory specific emission factors to their corresponding activity data. To calculate uncertainty, we first used bootstrapping with replacement ($n = 10,000$) to develop a distribution of emission factors for each source subcategory (e.g., sewer WUH, channel, river). Then, we fit a statistical distribution to the bootstrapped emission factors first by visualizing the best fit through a Pearson plot (i.e., also known as a Cullen and Frey graph) of the square of skewness versus the kurtosis of the bootstrapped emission factors. We fitted the distributions to the bootstrapped emission factors using the "fitdist" package in R-Studio (v.2022.12.0), which were either a normal or gamma distribution. For the activity data, we used two separate approaches for WUH activity data and urban water bodies. For sewer WUH counts, we calculated the standard error about the slope and y-intercept of the linear models of population versus WUH counts using the "LINEST" function in Excel to obtain upper and lower estimates. For other WUH types, we calculated the standard error of the slope and y-intercept of the linear regression for total WUH counts, and combined these data with the ranges obtained for the sewer WUH counts to obtain an upper and lower estimate of other WUHs. We fit activity data estimates to a triangular distribution with the upper and lower WUH counts set as the upper and lower bounds. For urban water bodies, we assumed a triangular distribution with upper and lower bounds of 20% of the best estimate of the areal cover of the urban water body type. We calculated uncertainty estimates using the 2.5th and 97.5th percentiles of a Monte Carlo simulation ($n = 1,000,000$) multiplying the generated activity data and emission factors.

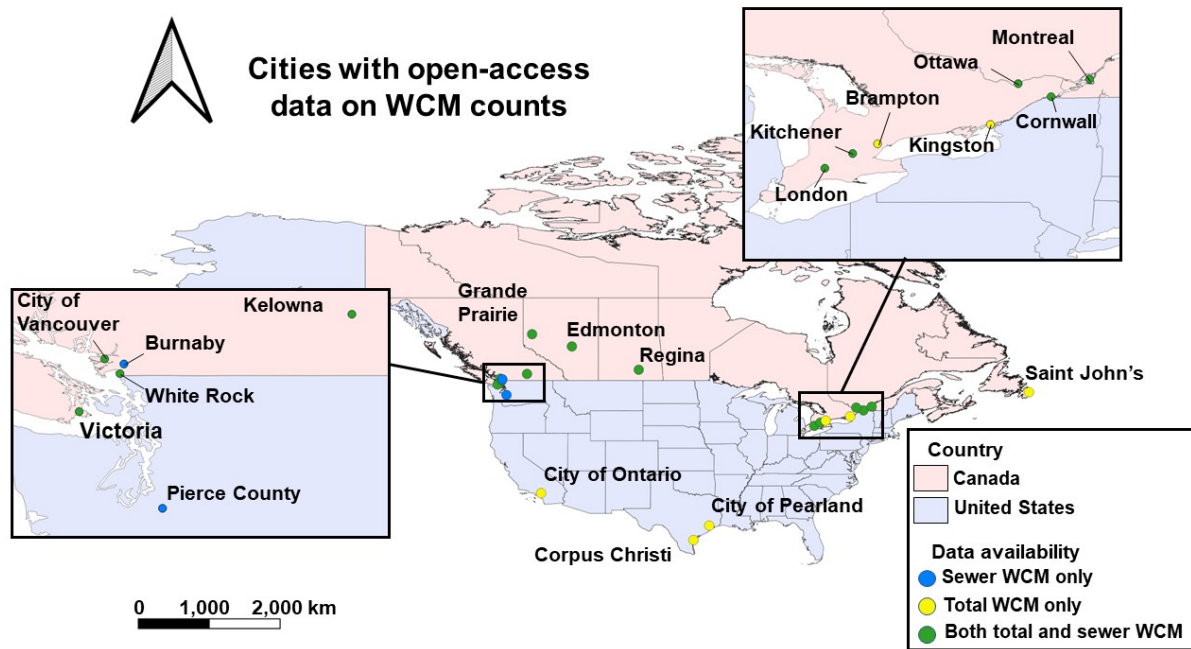


Figure 6.2: Map of all cities in Canada and the U.S. with open-access data related to WUH counts. Points are coloured according to the available data regarding the counts per type of WUH.

6.3 Results

6.3.1 Wastewater collection systems

The total population in the GTA was 5,928,040 in 2016 (Statistics Canada, 2011a). The total population of the Canadian cities we used for this analysis totaled 6,634,917 people for total WUHs, and 6,096,265 people for sewer WUHs, which makes up 25.7% and 23.6% of the total population in medium and large population centres in Canada, respectively. We found strong correlations for both total WUH counts and sewer WUH counts with city populations with R^2 values of 0.92 and 0.85 respectively. Based on the linear relationships, we estimate a total of 946,464 WUHs and 374,448 sewer WUHs in urban areas in Canada, which leaves a total of 572,016 other WUHs (SI - Figure 6.8).

We compiled a total of 238 individual source measurements of methane emissions from WUHs from Chapter 5 of this thesis and one other study (Fries et al., 2018) which include 22 measure-

ments we made from WUHs in Toronto, Canada. We found that the average methane emission rate from all WUHs was 1.3 g/hour. We classified 116 of these measurements as sewer WUHs and 122 from other WUHs. The average methane emission rate from sewer WUHs was 2.7 (95% c.i., 0.6 to 5.2) g/hour while the average emission rate from other WUHs was two orders of magnitude smaller at 3.1×10^{-2} (95% c.i., 0.2×10^{-2} to 8.6×10^{-2}) g/hour of methane (Figure 6.3). The highest emitting WUH was measured at 89 g/hour from a sewer WUH in Toronto which was located within the group of 13 high emitting WUHs in the northeastern corner of High Park, Toronto. The cluster of 13 WUHs in High Park collectively emitted methane at a rate of 358 g/hour when we measured them in October, 2021. We also found that this cluster of high-emitting WUHs were all characterized by a strong odour of sewage, water rushing audibly below the WUHs, and high volumetric flowrates of gas exiting the manholes which could be physically felt while standing over the sites.

Urban water bodies

We found that the total area covered by the NHN (i.e., absent water body classifications) data-set in the GTA was 15.4 km² compared the total area covered by named urban water bodies from the Statistics Canada (StatsCan) geospatial data-set at 8.8 km², or 64% of the NHN data. For the GTA, we found that 89.3% of areal extent of water bodies in the Statistics Canada database received some sort of classification. After visual investigation of the unclassified water bodies, we re-categorized all of the unnamed water bodies as ponds (i.e., isolated small water body). In addition, we changed the classification of one named water body from "Lake" to "Pond" for the Grenadier Pond. Based on a breakdown of the water body classifications provided within the StatsCan data, the most abundant urban water body type was rivers and lakes, followed by bays, creeks, ponds, and channels (Table 1). Lakes and rivers collectively made up 83.5% of the total distribution of urban water bodies.

We analyzed a total of 212 flux measurements from urban water bodies in the GTA. Of the 212 flux measurements, 64 were from ponds, 52 were from bays, 52 were from channels, and 44 were

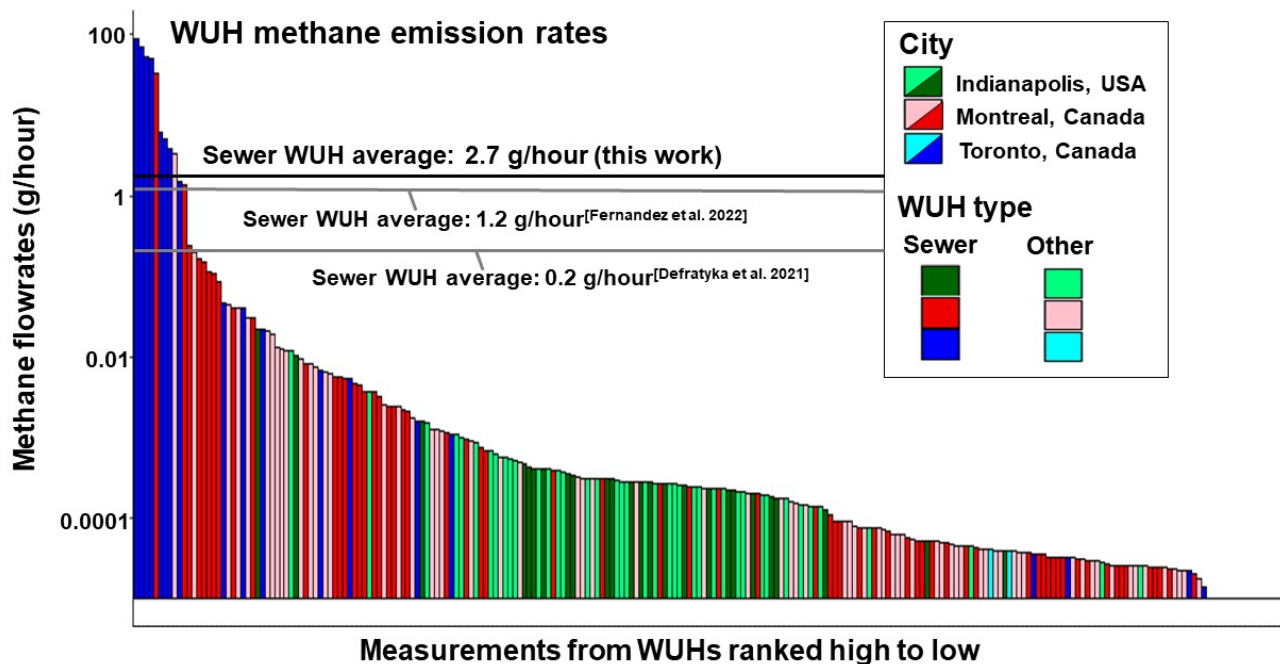


Figure 6.3: Barplot of methane emission rates measured from WUHs in Toronto and Montreal (Chapter 5), Canada, and Indianapolis, United States (Fries et al., 2018). Bars are coloured according the type of WUH. Average methane rates from sewer WUHs for this work and others (Defratyka et al., 2021; Fernandez et al., 2022) are shown by horizontal lines.

Table 6.1: Total area covered by urban water bodies (i.e., lakes, canals, creeks, bays, rivers, and ponds) in urban areas in the Greater Toronto Area, Canada.

Urban water body type	Area covered	% of total area
Lakes	2.09 km ²	13.5%
Channels	0.06 km ²	0.4%
Bays	1.34 km ²	8.7%
Rivers	10.82 km ²	70.0%
Ponds	1.14 km ²	7.4%
Total	15.45 km ²	100.0%

from rivers. We used the combined 160 measurements from rivers, bays, and ponds, as our flux rates representative of lakes because ponds, bays, and rivers all represent naturally occurring water bodies located in urban environments, whereas the urban canal (i.e. Keating Channel) measured in this work is a constructed waterway (SI - Section 6.6.2). We classified a total of 100 methane fluxes

as diffusive fluxes, and a further 112 as ebullition. The highest diffusive fluxes were measured from bays at $0.767 \mu\text{g}\cdot\text{m}^{-2}\cdot\text{sec}^{-1}$, whereas the other water body types had diffusive flux rates below $0.400 \mu\text{g}\cdot\text{m}^{-2}\cdot\text{sec}^{-1}$ (Figure 6.4). The highest mass of methane emitted from ebullition events were from channels and ponds at 19,470 and 13,000 $\mu\text{g}\cdot\text{m}^{-2}$ respectively, whereas mass of methane emitted from ebullition events from the remaining water body types were all below 2,000 $\mu\text{g}\cdot\text{m}^{-2}$ (Figure 6.4). The total fluxes from each water body type (i.e., diffusion and ebullition combined) were highest for channels and ponds at 82 (95% c.i., 54 - 113) $\mu\text{g}\cdot\text{m}^{-2}\cdot\text{sec}^{-1}$ and 33 (95% c.i., 19 - 50) $\mu\text{g}\cdot\text{m}^{-2}\cdot\text{sec}^{-1}$ respectively. The remaining water body types all had total methane fluxes below 20 $\mu\text{g}\cdot\text{m}^{-2}\cdot\text{sec}^{-1}$ (Table 2).

Temporal variability in emissions

We processed mobile surveying data from a total of 15 surveys near the northeastern corner of High Park, Toronto, and 41 surveys near the Keating Channel for a total of 56 surveys and 122,180 measurements within a 1 km radius of each site. The mobile surveys spanned four years for High Park and five years for the Keating Channel. A total of 38 methane plumes were measured from 13 surveys near High Park, with two surveys not detecting any proximal (i.e., within 500 meters) methane plumes. For the Keating Channel, a total of 315 methane plumes were measured from all 41 surveys near the channel, with no surveys without at least one detectable methane plume (Figure 6.5). For both sites, methane plumes were detected in all four seasons, with the majority of plumes detected in the warmer months of spring and summer which also corresponded to the highest number of mobile surveys. We found that methane plumes were measured during all of the surveys conducted in the fall and winter (Figure 6.5).

Annual methane emission estimates

We found that annual methane emissions from WUHs in urban areas in the GTA amounted to 9,112 (95% c.i., 13.5 - 84.1) t/year of methane which places them as the third highest methane source in the GTA compared to the Pak et al. (2021) methane inventory (Table 6.2), lower only than

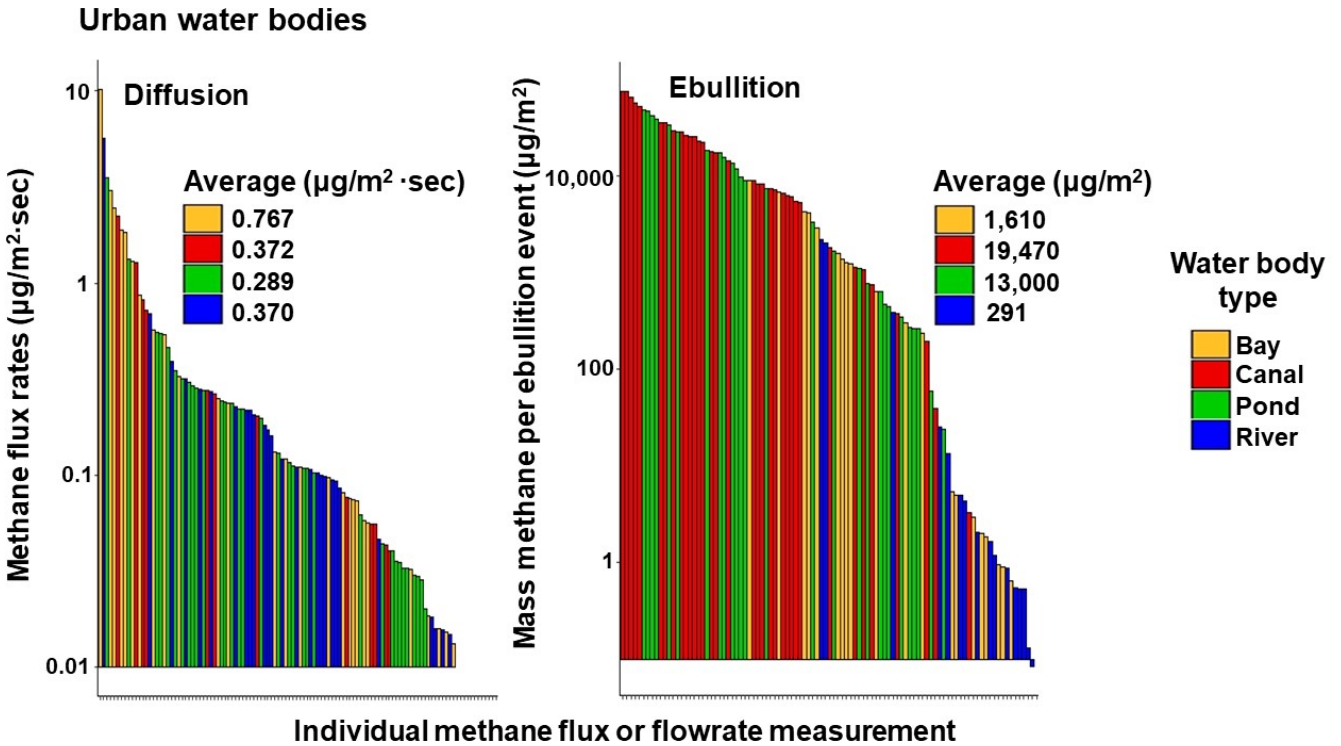


Figure 6.4: Barplots of methane flux rates from urban water bodies in Canada. Sections are coloured according to the categorization of urban water body and separated by diffusive fluxes (left) and ebullition fluxes (right). Measurements for lakes are made up of all measurements from urban water bodies except for those from canals. Average flux rates are shown for each classification with confidence intervals (95% c.i. after bootstrapping with replacement, $n = 10,000$) shown in parenthesis. Counts on the y-axis represent the number of measurements multiplied by the density.

methane emissions from large and small landfills (Figure 6.6). We found that methane emissions from WUHs were strongly influenced by sewer WUHs, which accounted for over 99% of total emissions from this source. Furthermore, we found that the high contribution from sewer WUHs are driven by a difference in emission factors (Table 6.2) rather than total counts of WUHs since sewer WUHs make up 40% of the total WUH counts based on our population-based linear model. Our estimate of annual methane emissions from WUHs also places them higher than the current methane emissions from wastewater treatment plants, which is a comparable category in Canada's

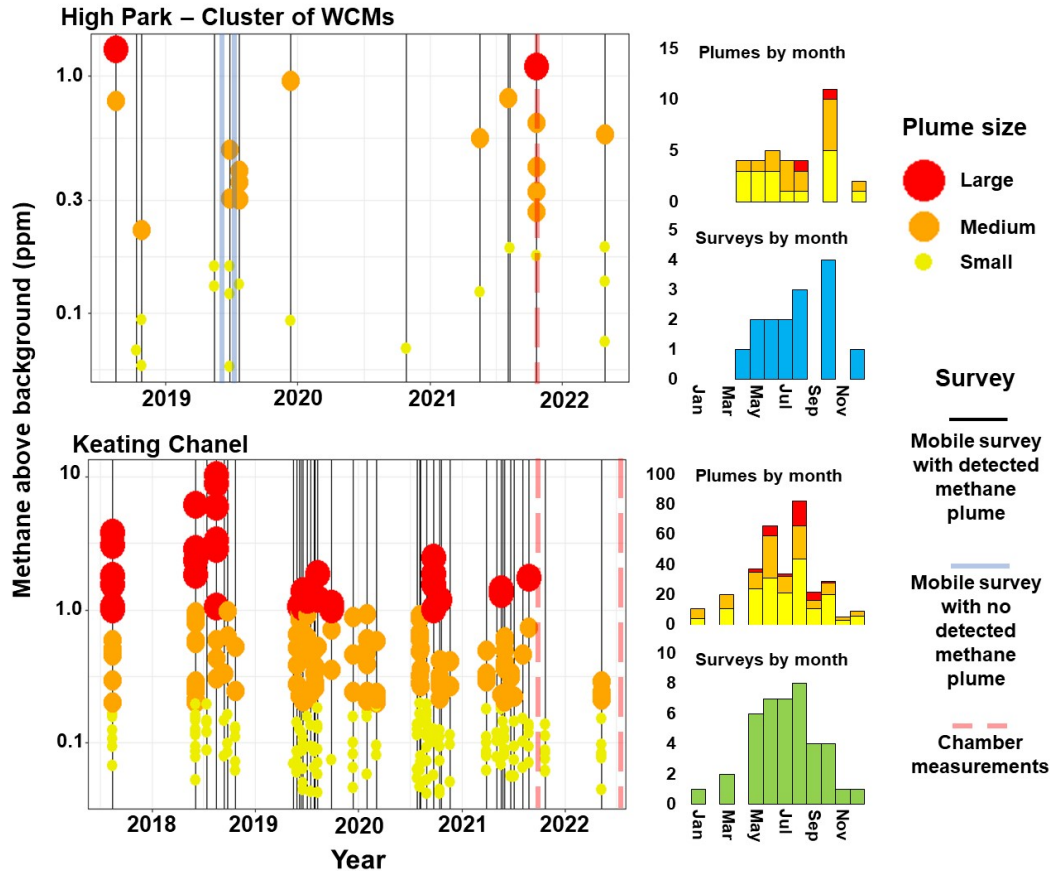


Figure 6.5: Methane plumes measured during mobile surveys from the cluster of wastewater utility holes in High Park (top), and the Keating Channel (bottom). Plumes are categorized according to size following the criteria outlined in (Ars et al., 2020). Methane plumes are categorized by the maximum plume height in methane excess concentration above background (ppm). The time of mobile surveys and/or chamber measurements are shown by the vertical lines. Number of surveys and detected methane plumes by month are shown in the barplots on the right.

greenhouse gas inventory. Methane emissions from WUHs made up 10.6% of the total methane emissions from the GTA according to the Pak et al. (2021) inventory.

We calculated annual methane emissions from urban water bodies in Canada to be 2,737 t/year of methane (95% c.i., 1,252 - 4,220) (Table 2). This places urban water bodies as the sixth highest methane source in the GTA according to the Pak et al. (2021) methane inventory. Within the AFOLU sector, we find that methane emissions from urban water bodies would be the third highest methane source in the sector, lower only than methane emissions from enteric fermentation and

Table 6.2: Summary of activity data, methane emission factors, and annual methane emissions estimates for each source category of urban water bodies and WUHs. Uncertainty bounds are shown in parenthesis.

Source category	AD (1000's WUHs)	EF (g/hour)	Annual emissions (t/year)
Sewer	374 (330 - 432)	2.7 (0.6 - 5.2)	8,960 (3,011 - 18,210)
Other	572 (448 - 688)	0.03 (≥ 0.00 - 0.09)	152 (8 - 505)
Total	-	-	9,112 (3,019 - 18,715)
Source category	AD (km ²)	EF ($\mu\text{g}\cdot\text{m}^{-2}\cdot\text{sec}^{-1}$)	Annual emissions (t/year)
Rivers	10.8 (8.7 - 13.0)	0.9 (0.1 - 1.9)	293 (0 - 633)
Ponds	1.14 (0.91 - 1.37)	33 (19 - 50)	1,191 (631 - 1,793)
Channels	0.06 (0.05 - 0.07)	82 (54 - 113)	161 (100 - 228)
Bays	1.34 (1.06 - 1.61)	4.4 (1.7 - 7.7)	185 (58 - 185)
Lakes	2.09 (1.67 - 2.51)	13.8 (7.6 - 20.9)	907 (463 - 1,381)
Total	-	-	2,737 (1,252 - 4,220)

wetlands (Figure 6). Our breakdown of methane emissions from urban water bodies shows that the majority of emissions occur from ponds and lakes (i.e., 77%), followed by river, bays, and channels (Table 2). Notably, channels accounted for 6% of cumulative methane emissions from urban water bodies despite making up only 0.4% of the total areal extent of urban water bodies in the GTA for an emissions intensity (i.e., percentage of total methane emissions divided by percentage total area) of 14.5. We observe a similar trend with ponds, which contributed 14% of cumulative methane emissions from urban water bodies despite making up 7.4% of the total areal extent covered by urban water bodies for a methane emissions intensity of 5.9.

6.4 Discussion

Our findings show that both WUHs and urban water bodies are significant methane sources at the national level for Canada, and likely in other countries as well. At the municipal scale, methane emissions from these biogenic sources could account for some of the discrepancy observed between top-down studies (Anderson et al., 2021; de Foy et al., 2023; Pitt et al., 2022; Plant et al., 2022, 2019) and current bottom-up methane inventories.

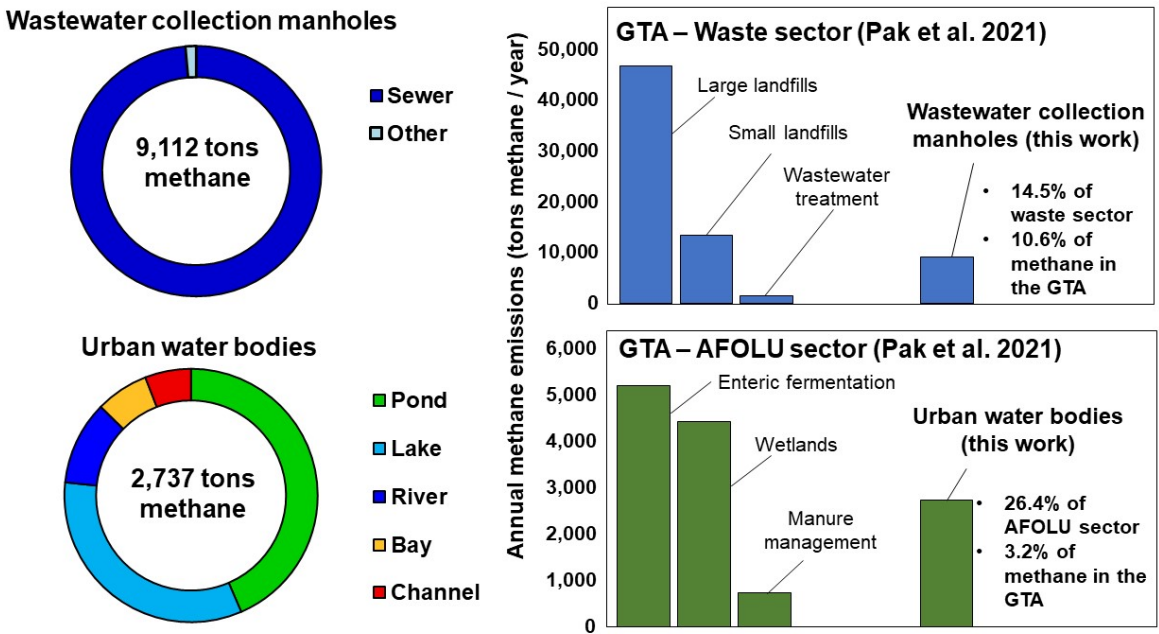


Figure 6.6: Relative contributions annual methane emissions from source subcategories of wastewater utility holes and urban water bodies (left). Barplots of annual methane emissions from the FLAME-GTA methane inventory (Pak et al., 2021) inventory report for the waste and agriculture, forestry, and other land-use (AFOLU) sectors (right).

6.4.1 Comparisons to prior measurements

Our annual methane emissions estimates for WUHs are strongly influenced by sewer WUHs. Methane flowrate measurements from WUHs follow an extremely skewed distribution, with the top 5% of emitters accounting for 97% of cumulative emissions. As such, it is important that the emission factors we use are representative. To our knowledge, there are three empirical studies that have estimated annual methane emissions from sources comparable or analogous to WUHs (i.e., termed "sewage" (Defratyka et al., 2021), "wastewater" (Fernandez et al., 2022), and we assume "microbial" from Maazallahi et al. (2020)) and extrapolated those values to city-wide estimates (Fernandez et al., 2022; Defratyka et al., 2021; Maazallahi et al., 2020). Based on our analysis of these studies (SI - Section 6.6.1) the methane emission factor for sewer WUHs in Paris (France) was 0.2 g/hour (Defratyka et al., 2021), in Bucharest (Romania) the emission factor was higher at 1.2 g/hour (Fernandez et al., 2022), and in Hamburg (Germany) the emission factor was 0.2 g/hour

(Maazallahi et al., 2020) (Figure 6.2). Both are lower than our emission factor for WUH sewers at 2.7 (95% c.i. 1.0 - 6.6)g/hour, but we do see overlap in terms of uncertainty bounds from the emission factor from Bucharest. Furthermore, the extrapolation of methane emissions measurements to city-wide estimates from all three studies utilize total road kilometers as the basis for extrapolation, whereas we extrapolate methane emissions from WUHs based on population. The comparison we make between our sewer WUH emission factor to these studies may be biased due to uncertainties arising from differences in activity data extrapolation.

The emission factors we use for urban water bodies are comparable to other studies for some classifications of water bodies, although we see wide range of methane flux rates from literature. Based on a literature review by Herrero Ortega et al. (2019), the highest methane fluxes from urban water bodies ever published occurred from lakes in Velacruz (Mexico) at $33 \mu\text{g}\cdot\text{m}^{-2}\cdot\text{sec}^{-1}$ (Gonzalez-Valencia et al., 2014), rivers in Mexico City (Mexico) at $28 \mu\text{g}\cdot\text{m}^{-2}\cdot\text{sec}^{-1}$ Martinez-Cruz et al. (2017), and a dammed section of a river in China at $25 \mu\text{g}\cdot\text{m}^{-2}\cdot\text{sec}^{-1}$ (He et al., 2018). Our highest flux rates were measured from channels and are three times higher than these studies with a flux rate of $82 \mu\text{g}\cdot\text{m}^{-2}\cdot\text{sec}^{-1}$. Ars et al. (2020) previously quantified methane emissions from the Keating Channel using mobile surveys and found an average methane emission rate of 200 kg/day. Based on our emission factor for channels and a listed area of 32,922 m² for the Keating Channel, our estimated methane emissions from the Keating Channel would be 233 kg/day, which is similar to the results from Ars et al. (2020). We estimated a flux rate of $33 \mu\text{g}\cdot\text{m}^{-2}\cdot\text{sec}^{-1}$ from ponds, which is more than four times higher than the highest prior total flux rate from ponds at $7 \mu\text{g}\cdot\text{m}^{-2}\cdot\text{sec}^{-1}$ measured from a pond in Yichang (China) (Xiao et al., 2014). We see that the majority of the difference can be attributed to differences in estimates of ebullition fluxes, since our estimates for diffusive fluxes from ponds are similar on average than prior studies. A reason for this may be due to bias from our chamber deployments where ebullition events were captured more frequently, or that the ponds we sampled simply had higher ebullition rates than prior studies. We did see that the 4.4 and $0.9 \mu\text{g}\cdot\text{m}^{-2}\cdot\text{sec}^{-1}$ flux rates we measured for bays and rivers are all similar to prior studies which range from 0.2 to $5.8 \mu\text{g}\cdot\text{m}^{-2}\cdot\text{sec}^{-1}$ (Herrero Ortega et al., 2019).

6.4.2 Temporal patterns in methane emissions

Both the cluster of high-emitting WUHs and the Keating Channel represent high emitting sites that strongly influence emission factors and annual emission estimates. Therefore, it is important to assess their intermittence across seasons since these are biogenic sources with microbial processes generating methane. Based on our temporal analysis of methane emissions from both the Keating Channel and the cluster of high-emitting WUHs in Toronto, we found that methane emissions persisted over multiple seasons. For the cluster of WUHs in High Park, we cannot distinguish any clear temporal trends as the plumes were detected across all seasons, but the majority of these plumes were measured in October which coincides with a higher number of surveys for the site (Figure 6.5). Notably, the only two surveys where methane plumes were not detected were conducted in August and July of 2019, both warmer months when biogenic methane production would be expected to be high (Nisbet et al., 2019). On the same day that we conducted chamber measurements from these WUHs, we measured the highest number of methane plumes from the site through mobile surveying. Overall, our results show that methane emissions from these high emitting WUHs appear to be persistent across seasons which offers valuable insight on the temporal nature of methane emissions from WUHs.

For the Keating Channel, the high number of mobile surveys conducted near this source offer more detailed insights on temporal variability when compared to the data from the cluster of WUHs. In general, methane plumes measured near the Keating Channel do decrease in severity (i.e., the peak height of excess methane) in the colder months (Sept to Dec) from surveys conducted in the warmer months (May - August). This trend can be observed from the decrease of large methane plumes from mid-2019 to early-2020 (Figure 6.5). The decrease could be attributable to seasonal differences such as increases in ebullition with increased water temperature (Wang et al., 2021) in warmer months, or could coincide with the beginning of the three-month annual dredging of the Keating Channel, or a combination of several factors (e.g., freezing of the channel in winter). We quantified methane fluxes using chamber measurements from the Keating Channel on two separate occasions in the fall and winter (Figure 6.5). During the first measure-

ment campaign in October, 2021, we observed consistent ebullition throughout the channel with the largest mass of methane released during an ebullition event reaching above $20,000 \mu\text{g}\cdot\text{m}^{-2}$. During the return visit in December, 2022, the channel was undergoing construction modifications and had recently been dredged. Few ebullition events were observed during this return visit and total methane fluxes were low at around $0.16 \mu\text{g}\cdot\text{m}^{-2}\cdot\text{sec}^{-1}$ (i.e., or 0.5 kg/day from the Keating Channel). These findings expand on those from Ars et al. (2020) where quantified emissions from the channel peaked in June 2019 at ~ 400 kg/day and then lowered to ~ 100 kg/day in July 2019, and provide insights on methane emissions during the fall and winter.

6.4.3 Mitigation avenues

Research on the mitigation avenues of methane emissions from WUHs generally involve the chemical dosing of wastewater networks with compounds such as nitrates (Jiang et al., 2013), hydrochloric and free nitric acid (Jiang et al., 2011), ferric iron (Zhang et al., 2009), and hydroxide (Gutierrez et al., 2009), and oxygen injections (Ganigué and Yuan, 2014). However, all of these methods are untested at municipal scales with respect to methane reduction, and have potential drawbacks such as the production of nitrous oxide or negative impacts to downstream wastewater treatment. Based on our findings a small percentage of WUHs are emitting a majority of methane emissions, and therefore, mitigation efforts could also benefit from prioritizing these high emitting sites and improving on our characterization of WUHs. WUHs can connect to a variety of different types of wastewater systems, such as rising mains and pump/lift stations, gravity sewers, and combined sanitary and storm water systems.

The cluster of high emitting WUHs we measured at High Park all were characterized by audible water rushing beneath the site, which suggests the terminus of a pump/lift station from a rising main and further supported by the persistence of methane emissions from those sites over time (Figure 6.5). We propose three main causes of high methane emissions from WUHs, which would all differ in potential mitigation strategies: (1) a pump/lift station (continuous emissions); (2) a blockage within a gravity sewer system leading to increases in hydraulic retention time leading to

stagnant wastewater (intermittent emissions); (3) and either the formation or presence of a siphon in wastewater systems from regular or temporary increases to wastewater flow (continuous or intermittent) (Lowe, 2016). Methane emissions from blockages could be addressed relatively simply by clearing the blockage, whereas emissions from siphons or pump/lift stations could be addressed with passive methane capture, focused chemical dosing of wastewater, or modifications to wastewater network structures. Given that a strong odour was noticed at all high methane emitting WUHs, programs involving the public such as a municipal inventory of points where a passerby noticed a sewer odour could be beneficial in identifying high-emitting WUHs for further investigation.

Methane emission rates were strongest for ponds and channels based on our measurements, and therefore we focus on mitigation options for these types of urban water bodies. We have already noted one mitigation option for channels with the dredging of the Keating Channel and the drop in methane emission rates from chamber measurements before (~ 233 kg/day) and after (~ 0.5 kg/day) dredging. However, it is unclear whether the emission reductions from dredging are re-distributed to the location where the material is stored. Notably, the location where the dredged material is deposited is also flagged as a methane source of unknown origin in Ars et al. (2020). As a preventative approach, urban channels and canals should be constructed to prevent the build-up of material within the system. For example, the Keating Channel is characterized by a sharp bend at the outlet of the Don River (Figure 6.1) where material can accumulate and settle (Taylor, 2007). With regards to ponds, one driver of methane emissions is nutrient loading (i.e., phosphates) leading to eutrophication (Malyan et al., 2022; Audet et al., 2020). Therefore, limiting nutrient inputs to urban ponds or installing pond aeration systems to avoid eutrophication would be mitigation avenues to consider for urban ponds.

6.4.4 Future work

This study has contributed to the growing literature on methane emissions from urban water bodies and the lack of direct measurement data from WUHs. The lack of direct measurement data from WUHs is a notable gap in literature given their significant contributions of methane emissions

at the municipal level. While future work would benefit from additional measurements, future studies should also prioritize a more detailed classification of WUH types so that insights can be drawn for both future measurement studies and mitigation strategy development. Pairing site-level measurement platforms that can distinguish biogenic methane emissions with more focused direct measurements would be especially useful in characterizing the high methane emitting WUHs that we see contributing the majority of methane emissions. For urban water bodies, our results show that despite making up a minority of the areal coverage, ponds and channels are strong sources of methane emissions. Methane emissions from urban ponds have received growing attention in literature, although there are a lack of direct methane quantification studies that target urban channels. Our results show that urban biogenic sources of methane emissions are a significant source at the national scale in Canada, and are likely significant in other countries as well. Quantifying methane emissions from these urban biogenic sources can partially explain the discrepancies observed in municipal inventories versus third party studies, and will ultimately allow policy-makers and scientist to make informed decisions regarding the mitigation of methane emissions.

6.5 Acknowledgements

We would like to thank McGill Sustainability Systems Initiative New Opportunities Award - Adapting Urban Environments for the Future awarded to MK, Natural Sciences and Engineering Research Council CGS-D awarded to JPW (reference ID: CGS-D 559246-2021), Mitacs Accelerate Grant awarded to MK and JPW, and McGill Engineering Doctoral Award to JPW for providing funding. We would also like to thank Anthony Fabien from Environment and Climate Change Canada for his work in gathering measurements from urban water bodies in the GTA.

6.6 Supplementary information

6.6.1 Methane emission rates and activity data

Wastewater utility holes

We obtained methane flowrate measurements from WUHs from our measurements made in Chapter 5 in Montreal and one other study (Fries et al., 2018) including an additional 22 measurements we made from WUHs in Toronto. For the Fries et al. (2018) study, we removed all measurements categorized as thermogenic since our focus is on biogenic methane emissions from wastewater. Some of the measurements obtained from (Fries et al., 2018) were presented in the form of methane screening levels and not methane flowrates. For these measurements, we used a linear relationship between screening methane levels and methane flowrates ($R^2 = 0.71$) from the data within (Fries et al., 2018) to convert all measurements within the study to methane flowrates (SI - Figure 6.7). All of the methane flowrates from the (Fries et al., 2018) study were below 20 mg/hour, meaning that the uncertainty related to the extrapolation of screening values to methane flowrates had little impact on the calculation emission factors since they all were close 0 compared to the highest emitting WUHs.

Urban water bodies

Methane emissions from urban water bodies occurred either as steady diffusive fluxes, or as intermittent ebullition events. Emission factors for diffusive fluxes were calculated as an average, like WUHs. For ebullition, we calculated emission factors for the different water body types by the total mass of methane per unit area emitted from ebullition divided by the total duration of time the chamber was measuring in that water body type. The total duration of time spent measuring urban water body fluxes at each water body type was 178.2 minutes for ponds, 155.8 minutes for bays, 155.2 minutes for rivers, and 142.2 minutes for canals.

6.6.2 Representativity of emission factors

Wastewater utility holes

As an assessment of representativity, we compared the percentage of high-emitting WUHs within our dataset to the results of (Fernandez et al., 2022). In (Fernandez et al., 2022), the city of Bucharest was surveyed repeatedly using a mobile surveying platform with a vehicle-mounted CRDS greenhouse gas analyzer. Methane leaks were identified using a minimum excess methane enhancement of 0.2 ppm measured when driving, which corresponds to a minimum methane leak of approximately 42 g/hour based on the (Weller et al., 2020) quantification method used in (Fernandez et al., 2022). After extensive surveying of Bucharest, they found a methane leak frequency of 1.6 leaks/km, which scaled up to the entire city (i.e., 3399 km) gives a total 5,438 methane leaks. Following the same approach used in (Fernandez et al., 2022), 63% of these leaks (i.e., 3,426 methane leaks) can be classified as biogenic based on the geochemical analysis they performed using $C_2:C_1$ ratios, $\delta^{13}C-CH_4$, and δ^2H-CH_4 . Since there are no landfills within the city boundaries for the (Fernandez et al., 2022) study, these leaks are further categorized as originating from wastewater. Based on our relationship of population to WUH counts, we estimate that there are approximately 263,900 total WUHs and 102,855 sewer WUHs in Bucharest. Assuming that all biogenic methane leaks originated from sewers, this gives a total of 3.3% of all sewer WUHs having a minimum methane leak rate of at least 42 g/hour. Our empirical dataset has a similar distribution, with 3.4% of measurements from sewer WUHs (i.e., 4 of 116) having a methane emission rate above 42 g/hour. The assumptions that we make in this comparison include: that all biogenic leaks estimated in Bucharest originate from WUHs and not other potential biogenic sources (e.g., historic landfills); that the number of WUHs in Bucharest follows the same linear trend as we observed in Canadian cities; that the extrapolations used within (Fernandez et al., 2022) for both the total methane leaks counts for the city and the distribution of biogenic sources are accurate and representative; and that the city-wide observations for Bucharest are representative to those of Canadian cities.

Urban water bodies

From urban water bodies, we combined our measurements from bays, rivers, and ponds to calculate emission factors for lakes, which we did not measure directly in this work. This assumption was made since lakes represent 13.5% of all water bodies in the GTA, and likely represent a notable percentage of urban water bodies in other cities as well. We did not include measurements from canals in this calculation because ponds, bays, and rivers all represent naturally occurring water bodies located in urban environments, whereas the urban canal (i.e. Keating Channel) measured in this work is a constructed waterway which differs from other water bodies in its geomorphology. Furthermore, our calculated emission factors for canals were the highest among the different water body types we measured by a wide margin, which implies that it is an outlier in terms of the different water body types.

Table 6.3: Classification of urban water bodies according to sub-types included in the Government of Canada geospatial data-set.

Water body classification	Sub-types included in classification
Rivers	River, Arm, Creek, Inlet, Brook, Stream
Channels	Canal, Channel
Bays	Bay, Harbour, Port, Cove
Ponds	Pond, Slough
Lake	Lake, Reservoir

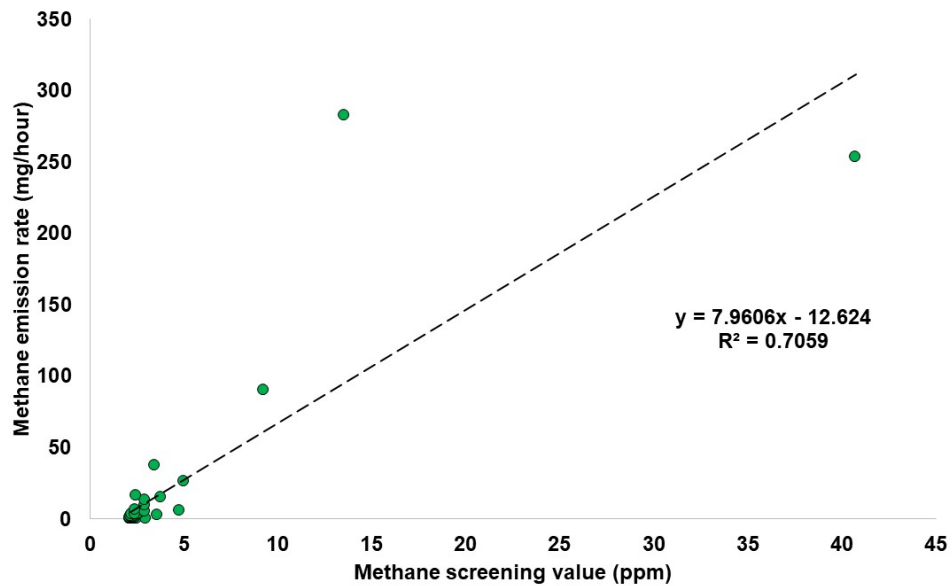


Figure 6.7: Linear regression of methane screening value (ppm) versus the measured methane flow rate for 43 wastewater utility holes measured in Indianapolis, Ohio. Data collected from (Fries et al., 2018).

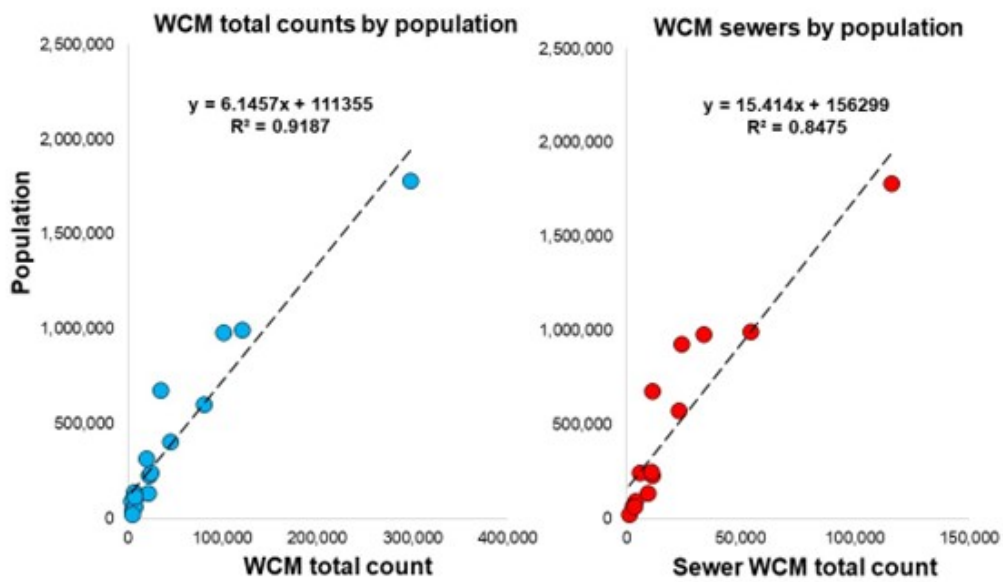


Figure 6.8: Linear regressions of total population counts versus total (left) and sewer WUH counts (right) by population. The equations representing linear regressions and the corresponding R^2 values are shown in each plot.

Bibliography

- Anderson, D. C., Lindsay, A., DeCarlo, P. F., and Wood, E. C.: Urban emissions of nitrogen oxides, carbon monoxide, and methane determined from ground-based measurements in Philadelphia, *Environmental Science & Technology*, 55, 4532–4541, 2021.
- Ars, S., Vogel, F., Arrowsmith, C., Heerah, S., Knuckey, E., Lavoie, J., Lee, C., Pak, N. M., Phillips, J. L., and Wunch, D.: Investigation of the spatial distribution of methane sources in the Greater Toronto Area using mobile gas monitoring systems, *Environmental Science & Technology*, 54, 15 671–15 679, 2020.
- Audet, J., Carstensen, M. V., Hoffmann, C. C., Lavaux, L., Thiemer, K., and Davidson, T. A.: Greenhouse gas emissions from urban ponds in Denmark, *Inland Waters*, 10, 373–385, 2020.
- Baron, A., Dyck, L., Amjad, H., Bragg, J., Kroft, E., Newson, J., Oleson, K., Casson, N., North, R., Venkiteswaran, J., et al.: Differences in ebullitive methane release from small, shallow ponds present challenges for scaling, *Science of the Total Environment*, 802, 149 685, 2022.
- Calvo Buendía, E., Tanabe, K., Kranjc, A., Jamsranjav, B., Fukuda, M., Ngarize, S., Osako, A., Pyrozhenko, Y., Shermanau, P., and Federici, S.: 2019 Refinement to the 2006 IPCC Guidelines for National Greenhouse Gas Inventories, 2019.
- de Foy, B., Schauer, J. J., Lorente, A., and Borsdorff, T.: Investigating high methane emissions from urban areas detected by TROPOMI and their association with untreated wastewater, *Environmental Research Letters*, 2023.
- Defratyka, S. M., Paris, J.-D., Yver-Kwok, C., Fernandez, J. M., Korben, P., and Bousquet, P.: Mapping urban methane sources in Paris, France, *Environmental science & technology*, 55, 8583–8591, 2021.
- DelSontro, T., Beaulieu, J. J., and Downing, J. A.: Greenhouse gas emissions from lakes and impoundments: Upscaling in the face of global change, *Limnology and Oceanography Letters*, 3, 64–75, 2018.
- Eggleston, H., Buendia, L., Miwa, K., Ngara, T., and Tanabe, K.: 2006 IPCC guidelines for national greenhouse gas inventories, 2006.
- Fernandez, J., Maazallahi, H., France, J., Menoud, M., Corbu, M., Ardelean, M., Calcan, A., Townsend-Small, A., van der Veen, C., Fisher, R., et al.: Street-level methane emissions of Bucharest, Romania and the dominance of urban wastewater., *Atmospheric Environment: X*, 13, 100 153, 2022.
- Fries, A. E., Schifman, L. A., Shuster, W. D., and Townsend-Small, A.: Street-level emissions of methane and nitrous oxide from the wastewater collection system in Cincinnati, Ohio, *Environmental Pollution*, 236, 247–256, 2018.
- Ganigué, R. and Yuan, Z.: Impact of oxygen injection on CH₄ and N₂O emissions from rising main sewers, *Journal of environmental management*, 144, 279–285, 2014.

- Gonzalez-Valencia, R., Sepulveda-Jauregui, A., Martinez-Cruz, K., Hoyos-Santillan, J., Dendooven, L., and Thalasso, F.: Methane emissions from Mexican freshwater bodies: correlations with water pollution, *Hydrobiologia*, 721, 9–22, 2014.
- Gutierrez, O., Park, D., Sharma, K. R., and Yuan, Z.: Effects of long-term pH elevation on the sulfate-reducing and methanogenic activities of anaerobic sewer biofilms, *Water research*, 43, 2549–2557, 2009.
- He, B., He, J., Wang, J., Li, J., and Wang, F.: Characteristics of GHG flux from water-air interface along a reclaimed water intake area of the Chaobai River in Shunyi, Beijing, *Atmospheric Environment*, 172, 102–108, 2018.
- Herrero Ortega, S., Romero González-Quijano, C., Casper, P., Singer, G. A., and Gessner, M. O.: Methane emissions from contrasting urban freshwaters: Rates, drivers, and a whole-city footprint, *Global change biology*, 25, 4234–4243, 2019.
- Holgerson, M. A.: Drivers of carbon dioxide and methane supersaturation in small, temporary ponds, *Biogeochemistry*, 124, 305–318, 2015.
- Jiang, G., Gutierrez, O., Sharma, K. R., Keller, J., and Yuan, Z.: Optimization of intermittent, simultaneous dosage of nitrite and hydrochloric acid to control sulfide and methane productions in sewers, *Water research*, 45, 6163–6172, 2011.
- Jiang, G., Sharma, K. R., and Yuan, Z.: Effects of nitrate dosing on methanogenic activity in a sulfide-producing sewer biofilm reactor, *Water research*, 47, 1783–1792, 2013.
- Kang, M., Kanno, C. M., Reid, M. C., Zhang, X., Mauzerall, D. L., Celia, M. A., Chen, Y., and Onstott, T. C.: Direct measurements of methane emissions from abandoned oil and gas wells in Pennsylvania, *Proceedings of the National Academy of Sciences*, 111, 18 173–18 177, 2014.
- Klausner, T., Mertens, M., Huntrieser, H., Galkowski, M., Kuhlmann, G., Baumann, R., Fiehn, A., Jöckel, P., Pühl, M., and Roiger, A.: Urban greenhouse gas emissions from the Berlin area: A case study using airborne CO₂ and CH₄ in situ observations in summer 2018, *Elementa: Science of the Anthropocene*, 8, 2020.
- Lowe, S.: Sewer ventilation: factors affecting airflow and modeling approaches, *Journal of Water Management Modeling*, 2016.
- Maazallahi, H., Fernandez, J. M., Menoud, M., Zavala-Araiza, D., Weller, Z. D., Schwietzke, S., Von Fischer, J. C., Denier Van Der Gon, H., and Röckmann, T.: Methane mapping, emission quantification, and attribution in two European cities: Utrecht (NL) and Hamburg (DE), *Atmospheric Chemistry and Physics*, 20, 14 717–14 740, 2020.
- Malyan, S. K., Singh, O., Kumar, A., Anand, G., Singh, R., Singh, S., Yu, Z., Kumar, J., Fagodiya, R. K., and Kumar, A.: Greenhouse gases trade-off from ponds: an overview of emission process and their driving factors, *Water*, 14, 970, 2022.

- Marcotullio, P. J., Sarzynski, A., Albrecht, J., Schulz, N., and Garcia, J.: The geography of global urban greenhouse gas emissions: An exploratory analysis, *Climatic Change*, 121, 621–634, 2013.
- Martinez-Cruz, K., Gonzalez-Valencia, R., Sepulveda-Jauregui, A., Plascencia-Hernandez, F., Belmonte-Izquierdo, Y., and Thalasso, F.: Methane emission from aquatic ecosystems of Mexico City, *Aquatic Sciences*, 79, 159–169, 2017.
- Natural Resources Canada: National Hydro Network - NHN - GeoBase Series, <https://open.canada.ca/data/en/dataset/a4b190fe-e090-4e6d-881e-b87956c07977>, accessed 2023-04-27, 2022.
- Nisbet, E. G., Manning, M., Dlugokencky, E., Fisher, R., Lowry, D., Michel, S., Myhre, C. L., Platt, S. M., Allen, G., Bousquet, P., et al.: Very strong atmospheric methane growth in the 4 years 2014–2017: Implications for the Paris Agreement, *Global Biogeochemical Cycles*, 33, 318–342, 2019.
- Pak, N. M., Heerah, S., Zhang, J., Chan, E., Worthy, D., Vogel, F., and Wunch, D.: The facility level and area methane emissions inventory for the Greater Toronto Area (FLAME-GTA), *Atmospheric Environment*, 252, 118 319, 2021.
- Pitt, J. R., Lopez-Coto, I., Hajny, K. D., Tomlin, J., Kaeser, R., Jayarathne, T., Stirm, B. H., Floerchinger, C. R., Loughner, C. P., Gately, C. K., et al.: New York City greenhouse gas emissions estimated with inverse modeling of aircraft measurements, *Elem Sci Anth*, 10, 00 082, 2022.
- Plant, G., Kort, E. A., Floerchinger, C., Gvakharia, A., Vimont, I., and Sweeney, C.: Large fugitive methane emissions from urban centers along the US East Coast, *Geophysical research letters*, 46, 8500–8507, 2019.
- Plant, G., Kort, E. A., Murray, L. T., Maasackers, J. D., and Aben, I.: Evaluating urban methane emissions from space using TROPOMI methane and carbon monoxide observations, *Remote Sensing of Environment*, 268, 112 756, 2022.
- Song, C., Zhu, J.-J., Willis, J. L., Moore, D. P., Zondlo, M. A., and Ren, Z. J.: Methane Emissions from Municipal Wastewater Collection and Treatment Systems, *Environmental Science & Technology*, 57, 2248–2261, 2023.
- Statistics Canada: Water File - Lakes and Rivers (polygons) - 2011 Census, <https://open.canada.ca/data/en/dataset/448ec403-6635-456b-8ced-d3ac24143add>, accessed 2023-04-27, 2011a.
- Statistics Canada: Water File - Lakes and Rivers (polygons) - 2011 Census, <https://open.canada.ca/data/en/dataset/448ec403-6635-456b-8ced-d3ac24143add>, accessed 2023-04-27, 2011b.
- Taylor, K.: Urban environments, *Environmental sedimentology*, pp. 190–222, 2007.
- Walsh, C. J., Roy, A. H., Feminella, J. W., Cottingham, P. D., Groffman, P. M., and Morgan, R. P.: The urban stream syndrome: current knowledge and the search for a cure, *Journal of the North American Benthological Society*, 24, 706–723, 2005.

- Wang, G., Xia, X., Liu, S., Zhang, L., Zhang, S., Wang, J., Xi, N., and Zhang, Q.: Intense methane ebullition from urban inland waters and its significant contribution to greenhouse gas emissions, *Water Research*, 189, 116 654, 2021.
- Weller, Z. D., Hamburg, S. P., and von Fischer, J. C.: A national estimate of methane leakage from pipeline mains in natural gas local distribution systems, *Environmental science & technology*, 54, 8958–8967, 2020.
- Whiting, E., Plant, G., and Kort, E. A.: Estimating Urban Methane Emissions from Space using TROPOMI CH₄: CO Enhancement Ratios, in: *AGU Fall Meeting Abstracts*, vol. 2022, pp. A45R–2110, 2022.
- Wunch, D., Toon, G. C., Hedelius, J. K., Vizenor, N., Roehl, C. M., Saad, K. M., Blavier, J.-F. L., Blake, D. R., and Wennberg, P. O.: Quantifying the loss of processed natural gas within California’s South Coast Air Basin using long-term measurements of ethane and methane, *Atmospheric Chemistry and Physics*, 16, 14 091–14 105, 2016.
- Xiao, S., Yang, H., Liu, D., Zhang, C., Lei, D., Wang, Y., Peng, F., Li, Y., Wang, C., Li, X., et al.: Gas transfer velocities of methane and carbon dioxide in a subtropical shallow pond, *Tellus B: Chemical and Physical Meteorology*, 66, 23 795, 2014.
- Zhang, L., Keller, J., and Yuan, Z.: Inhibition of sulfate-reducing and methanogenic activities of anaerobic sewer biofilms by ferric iron dosing, *Water research*, 43, 4123–4132, 2009.

Chapter 7

General discussion and conclusions

The overall goal of this thesis was to directly measure a variety of diffuse methane sources using the static chamber methodology to better characterize the overall methane contributions from sources with emission factors of ~ 10 g/hour but large activity data values (i.e., $\geq 10^5$). In this final chapter we discuss the implications of our findings, in addition to the limitations of all chapters presented in this thesis with context to prior work, and discuss recommendations from both research- and policy-based standpoints. We end with a brief concluding statement.

7.1 General discussions

In Chapter 3 of this thesis, we found an overall accuracy of $\pm 14\%$ for the static chamber method over these flowrate ranges, which exceeds the quantification accuracy of other indirect measurement methods such as satellite, aircraft, and mobile laboratory sampling platforms (Johnson et al., 2023; Edie et al., 2020; Sherwin et al., 2023), and direct measurement methods such as the Hi-Flow Sampler (Riddick et al., 2019; Klotz, 2023). Our findings suggest that the presence of interior chamber mixing is important for accuracy, especially for larger chamber sizes, which is an important guideline for chamber design and field deployment. The use of optimal chamber designs increased the accuracy of the static chamber method to $\pm 5\%$, which effectively makes the static chamber method one of the most accurate methane quantification methods currently available.

Many sectors in GHG inventories are based on bottom-up extrapolations using measurements at the component- and/or equipment-level, and our findings show that the static chamber method can be an accurate measurement method to gather these measurements.

In our controlled release experiments, the effects of leak properties were tested, which is a novel factor to test for the static chamber method and many other methods as well. Leak properties are important to investigate as methane sources can have differing methane concentrations (e.g., biogas versus NG). Our study also utilized known methane standards, whereas others typically utilize stock NG whose true methane concentration is a source of uncertainty (Riddick et al., 2022; Morales et al., 2022; Kumar et al., 2022).

In Chapter 4 of this thesis we present a synthesis of direct measurement data and activity counts for AOG wells. Since our synthesis of methane measurements from AOG wells presented in Chapter 4, there have been several additional studies that have quantified methane emissions from AOG wells (Lebel et al., 2020; El Hachem and Kang, 2022; Townsend-Small and Hoschouer, 2021; Etiope et al., 2019; Riddick et al., 2020). Our revised calculations of annual methane emissions from AOG wells did show that inventory estimates were low. Moreover, the number of AOG wells in Canada and the U.S. are likely to continue to grow, meaning that the contribution of methane emissions from AOG wells will likely increase as years pass if mitigation is not prioritized.

We found that emission factors for AOG wells varied from 1.8×10^{-3} g/hour to 48 g/hour depending on the region, well type, and plugging status. Similar results were observed from Lebel et al. (2020) and Townsend-Small and Hoschouer (2021), who found emission factors for AOG wells in California and Texas to be 10.9 and 6.2 g/hour respectively. Notably, El Hachem and Kang (2022) and Lebel et al. (2020) identified new AOG well characteristics that could influence methane emission rates. El Hachem and Kang (2022) found that AOG wells emitting H₂S emitted at higher rates (i.e., 16.6 g/hour) than non-H₂S producing wells. Lebel et al. (2020) showed that "idle" wells emit at higher rates (i.e., 35.4 g/hour) than other AOG wells. Furthermore, a large indirect sampling campaign utilizing mobile surveying data by Vogt et al. (2022) quantified methane emissions from suspended well sites in western Saskatchewan, and found that if their contributions

are ignored that methane emissions inventories would underestimate total emissions from the O&G sector by around 25%.

Chapters 5 and 6 of this thesis focus on methane emissions from urban environments, which have been identified as major contributor of global methane emissions (de Foy et al., 2023; Marcotullio et al., 2013). Historic landfills, WUHs, and urban water bodies are all biogenic methane sources that were identified in Chapters 5 and 6 as significant contributors of methane emissions in their cities' respective methane inventories despite not being included in municipal, provincial, or federal GHG inventories, which confirms our initial hypothesis. Urban areas are distinctive in that they are complex environments with multiple methane sources (Pak et al., 2021; Lamb et al., 2016; Plant et al., 2022) but are also uniquely positioned to implement mitigation strategies (Hopkins et al., 2016). Multiple top-down studies based in the U.S. have highlighted that municipal methane inventories underestimate their annual emissions (Plant et al., 2019, 2022; de Foy et al., 2023), and some of the potential reasons for this underestimation are listed as either the accounting of certain methane sources, or the poor characterization of known methane sources.

Our findings in Chapter 5 highlight the large contributions of methane emissions from residential meter-sets and third party breaks to overall emissions from NG distributions systems, and we show that methane emissions from WUHs and historic landfills are both significant (i.e., second and third highest methane sources in the city) relative to Montreal's methane inventory despite not being included in municipal, provincial, or federal GHG inventories. We found that emission factors for residential meter-sets were low at 0.23 g/hour with a maximum methane emission rate below 10 g/hour. Despite not measuring any residential meter-sets that would be readily captured via indirect methods, we found their annual contributions made up ~40% of total methane emissions from the NG distribution sector. This supports our hypothesis that small diffuse methane sources can be significant contributors to cumulative methane emissions.

Our estimates for annual methane emissions from urban water bodies in the GTA confirms our initial hypothesis that their annual methane emissions were substantial (i.e., ~15% of total methane emissions in the GTA). In terms of different types of urban water bodies, we found that

methane emissions from ponds and canals are notable, despite making up less than 10% of the total areal extent of urban water bodies in the GTA. Urban ponds have already been identified as a significant methane source in prior research (Herrero Ortega et al., 2019; Wang et al., 2021; Holgerson, 2015; DelSontro et al., 2018), but few studies have quantified methane emissions from urban canals (Ars et al., 2020) which are a heavily modified urban water body that differs from the other types. The emission factor we calculated for urban canals (i.e., $75 \mu\text{g}\cdot\text{m}^{-2}\cdot\text{sec}^{-1}$) in the GTA was more than twice as high as the highest emissions previously observed from urban water bodies (Martinez-Cruz et al., 2017). It is unclear whether all urban canals emit methane at rates similar to those observed at the Keating Channel, but measurements from canals in other cities would help improve our understanding of their contributions at regional and global scales. Furthermore, we were able to confirm the hypothesis of Ars et al. (2020) regarding the annual emissions from the Keating Channel, and our direct measurement aligned well with the estimates obtained from the mobile surveying data.

7.2 Limitations and Uncertainties

Our work in Chapter 3 highlights the usefulness of the static chamber method (and also other direct measurement techniques) in the quantification of methane emissions from lower emitting sites and the high resolution in terms of source attribution. However, there are many situations where direct measurement methods are not suitable, either due to safety concerns or logistical constraints. For sites where direct access is impossible or dangerous, indirect measurement techniques would be more suitable. In other cases, such as measuring methane emissions from H_2S emitting AOG wells, safety concerns (i.e., H_2S is a highly toxic gas) can be overcome with additional safety precautions such as wearing a self-contained breathing apparatus (El Hachem and Kang, 2022).

In addition to potential safety and logistical concerns, direct measurement methods also face the downside of missing sources when extrapolating individual measurements to larger scales (i.e., facility, regional, and global levels) and are limited by small sample sizes, which is evident in

multiple studies highlighting the discrepancy between GHG inventories created from bottom-up measurements and top-down studies (Alvarez et al., 2018; Plant et al., 2022; MacKay et al., 2021). Although Rutherford et al. (2021) found agreement between their bottom-up inventory of methane emissions from the U.S. energy production sector and other top-down inventories, and highlight that compiling larger data-sets of measurements could potentially address the discrepancies observed between bottom-up and top-down inventory approaches, the limitations of direct measurement methods and bottom-up inventory development are well established. Ideally, combinations of indirect and direct methods should be utilized to establish methane emissions distributions curves for sites emitting methane at levels not detectable via indirect methods, and to establish the contributions of less populous but significant super-emitting sites (Fox et al., 2019).

Our compilation of component-level emission factors from the Intergovernmental Panel on Climate Change (2022) represents only what is contained within the database itself, and does not necessarily represent the full range of component-level emission factors found in the world, or their importance relative to cumulative methane emissions. Moreover, in our compilation of controlled release studies based on a Goggle Scholar search (as of June 2023), some studies may have been overlooked and newer studies may not have been available. Both the compilation of component-level emission factors and controlled release studies would benefit from a more comprehensive literature search utilizing key search terms, similar to the literature review performed by El Hachem and Kang (2023).

Another limitation of the controlled release tests we performed in this work is the lack of exact replicates for each release. Our controlled releases were performed with a single replicate for each combination of investigated factors, which leaves the potential for data outliers to overly influence results. We did observe skewed distribution of measurement accuracy values from our tests, which implies that the use of replicates could constrain these numbers and better illustrate the true accuracy of the static chamber method. In the context of prior studies testing the static chamber method, both Pihlatie et al. (2013) and Christiansen et al. (2011) focused on extremely small flux rates rather than flowrates, and Riddick et al. (2022) used three replicates the three

different flowrates for nine total releases. Additionally, the results of the static method testing in Riddick et al. (2022) were not reported due to safety concerns from the experiment.

For the limitations of our research presented in Chapter 4, 5 and 6, our estimates for annual methane emissions are based on a compilation of direct measurement data. We have already highlighted the drawbacks of direct measurement data, such as the small sample sizes and potential to miss super-emitting sites. For Chapter 4, all of the measurements from AOG wells that were included in our compilation of measurements were sites where site access permissions were obtained, which could bias our emission rate data by missing AOG well sites that are still owned by private companies (e.g., suspended and idle wells), such as the sites measured in Vogt et al. (2022). The limitations of Chapters 5 and 6 are similar to those observed in Chapter 4 with regards to the utilization of direct measurement data for the extrapolation of methane emissions to annual estimates. Notably, our sample set of direct measurements from WUHs in Montreal and the GTA represents an even smaller percentage (i.e., $\leq 0.05\%$) of the total sampled population when compared to our measurements from AOG wells.

The measurements we compiled in Chapter 4 represent the available measurement data at the time, but we did not have measurements from two of the regions containing the highest numbers of AOG wells (i.e. Alberta and Texas). Geographic region was identified in El Hachem and Kang (2023) as a factor that influenced AOG well leakage, and therefore the inclusion of measurements from these regions would provide a more representative emission measurement dataset. The same limitations also extend to most our direct measurement data gathered from urban areas in Chapters 5 and 6, with the exceptions of NG branch and gate stations for Montreal where we measured 100% and 67% of the cities within the city.

Another limitation of this work is our classification of plugged and vented wells from Kang et al. (2016) in our emission factors for plugged wells. While we do acknowledge in this work the impacts of regional well plugging practices, separating plugged and vented wells into a separate category would better represent the total methane emissions and geospatial distributions of methane emissions from plugged wells. There are also uncertainties associated with the classi-

fication of WUH types. Without a detailed map of the wastewater collection infrastructure, it is challenging to attribute our direct measurements from WUHs to the exact type of wastewater collection system they were connected to, which would provide valuable data for our annual emission estimates and for both policy-makers. For urban water bodies, the classifications for urban water bodies relied on the definitions provided by the Statistics Canada geospatial data which could be outdated or poorly characterized. In addition, several studies showed that methane emissions from urban water bodies vary over seasons (Herrero Ortega et al., 2019; Peacock et al., 2021), meaning that our measurements conducted in October and December may be biased.

For our measurements from historic landfills, we performed multiple single-point flux measurements over sections of the landfill sites and then interpolated those measurements using inverse distance weighting. In terms of geospatial analysis, kriging provides more informative data by also quantifying interpolation uncertainties over space. Furthermore, interpolations of flux chamber measurements are likely to underestimate overall methane emissions from landfills since emissions are heterogeneous over space and time (Mønster et al., 2019). Therefore, there are opportunities to apply advanced geostatistical methods to reduce uncertainties and gain new insights.

Finally, for Chapter 4, 5, and 6 we did not incorporate the measurement accuracy of the static chamber method into our annual emission rates calculations to better represent the uncertainty of these estimates. This could be accomplished during the bootstrapping process used to calculate emission factors and uncertainty, where each individual measurement is represented by a normal probability distribution with the mean set as the measured flowrate and the standard deviation as the measurement uncertainty.

7.3 Recommendations

7.3.1 Future research directions

From a research-based perspective, it would be beneficial to test other factors that could influence the accuracy of the static chamber method, such as the effectiveness of the chamber seal, impacts

of infrastructure within the chamber, different methods for mixing air within the chamber volume, and different sampling points. In addition, testing the effectiveness of the static chamber method in capturing temporally varying flowrates would also be beneficial, as many component/equipment level sources are known to have flowrates that vary over time (e.g., pneumatics, AOG wells, urban water bodies) (Allen et al., 2013; Riddick et al., 2020; Herrero Ortega et al., 2019). More in-depth controlled release testing, with the use of replicates, would aid in quantifying the accuracy of the static chamber method under the wide range of conditions likely to be encountered in field settings.

For AOG wells, future research would benefit from additional direct measurements given the low methane flowrates common to AOG well sites (Chapter 4). Focusing on measuring AOG wells in regions with the highest populations of AOG wells would be beneficial since geographic region has been identified as a indicator of well leakage (El Hachem and Kang, 2023). In addition, broadening the well status classifications of AOG well measurements (both for past and future work) will aid in improving the representivity of methane emissions calculations and identifying specific provinces/states/territories with the highest methane emissions. Studies that investigate the impacts of the plugging status of AOG wells on methane emissions, soil gas migration, and groundwater contamination will help determine the environmental impacts of plugging AOG wells which is important data for policy-makers.

For future research on methane measurement studies for urban environments, we have several recommendations. The first recommendation would be to develop a detailed inventory of activity data for the target city, including the compilation of a detailed network of wastewater collection infrastructure and historic landfills, which may be challenging given open access data availability issues. This compilation of activity data will help in the design of measurement campaigns and the later source attribution stages, which addresses two limitations we note in our urban measurement studies. With regards to wastewater collection infrastructure, most cities offer detailed maps of sewer infrastructure for specific plots of land at a variable cost between cities. To avoid the large costs of purchasing the entire suite of maps for a city, the detailed maps could be purchased based on locations obtained from the measurement data.

For the design of measurement campaigns of urban areas, rather than initially performing direct measurements, we recommend developing a comprehensive data-set of indirect measurements to cover the entire city over multiple seasons. Indirect measurements performed at multiple spatial scales would also be useful, for example using satellite-based observations to estimate total city methane emissions (e.g., TROPOMI) in tandem with extensive mobile surveying data to identify the emission rates and locations of persistent methane sources. Direct measurements can follow the indirect measurements to determine the specific leaking components from sites identified through the indirect sampling, and to establish the contributions from the lower-emitting sites not easily detected from the indirect methods. In a similar way, measurements at larger spatial scales would also be valuable for AOG well methane emissions estimates, especially to identify super-emitting sites.

Furthermore, factors that are easily measured for wastewater collection systems should be investigated in tandem with methane emission rate data to determine whether any relationships can be established. This would allow for a more representative spatial presentation of methane emissions from wastewater collection systems which is critical for developing mitigation strategies. An example of this approach would be loss rate calculations for active O&G wells where a relationship between production and methane emission rates was established (Omara et al., 2022), where site-level methane emissions measurements are divided by the daily production values of the site to determine the percentages of methane lost from the production stream.

While we do investigate several methane sources that are either poorly characterized or not included in GHG inventories, there are likely others as well. For example, methane emissions downstream of a tropical hydroelectric dam in the central Amazon basin were found to represent 3% of the cumulative methane emissions from the central Amazon floodplain (Kemenes et al., 2007). Other sources such as beyond-the-meter methane emissions have also been identified and are a recent inclusion to the U.S. and Canadian GHG inventories, but are limited to data from a small number of measurement studies (Saint-Vincent and Pekney, 2019; Lebel et al., 2022; Klotz,

2023). Studies that investigate these unknown/poorly characterized sources will be valuable in developing methane mitigation strategies.

7.3.2 For policy-makers

Throughout this thesis we present several policy relevant findings that are actionable and can be immediately applied. Below we present several examples of these actions that can be utilized by policymakers to increase or encourage mitigation action to reduce methane emissions.

From a policy-based perspective, all studies that have directly measured AOG wells have highlighted lower emission rates from plugged wells when compared to unplugged wells (El Hachem and Kang, 2022; Williams et al., 2019; Kang et al., 2014, 2016; Lebel et al., 2020; Townsend-Small et al., 2016), which does imply that established well plugging practices would be effective in reducing methane emissions from AOG wells. Furthermore, a detailed review of factors linked to high-emitting O&G wells by El Hachem and Kang (2023) found that geographic location, well deviation, plugging status, and casing quality were all linked with well leakage. However, as indicated in Kang et al. (2021) and Jackson et al. (2020), there is a lack of knowledge on the leakage potential of plugged wells, and requires further research. There are multiple environmental factors to consider in addition to methane emissions when evaluating the impacts of well plugging, such as groundwater contamination, soil degradation, damage to ecosystems, or lead to the increased likelihood of groundwater pollution.

As part of the USD \$65 billion Bipartisan Infrastructure Law passed in the U.S. in 2021, USD \$4.7 billion has been pledged to remediate orphaned AOG wells (Kang et al., 2023; Boutot et al., 2022). In Canada, CAD \$1.7 billion has been committed to plug orphaned wells and support O&G workers (Kang et al., 2021). Orphaned wells are a category of AOG well with no legal responsible party (Kang et al., 2021), for example, a by-product of an O&G company going bankrupt without providing the necessary funds for subsequent plugging (Boutot et al., 2022). For other types of unplugged wells with owners (e.g., suspended, idle, temporarily inactive AOG wells), implementing regulations that require additional financial assurances, justifications for im-

plementing/maintaining inactive status, limit the number of inactive wells an operator can hold, or requiring/enforcing regular maintenance can be used (Statistics Canada, 2021).

One of the key limitations we outline for our urban measurement studies in Chapters 5 and 6 is the lack of data availability for both comprehensive wastewater collection infrastructure and historic landfills. While we did have access to historic landfills maps and geospatial data on the number of sewer and storm drain WUHs in Montreal (Ville de Montréal, 2022a,b) this does not appear to be a common in many cities. For other cities where historic landfill sites are not mapped, there are geophysical techniques such as non-invasive seismic methods that can be used to delineate their locations (Baker and Gabr, 2011; Brand, 1991). Methods of estimating the numbers and types of WUHs in cities could also be improved, most readily through increased transparency from cities regarding the availability of detailed wastewater collection infrastructure for researchers. Ultimately, open-source detailed maps of wastewater collection infrastructure for cities would address most of the issues related to site classifications for both emission factors and activity data we observe for methane emissions from WUHs.

Evaluating the effectiveness of specific mitigation strategies for wastewater collection systems is difficult as most of the studies on mitigation methods for methane production in sewers are not tested in field settings and have potential drawbacks (e.g., production of N_2O). However, we did note that the high-emitting WUHs we measured were characterized by a strong odour of sewage, therefore municipal programs that allow the public to report instances and locations of foul odours relating to sewage could be used to identify targets for measurement and potential mitigation.

Historic landfill sites are old and not fed a constant rate of waste, meaning that mitigation options such as gas collection systems would be expected to produce less biogas than younger sites (Barlaz et al., 2009). However, our work shows that historic landfills can emit significant amounts of methane (i.e., second highest methane source in Montreal), and that the installation of gas collection systems at high-emitting landfills can be done at low cost. Either direct or indirect measurements would be needed to classify historic landfill sites as high-emitting versus the relatively lower-emitting sites.

For residential meter-sets, we found that implementing LDAR programs results in high costs due to the large number of sites, implying that the current mitigation measures (i.e., customer reporting of NG odour) may be sufficient for the time being. For third party breaks, we found that the most realistic mitigation option is the enforcement of pipeline checks prior to excavation activities.

For urban water bodies, we found that the highest emitting types were ponds and canals. For urban ponds, the construction of pond aeration systems could reduce methane emissions through the prevention of eutrophication. For urban canals, mitigation could be addressed both proactively and retroactively, through consideration in the construction or reconstruction of canals to prevent the retention of organic material.

7.4 Conclusions

Concentrations of methane in the atmosphere are growing (Nisbet et al., 2020, 2014, 2019). The reduction of methane emissions will be a key component in any strategies developed to mitigate the effects of climate change given the cost-effective mitigation options that exist (Ocko et al., 2021) and the potency of methane as a greenhouse gas (IPCC, 2022). In this thesis, we emphasize the importance of direct measurements of methane emissions and the contributions of diffuse methane emissions from sources with low emission factor values but high activity data counts. Direct measurements also offer valuable data in terms of source attribution, which is valuable information for developing cost-effective methane mitigation strategies. Furthermore, the identification of specific methane emission sources offers additional benefits by identifying potential avenues for methane recovery and emissions reductions (Mazzotti et al., 2009; Lusk, 1998; Thompson et al., 2009), which could off-set or provide net benefits of implementing methane mitigation technologies.

Throughout this thesis, we identified several methane emission sources that are either poorly characterized (i.e., AOG wells), or are not included in any GHG inventories (i.e., residential NG meter-sets, WUHs, urban water bodies, historic landfills). These methane sources generally emit

methane at rates that are not easily detectable via indirect measurement methods. In addition to these sources that we investigate, there are likely several other methane sources that have not been included in GHG inventories such as hydroelectric dams (Kemenes et al., 2007), or are poorly depicted in GHG inventories and would benefit from additional measurements (e.g., beyond-the-meter methane sources Saint-Vincent and Pekney (2019); Lebel et al. (2022)). While many high emitting methane sources can be captured using indirect methane measurement techniques, direct measurements will continue to be needed for many sources, both to quantify the emissions from lower-emitting sites and to identify the specific components/equipment responsible for emissions which is valuable information for policy-makers. Ultimately, this work will contribute towards the growing need for measurement-based studies in the quantification, identification, and mitigation of methane emissions from the variety of sources that exist around the world, and add to the science-based approach towards reducing our GHG emissions and mitigating the impacts of climate change.

Bibliography

- Allen, D. T., Torres, V. M., Thomas, J., Sullivan, D. W., Harrison, M., Hendler, A., Herndon, S. C., Kolb, C. E., Fraser, M. P., Hill, A. D., et al.: Measurements of methane emissions at natural gas production sites in the United States, *Proceedings of the National Academy of Sciences*, 110, 17 768–17 773, 2013.
- Alvarez, R. A., Zavala-Araiza, D., Lyon, D. R., Allen, D. T., Barkley, Z. R., Brandt, A. R., Davis, K. J., Herndon, S. C., Jacob, D. J., Karion, A., et al.: Assessment of methane emissions from the US oil and gas supply chain, *Science*, 361, 186–188, 2018.
- Ars, S., Vogel, F., Arrowsmith, C., Heerah, S., Knuckey, E., Lavoie, J., Lee, C., Pak, N. M., Phillips, J. L., and Wunch, D.: Investigation of the spatial distribution of methane sources in the Greater Toronto Area using mobile gas monitoring systems, *Environmental Science & Technology*, 54, 15 671–15 679, 2020.
- Baker, H. and Gabr, A.: Using Geophysical and Geotechnical Techniques to Delineate a Landfill in a Residential Area, in: *First EAGE International Conference on Engineering Geophysics*, pp. cp–273, EAGE Publications BV, 2011.
- Barlaz, M. A., Chanton, J. P., and Green, R. B.: Controls on landfill gas collection efficiency: instantaneous and lifetime performance, *Journal of the Air & Waste Management Association*, 59, 1399–1404, 2009.
- Boutot, J., Peltz, A. S., McVay, R., and Kang, M.: Documented Orphaned Oil and Gas Wells Across the United States, *Environmental Science & Technology*, 56, 14 228–14 236, 2022.
- Brand, S. G.: Evaluation of three geophysical methods to locate undocumented landfills, Ph.D. thesis, Texas A&M University, 1991.
- Christiansen, J. R., Korhonen, J. F., Juszczak, R., Giebels, M., and Pihlatie, M.: Assessing the effects of chamber placement, manual sampling and headspace mixing on CH₄ fluxes in a laboratory experiment, *Plant and soil*, 343, 171–185, 2011.
- de Foy, B., Schauer, J. J., Lorente, A., and Borsdorff, T.: Investigating high methane emissions from urban areas detected by TROPOMI and their association with untreated wastewater, *Environmental Research Letters*, 2023.
- DelSontro, T., Beaulieu, J. J., and Downing, J. A.: Greenhouse gas emissions from lakes and impoundments: Upscaling in the face of global change, *Limnology and Oceanography Letters*, 3, 64–75, 2018.
- Eddie, R., Robertson, A. M., Field, R. A., Soltis, J., Snare, D. A., Zimmerle, D., Bell, C. S., Vaughn, T. L., and Murphy, S. M.: Constraining the accuracy of flux estimates using OTM 33A, *Atmospheric Measurement Techniques*, 13, 341–353, 2020.
- El Hachem, K. and Kang, M.: Methane and hydrogen sulfide emissions from abandoned, active, and marginally producing oil and gas wells in Ontario, Canada, *Science of The Total Environment*, 823, 153 491, 2022.

- El Hachem, K. and Kang, M.: Reducing oil and gas well leakage: a review of leakage drivers, methane detection and repair options., *Environmental Research: Infrastructure and Sustainability*, 2023.
- Etiopie, G., Schwietzke, S., Helmig, D., and Palmer, P.: Global geological methane emissions: An update of top-down and bottom-up estimates, *Elementa: Science of the Anthropocene*, 7, 2019.
- Fox, T. A., Barchyn, T. E., Risk, D., Ravikumar, A. P., and Hugenholtz, C. H.: A review of close-range and screening technologies for mitigating fugitive methane emissions in upstream oil and gas, *Environmental Research Letters*, 14, 053 002, 2019.
- Herrero Ortega, S., Romero González-Quijano, C., Casper, P., Singer, G. A., and Gessner, M. O.: Methane emissions from contrasting urban freshwaters: Rates, drivers, and a whole-city footprint, *Global change biology*, 25, 4234–4243, 2019.
- Holgerson, M. A.: Drivers of carbon dioxide and methane supersaturation in small, temporary ponds, *Biogeochemistry*, 124, 305–318, 2015.
- Hopkins, F. M., Ehleringer, J. R., Bush, S. E., Duren, R. M., Miller, C. E., Lai, C.-T., Hsu, Y.-K., Carranza, V., and Randerson, J. T.: Mitigation of methane emissions in cities: How new measurements and partnerships can contribute to emissions reduction strategies, *Earth's Future*, 4, 408–425, 2016.
- Intergovernmental Panel on Climate Change: IPCC Emission Factor Database., <https://www.ipcc-nggip.iges.or.jp/EFDB/main.php>, accessed 2022-12-14, 2022.
- IPCC: Climate Change 2022: Mitigation of Climate Change. Contribution of Working Group III to the Sixth Assessment Report of the Intergovernmental Panel on Climate Change, Cambridge University Press, Cambridge, UK and New York, NY, USA, <https://doi.org/10.1017/9781009157926>, https://www.ipcc.ch/report/ar6/wg3/downloads/report/IPCC_AR6_WGIII_FullReport.pdf, 2022.
- Jackson, R. E., Dusseault, M. B., Frape, S., Phan, T., and Steelman, C.: Investigating the origin of elevated H₂S in groundwater discharge from abandoned gas wells, Norfolk County, Ontario, *Geoconvention 2020*, 2020.
- Johnson, M. R., Tyner, D. R., and Conrad, B. M.: Origins of Oil and Gas Sector Methane Emissions: On-Site Investigations of Aerial Measured Sources, *Environmental Science & Technology*, 57, 2484–2494, 2023.
- Kang, M., Kanno, C. M., Reid, M. C., Zhang, X., Mauzerall, D. L., Celia, M. A., Chen, Y., and Onstott, T. C.: Direct measurements of methane emissions from abandoned oil and gas wells in Pennsylvania, *Proceedings of the National Academy of Sciences*, 111, 18 173–18 177, 2014.
- Kang, M., Christian, S., Celia, M. A., Mauzerall, D. L., Bill, M., Miller, A. R., Chen, Y., Conrad, M. E., Darrah, T. H., and Jackson, R. B.: Identification and characterization of high methane-emitting abandoned oil and gas wells, *Proceedings of the National Academy of Sciences*, 113, 13 636–13 641, 2016.

- Kang, M., Brandt, A. R., Zheng, Z., Boutot, J., Yung, C., Peltz, A. S., and Jackson, R. B.: Orphaned oil and gas well stimulus—maximizing economic and environmental benefits, *Elem Sci Anth*, 9, 00 161, 2021.
- Kang, M., Boutot, J., McVay, R. C., Roberts, K. A., Jasechko, S., Perrone, D., Wen, T., Lackey, G., Raimi, D., Digiulio, D. C., et al.: Environmental risks and opportunities of orphaned oil and gas wells in the United States, *Environmental Research Letters*, 18, 074 012, 2023.
- Kemenes, A., Forsberg, B. R., and Melack, J. M.: Methane release below a tropical hydroelectric dam, *Geophysical research letters*, 34, 2007.
- Klotz, L.: Methane Emissions and Environmental Impacts of Oil and Gas Systems: Post-meter natural gas systems and well sites in northern regions, 2023.
- Kumar, P., Broquet, G., Caldow, C., Laurent, O., Gichuki, S., Cropley, F., Yver-Kwok, C., Fontanier, B., Lauvaux, T., Ramonet, M., et al.: Near-field atmospheric inversions for the localization and quantification of controlled methane releases using stationary and mobile measurements, *Quarterly Journal of the Royal Meteorological Society*, 148, 1886–1912, 2022.
- Lamb, B. K., Cambaliza, M. O., Davis, K. J., Edburg, S. L., Ferrara, T. W., Floerchinger, C., Heimburger, A. M., Herndon, S., Lauvaux, T., Lavoie, T., and Lyon, D.: Direct and indirect measurements and modeling of methane emissions in Indianapolis, Indiana, *Environmental Science & Technology*, 50, 8910–8917, 2016.
- Lebel, E. D., Lu, H. S., Vielstadte, L., Kang, M., Banner, P., Fischer, M. L., and Jackson, R. B.: Methane emissions from abandoned oil and gas wells in California, *Environmental Science & Technology*, 54, 14 617–14 626, 2020.
- Lebel, E. D., Finnegan, C. J., Ouyang, Z., and Jackson, R. B.: Methane and NO_x emissions from natural gas stoves, cooktops, and ovens in residential homes, *Environmental science & technology*, 56, 2529–2539, 2022.
- Lusk, P.: Methane recovery from animal manures the current opportunities casebook, Tech. rep., National Renewable Energy Lab.(NREL), Golden, CO (United States), 1998.
- MacKay, K., Lavoie, M., Bourlon, E., Atherton, E., O’Connell, E., Baillie, J., Fougère, C., and Risk, D.: Methane emissions from upstream oil and gas production in Canada are underestimated, *Scientific reports*, 11, 1–8, 2021.
- Marcotullio, P. J., Sarzynski, A., Albrecht, J., Schulz, N., and Garcia, J.: The geography of global urban greenhouse gas emissions: An exploratory analysis, *Climatic Change*, 121, 621–634, 2013.
- Martinez-Cruz, K., Gonzalez-Valencia, R., Sepulveda-Jauregui, A., Plascencia-Hernandez, F., Belmonte-Izquierdo, Y., and Thalasso, F.: Methane emission from aquatic ecosystems of Mexico City, *Aquatic Sciences*, 79, 159–169, 2017.
- Mazzotti, M., Pini, R., and Storti, G.: Enhanced coalbed methane recovery, *The Journal of Supercritical Fluids*, 47, 619–627, 2009.

- Mønster, J., Kjeldsen, P., and Scheutz, C.: Methodologies for measuring fugitive methane emissions from landfills—A review, *Waste Management*, 87, 835–859, 2019.
- Morales, R., Ravelid, J., Vinkovic, K., Korbeń, P., Tuzson, B., Emmenegger, L., Chen, H., Schmidt, M., Humbel, S., and Brunner, D.: Controlled-release experiment to investigate uncertainties in UAV-based emission quantification for methane point sources, *Atmospheric Measurement Techniques*, 15, 2177–2198, 2022.
- Nisbet, E., Fisher, R., Lowry, D., France, J., Allen, G., Bakkaloglu, S., Broderick, T., Cain, M., Coleman, M., Fernandez, J., and Forster, G.: Methane mitigation: Methods to reduce emissions, on the path to the Paris Agreement, *Reviews of Geophysics*, 58, e2019RG000 675, 2020.
- Nisbet, E. G., Dlugokencky, E. J., and Bousquet, P.: Methane on the rise—again, *Science*, 343, 493–495, 2014.
- Nisbet, E. G., Manning, M., Dlugokencky, E., Fisher, R., Lowry, D., Michel, S., Myhre, C. L., Platt, S. M., Allen, G., Bousquet, P., et al.: Very strong atmospheric methane growth in the 4 years 2014–2017: Implications for the Paris Agreement, *Global Biogeochemical Cycles*, 33, 318–342, 2019.
- Ocko, I. B., Sun, T., Shindell, D., Oppenheimer, M., Hristov, A. N., Pacala, S. W., Mauzerall, D. L., Xu, Y., and Hamburg, S. P.: Acting rapidly to deploy readily available methane mitigation measures by sector can immediately slow global warming, *Environmental Research Letters*, 16, 054 042, 2021.
- Omara, M., Zavala-Araiza, D., Lyon, D. R., Hmiel, B., Roberts, K. A., and Hamburg, S. P.: Methane emissions from US low production oil and natural gas well sites, *Nature Communications*, 13, 2085, 2022.
- Pak, N. M., Heerah, S., Zhang, J., Chan, E., Worthy, D., Vogel, F., and Wunch, D.: The facility level and area methane emissions inventory for the Greater Toronto Area (FLAME-GTA), *Atmospheric Environment*, 252, 118 319, 2021.
- Peacock, M., Audet, J., Bastviken, D., Cook, S., Evans, C., Grinham, A., Holgerson, M., Högbom, L., Pickard, A., Zieliński, P., et al.: Small artificial waterbodies are widespread and persistent emitters of methane and carbon dioxide, *Global Change Biology*, 27, 5109–5123, 2021.
- Pihlatie, M. K., Christiansen, J. R., Aaltonen, H., Korhonen, J. F., Nordbo, A., Rasilo, T., Benanti, G., Giebels, M., Helmy, M., Sheehy, J., et al.: Comparison of static chambers to measure CH₄ emissions from soils, *Agricultural and forest meteorology*, 171, 124–136, 2013.
- Plant, G., Kort, E. A., Floerchinger, C., Gvakharia, A., Vimont, I., and Sweeney, C.: Large fugitive methane emissions from urban centers along the US East Coast, *Geophysical research letters*, 46, 8500–8507, 2019.
- Plant, G., Kort, E. A., Murray, L. T., Maasackers, J. D., and Aben, I.: Evaluating urban methane emissions from space using TROPOMI methane and carbon monoxide observations, *Remote Sensing of Environment*, 268, 112 756, 2022.

- Riddick, S. N., Mauzerall, D. L., Celia, M. A., Kang, M., Bressler, K., Chu, C., and Gum, C. D.: Measuring methane emissions from abandoned and active oil and gas wells in West Virginia, *Science of the Total Environment*, 651, 1849–1856, 2019.
- Riddick, S. N., Mauzerall, D. L., Celia, M. A., Kang, M., and Bandilla, K.: Variability observed over time in methane emissions from abandoned oil and gas wells, *International Journal of Greenhouse Gas Control*, 100, 103 116, 2020.
- Riddick, S. N., Ancona, R., Mbua, M., Bell, C. S., Duggan, A., Vaughn, T. L., Bennett, K., and Zimmerle, D. J.: A quantitative comparison of methods used to measure smaller methane emissions typically observed from superannuated oil and gas infrastructure, *Atmospheric Measurement Techniques*, 15, 6285–6296, 2022.
- Rutherford, J. S., Sherwin, E. D., Ravikumar, A. P., Heath, G. A., Englander, J., Cooley, D., Lyon, D., Omara, M., Langfitt, Q., and Brandt, A. R.: Closing the methane gap in US oil and natural gas production emissions inventories, *Nature communications*, 12, 4715, 2021.
- Saint-Vincent, P. M. and Pekney, N. J.: Beyond-the-meter: Unaccounted sources of methane emissions in the natural gas distribution sector, *Environmental science & technology*, 54, 39–49, 2019.
- Sherwin, E., Rutherford, J., Zhang, Z., Chen, Y., Wetherley, E., Yakovlev, P., Berman, E., Jones, B., Thorpe, A., Ayasse, A., et al.: Quantifying oil and natural gas system emissions using one million aerial site measurements, 2023.
- Statistics Canada: Idle and orphan oil and gas wells: state and provincial regulatory strategies 2021, https://iogcc.ok.gov/sites/g/files/gmc836/f/iogcc_idle_and_orphan_wells_2021_final_web.pdf, accessed 2023-08-13, 2021.
- Thompson, S., Sawyer, J., Bonam, R., and Valdivia, J.: Building a better methane generation model: Validating models with methane recovery rates from 35 Canadian landfills, *Waste management*, 29, 2085–2091, 2009.
- Townsend-Small, A. and Hoschouer, J.: Direct measurements from shut-in and other abandoned wells in the Permian Basin of Texas indicate some wells are a major source of methane emissions and produced water, *Environmental Research Letters*, 16, 054 081, 2021.
- Townsend-Small, A., Ferrara, T. W., Lyon, D. R., Fries, A. E., and Lamb, B. K.: Emissions of coalbed and natural gas methane from abandoned oil and gas wells in the United States, *Geophysical Research Letters*, 43, 2283–2290, 2016.
- Ville de Montréal: Carte de localisation des anciennes carrières et des dépôts de surface de la Ville de Montréal, Tech. rep., <https://environnementmtl.maps.arcgis.com/apps/webappviewer/index.html?id=eddf22f7ef54982a6545e8eb3c86a9a>, 2022a.
- Ville de Montréal: Regards d’égouts, Tech. rep., <https://donnees.montreal.ca/ville-de-montreal/regards-egouts>, 2022b.

- Vogt, J., Laforest, J., Argento, M., Kennedy, S., Evelise, B., Lavoie, M., and Risk, D.: Active and inactive oil and gas sites contribute to methane emissions in western Saskatchewan, Canada, *Elementa*, 10, 2022.
- Wang, G., Xia, X., Liu, S., Zhang, L., Zhang, S., Wang, J., Xi, N., and Zhang, Q.: Intense methane ebullition from urban inland waters and its significant contribution to greenhouse gas emissions, *Water Research*, 189, 116 654, 2021.
- Williams, J. P., Risk, D., Marshall, A., Nickerson, N., Martell, A., Creelman, C., Grace, M., and Wach, G.: Methane emissions from abandoned coal and oil and gas developments in New Brunswick and Nova Scotia, *Environmental monitoring and assessment*, 191, 1–12, 2019.